FAULT LOCATION IN POWER DISTRIBUTION GRIDS USING PHASOR MEASUREMENT UNITS

BY

MUSTAFA M. AL-KHABBAZ

A Thesis Presented to the

DEANSHIP OF GRADUATE STUDIES

KING FAHD UNIVERSITY OF PETROLEUM & MINERALS

DHAHRAN, SAUDI ARABIA

In Partial Fulfillment of the

Requirements for the Degree of

MASTER OF SCIENCE

In

ELECTRICAL ENGINEERING

JANUARY 2018

KING FAHD UNIVERSITY OF PETROLEUM & MINERALS

DHAHRAN- 31261, SAUDI ARABIA

DEANSHIP OF GRADUATE STUDIES

This thesis, written by **MUSTAFA MOHAMMED JAMAL AL-KHABBAZ** under the direction of his thesis advisor and approved by his thesis committee, has been presented and accepted by the Dean of Graduate Studies, in partial fulfillment of the requirements for the degree of **MASTER OF SCIENCE IN ELECTRICAL ENGINEERING.**

Dr. Mohammad A. Abido
(Advisor)

Dr. Ali A. Al-Shaikhi
Department Chairman

Dr. Ibrahim M. El Amin
(Member)

Dr. Salam A. Zummo
Dean of Graduate Studies

Dr. Mohammed M. Al-Muhaini
(Member)

٣/١٠/١٢

Date

THIS THESIS IS DEDICATED TO

THE MEMORY OF MY FATHER 1945-2017

DEAR MOTHER

BROTHERS

SISTERS

AND

BELOVED WIFE

ACKNOWLEDGMENTS

First and foremost, I would like to thank Almighty God for enabling me to complete this thesis. During the process of developing the objectives, I realized the gift of analysis, ambition and structured thinking. The power of believing in my passion allowed me to pursue my dream. I could never have achieved this without my faith in you, the Almighty.

I gratefully acknowledge and appreciate the support provided by King Fahd University of Petroleum and Minerals (KFUPM), especially from my thesis advisor Professor Dr. Mohammed A. Abido for facilitating the work and for the encouragement. It is my pleasure to work with him as he is an intelligent, competent, cooperative and inspiring professor. His guidance and tips made it possible to produce high impacts achievements under my thesis work.

The gratitude is, also, extended to both Dr. Ibrahim M. El Amin and Dr. Mohammed M. Al-Muhaini, the other committee members of my thesis. Their times and efforts in supporting the research and providing appropriate guidance are truly appreciated.

Last but not least, I would like to pass special thanks to my family for their encouragement to improve my competencies. I am grateful to my late father and mother who taught me by example that there is no end for education. The appreciation is also extended to my brothers (especially Mosa who is always around for help), sisters and beloved wife. Their concerns and supports made my study at KFUPM enjoyable. My family is the first and last and will remain my top priority.

TABLE OF CONTENTS

LIST OF TABLES

LIST OF FIGURES

LIST OF ABBREVIATIONS

ABC	:	Artificial Bee Colony
BFS	:	Backward\forward Sweep
BM	:	Branch matrix
CT	:	Current transformer
DL	:	Distribution line
EBFS	:	Enhanced backward/ forward Sweep
EHV	:	Extra high voltage
EMS	:	Energy management system
ETAP	:	Electrical transient analysis program
FACTS	:	Flexible alternative current system
GIMM	:	Global-based inaccuracy mitigation measure
GMD	:	Geometric mean distance
GMR	:	Geometric mean radius
GPS	:	Global positioning system
HIF	:	High impedance fault
IMM	:	Inaccuracy mitigation measure

KCL	:	Kirchhoff current law
LG	:	Line-to-ground
LIMM	:	Local-based inaccuracy mitigation measure
LL	:	Double line
LLG	:	Double line-to-ground
MAD	:	Mean absolute deviation
MAPE	:	Mean absolute percentage error
MSE	:	Mean square error
OFT	:	Ohm’s formula technique
OPEX	:	Operation expenses
OPP	:	Optimal placement problem
PCC	:	Power control centres
PMU	:	Phasor measurement units
RMSE	:	Root mean square error
RTU	:	Remote terminal unit
SCADA	:	Supervisory control and data acquisition
SCTM	:	Symmetrical component transformation matrix

SMT	:	Single measurement technique
SPEA	:	Strength Pareto evolutionary algorithm
TPCMT	:	Two-port circuit measurement technique
UHV	:	Ultra-high voltage

ABSTRACT

Full Name : Mustafa Mohammed Jamal Al-Khabbaz

Thesis Title : Fault Location in Power Distribution Grids using Phasor Measurement Units

Major Field : Electrical Engineering

Date of Degree : January 2018

This thesis proposes utilization of an impedance-based model in power distribution systems equipped with phasor measurement units (PMUs) for fault location purpose. The model has been further improved so it can locate faults in inhomogeneous distribution lines. This is achieved by the first-time introducing for a novel homogeneous-to-inhomogeneous relation (H2IR). Additionally, novel inaccuracy mitigation measures are developed under the model to improve the accuracy of fault location and hence advance power restoration. The model effectiveness is validated for different case studies using different statistical measures. The results have demonstrated the model robustness in locating faults in distribution grids accurately. This topic is studied due to the limited efforts in literature of high accuracy impedance-based fault location at the distribution level with the use of PMUs.

Additionally, a fault type classification scheme is, also, developed to identify the faulty phase(s) and the type of fault based on real-time PMU phasor signals. Distribution line parameters are identified online by three different methods using synchronized measurements from the PMUs. The work, also, includes the first problem of deploying PMUs in distribution which is optimal placement. The objective is formulated to maintain full network observability, while improving the redundancy and reducing the investment cost associated with PMUs installation. Two novel approaches for determining the load flow for distribution systems are offered. The first approach is an enhancement to backward/ forward Sweep. The second provides a new method namely Zig Zag-based load flow. Both approaches are applicable for extended radial distribution systems where multiterminal lines exist. These will result in reduction of the number of iterations while maintaining the required load flow accuracy.

Master of Science Degree

King Fahd University of Petroleum and Minerals

Dhahran, Saudi Arabia

ملخص الرسالة

الاسم الكامل: مصطفى محمد جمال الخباز

عنوان الرسالة: تحديد موقع الأعطال في شبكة التوزيع الكهربائية بإستخدام وحدات قياس أطوار الكميات الكهربائية

التخصص: الهندسة الكهربائية

تاريخ الدرجة العلمية: يناير 2018م

يعتبر توفير شبكة توزيع كهربائية ذات إعتمادية عالية تحدياً لمزودي الطاقة الكهربائية, إعتمادية الشبكة تتأثر بالأعطال و التي قد تتسبب في انقطاع التيار عن المستخدمين, ولذلك هناك حاجة ماسة إلى تقنيات سريعة و دقيقة في تحديد الأعطال للتعجيل في إستعادة التيار و بالتالي تقليل فترة الإنقطاع. في الآونة الأخيرة تم تطوير و تركيب كميات لا بأس بها من وحدة قياس الأطوار المتزامن للكميات الكهربائية (Phasor Measurement Units), هذا الجهاز يعتمد على النظام العالمي لتحديد المواقع (GPS) و الذي سيشكل مستقبل أنظمة الطاقة الكهربائية, هذه التقنية يمكن إستخدامها لحل مشكلة إيجاد موقع الأعطال بسرعة و دقة عاليتين.

تقترح هذه الأطروحة نموذجاً قائماً على المقاومة لغرض تحديد موقع العطل في أنظمة توزيع الطاقة المتجانسة بإستخدام وحدات قياس الأطوار المتزامن للكميات الكهربائية. وقد تم تطوير النموذج بشكل أكبر بحيث يمكن تحديد الأعطال في خطوط التوزيع غير المتجانسة. ويتحقق ذلك من خلال خوارزميات جديدة لتحويل القيم المتجانسة إلى غير متجانسة يرمز إليها بـ (H2IR). بالإضافة إلى ذلك، تم تطوير تدابير لزيادة دقة موقع العطل، وبالتالي استعادة الطاقة بشكل أسرع. تم التحقق من فعالية النماذج بدراسة حالات متعددة جرى تقييمها بإستخدم مقاييس إحصائية مختلفة. أظهرت النتائج الفعالية العالية للنماذج في تحديد الأعطال في شبكات التوزيع بدقة أعلى من دراسات مشابهة. تم دراسة هذا الموضوع نظرا للجهود المحدودة المبذولة في مجال تحديد موقع العطل في أنظمة التوزيع بالإستعانة بوحدة قياس الأطوار المتزامن للكميات الكهربائية .

بالإضافة إلى ذلك، تمت تطوير خوارزميات لتصنيف نوع العطل و تحديد مقاومة خط التوزيع معتمدة على قياس أطوار الجهد والتيار بشكل متزامن. وتشمل هذه الرسالة أيضا على تركيب وحدات قياس الأطوار المتزامن للكميات الكهربية بالشكل الأمثل, وذلك لأن تركيبها في شبكات التوزيع يحتاج إلى دراسة و تقنين من حيث المكان والعدد و الهدف لإعتبارات إقتصادية. تم تقديم نهجين جديدين لتحديد تدفق الطاقة في أنظمة التوزيع؛ النهج الأول تطويرلـ (backward/ forward Sweep). والثاني يوفر طريقة جديدة وهي الحركة التموجية لتحديد التدفق في شبكات التوزيع. وينطبق كلا النهجين على أنظمة التوزيع الخطي و الخطي الموسع.

درجة الماجستير في العلوم

جامعة الملك فهد للبترول والمعادن

الظهران ، المملكة العربية السعودية

CHAPTER 1

INTRODUCTION

1.1 Overview

The electrical power consumption has been increasing dramatically over the past years due to mainly population growth, industrialization and the improved quality of life. The projections show that the power need will continue to raise for the upcoming decade, following the previous trend. In the case of the Kingdom of Saudi Arabia (KSA), the power escalation rate is forecasted to be 8% annually [1], [2]. This represents a challenge to the kingdom and the rest of the world to meet the demand increase rate while maintaining vast, highly diversified and reliable electrical networks. Allocation of enormous amount of investment is required to meet the demand in reliable and economic manners. With the intention of the kingdom toward competitive electricity market, the economic factor will play a key role in any investment, operation and maintenance decision. This will impose modernization of the electrical system by improving the automation and control schemes, deploying advance measurements and capitalizing on the other emerging technologies. Modernizing the electrical network will permit the continuous monitoring and management of the energy transferred from generation sources to meet the demand of end-customers.

Fault location function is classified as primarily important among the other capabilities of modern networks. This is to ensure that the faulty part of the system is discovered and located

accurately at the earliest to ensure the prompt restoration of power supply. The current power networks are approaching their maximum limits which imply that the spare capacity in healthy circuits is more likely insufficient to substitute the failed distribution lines. The economic, reliability and customer satisfaction are effected once the interruption period is extended.

Distribution lines are categorized into three main categories in terms of installation; underground, overhead, and submarine. There are several causes of line failures associated with each type of installation.

Buried cable faults are caused mainly by accidentally hitting and damaging the cables during machinery excavations, stressing the cables by heavy above ground structures (such as utilities hydrocarbon or water tanks), and cable insulation failure, etc.

Distribution aerial lines have lower reliability index compared to the underground installations. The faults result from various factors, for instance downed-conductors. Detection and location of downed live conductors represent a serious challenge to distribution network operators, especially when the conductor falls on a high resistivity soil. Various areas in the kingdom are exposed to the fallen conductors on a high impedance ground. Examples of these areas are Shaybah and Al Hasa vicinity cities, namely Udhailiyah, Uthmaniyah, Hawiyah and Haradh, etc. Other sources of the overhead faults are due to insulation breakdown, broken conductors and broken towers which will result in a connection with ground. These phenomena are caused primarily from high windstorms occurrence, weather conditions, lightning strokes striking the lines, wooden and steel poles deterioration, aging and defective parts. In addition, the connecting path to ground takes place when an animal, tree, or other external object ground the circuit intentionally or accidentally. The significantly

high failure rate in aerial lines is worth devoting considerable resources to study the line protection and fault location.

Submarine cable damage results from fishing, trawl, anchors and other causes.

The mainstream, electrical fault root causes are thoroughly investigated prior to the power restoration to clear the resulted safety risks and repair associated mechanical damages. Restoring the power can be accelerated by the expeditious identification of fault location with reasonable distance accuracy.

Fault classification represents an important building block of fault location algorithms. Power system faults are divided into two three-phase symmetrical (balanced) and three asymmetrical (unbalanced). Three unsymmetrical fault types are one line-to-ground (LG), line-to-line (LL) and double line-to-ground (LLG). The two symmetrical fault types are triple lines shorted together and triple lines-to-ground. A total of eleven (11) cases are generated out of these five fault types based on selected phase(s) (A, B & C).

Faults are categorized into three types in terms of fault resistance which are solid (bolted), low impedance, and high impedance faults. In short circuit (phase to phase) faults, the two or three phases could be exposed to connection through impedance.

1.2 Motivations

The need of automated, prompt, and accurate fault location technologies increases every day. Researchers continue to pay more attentions to the importance of fault location, addressing the market issues. Utilities stakeholders' expectations will be satisfied with the availability of

fast fault location techniques. The classical stakeholders along with their expectations are as follows:

1- Customers: Will be satisfied with a reliable and safe electrical utility network with less number of interruptions and lower distribution intervals.
2- Personnel: Prefers to work with automated technologies to facilitated their daily activities and remove a huge burden from their schedules.
3- Shareholders: Will avoid spending more money on the fault location resources and save substantial cash that could be revenue lost from the customers due to the extended interruption periods.

It is in favor of all stakeholders to adopt new technology that helps in fast repair of faulty parts, expedite power restoration and therefore improve distribution power network reliability.

Distribution systems experience permanent and momentary faults. Momentary faults are more frequent in aerial circuits and will be cleared at the same instance by auto-recloser devices. This type of temporary faults will not cause a considerable interruption duration and hence outside the scope of this study.

This study focuses on the permanent faults in which the operators and maintenance crew interventions are required to investigate the root causes and effects of the fault after its occurrence. One of the due diligence required to put the line back in service is to identify the exact fault position. The traditional way is to patrol and inspect the whole length of the line which is not efficient in all aspects; time, money and resources. Additionally, the ownership, maintenance and operation jurisdiction, in several occasions, is divided between different

entities. This will require a lot of coordination and communications that could be avoided easily by discovering the actual fault location and assigning it to the responsible organization.

Fault location in distribution networks has the same, if not more, criticality level comparing to transmission due to the following reasons:

1. In numerous cases, Distribution lines (DL) are installed underground, especially in residential and industrial areas for different justification. The justifications include that the aerial lines could be safety risky to people and affecting scene of the city. However, underground installation usually crosses roads and passes under third parties' territories which make the coordination more complicated. The issue is exacerbated further by the fact that underground circuits require feet patrolling and inspection in case of maintenance and abnormal situations. Patrolling to inspect aerial transmission lines is performed by vehicles.
2. Live downed-conductors are common problems in distribution networks which create a safety risk. Hence, quick and accurate protective and fault location schemes are necessary.
3. Transmission lines are designed with acceptable redundancy to tolerate any planned and forced outages. Therefore, the faults could cause line outages but not necessarily power interruption to the customers. Unlike transmission, most of distribution circuits are designed to be radial type. Accordingly, any fault in the radial configuration DL will cause interruptions. This could result in tremendous amount of opportunity loss and actual money loss.
4. Distribution system faults account for more than 80% of customer interruptions [3]. This large percentage confirms the high priority of fault location in distribution grids.

The above four considerations justify the innovation and creation for swift and accurate fault location in distribution networks.

1.3 Thesis Objectives

This thesis provides optimally placed phasor measurement units (PMUs) and impedance-based algorithms for the location of the faults in distribution grids. The following objectives will be accomplished by the end of this work:

1. Apply multi- and single objectives population-based algorithms to minimize the number of PMU installation in distribution networks while maintaining the full system monitoring and enhancing the observability redundancy.
2. Propose an impedance-based approach for fault location in a distribution system by the utilization of the fundamental frequency component of voltage and current signals obtained from PMUs.
3. Evaluate robustness of the proposed impedance-based fault location techniques using PMU for different scenarios, including changing fault distance, fault resistance, fault type and loading conditions.

1.4 Contributions

The major achieved contributions resulted from this thesis work are itemized as follows:

1. Conducted a comprehensive panoramic review for the available publications in literature on the application of PMU for fault location in both transmission and distribution.
2. Proposed novel impedance-based fault location models for symmetrical and asymmetrical faults in homogeneous and inhomogeneous distribution grids. This is achieved by the utilization of the fundamental frequency component of voltage and current signals obtained from PMUs. Additionally, novel accuracy improvement measures have been established to reduce the error of fault location estimations and hence advance power restoration.
3. Analyzed and recommended the use of online DL parameters identification methods in the proposed impedance based model, especially for asymmetrical faults. The proposed approach is independent of any information provided from the electric utility Bureaus. The recommendations supported the fault location models and have significant impacts on their accuracy.
4. Introduced two novel load flow analysis for distribution networks that resulted in in reduction of the number of iterations compared to backward\forward Sweep (BFS), while maintaining the required load flow accuracy.
5. Placed PMUs in distribution networks optimally by using single and multi-objective intelligent optimization algorithms, namely Artificial Bee Colony (ABC) and Strength Pareto evolutionary algorithm (SPEA). They are robust and

reliable techniques to find the optimal solution. Using multi-objective approach will give diversified optimal options to the decision makers to select the most appropriate choice that meets their stakeholder expectations.

1.5 Thesis Methodology and Structure

The methodology of this thesis is categorized into five main aspects to achieve the main objective (fault location). The five aspects are data collection (literature survey), load flow, PMUs optimal placement, DL parameters identification and fault location.

The first aspect is the relevant data collection which is completed through surveying the related works reported in literature. Load flow analysis represents the second aspect toward fault location. It is required to find the per-fault voltage and current signals at the two terminals of the faulty line. The system conditions observability is necessary to locate faults in the network which comes as the third aspect. The system observability will provide the required pre- and post-fault input data to the fault location model. The full system observability is ensured by optimally placing PMUs in distribution grids. The proposed fault location model is based on the faulty line impedance. Basing the line parameters estimation on off-line techniques or pre-identified information will reduce the accuracy level of the fault location. Therefore, it is proposed to determine the parameters online using the PMUs. The line parameters identification is the fourth aspect of this study methodology. By having the aforementioned four aspects, the fault location model is developed accordingly as the last aspect. Impedance-based algorithms have been developed to locate faults in asymmetrical and symmetrical, homogenous and inhomogeneous DLs. The five study methodology aspects are illustrated in Figure 1-1.

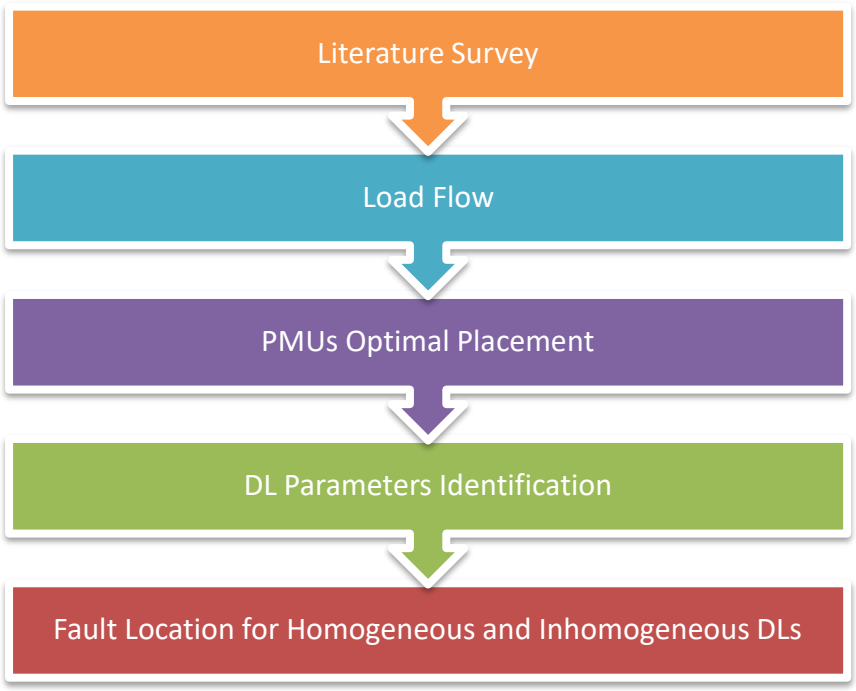

Figure 1-1: Thesis methodology flowchart

This thesis is organized into nine chapters. After the introduction in Chapter 1, an exhaustive literature survey of PMU-based fault locations is presented in Chapter 2. Chapter 3 discusses load flow analysis in distribution grids. The PMUs optimal placement problem (OPP) problem in distribution grids is formulated in Chapter 4. Chapter 5 offers online identification of DL parameters using PMUs. In Chapter 6, inaccuracy prediction and mitigation for asymmetrical and symmetrical impedance-based fault location are proposed. Fault location for inhomogeneous DLs is developed in Chapter 7. Last but not least, the thesis outcomes and recommendations addressing the future work is presented in Chapter 8.

CHAPTER 2

LITERATURE REVIEW

Electricity providers require sustaining high reliability of electrical networks starting from generation to end-customers. Reliability of the electrical system could be affected by faults, which could cause customer interruptions. Subsequently, prompt and accurate fault location techniques are needed to reduce the interruption period by expediting power restoration. Recently, phasor measurement units (PMUs) have been rapidly deployed in the electrical networks that could be used for solving the fault location problem. This chapter presents a comprehensive survey on the work reported in literature since 2000 till 2017 addressing this problem. To the best of my knowledge, this chapter is exhaustive to all available researches in the subject of PMU use for fault location. These publications have been tabulated to summarize the discussed problems, pros and cons, accuracy, methods implemented, and locations with respect to energy chain. This manuscript will support power system engineers and academic researchers as a reference for their prospective relevant problems. Finally, the challenges and important aspects have been highlighted for further investigation in future.

2.1 Introduction

Power system fault location utilizing PMU is an evolving subject that has been considered by several researchers and utilities. Recently, the installation of PMUs have been substantially increased and the associated standards have been developed [4]. The PMU application for fault location is demanding due to their extraordinary synchronization. This chapter aims to

promote improvements in the power system fault location using PMUs by surveying the associated added-value efforts. Literature survey covered by search includes publications from different well-known journals, databases, and conferences in the period of 2000 through mid of 2017. More than 1000 publications in related subjects have been reviewed. A total of 73 publications are found to be closely related to the subject of PMU application to fault location.

The major problems presented in the surveyed publications can be categorized based on the location in the electric energy chain into transmission and distribution. Four technique-based subcategories are discussed within both the transmission and distribution categories as follows:

1. Impedance
2. Wavelet
3. Travelling wave
4. Others

Under these subcategories, the discussed problems, pros and cons, accuracy, required terminal data (one, two and multi-terminals) are analyzed. The accuracy is calculated considering the simulated cases in each respective study. Additionally, line configuration (double-circuit configuration and series-compensated line) associated studies are summarized. Additional specific problems such as system configuration, optimal PMU placement, and distributed generations associated with each study are briefed.

The other technologies used for locating the power system faults are not part of the scope of this study. This includes other time synchronization techniques [5]–[7] such as internet based

or wide-area synchronization. Traditional fault locator with time synchronization device such as an intelligent electronic device (IED) [8] are also not covered in this study.

Reference [9] explores the published papers regarding fault location utilizing synchronized measurements. However, it covers a wide range of synchronization techniques. Furthermore, the research is non-exhaustive to all available publications in the subject of for fault location. Aminifar et al. [10] presented a survey to the synchrophasor articles published in specific journals where different uses of the synchrophasor are categorized and briefed. However, the survey has a limited scope in terms of the journals and databases covered. Reference [11] introduced a review on the fault location techniques that are associated with distribution system, namely impedance, knowledge-based, and travelling wave techniques. Additionally, it highlighted the research opportunities of fault location in distribution network. However, it does not address critical evolving subjects in details such as the PMU use for the fault location.

This research is an integration to the previous efforts and covers fault location problem using PMUs in both transmission and distribution networks.

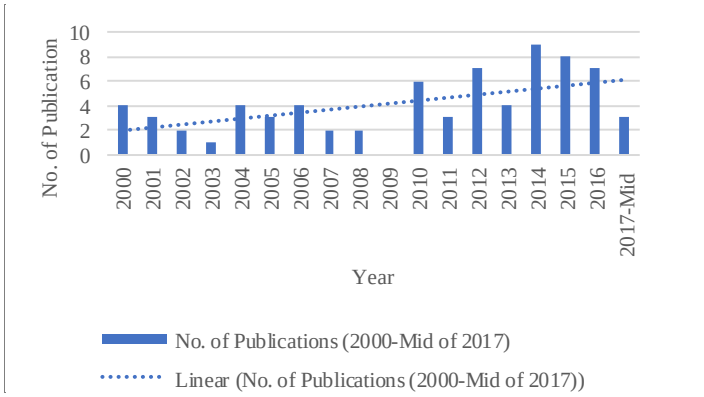

Figure 2-1: Number of publications per year (2000-Mid of 2017)

Measurement units represent a cross element to modernizing the power grid. They are enablers for system continuous monitoring, control, protection, optimized operation, and failure production, etc.

Figure 2-1 shows the number of papers published per year since 2000. An increasing chronological trend is demonstrated in the figure, which reflects the realization of this subject importance by the researches and industries. Figure 2-2 (a) illustrates that the majority (53%) of papers have been published in journals which further proves the importance of this subject. Only 14% out of the total publications discuss the problem of PMUs for fault location in distribution network as shown in Figure 2-2 (b).

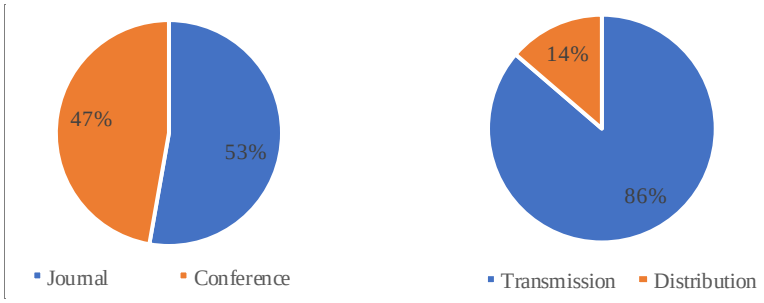

(a) Journal vs. Conference **(b) Transmission vs. Distribution**

Figure 2-2: Percentage of publications distribution (2000-Mid of 2017)

2.2 PMUs for Fault Location in Transmission Networks

The majority of PMU-based fault location techniques have been developed for transmission. Impedance principle-based technique accounts for 75% of the total publications, see Figure 2-3. This technique depends on the fundamental voltage and current phasors. Fault location algorithms based on wavelet, travelling wave phenomenon and others have also been developed.

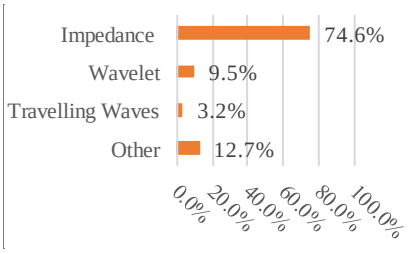

Figure 2-3: Percentage of publications based on technique for transmission system

The accessibility of obtaining the system conditions decides if the fault location algorithms should be one, two, or multiterminal. Two terminals-based technique is the most common (52% as per Figure 2-4) which is proven reliable and robust under different conditions.

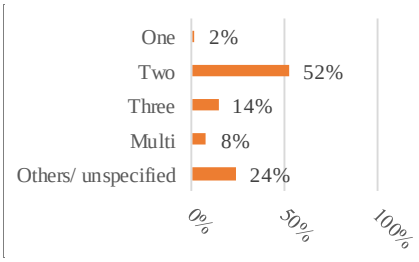

Figure 2-4: Percentage of publication distribution based on required terminal data (one, two, three and multi-terminals)

The accuracy of the proposed methods in the publications has been evaluated, considering the studied system. The fault location accuracy takes into account different additional specific subjects, including the following:

1. One, two, three and multiterminal techniques
2. Double-circuit configuration
3. Series-compensated line
4. Transpose, un-transpose and mesh
5. Extra high voltage network
6. Optimal PMU placement

7. Voltage measurement
8. Arcing faults
9. Inhomogeneous lines
10. Dynamic conditions
11. Online parameter calculation
12. Realistic examples

The rest of this section digests the above subjects under the four technique-based subcategories and cites the relevant sources.

2.2.1 Impedance-based Methods

Most of efforts devoted in developing PMU-based fault location in transmission networks are in impedance-based technique. This technique measures fundamental voltage and current signals in phasor form at one, two, or multiterminal of the line and uses mathematical model to locate the fault. Due to the importance of the impedance-based technique and the intense efforts spared for this subject, it is discussed in the following sub-sections.

A. One, Two, Three and Multiterminal Techniques

The majority of PMU-based fault location techniques are based on two terminals and multiterminal system conditions measurements as per Figure 2-4. One-terminal methods utilize one-terminal voltage and current phasors, therefore the accuracy of fault location is adversely impacted by the fault resistance and the other terminal impedance [12]–[14].

Two terminals algorithms have been introduced to enhance the fault location accuracy [15]–[17]. PMU-based two terminals fault location algorithms have been proposed recently in [18]–[20]. Reference [21] introduced an algorithm that is based on multiple fault current readings.

Jiang et al. in [22] discussed a technique that includes fault observability and distributed parameter line model. The technique avoids uncertainties in fault inception angle and fault path resistance. Both [23] and [24] are for transposed and un-transposed lines. The presented method in [24] is independent of the nature of fault and loading conditions. Unlike [24], it is a disadvantage for Reference [25] to use different formulas for different fault types. Analysis of the PMU errors impact on the accuracy of fault location was studied by Dehghanian and Kezunovic in [26]. Online parameters calculation is presented in [27] for both symmetrical and asymmetrical overhead lines using an adaptive simplified approach [28]. Temporary (or arcing) fault recognition was studied in [29] and [30]. The methods can identify the permanent and transient faults for short transmission lines. PMU-based fault location under dynamic state was investigated by [31]–[33]. Time span effects was considered by [31] which is independent of fault types, [32] is for interconnected networks and [33] used a dynamic variable and a time-changing angular frequency. Inhomogeneous lines fault location was analyzed in [34], [35].

The two terminals-based fault location methods have been developed using different sets of system condition signals obtained from PMUs. The methods could be based on the three-phase signals of either current, voltage or both at the two ends. The latter is extended to include using the two ends voltage signals and only one end current signal or vice versa. The summary of the aforementioned two terminals-based papers, including the pros and cons and accuracy, are shown in Table 2-1.

With the advancement of modern electrical networks, the system configurations become more complicated. The complication lies in the multiterminal configuration that is formed for different reasons. In some cases, it is more economical to provide power supply to a certain

load with a tapped line. This could also be a temporary solution for a temporary load or a growing load until the growth justifies building a substation. The fault location in multiterminal lines becomes a challenge due to the possibility of different sources to contribute to the fault. It is assumed that no measurement exists at the tap points. Subsequently, there is a need for three and multiterminal techniques. Some fault location techniques for three-terminal circuits have been offered [35]–[46]. Additionally, there is few fault location algorithms for multiterminal lines due to the problem complexity [47]–[50]. A new multiterminal fault location technique was presented in [48]. The authors applied two terminals fault location method to N-terminal transmission lines where N is greater than three. Then, a fault locator (fault section selector) was materialized. [46] and [48] introduced approaches for three and multiterminal lines, respectively, that uses two terminals techniques. Line parameter are calculated online in [45] and [49]. A new algorithm for lines with tapped legs proposed by [39] and [40]. The latter did not require the model of the tapped leg. The algorithm in [44] introduced single phase to ground fault problem with no simplifying assumptions or limits to the fault resistance. Reference [47] avoided source impedances using a two-stage un-iterative technique. PMU-based fault location under dynamic state was investigated by [38].

Further discussions of the three and terminal techniques are presented in Table 2-1. This includes pros, cons and accuracy of each study.

B. One and Two-Circuit Lines

Due to the challenges associated with the transmission right-of-way acquisition, numerous double-circuit transmission lines have been installed in power systems. Therefore, fault location techniques should take into consideration this type of installation. The majority and

most common fault location techniques in the previous decades are for single-circuit line fault location [16], [51]–[54]. Double-circuit lines fault location techniques have been developed in [12]–[14], [55]–[63]. References [64] and [65] presented a technique for double-circuit lines that utilizes current readings from one or more branches. The latter did not require measurement from the same faulted section. The charging current was accounted for in [66] which is custom-made for extra high voltage (EHV).

C. Series-Compensated Lines

Series compensation serves to increase power transfer, improve system stability, and regulate voltage. A series compensation can be categorized into fixed, thyristor-controlled, and gate turn-off thyristor based devices. Series capacitor, thyristor-controlled series capacitor and static synchronous series compensator are examples of the three categories, respectively. Non-linearity feature associated with the series compensation will introduce challenges in calculating the compensation voltage. Any inaccuracy of the series capacitor voltage will lead to inaccuracy of fault current and subsequently in the fault location. To overcome these problems, PMU-based schemes have been introduced. References [18] and [19] introduced an approach that uses pure fault resistance in lieu of impedance and [67] can be applied to series flexible alternative current system (FACTS) devices. The approach proposed by Apostolopoulos and Korres in [68] did not utilize the model of the series compensation and hence eliminated its associated errors. The missing voltage signals can be calculated using the method in [69] for EHV.

The pros, cons and accuracy of series-compensated lines related papers discussed above are highlighted in Table 2-1.

D. Other Specific Subjects

Optimal placement of PMU for fault observability are presented in References [70] and [71]. Real networks simulation was considered in [35]–[37], [72] for Taiwan, [41]–[43] for Saudi Arabiya and [32] for Egypt. Voltage measurement based methods were also discussed to eliminate the inherent error associated with the current transformer (CT). Brahma in [73] presented a new simplified approach that identifies the faulted section and locate the fault. Reference [74] required both synchronized and unsynchronized positive-sequence, [75] applied superposition theorem, Venugopal and Tiwari in [76] consider the variation in source and load impedances, [50] was for transposed and un-transposed, and [77] targeted large networks.

Table 2-1 summarizes the pros, cons and accuracy of the papers discussed above.

Table 2-1: Summary of problems, pros, cons and accuracy of the surveyed papers under impedance-base technique for transmission

Ref	Proposal	Pros/(cons)	Accuracy
[18], [19]	Introduced a new powerful fault location algorithm for series-compensated lines.	- (Pure fault resistance in lieu of impedance). - (Known fault type). - (Using series capacitors for line compensation leads major problems in the fault location processes).	99.9%

Ref	Proposal	Pros/(cons)	Accuracy
[21]	Introduced a novel algorithm that is based on multiple fault current readings.	- Readings can be obtained from other un-faulted lines.	99.8%
[22]	Discussed a technique that includes fault observability and distributed parameter line model.	- Avoids uncertainties in fault inception angle and fault path resistance.	97.8%
[23]	Provided a non-iterative wide-area approach for un-transposed and meshed networks.	- Requires limited readings.	99.0%
[24]	Proposed an adaptive fault detection, location and protection scheme for both transposed and un-transposed parallel transmission lines.	- Independent of the nature of fault and load flows.	99.7%
[25]	Discussed different formulas that use both voltage and current signals.	- (Different formulas for different fault types).	99.6%
[26]	Analyzed the PMU errors impact of hardware limitation on the accuracy of fault location.	- (Does not provide a solution to overcome the impacts).	97.0%
[27]	Offered a flexible numerical approach for overhead lines faults	- Does not require prior knowledge to the line parameters.	Note 1

Ref	Proposal	Pros/(cons)	Accuracy
	including both symmetrical and asymmetrical.		
[28]	Provided a new adaptive algorithm with online parameter calculation for single, parallel and teed lines.	- Novel and simplified approach.	97.8%
[29]	Proposed a new numerical method that includes arcing faults recognition.	- Able to identify if the fault permanent or transient. - (Applicable to short transmission line).	Note 1
[30]	Analyzed a new numerical method for single LG faults in short overhead lines.	- Considers arcing and tower footing resistance.	Note 1
[31]	Presented algorithms for a power system under dynamic conditions that is extended from conventional fault location method.	- Independent of fault types.	98.7%
[32]	Discussed a technique for interconnected networks.	- Actual Egyptian power network was used for simulation.	99.8%
[33]	Proposed a method that considers dynamic conditions impacts on the line parameters using a dynamic	- (Additional computation is required).	99.8%

Ref	Proposal	Pros/(cons)	Accuracy
	variable and time-changing angular frequency.		
[34]	Offered an approach for combined overhead and underground lines.	- Detects faults in underground section of the line.	98.6%
[35], [36], [37]	Proposed a three-terminal algorithm for multi-section inhomogeneous lines, combining overhead and underground power circuits.	- Actual field test has been achieved in Taiwan power system.	98.1%
[38]	Provided algorithms for a power system under dynamic conditions such as power oscillation.	- Considers time span effects.	98.7%
[39]	Presented a novel faulted section discrimination index that considers the tapped lines.	- Considers the tapped lines.	99.7%
[40]	Proposed a new algorithm for lines with tapped legs.	- Does not require the tapped leg model.	99.4%
[41], [42], [43]	Developed and test adaptive technique for the interconnected networks.	- Actual system simulation for Electricity Company-Eastern Operating Area network of Saudi Arabiya.	99.7%

Ref	Proposal	Pros/(cons)	Accuracy
[44]	Discussed an approach for single phase to ground.	- No simplifying assumptions. - No limits fault resistance magnitude.	99.9%
[45]	Provided a fully adaptive technique for three-terminal lines.	- Does not require data form the electric utility.	97.9%
[46]	Presented a new approach for three-terminal lines using two terminals data.	- Under different fault and pre-fault conditions.	99.5%
[47]	Presented a two-stage un-iterative technique.	- Avoids using the source impedances.	99.9%
[48]	Introduced a universal approach for multiterminal lines that uses two- terminal techniques for several terminals lines.	- Applies to arbitrary configurations including power source behind each terminal.	99.0%
[49]	Described a new iterative scheme for single multiterminal lines.	- Online calculation to the system parameters.	99.6%
[50]	Proposed a method that utilizes voltage measurements to eliminate the inherent error associated with the CT.	- Applicable to transposed and un-transposed lines.	97.2%
[64]	Proposed a new adaptive algorithm for double-circuit lines.	- Applies to double-circuit line.	99.6%

Ref	Proposal	Pros/(cons)	Accuracy
[65]	Provided a novel technique for double-circuit lines that utilizes current readings from one or more branches.	- Does not require fault section measurements.	99.5%
[66]	Provided a new modal components-based algorithm for EHV double-circuit lines.	- Compensates charging current effect.	Note 1
[67]	Proposed a new series-compensated lines that can be applied to series FACTS devices.	- Does not require prior knowledge to the system conditions.	99.5%
[68]	Offered a method for series-compensated double-circuit lines.	- Does not utilize the model of the series compensation and hence eliminate its associated errors.	96.7%
[69]	Proposed a method for EHV series-compensated lines.	- Able to calculate the missing voltage signals.	Note 1
[70]	Offered a novel method that includes faulted section identification.	- Uses limited coverage of PMUs.	Note 1
[71]	Applied an approach that includes system observability for both pre- and post-fault.	- Does not necessitate complete system observability.	Note 1

Ref	Proposal	Pros/(cons)	Accuracy
[72]	Developed a two-step method that combines both fault location algorithm and faulted line identification.	- Uses realistic example for simulation form Taiwan Power Company system.	95.5%
[73]	Provided a new simple approach that identifies the faulted section and locate the fault.	- Avoids the CT errors.	97.0%
[74]	Developed a novel wide-area approach that requires both synchronized and unsynchronized positive-sequence voltage measurements.	- Avoids CT saturation and zero-sequence parameters.	99.3%
[75]	Analyzed all possible fault points using voltage data and applying superposition theorem.	- Uses simplified equations.	98.0%
[76]	Introduced a novel method that considers the variation in source and load impedances.	- Less dependent on CT.	98.2%
[77]	Developed a universal method for large networks that utilizes voltage measurements.	- (May fail for high impedance faults).	99.0%

Ref	Proposal	Pros/(cons)	Accuracy
[78]	Discussed a scheme for overhead line that uses superposed positive-sequence voltage and current signals.	- (Lack of novelty as the work was already considered in [28]).	99.6%

Note 1: Either unidentified, undetailed or associated with low accuracy

2.2.2 Wavelet

Wavelet is a mathematical model used for digital signal processing with similar principles to Fourier analysis. It is suitable for analysis of short-term and transient signals that commonly exist in power networks. The technique can extract valuable data from voltage and current measurements. The model has a unique time-frequency property so it can be used to locate faults.

A total of six sources are found under wavelet-based techniques as per Table 2-2. References [79] and [80] presented a new adaptive technique for EHV and ultra-high voltage (UHV) transmission lines. This eliminates the system noise and measurement errors. Development of fault detection and location technique considering both permanent and arcing faults was presented in two papers ([81] and [82]). [83] included different fault types and faulted section identification. Lee et al. in [84] introduced a new numerical method that is divided into short and long lines with and without shunt capacitance, respectively. In general, the problems studied under this category is similar to the problems investigated under impedance-based techniques.

The average accuracy of wavelet-based fault location is calculated to be 99.7% based on the tabulated publications. This accuracy is superior to the average accuracy of impedance-based method for transmission, which is 93.5%.

Table 2-2: Summary of problems, pros, cons and accuracy of the surveyed papers under wavelet-base technique for transmission

Ref	Proposal	Pros/(cons)	Accuracy
[79], [80]	Developed a new adaptive technique for EHV and UHV transmission line.	- Eliminates system noise and measurement errors.	99.9%
[81], [82]	Developed fault detection and location technique considering arcing fault.	- Applicable to both arcing and permanent faults.	99.6%
[83]	Presented a novel technique for different fault types.	- Includes faulted section identification.	Note 1
[84]	Provided a new numerical method that is divided into short and long lines without and with shunt capacitance, respectively.	- Relatively simple.	99.6%

Note 1: Either unidentified, undetailed or associated with low accuracy

2.2.3 Travelling Waves

Travelling wave is used to capture the travelling time of the signal along the monitored lines between the fault point and the PMU. This technique is mainly applicable for long transmission lines in which the reading could be obtained from one or two terminals. This

method is less influenced by system conditions, fault types and resistance, etc. Two PMU-based publications for fault location using travelling waves are found in [85], [86]. The first was for interconnected power systems and the latter represented a high-level review for different techniques as summarized in Table 2-3.

Travelling waves-based techniques using PMUs for fault location offer an acceptable accuracy. To get the full benefits out of these techniques, a high-speed communication medium is required such as fiber optic cables. The accuracy of this type is highly affected by noise.

Table 2-3: Summary of problems, pros, cons and accuracy of the surveyed papers under travelling waves base technique for transmission

Ref	Proposal	Pros/(cons)
[85]	Introduced an approach for interconnected power systems.	- Works with very few PMUs.
[86]	Reviewed different techniques.	- (High-level).

2.2.4 Others

An intelligent strategy and Particle Swarm Optimization were presented in [87] and [88]. The latter considered limited number of PMU installation and hence limited measurements. It simulated a realistic model for West Texas, United States. These two approaches are the only publications that employed intelligent-based algorithms for fault location using PMUs.

Reference [89] introduced a system-wide method for transmission network using the oscillation propagation phenomena of electromechanical waves. Double-circuit three-terminal lines that includes both transposed and un-transposed lines were established in [90].

Symmetrical and unsymmetrical considerations were discussed in [91], whereas adaptive technique was presented in [92]. [93] demonstrated high-speed synchrophasor data that is not impacted by fault resistance, inhomogeneous voltage angles and mutual coupling. Zheng and Pang in [94] integrated PMUs, supervisory control and data acquisition (SCADA), and other intelligent electronic devices to improve the effectiveness. Table 2-4 summarizes pros, cons, and accuracy of the aforementioned discussed papers.

Table 2-4: Summary of problems, pros, cons and accuracy of the surveyed papers under others for transmission

Ref	Proposal	Pros/(cons)	Accuracy
[87]	Introduced an intelligent algorithm.	- With higher fault detection speed.	Note 1
[88]	Discussed a method that considers limited number of PMU installation and hence limited measurements.	- Simulated actual system for West Texas.	92.0%
[89]	Introduced a novel system-wide method for transmission network using the oscillation propagation phenomena of electromechanical waves.	- Measurements from sparsely located PMUs.	98.8%
[90]	Established new approach for double-circuit three-terminal lines	- Able to distinguish between internal and external faults.	Note 1

	that includes both transposed and un-transposed lines.		
[91]	Presented a new approach for series-compensated lines for symmetrical and unsymmetrical.	- Automotive line parameters calculation.	98.9%
[92]	Developed an integrated adaptive PMU-based fault location and a computer network routing algorithm.	- Results in minimal signals delay.	Note 1
[93]	Demonstrated high-speed synchrophasor data.	- Not affected by fault resistance, inhomogeneous voltage angles and mutual coupling.	97.9%
[94]	Integrated PMUs, SCADA and other intelligent electronic devices.	- The integration improved the effectiveness.	96.3%

Note 1: Either unidentified, undetailed or associated with low accuracy

Figure 2-5 summarizes the discussed topics and categories of PMU-based fault location for transmission. It shows that researchers are more interested in the works associated with impedance-based, two terminals, series-compensated, voltage measurement, dynamic conditions, online parameter calculation and realistic examples. Little efforts have been devoted for travelling wave, one-terminal, and inhomogeneous lines. These subjects should receiver more attention, especially for inhomogeneous lines as there is a considerable quantity of inhomogeneous lines exist in the electrical system network.

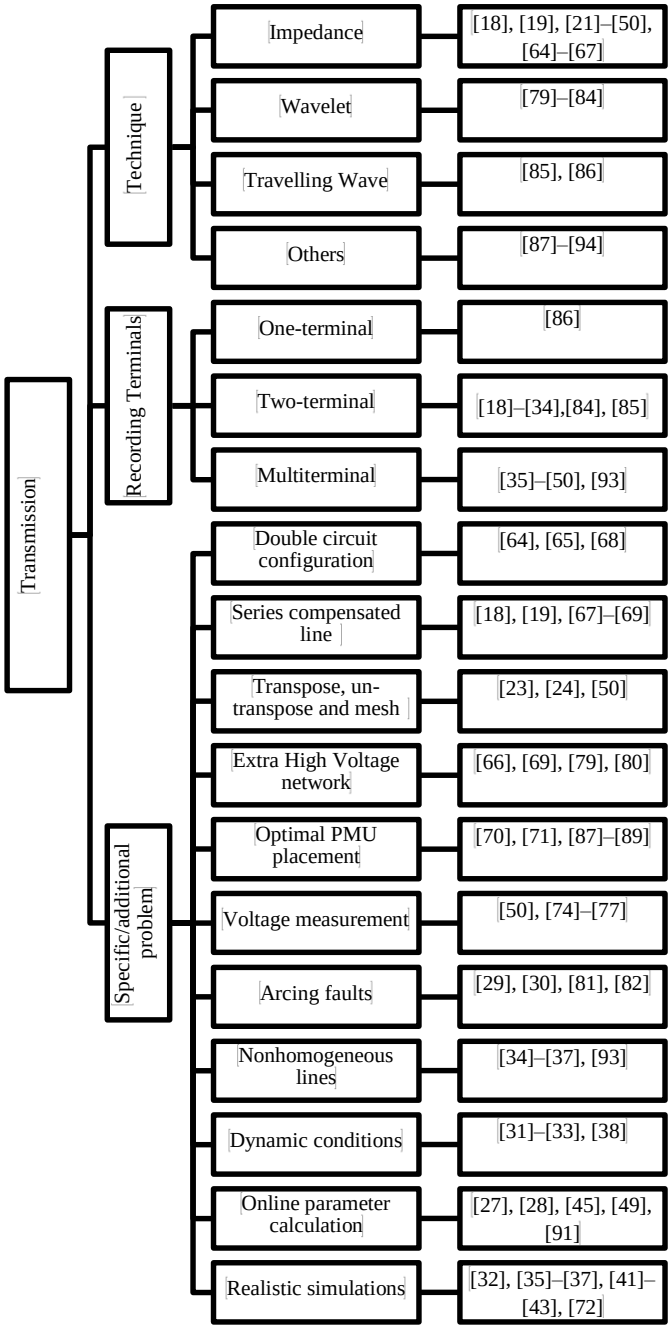

Figure 2-5: Simplified hierarchy for the techniques, recording terminals and specific problems under transmission

2.3 PMUs for Fault Location in Distribution Networks

The majority of PMU-based fault location techniques have been developed for transmission. The available work associated with the fault location application of PMUs at distribution grids is very limited. A total of only 10 out 73 publications has been developed for distribution.

Fault location in distribution networks has the same if not more critical comparing to transmission due to the following reasons:

1. DLs in most cases are installed underground in residential and industrial cases for different justification. The aerial could be risky to the people and effect the city scene. Underground installation usually crosses roads and passes under third parties' territories. If aerial circuits require vehicle patrolling, underground cables will mandate feet patrolling and inspection.
2. Distribution downed live conductors is a safety risk to the people.
3. Transmission line are designed with acceptable redundancy to tolerate any planned and forced outages. Therefore, the faults could cause line outages but not necessarily power interruption to the customers. Unlike transmission, most of distribution circuits are designed to be radial type.
4. Distribution system faults account for more than 80% of customer interruptions [3].

The above four considerations justify the innovation and creation for swift and accurate fault location in distribution networks.

Fault location methods in distribution network could be organized into the same four main categories as transmission. The four methods are detailed in the proceeding sections. Figure 2-6 shows the number publication based on technique for distribution system. A total of five

publications have been developed using impedance-based method, two wavelets, one travelling wave, and two under “others”.

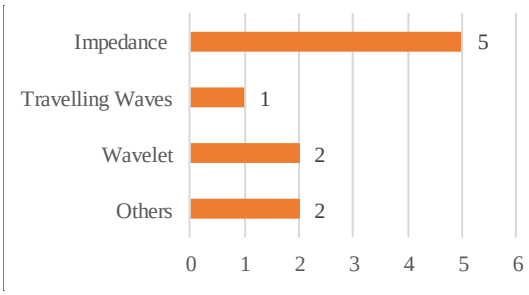

Figure 2-6: Number of publication distribution based on technique for distribution system

2.3.1 Impedance-based Methods

In general, available work associated with the impedance-based fault location application of PMUs at distribution grid is very limited. Paper [95] presented a method that works for different networks including active and passive, radial and looped with ranging precision in order of magnitude of 1%. A new PMU-based method was introduced in [96] to locate faults in distribution network and the method was proven via simulations using MATLAB/Simulink for different types of faults. In Reference [97], an algorithm for optimal PMU placement was validated for a 7-bus test circuit in addition to IEEE 14 and 30 buses networks. The optimal PMU placement was performed to identify the fault location in both ring and radial type distribution systems, which was tested using 11-bus radial, and 14-bus ring networks. Patynowski et al. in [98] discussed a new approach that collects the data from different sources for high impedance grounded or ungrounded lines. A new algorithm for high impedance fault (HIF) was introduced in [99] by Kargar and Zanjani. This type of faults is difficult to detect by over current protection relays because of low fault current. The algorithm is sensitive to any change in current phasor.

Apart of the aforementioned five publications [95]–[99] tabulated in Table 2-5, there is no study that explores the deployment of PMU technology in distribution network to estimate fault location using an impedance-based technique. It is noticed from Table 2-5 that the accuracy of the proposed impedance-based techniques is not significantly high. The maximum accuracy is 99.0 % recorded in References [95] and [96].

Table 2-5: Summary of problems, pros, cons and accuracy of the surveyed papers under impedance-base technique for distribution

Ref	Proposal	Pros/(cons)	Accuracy
[95]	Proposed a method that works for different networks including active and passive, radial and looped.	- Not limited to a certain PMU placement. - (The number of simulated studies is not clear in which the accuracy was decided to be within 1% of the line length).	99.0%
[96]	Offers a new algorithm for the multi-source system.	- Includes multi-source.	99.0%
[97]	Presented a technique for both radial and ring type feeders.	- Considers DGs.	98.0%
[98]	Discussed a new approach that collects the data from different sources for high impedance grounded or ungrounded lines.	- (An additional device namely phasor Data Concentrator device is required).	88.9%

Ref	Proposal	Pros/(cons)	Accuracy
[99]	Introduced a new algorithm for HIF.	- Considers the little change of current phasor.	Note 1

Note 1: Either unidentified, undetailed or associated with low accuracy

2.3.2 Wavelet

Two publications fall under this category, [100] and [101] as shown in Table 2-6. The first presents an adaptive scheme for aged power cable that overcomes cable changing parameters. The latter presents a technique that uses voltage information recorded at a certain set of buses, considering the optimal PMU placement. The technique is capable to measure the voltage sag magnitudes.

2.3.3 Travelling Waves

Only one paper [102] discussed the travelling wave-based technique for locating fault in distribution system using PMUs, see Table 2-6. It described an automated algorithm that also identified fault type. The method is applicable for active and passive network.

2.3.4 Others

Reference [103] presented a unique fault location technique on state estimation. It provided a real-time fault detection and location functionalities calculated form parallel PMU. The presented technique is applicable for both active and passive networks. The technique in [104] offers PMU optimal placement using Tabu search algorithm to improve the fault location accuracy. The summary of the two references is tabulated in Table 2-6.

Table 2-6: Summary of problems, pros, cons and accuracy of the surveyed papers under wavelet, travelling wave and others techniques for distribution

Ref	Proposal	Pros/(cons)
[100]	Proposed an adaptive scheme for aged power cable.	- Overcomes cable changing parameters. - It is associated with high accuracy (99.8%). - (Does not work for the fault of B-C).
[101]	Presented a technique that uses voltage information recorded at a certain set of buses.	- Able to measure the voltage sag magnitudes.
[102]	Described an automated algorithm that also identifies fault type.	- (Effect of non-coincident load variation is not clear).
[103]	Provided a real-time fault detection and location functionalities calculated form parallel PMU-based state estimators.	- Applicable for active and passive. - (Requires Knowledge of the network admittance matrix).
[104]	Offered PMU optimal placement using a Tabu Search Algorithm to improve the fault location accuracy.	- (Does not detail the fault location method).

Figure 2-7 presents the discussed topics and subcategories of PMU-based fault location for distribution along with their associated sources in hierarchy format. It shows that the majority of efforts have been devoted for topics associated with impedance-based, two terminals, and optimal PMU placement. Only a few interests are related to travelling wave and cable aging.

The latter is a critical and common problem for a number of utilities that should be paid adequate attention to avoid the cable replacement due to reliability (mean time to repair) issue.

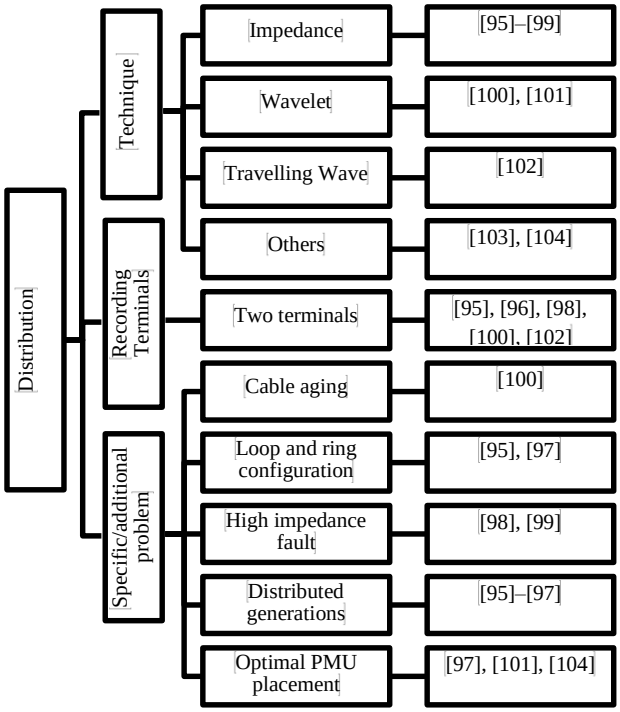

Figure 2-7: Simplified hierarchy for the techniques, recording terminals and specific problems under distribution

2.4 Outcomes and Recommendations

To reduce the interruption period associated with power system faults, prompt and accurate fault location techniques are required. This needs a comprehensive assessment for all available works in the subject of PMU-based fault location. Based on that, the associated added-value efforts have been surveyed, identifying their appropriate applications, pros, cons and accuracy. The outcomes of this analysis along with associated recommendations are as follows:

1. Investigate further actual systems simulations, experiments and field piloting. This is to increase the utilities confidence of deploying PMUs in wide scales.
2. Study the aged and inhomogeneous lines fault locations as they are critical and common problems for a number of utilities. This is to avoid cable replacement due to reliability (mean time to repair) issue.
3. Continue using the two- and multiterminal-based techniques are they are proven reliable and robust under different conditions.
4. Consider both impedance and wavelet-based techniques for distribution as the work is very limited and the they should provide the same accuracy level as in transmission.
5. Explored more wavelet-base techniques for transmission due to its improved accuracy which is superior to the recorded average impedance-based. The investigation in this area is more promising which may achieve super accuracy results comparing to the others as the accuracy matters the most.
6. Research for PMU-based fault location at the generation side. Although the distance is not that long from the generation unit to the substation, the expeditious and accurate fault location is required. This is to put back into surface the affected unit and avoid unnecessary additional excavation which might damage other cables in the process.
7. Consider PMU-based fault location at the load side. Prompt and accurate fault location for loads is important, especially when the cables are in critical process area where hand digging is the only permitted option. This is associated with very high cost and execution time. The lines supplying offshore hydrocarbon facilities are also very critical and require more cost and time for power restoration.

8. Study renewable integration with the conventional grid which has not been paid adequate attention and this type of systems are increasing.

2.5 Conclusion

This chapter presents an exhaustive and scrutinized survey on PMU application for fault location and its associated publications. The publications trend has been increasing substantially since 2000. In general, most of studies have been developed for transmission. The available work at distribution grid is very limited. Additionally, there is a lack of publications on the other electrical energy chain, mainly generation, and end-customer sides. Accurate fault location for loads is important, especially when the cables are in critical process area or for offshore hydrocarbon facilities. Furthermore, renewable integration with the conventional grid has not been paid adequate attention. Subsequently, these areas along with others are opportunities for researchers to explore and develop novel approaches, addressing their respective challenges.

CHAPTER 3

IMPROVED LOAD FLOW IN DISTRIBUTION NETWORKS

This chapter proposes two novel approaches for determining the load flow in distribution systems. The first approach is an enhancement to backward\forward Sweep (BFS). The second offers a new method namely Zig Zag-based load flow. Both approaches are applicable for extended radial distribution systems where multiterminal lines exist. These will result in reduction of the number of iterations while maintaining the required load flow accuracy. For this purpose, nine case studies are established to confirm the performance of the proposals. The study state simulation results reveal that the proposed approaches have excellent capabilities in calculating the load flow. Load flow is required for the proposed fault location models as they use the pre- and post- voltage and current values.

3.1 Introduction

Load flow analysis represents the first building block toward any power system related study. This includes energy forecast, voltage drop and stability analysis in its three parts; steady state, dynamic and transient. The latter requires load flow to calculate the initial conditions. The key feature of the distribution system is that the X/R ratio is relatively low. Additionally, the majority of distribution systems have the radial structure configuration. Hence, Newton

Raphson, Fast Decoupling and Gauss Seidel will show weakness in distribution network [105]. These techniques were created mainly for transmission systems where the X/R is more than 10.

BFS power flow, enhanced BFS and Zig Zag approaches are developed in this research to get accurate distribution load flow results. BFS is one of the robust techniques that is widely used in distribution network analysis for load flow in radial distribution systems [106]–[109]. The radial network is simple to construct, low capital cost and used in low voltage level. The radial configuration entails that there are no connected loops in the system and each node is linked to the source via one way. Loops might exit but separated via a normally open breaker. Distribution system, also, combines single, two and three-phase circuits, delta-connected and unbalanced loads that are considered challenging. It is the most economical power supply and has an acceptable reliability index to certain types of customers. The radial distribution configuration is widely used in sparsely populated areas and in the remote scattered hydrocarbon facilities.

Several resources discussed BFS and applied modifications for different purposes. Reference [110] adopted the linear proportion concept to calculate the bus voltages by identifying the real to imaginary ratio of the voltage. It updated the voltages by multiplying their real and imaginary parts with the corresponding ratios. Jia-jia and Jun-yong in [111] applied hybrid particle Swarm method to reconfigure distribution networks with distributed power generations. The authors used the node-layer incident matrix to find the load flow. BFS was, also, used to perform load flow analysis distribution network with distributed generators by Kaur and Singh in [112]. A power flow technique for unbalanced distribution radial network

was introduced in [113]. The proposed method considered the mutual coupling between the phases to obtain higher accuracy. Fast decoupled and BFS methods were compared in [114] for solving power flow for distribution network.

In this chapter, two different approaches are proposed for distribution system power flow analysis. The proposed methods are enhanced backward/ forward Sweep (EBFS) and Zig Zag-based load flow. Both approaches are applicable for extended radial system where multiterminal lines exist. Main idea behind these two methodology is to reduce the number of iterations while maintaining the required accuracy. In Section 3.2, the two proposed methods along with BFS are described. Nine case studies are established to confirm the performance of the proposals in Section 3.3. Finally, Section 3.4 concludes this chapter and summarizes its outcomes.

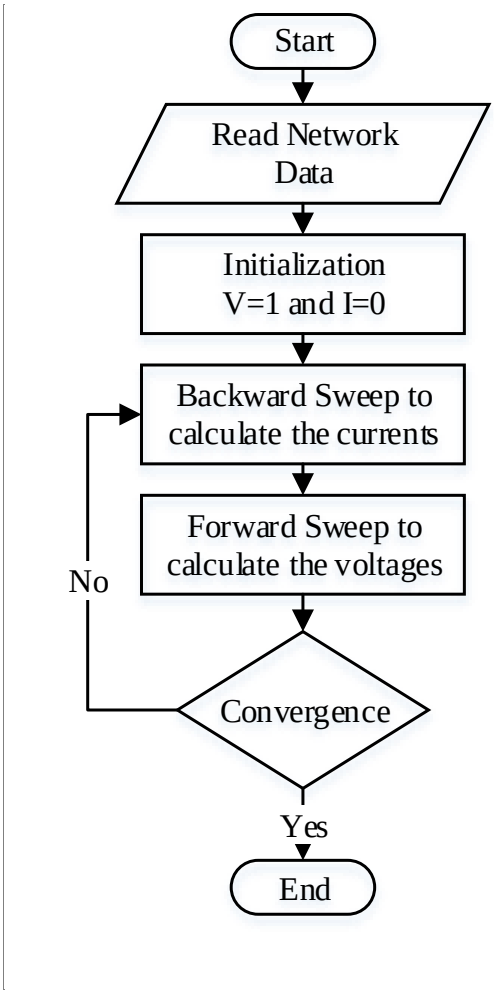

Figure 3-1: Flowchart of BFS

3.2 Load Flow Analysis

3.2.1 Backward/ Forward Sweep

Forward/backward Sweep load flow method is commonly applied to distribution networks. This is due to its effectiveness for radial and weak meshed systems.

FBS calculates, first, the currents across each branch, starting with the last layer in the system. Then, it moves backward to the branches connected to Swing bus which is usually bus no. 1. The currents are calculated using the following formula:

$$I_i = (\frac{S_i}{V_i})^* + \sum_{k=a,b,c,\dots etc} I_k \quad (3.1)$$

Where i is a specific branch in which the current will be calculated. The symbols a, b and c, etc. represent the branches connected to Branch i from the load side. The quantities S, V and I stand for complex power, voltage and current in per unit quantities, respectively.

Next, the method calculates the voltage across each bus in a forward manner. It starts with the Swing bus and covers all the other buses in the network. The calculation is performed using the voltage drop formula.

$$V_i = V_j - I_{ij} Z_{ij} \quad (3.2)$$

Where i is a specific bus that is under calculation. The symbol j is a bus with a former index ($j < i$) that is directly connected to i. I_{ij} and Z_{ij} are the current and impedance between buses i and j. Figure 3-1 shows the flowchart of the BFS and the calculation results are shown in Section 3.3.

3.2.2 Enhanced Backward/ Forward Sweep

The proposed enhanced backward/ forward Sweep (EBFS) based load flow provides additional improvement to the conventional BFS. The latter identifies the currents based on the initiations and then based on the calculated voltages. The proposed method updates the

currents within each voltage calculation step to accelerate the convergence by reducing the number of iterations.

The proposed method includes three components: Forward and backward sweeps in addition to intermediate currents update. In the backward sweep, power formula and nodal analysis are used to calculate the currents at each downstream branch moving toward the root (Swing Bus). In the forward sweep, Kirchhoff Current Law and Kirchhoff Voltage Law are utilized to identify the voltages across the upstream buses. It starts with the root, moving toward the tail (end-customer side). During this stage, the currents values will be updated to obtain more accurate voltages as the voltage calculation moves toward the load side.

To start the current update process, the present iteration currents should be availed by the following formula:

$$I_{ij}^{q} = \left(\frac{S_i}{V_i^{q-1}}\right)^{*} + \sum_{k=a,b,c,\dots etc} I_k^q \tag{3.3}$$

Where q reflects the iteration number.

The voltage across specific Bus i at Iteration q is provided by the below equation:

$$V_i^q = V_j^q - I_{ij}^q Z_{ij} \tag{3.4}$$

Then, the updated current ($I_i^{q\prime}$) will be calculated based on the below relation by including the latest corresponding voltage (V_i^q) value.

$$I_i^{q\prime} = \left(\frac{S_i}{V_i^q}\right)^{*} + \sum_{k=a,b,c,\dots etc} I_k^q \tag{3.5}$$

The voltage will be updated using the below equation which incorporates the updated current to get the updated voltage ($V_i^{q\prime}$).

$$V_i^{q\prime} = V_j^q - I_{ij}^{q\prime} Z_{ij} \tag{3.6}$$

The current update process will be performed for all buses except the slack bus where its value is controlled by the power source.

The iteration process terminates when the deviation between the previous iteration voltage and the current one is less than a specific tolerance value. Otherwise, the process will continue to repeat till the convergence takes place. Figure 3-2 illustrates the flowchart of the proposed EBFS and the calculation results are shown in Section 3.3.

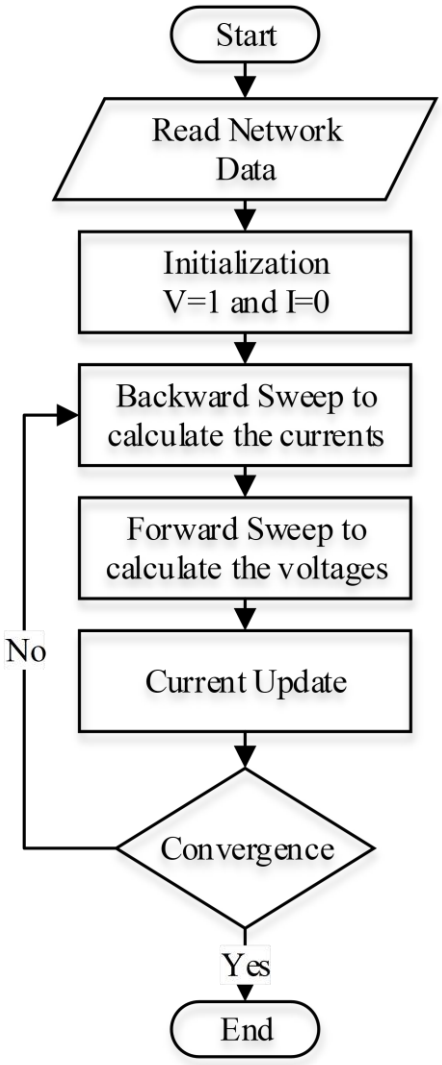

Figure 3-2: Flowchart of EBFS (Proposal 1)

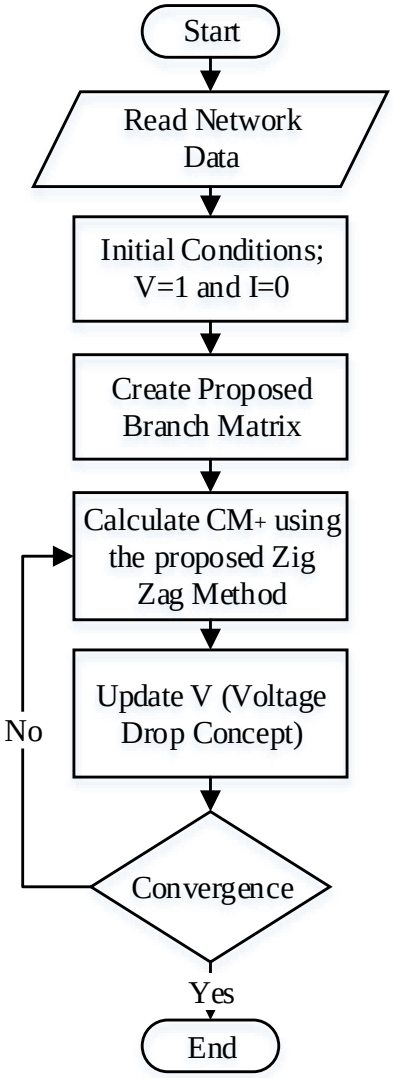

Figure 3-3: Flowchart of the Zig Zag method (Proposal 2)

3.2.3 Zig Zag-based Load Flow

The Zig Zag-based load flow method comprises the following steps:

1- Creating branch matrix (BM) where the number of rows reflects the number of branches and the number of columns represents the number of buses. The BM matrix for the 5-bus test circuit shown in Figure 3-4 is as follows:

$$BM = \begin{bmatrix} 1 & 1 & 1 & 1 & 0 \\ 0 & 0 & 1 & 0 & 1 \end{bmatrix} \tag{3.7}$$

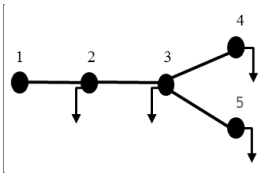

Figure 3-4: The 5-bus test circuit

2- A parameter called node current (NC) can is given as follows:

$$NC_i = \left[\frac{I_i}{K_i}\right] \tag{3.8}$$

Where I_i represents the load current of Bus i. The symbol K reflects the number of links connected to a specific Bus i. Multiplying NC_i with the corresponding elements in BM results in a new matrix called nodal current matrix (CM). For the 5-bus test circuit displayed in Figure 3-4, the CM matrix is given as follows:

$$CM = \begin{bmatrix} \frac{I_1}{K_1} & \frac{I_2}{K_2} & \frac{I_3}{K_3} & \frac{I_4}{K_4} & 0 \\ 0 & 0 & \frac{I_3}{K_3} & 0 & \frac{I_5}{K_5} \end{bmatrix} \tag{3.9}$$

3- The method will find the currents for the system branches in a Zig Zag manner and record them an updated matric denoted by CM_+ matrix. Each bus will have its own current tagged with the branch. The CM_+ matrix for the 5-bus test circuit presented in Figure 3-4 is formulated as follows:

$$CM_+ = \begin{bmatrix} I_{1+} & I_{2+} & I_{3+} & I_{4+} & 0 \\ 0 & 0 & I_{3+} & 0 & I_{5+} \end{bmatrix} \tag{3.1}$$

4- The voltage will be identified using the voltage drop concepts and will be calculated, starting from upstream through downstream.

The above steps will be repeated iteratively until the deviation between the load voltage and the previous voltage is below a specified tolerance for the process to converge. The main contribution of this method that it performs the calculation with the uses of matrices. Figure 3-4 presents the flowchart of the proposed Zig Zag method and the calculation results are shown in Section 3.3.

The Zig Zag method is used to confirm the steady state load flow for the fault location models. This is required as the proposed models use the pre- and post- voltage and current values.

3.3 Simulations and Results

Algorithms of the three methods (BFS, EBS and Zig Zag) have developed and tested using 5, 7, 11, 25, 28, 30, 33, 34, and 69 - bus distribution systems. The details of these systems line and bus data are tabulated in Appendix A. The simulation results are tabulated in below Table 3-1, Table 3-2 and Table 3-3.

Accuracy of the methods are identified based on the differences between last two iterations. Table 3-1 shows that the proposed EBFS and Zig Zag are superior in accuracy by 33% and 58%, respectively, compared to BFS technique.

Table 3-1: Deviation of the last two iterations

System	Conventional (BFS)	Proposal 1 (EBFS)	Proposed 2 (Zig Zag)
5	5.61E-06	4.64E-06	2.85E-06
7	2.69E-06	2.69E-06	2.69E-06
11	2.95E-06	2.95E-06	2.95E-06
25	7.75E-06	5.84E-06	4.10E-06
28	9.53E-06	7.80E-06	6.45E-06
30	9.35E-06	5.85E-06	2.13E-06
33	7.93E-06	4.89E-06	2.16E-07
34	9.23E-06	5.41E-06	3.63E-06
69	7.87E-06	1.95E-06	1.44E-06
Average	**6.99E-06**	**4.67E-06**	**2.94E-06**

The average iterations required by BFS to converge is approximately five times the iterations required by the proposed EBFS and Zig Zag as demonstrated in Table 3-2 (42 iterations compared to 10 for EBFS and 9 for Zig Zag). The number of iterations associated with each case study for the three techniques are presented in Table 3-2. For example, the results for the 5-bus test circuit will converge after seven iterations for the Zig Zag and will result in a difference between the last iteration and the one before of 2.85E-06. This shows the robustness and the effectiveness of the Zig Zag method.

Table 3-2: Required iterations to converge for the three methods

System	Conventional (BFS)	Proposal 1 (EBFS)	Proposed 2 (Zig Zag)
5	9	9	7
7	8	8	8
11	9	9	9
25	42	10	7
28	141	26	23
30	44	9	7
33	25	5	4
34	46	9	7
69	50	8	7
Average	**42**	**10**	**9**

In terms of elapsed time, though EBFS algorithm can provide comparatively outstanding results when compared to BFS, the time taken by EBFS is a little bit longer compared to BFS. An observation of Table 3-3 reveals that the time taken by the Zig Zag algorithm is in the same order of magnitude when compared to the BFS, and also the quality of the solution is better. As a result, a conclusion can be made that Zig Zag method is the best technique for the studied systems and results in considerably better solutions. There is a chance to achieve better convergence time from the two proposed techniques by further optimization to their respective MATLAB codes.

Table 3-3: Elapsed time taken by each method to converge

System	Conventional (BFS)	Proposal 1 (EBFS)	Proposed 2 (Zig Zag)
5	0.024248	0.024915	0.024681
7	0.020715	0.02723	0.031041
11	0.021658	0.029722	0.035335
25	0.027870	0.043076	0.034460
28	0.039134	0.067354	0.059562
30	0.029935	0.049992	0.034840
33	0.028292	0.050972	0.027398
34	0.038784	0.050095	0.032420
69	0.041999	0.170685	0.049108
Average	**0.030293**	**0.057116**	**0.036538**

The voltage profiles of the simulated systems 5, 7, 11, 25, 28, 30, 33, 34, and 69 - bus distribution systems are displayed in Figure 3-5 to Figure 3-13. The three methods are shown in each figure to compare the load flow results. The figures prove the effectiveness of the proposed methods as they have provided exactly the same results as obtained by BFS.

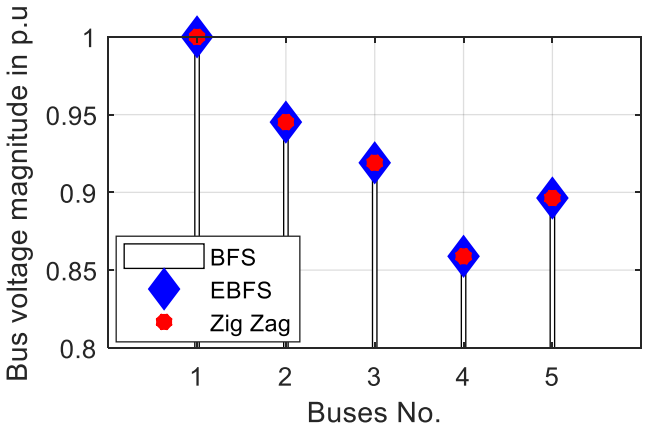

Figure 3-5: Voltage profile of IEEE 5 node radial distribution network using the conventional and proposed techniques

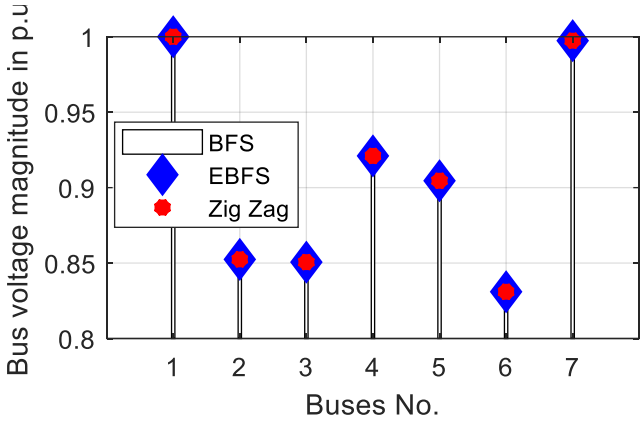

Figure 3-6: Voltage profile of IEEE 7 node radial distribution network using the conventional and proposed techniques

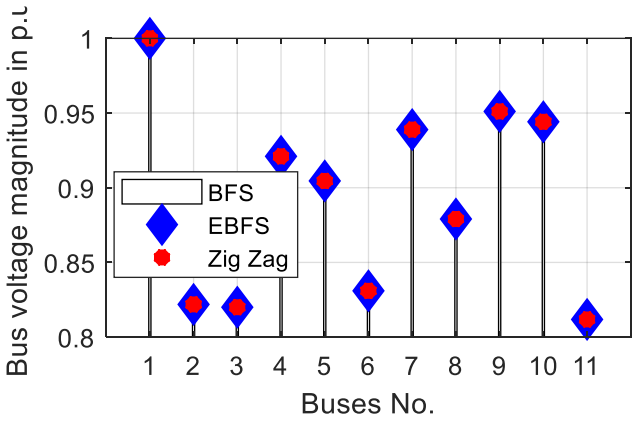

Figure 3-7: Voltage profile of IEEE 11 node radial distribution network using the conventional and proposed techniques

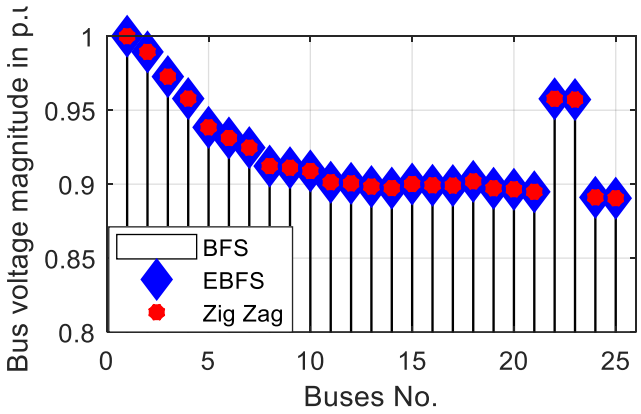

Figure 3-8: Voltage profile of IEEE 25 node radial distribution network using the conventional and proposed techniques

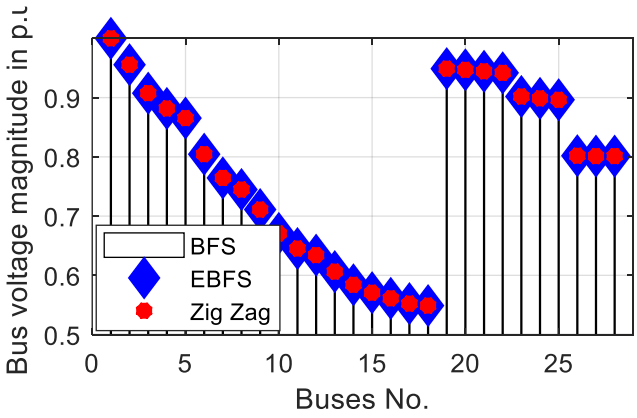

Figure 3-9: Voltage profile of IEEE 28 node radial distribution network using the conventional and proposed techniques

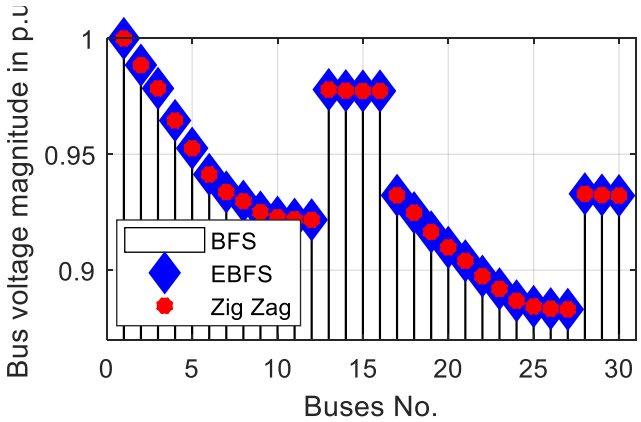

Figure 3-10: Voltage profile of IEEE 30 node radial distribution network using the conventional and proposed techniques

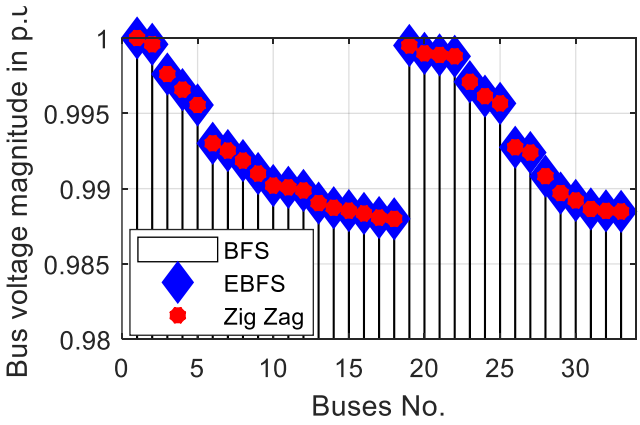

Figure 3-11: Voltage profile of IEEE 33 node radial distribution network using the conventional and proposed techniques

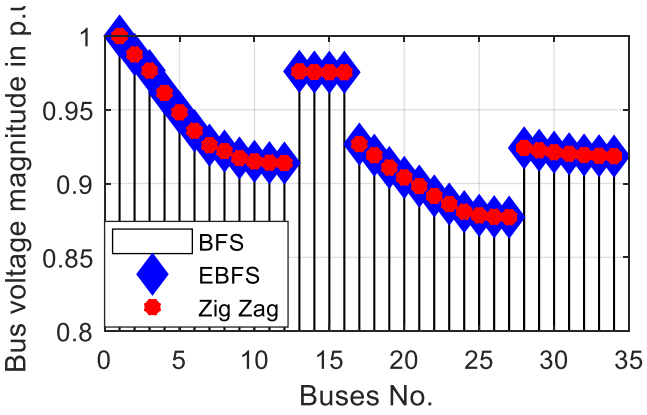

Figure 3-12: Voltage profile of IEEE 34 node radial distribution network using the conventional and proposed techniques

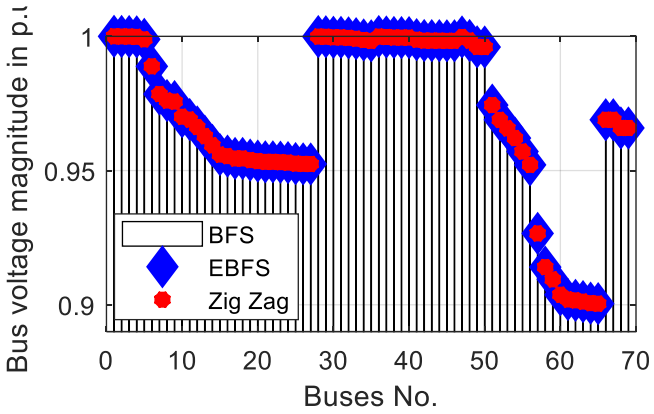

Figure 3-13: Voltage profile of IEEE 69 node radial distribution network using the conventional and proposed techniques

3.4 Conclusion

In this chapter, two novel load flow analysis for distribution networks are developed and compared against BFS. The approaches are EBFS and Zig Zag-based load flow analysis. Both approaches can be applied for extended radial system where multiterminal lines exist. A total of nine different cases are simulated to show the effectiveness of the proposed methods. The simulations models include 5, 7, 11, 25, 28, 30, 33, 34, and 69-bus IEEE distribution systems.

The numerical results demonstrate that these two methods are very robust and have excellent convergence characteristics. They will result in reduction of the number of iterations while maintaining the required load flow accuracy. It is concluded that Zig Zag is the best technique for the studied systems which results in considerably better solutions. There is a chance to achieve less convergence time from the two proposed techniques by further optimization to their respective MATLAB codes.

CHAPTER 4

OPTIMAL PLACEMENT OF PMUS IN DISTRIBUTION NETWORKS

This chapter presents optimal placement of PMUs for power distribution network observability. The placement problem is formulated to minimize the number of PMU installation while maintaining the full system monitoring and enhancing the redundancy. Single and multi-objective intelligent optimization techniques are used in 7, 11, and 14-bus distribution systems. The optimal placement conditions and criteria in distribution configuration are discussed. The one and dual optimization algorithms, namely Artificial Bee Colony (ABC) and Strength Pareto evolutionary algorithm (SPEA), are described, respectively. Then, the case studies and objective functions are established, considering both ABC and SPEA. Last but not least, conclusions and recommendations are stated at the end to recap the work efforts. The optimal placement for system conditions observability is necessary to locate faults in power networks. The system observability will provide the required pre- and post-fault input data to the fault location model.

4.1 Significant and Applications of Phasor Measurement Units

Phasor measurement units represent a cross element to modernizing the power grid. They are enablers for system continuous monitoring, control, protection, optimized operation, energy

efficiency, demand side management, forecasting, renewable integration, and embedded generators, etc. Additionally, the implementation of advance measurements will support transforming the existing gird to be smarter, providing the power control centres (PCCs) with enough information to optimally operate the system.

PMU is a mature technology not only to the academic sector but also to the industry. Nowadays, it represents a preferred solution to the custodies of power system networks. Other alternatives would provide less features than the ones available in the PMU. The PMUs are superior to the other technologies in terms of the frequency of samples and the time attached with the measurements.

This section presents a brief on the significant and applications of PMUs.

4.1.1 Significance of PMUs

PMU is considered to be a vital measurement device in future power networks with a capability of measuring electrical system conditions. It measures the magnitudes and phase angles of voltage and current waveforms at a certain bus, leveraging GPS and time stamp the measurements with extraordinary precision.

PMUs could be used in transmission and distribution electrical networks for several purposes including optimal power flow, fault detection, fault location, electrical system control and protection, and so on.

PMU is an advanced class of metering systems and recently considered for deployment by a number of worldwide utility entities

The sinusoidal signal can be replaced by a complex number called “phasor”. Assuming the following sinusoidal waveform:

$$y(t) = Y_m \cos(\omega t + \delta) \tag{4.1}$$

The signal can be represented by the below phasor:

$$Y = \frac{Y_m}{\sqrt{2}} e^{i\delta} \tag{4.2}$$

$$= \frac{Y_m}{\sqrt{2}} (\cos\delta + i \sin\delta) \tag{4.3}$$

It is observed from the above phasor equation that the angular frequency $\omega = 2\pi f$, which is in in radians per second, is not stated to be part of the formula. $\frac{Y_m}{\sqrt{2}}$ is the magnitude of the phasor representation in rms and $\delta = 2\pi f \tau$ is the phase angle. Note that f is the power system frequency and τ is the lagging time of the sinusoidal signal.

The aforementioned sinusoidal waveform and its phasor equivalent are shown in Figure 4-1.

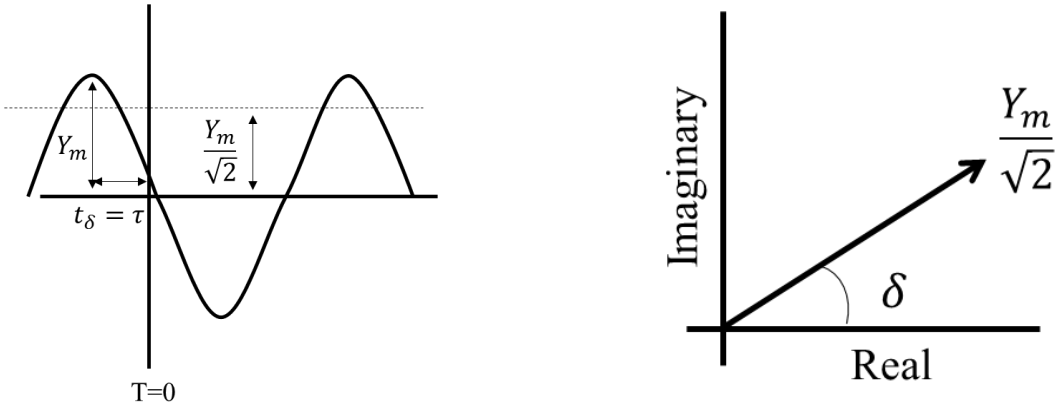

A) Sinusoidal waveform **B) Phasor equivalent**

Figure 4-1: Phasor equivalent of a sinusoidal waveform

Measurement of the phase angle is in a counterclockwise direction starting from the positive side x-axis. The clockwise measurement can also be considered; however, the phase angle of the waveform will be negative. All phasor quantities in the phasor equivalent diagram must have the same frequencies. This is due to the absence of the frequency in the phasor equivalent formula discussed above. Since the phasor equivalent is independent of time and frequency, the phasor representation is applicable only to the steady state condition. If there is any change in the system status in term of magnitude or frequency, the phasor equivalent will not be valid. Subsequently, new samples will be required and this is in line with what is offered by the PMU. The measurement device will record new samples every fraction of a second to update the phasor values.

4.1.2 PMU Applications

There is a wide range of applications for PMUs for different purposes such as enhancing power system reliability and stability. PMU related studies published in literature can be classified into ten categories itemized in Table 4-1.

Several PMUs have already been installed at numerous electrical systems of utilities industrial companies worldwide. The most important realized benefit of PMU is the precise synchronized samplings with the time stamp. This stamp is obtained from the GPS signals available all over the globe. One of the most important issues that need to be addressed in the emerging technology of PMUs is site selection. The economics is a major driver of the limiting the number of PMU in power system networks. The mass production will definitely drop the price in the future. Additionally, The PMU placement is limited by the availability of communication infrastructure which require a considerable investment which could be

even more than the PMU material and installation cost. The PMU placement problem is addressed in this chapter (Chapter 4).

Table 4-1: Classification of PMU related publications

Category	Description	References
1-	Overview, background, model and applications	[10], [115]–[125]
2-	Installation and integration issues	[126]–[129], [129]–[134]
3-	Planning	[135]
4-	Optimal placement	[136]–[150]
5-	State estimation	[151]–[156]
6-	Fault detection, location and classifications	[88], [99], [101], [136], [157]–[164]
7-	Transient, dynamic and steady state stability monitoring & its reliability, analysis and prediction	[165]–[188]
8-	System Protection	[189]–[199]
9-	Network Management	[116], [200]–[203]
10-	Line parameter identification	[204]–[218]

Recent PMUs can produce synchronous measurements and hence are more accurate compared to traditional management systems such as SCADA. Subsequently, PMUs improve the performance of state estimation significantly. PMU data are available to provide better inputs to contingency assessment and energy management system (EMS). Furthermore, tracking system angles to detect any potential of instabilities to take an advance action.

One of the major applications of PMU outputs is the detection, location and classification of power system faults. This application consists of three steps: First detect the faulted line and then find the fault location on this line and last to classify the fault type. This methodology makes use of local PMU outputs such as the synchronized voltage and current waveforms at two terminals of a DL.

4.2 Optimal Placement Problem in Distribution

PMU placement in distribution is more significant than the placement in transmission. This is due to the followings:

1- Distribution network is more complicated than transmission and consists of larger number of nodes. Subsequently, it is beneficial to reduce the number of PMU installation.

2- PMU cost in distribution plays an important role due to the relatively low investment required to construct the lines compared with the considerable amount of money to build transmission network. Therefore, the cost ratio of PMUs at distribution is more sensitive than transmission.

3- Communication infrastructure in transmission network is available in most of locations in which fiber optical wires run with the transmission lines. Therefore, measurement devices could be installed anywhere with no major infrastructure constraint compared with distribution. On the other hand, more than 70% of the distribution network is not supported by communication infrastructure. This will require additional constraint in the optimal location algorithm.

The above three justifications mandates studying the placement of PMUs in distribution.

The objective is to place the PMUs optimally in distribution using different optimization methods. ABC and Strength Pareto Evolutionary Algorithm (SPEA) which are, robust and reliable techniques, are implemented to find the optimal solutions. The used rules are presented in Figure 4-2 and further clarified in the following steps:

1- All buses surrounding a bus furnished with a PMU are observable.

2- String of buses connecting two terminals lines are observable if one of them is observable whether by calculation (indirect observation) or directly equipped with PMU.

3- Zero-Injection bus surrounded by observable buses is observable.

4- A node connected to an observable zero-injection bus is observable if all the other nodes connected to the zero-injection bus are observable.

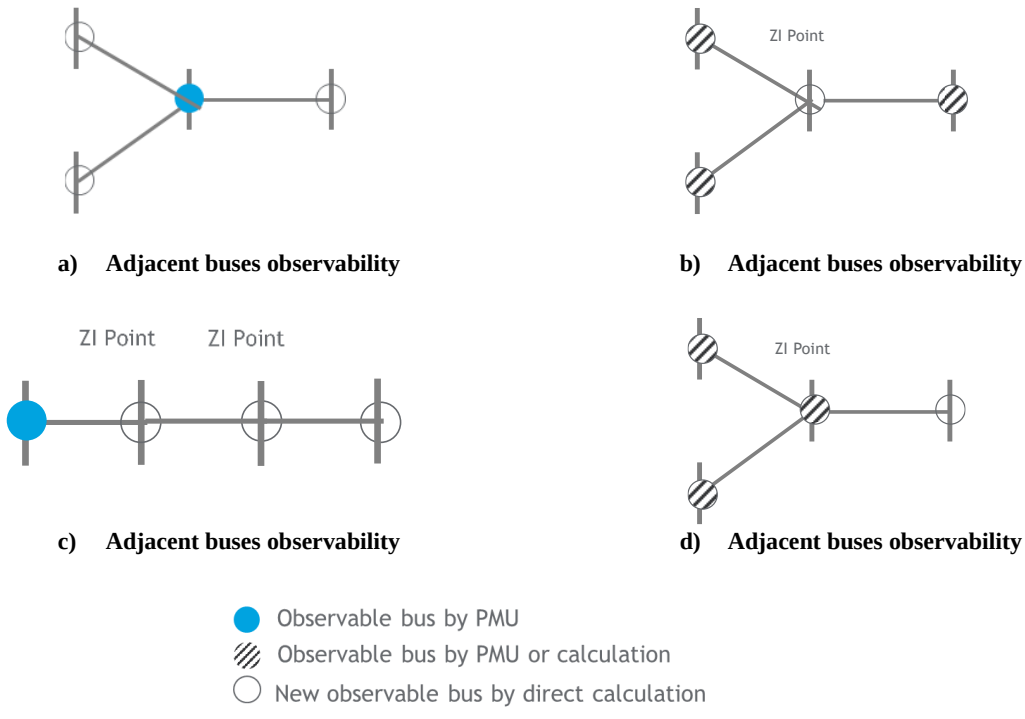

a) Adjacent buses observability **b) Adjacent buses observability**

c) Adjacent buses observability **d) Adjacent buses observability**

Figure 4-2: Rules of PMU placement in power distribution network

The building blocks of the optimal placement problem (OPP) can be categorized into a number of steps, considering the following:

Step 1 converts the bus admittance matrix into binary form using the below logic.

$$S_{j,k} = \begin{cases} 1, & if\ j\ is\ adjacent\ to\ k0 \\ 1, & if\ j = k \\ 0, & \text{Otherwise} \end{cases} \tag{4.4}$$

Step 2 puts the binary numbers generated in Step 1 in a square matrix S which is called node-incidence matrix. The below S matrix is for the 7-bus system used in this work and shown in Figure 4-5.

$$S = \begin{bmatrix} 1 & 1 & 0 & 0 & 0 & 0 & 0 \\ 1 & 1 & 1 & 0 & 0 & 1 & 1 \\ 0 & 1 & 1 & 1 & 0 & 0 & 1 \\ 0 & 0 & 1 & 1 & 1 & 1 & 0 \\ 0 & 0 & 0 & 1 & 1 & 0 & 0 \\ 0 & 1 & 0 & 1 & 0 & 1 & 0 \\ 0 & 1 & 1 & 0 & 0 & 0 & 1 \end{bmatrix} \tag{4.5}$$

Step 3 validates the observability of all the network buses using the following formula:

$$h_k = \sum_{i=1}^{m} S_{k,i} u_i \tag{4.6}$$

$$\sum_{i=1}^{m} h_k \geq 1 \tag{4.7}$$

The symbol of the availability of PMU at Bus k is u_i (binary number). If distribution of PMUs violates this condition, the code will return significantly high value to the objective function. Hence, this case will be rejected and new route will start again.

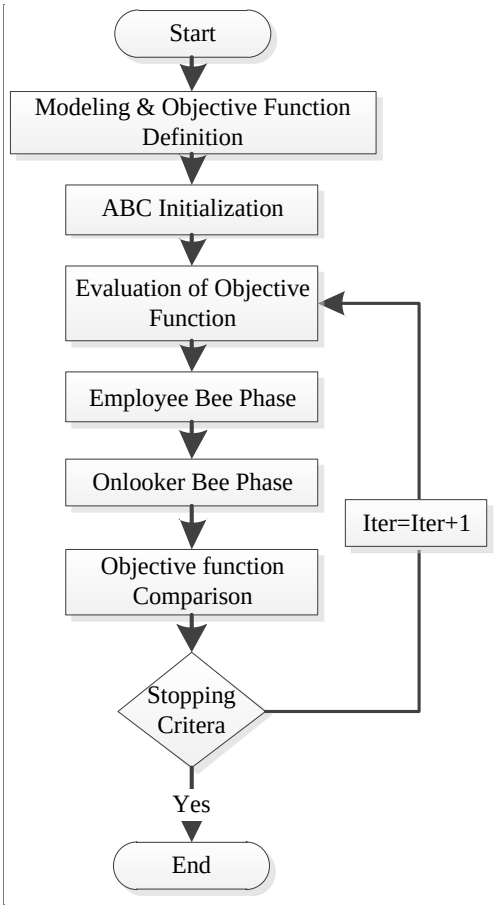

Figure 4-3: ABC algorithm flowchart

Step 4 comprises of a number of sub-steps to reflect the rules for optimal placement in distribution indicated in Figure 4-2.

Step 5 represents the objective function detailed in Section 4.5.

4.3 ABC Technique

The ABC search optimization is an inhabitants-based probabilistic search algorithm that is capable of providing global solutions. It was developed by Karaboga and Basturk [219] inspired from the foraging activities of honeybees for numerical search problems. The minimal model of honeybee swarm intelligence has three components: Employed bees,

onlooker bees and food sources; the nectar amount of a food source corresponds to the objective function.

In the ABC algorithm, the colony of artificial bees is categorized into three groups of bees: Employed bees, onlookers and scouts. The food source corresponds to a candidate solution of the optimization problem and the nectar amount of a food source corresponds to the quality (fitness) of the associated solution. Every food source has only one employed bee.

The various steps involved in the algorithm are as follows, refer to Figure 4-3.

A. Initialization of Employed Bees

This step involves defining the parameters for the ABC algorithm and the random initialization of the employed bees using the relation:

$$X_i = X_{i\,min} + \text{rand}\,(X_{i\,max} - X_{i\,min}) \tag{4.8}$$

The position of the employed bees is stored.

B. Fitness Evaluation and Finding the Best Values

In this step, the nectar amount or fitness of each employed bee is evaluated. The global best solution and the best solution are stored.

C. Perturbation

This step is to perturb the position of each of the employed bee and check the fitness of the perturbed position.

D. Update the Position

This process updates the position of employed bees based on a fitness comparison.

E. Global Best Updating

The global best for the bees is updated in this process by considering a comparison of global fitness.

F. Update Employed Bees

This process aims to update the position of employed bees through the Onlooker Bees (OBs).

G. Stopping Criteria

The pre-specified number of iterations for which the fitness function does not change is considered to be the stopping criterion.

4.4 Strength Pareto Evolutionary Algorithm

Multi-objective optimization algorithms, which address contradictory objectives, give rise to a set of optimal solutions instead of one. This is because most of engineering problems have diversified portfolio of solutions, i.e. the solution is not unique. Selectivity of the final solution depends on several factors, such as financial constraints, reliability & redundancy preference and so on and so forth.

This research uses SPEA that was presented by Zitzler and Thiele [220] to get the optimal placement of PMUs based on two objectives described in Section V. The algorithm steps could be summarized as follows:

A. Initialization of population and Pareto-optimal set

B. Update of Pareto-optimal set

C. Fitness value calculation

D. Selection of the population that give

E. Applying crossover and mutation

F. Checking for stopping criteria

The SPEA algorithm is outlined in Figure 4-4.

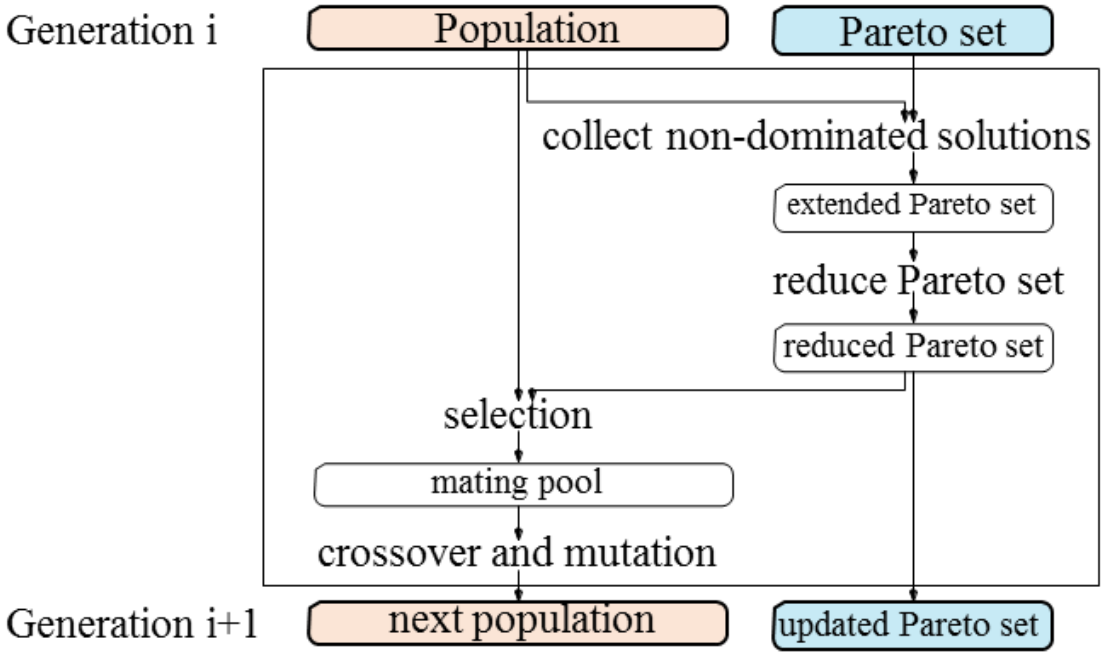

Figure 4-4: Outline of the SPEA [220]

4.5 Case Studies and Objective Functions

To simulate the placement of PMU devices in distribution networks single and multi-objective intelligent optimization techniques are used (ABC and SPEA). The placement has been simulated in 7, 11, and 14-bus distribution systems. The simulations have been performed considering the criteria and constraints described in Section 4.2.

For the single objective optimization algorithm (ABC), the following objective function is modeled:

$$Objective = \min\left(\sum_{i=1}^{N_b} C_i d_i + \sum_{i=1}^{N_b} P_i o_i + \sum_{i=1}^{N_b} \frac{1}{B_i r_i}\right) \quad (4.9)$$

N_b : System size (number of buses).

C_i : Cost of a new PMU Installation.

d_i : Detector for new PMU at Bus. It is set to one for new PMU and zero otherwise.

P_i : Penalty for a non-observable bus. This is to ensure the full system observability. P is set to be very high number for non-observability.

O_i : Detector for new non-observable Bus i. It is set to one for non-observability and zero otherwise.

B_i : An incentive of redundant observability. It is a large number.

r_i : Indicates the redundancy of observation. If a bus is observed once this number will be 1 and for twice observability it will be 2 and so on.

On the other hand, using dual-objective method Strength Pareto evolutionary algorithm (SPEA) is more useful as it produces a diversified portfolio of options to help the management to take decisions for investment. Two objectives are considered; the first objective to maintain the observability at all buses, whereas the second one targets higher redundancy. The two objective functions are as follows:

$$Objective\ 1 = \min\left(\sum_{i=1}^{N_b} C_i d_i + \sum_{i=1}^{N_b} P_i o_i\right) \tag{4.10}$$

$$Objective\ 2 = \min\left(\sum_{i=1}^{N_b} -B_i r_i\right) \tag{4.11}$$

4.6 Results and Discussions

The results considering the observability of all buses and the redundancy are shown in the below figures. First, the results of applying ABC at the 7-bus standard are presented in Figure 4-5. The ABC algorithm resulted in only two PMUs to observe the 7-bus network. The observation redundancy obtained from PMUs at each bus is presented in Figure 4-5 (c) which highlights that there is a redundancy of n+1 of observation at Bus 3. The remining buses will have a redundancy of n. The 7-bus system was selected as it is easier to be tracked manually to check the robustness of the developed algorithm.

Additionally, PMU placement in distribution is applied to 11-bus test distribution system as in Figure 4-6. A total of five PMUs are required for the system which leads to an improved observability redundancy. The redundancy of couple of buses are n+2. For example, in case Bus 4 PMU is lost, the bus conditions still can be monitored by the PMUs of Buses three and

ten. Testing the developed algorithms for 11-bus model with zero-injection buses results are indicated in Figure 4-7. The algorithms recognize the zero-injection bus and therefore reduce the number of PMUs as that bus can be observed by calculation. This is in accordance with the observability rules described in Section 4.2.

Furthermore, 14-bus system is simulated using ABC and the results are established in Figure 4-8. Despite the fact that the system has higher number of buses compared to the 11-bus model, still it needs the same number of PMUs while maintaining the required observability. This is an advantage of the OPP of PMUs using ABC.

The results of simulating the multi-objective technique for 14-bus test distribution network are displayed in Figure 4-9. The algorithms result in the same number of PMUs as obtained by ABC. However, this method will offer sets of solutions that will help the decision makers to select the most appropriate one.

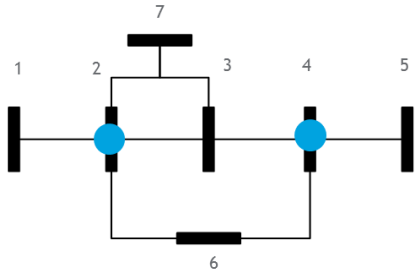

A) Optimal Location of PMUs labeled on the 7-bus test system

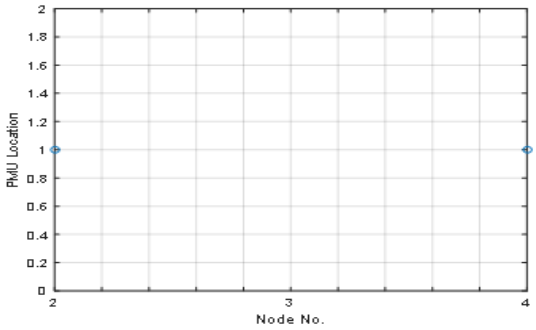

B) PMUs optimal location using ABC

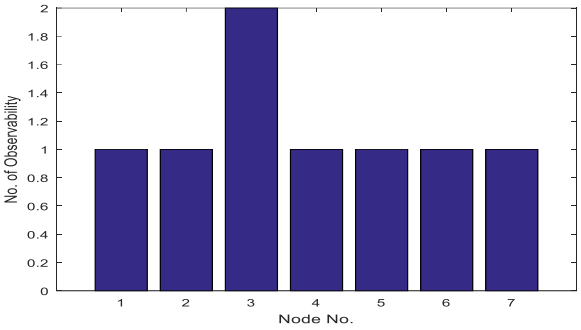

C) Observation redundancy obtained from PMUs at each bus

Figure 4-5: The results of the optimal placement of PMUs on a standard 7-bus distribution system using ABC

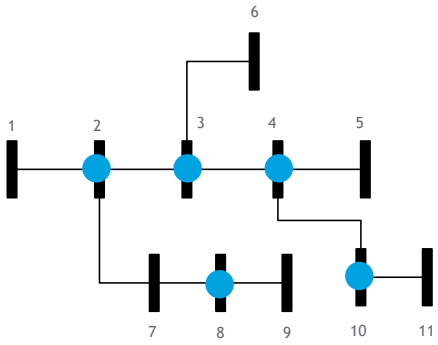

A) Optimal Location of PMUs labeled on the 11-bus test system

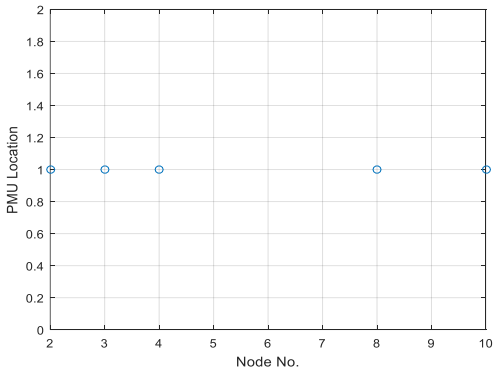

B) PMUs Optimal Location using ABC

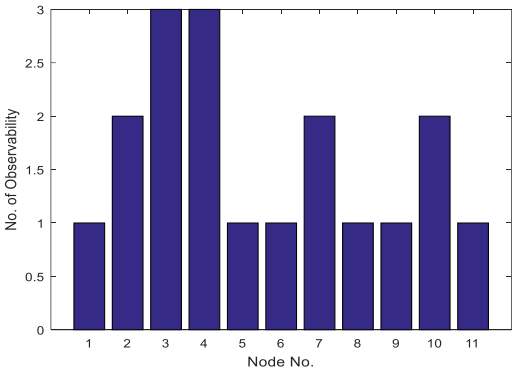

C) Observation Redundancy Obtained from PMUs at each bus

Figure 4-6: Optimal PMU placement results for a standard 11-bus distribution system using ABC

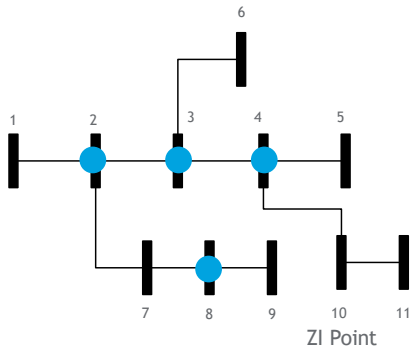

A) Optimal Location of PMUs labeled on the 11-bus test system with zero-injection bus

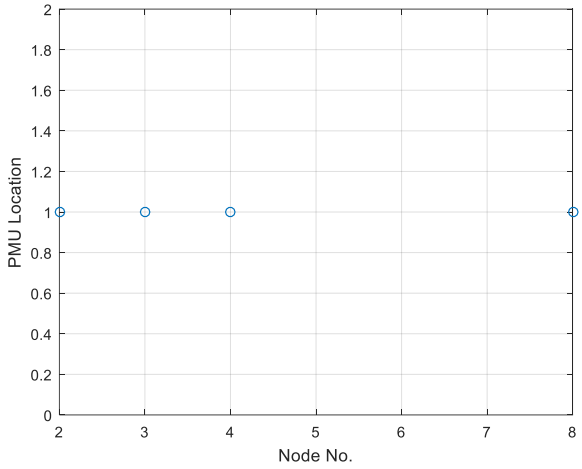

B) PMUs Optimal Location using ABC

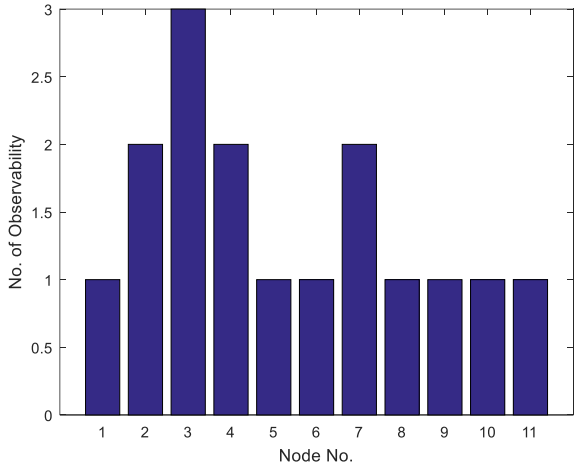

C) Observation Redundancy Obtained from PMUs at each bus

Figure 4-7: Optimal PMU placement results for a standard 11-bus distribution system with zero-injection bus using ABC

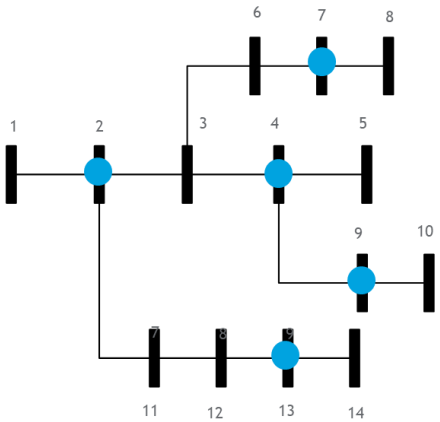

A) Optimal Location of PMUs labeled on the 14-bus test system

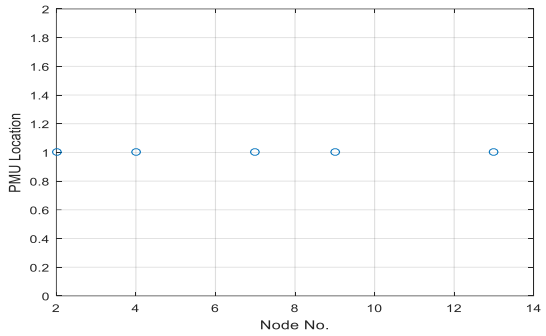

B) PMUs Optimal Location using ABC

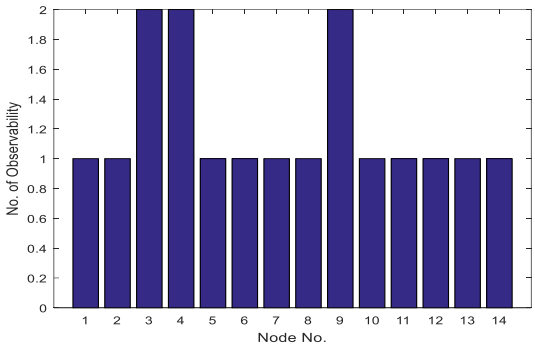

C) Observation Redundancy Obtained from PMUs at each bus

Figure 4-8: Optimal PMU placement results for 14-bus test distribution network with the redundancy chart by applying ABC

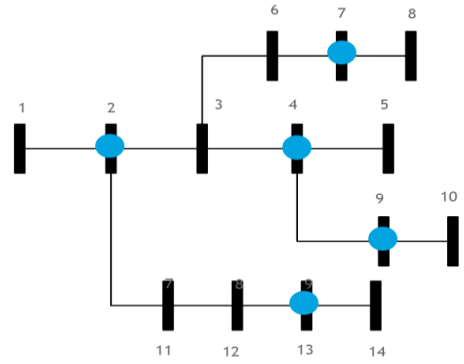

A) Optimal location of PMUs labeled on the 14-bus test system

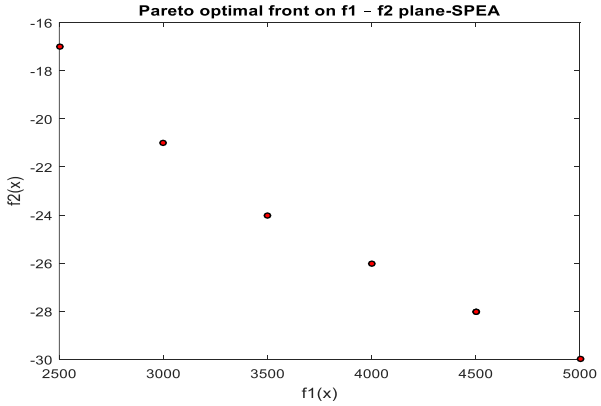

B) Pateto front for IEEE 14 Bus Distribution System

8	0 1 0 0 1 1 1 0 1 0 1 1 1 0	4000	-26
9	0 1 0 0 1 1 1 0 1 1 1 1 1 0	4500	-28
9	0 1 0 0 1 1 1 1 1 0 1 1 1 0	4500	-28
10	0 1 0 0 1 1 1 1 1 1 1 1 1 0	5000	-30
5	0 1 0 1 0 0 1 0 1 0 0 0 1 0	2500	-17
6	0 1 0 1 0 0 1 0 1 0 0 1 1 0	3000	-21
7	0 1 0 1 0 0 1 0 1 0 1 1 1 0	3500	-24

C) PMUs optimal location using SPEA at each bus

Figure 4-9: Optimal PMU placement results for 14-bus test distribution network with the redundancy chart by applying SPEA

4.7 Conclusion

The optimal placement of PMUs problem is considered first using single objective function (ABC). It is one of the robust and reliable techniques to find the optimal solution. It is applied to standard 7, 11, and IEEE 14-bus systems. Furthermore, multi-objective optimization technique (SPEA) is discussed. It represents a considerable contribution to the subject of PMUs in distribution. SPEA is applied to IEEE 14-bus system and the results revealed in a portfolio of optimal options. Using multi-objective approach will give diversified optimal options to the decision makers to select the most appropriate one that meet their needs.

CHAPTER 5

IDENTIFICATION OF DISTRIBUTION LINE PARAMETERS BY PHASOR MEASUREMENT UNITS

This chapter proposes to improve the accuracy associated with online distribution line parameters identification. Additionally, it introduces the concept of positive-sequence quantities for determining the line resistance, reactive inductance and shunt admittance. The positive-sequence based analysis is required for asymmetrical related studies such as unbalanced fault analysis. The chapter, also, includes the consideration of noisy distribution networks. It compares the performance of three line parameters identification techniques by using different statistical measures. A total of 12,960 different case studies are simulated and analyzed under six main loading scenarios and four categories with changing line parameters. The line parameters are calculated online using voltage and current signals obtained from phasor measurement units (PMUs) placed at the line two terminals. Finally, the study outcomes and the associated recommendations have been summarized for future works considerations.

5.1 Introduction

Distribution line (DL) parameters identification forms the basis for distribution power system studies, including dynamic & transient stabilities, state estimate, and protection setting, etc. The common practice in the industry, till today, is to determine the parameters using values from design datasheets, manufacture specification sheets and engineer estimation. The latter could base the calculation on conductor dimensions, sag, temperature, tower geometries, and other elements. These elements will be used to identify the DL data through different mechanisms such as calculating the geometric mean radius (GMR) and the geometric mean distance (GMD). Additionally, the official electrical transient analysis program (ETAP) model could be utilize to find the DL data, which is an off-line tool. Assumptions and approximations are included in the calculation process steps which will reduce the accuracy of data. Basing DL parameters estimation on off-line techniques or pre-identified information will reduce the accuracy level of the power system studies that depend on these values due to the following:

1. Conductor resistance and reactance vary with ambient conditions, conductor situation and the power flow.
2. A number of installed circuits are spliced with other conductors that are different in types and specifications. This will result in an inhomogeneity of the line sections.
3. The overhead conductor arrangements differ from section to another as the tower configurations changes, and transposition might apply.
4. Cable installation conditions such as grouping, underground, overhead, on cable trays, in conduits, and submarine, etc. play a major role in line parameter estimation.

5. Cable aging could impact the line parameters due to several factors such as degradation, tension and life cycle.

The above five factors are sources of conductor impedance and admittance identification errors. Accordingly, it is possible to develop more accurate DL impedance parameters estimation by online measurement techniques using the synchronized PMUs.

With the emergence of PMU technology, it is possible to obtain more accurate data about the system conditions with high frequency samples along with the corresponding time stamp.

The majority of research works to estimate the power system line parameters is transmission oriented. Numerous techniques have been introduced to calculate the transmission parameters using the synchronized measurement devices. A two-port ABCD parameter identification based technique is introduced in [221]. This method utilizes two sets of three samples of sending and receiving terminals' voltage and current signals. This is to find three estimates of ABCD parameters. The ABCD method is referred to in this research work as a "two-port circuit measurement technique". In Reference [222], four methods are discussed to identify short transmission line parameters by synchronized measurements. Reference [212] proposes a novel method to identify transmission line parameters for different cases, including short and long, transposed and un-transposed lines with balanced and unbalanced load conditions. The positive-sequence line parameters considering the effects of the line shunt capacitance is performed in [223], employing a two-terminal transmission line model. Likewise, Reference [224] aims to achieve the same objectives where a new estimation method is presented using synchronized phasor measurements at both line ends. The approach in [225] proposes the use of recursive parameter estimation to find the network branch parameters online and off-line.

The least-square technique is leveraged in [226] with the objective of obtaining the line parameters iteratively.

Unlike the abundance of publications on transmission line parameters estimation, the work in distribution is limited. The probability theory, which builds on voltage drop linear equivalent model, is used in [227]. The approach objective is to estimate the DL impedance and get precise parameters. Numerous works discuss the uncertainties of network parameters and inaccuracy of measurements. In particular, the DL parameters and measurement uncertainties are analyzed in [228]. A novel power system uncertainty analysis technique is proposed in [12], where a two-step approach based on static weighted least-squares analysis is used. A regular power flow calculations based technique is presented in [229], considering line parameter estimation. It resulted in a negligible deviation between simulation, experiment and the actual manufacturer specifications. The key outcomes of the DL parameters estimation studies are that the accuracy of line parameters is crucial for a number of applications including the grid control, stability analysis and fault location studies.

This chapter proposes the use of PMU to identify the DL parameters under the consideration of accuracy, positive-sequence and noise. The concept of symmetrical components is leveraged to extract the positive-sequence of the synchronized phasor voltage and current measurement signals. The online synchronized signals obtained from the PMUs will be used in calculating both the phase and positive-sequence DL parameters. Section 5.2 discusses the PMU definition and measurement methodology. In Section 5.3, three techniques have been developed to measure DL resistance, reactive inductance and shunt admittance. The proposed inaccuracy prediction and mitigation measures are presented in Section 5.4. Section 5.5 describes the used accuracy statistical measures to evaluate and compare the performance of

the three techniques. The developed case studies along with their results and discussion are presented in Sections 5.6 and 5.7, respectively. Finally, the study recommendations and outcomes are stipulated in Section 5.8.

5.2 PMU Definition and Measurement Methodology

Phasor measurement unit is a name for a device that produces phasors which have been calculated at an instant identified as the time stamp of the PMU. The simultaneous readings are the key driver of recommending PMU among others as it is essential to synchronize these time stamps. This is to have all phasor measurements obtained at the same instant are accurately simultaneous. Considering the notation T = 0 is the time stamp of the recorded input waveform, the PMU will produce the phasor equivalent using the input waveform samples. There is a filter at the PMU input which produces a phase delay as the sampled data are measured after the filter as shown in Figure 5-1. However, the PMU will substitute for this delay that depends on the characteristic of the filter.

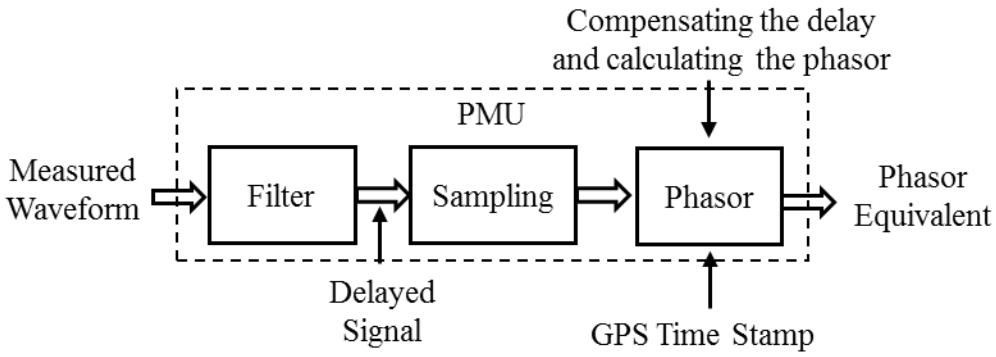

Figure 5-1: PMU structure including filter, sampling and phasor calculation (the concept is obtained from [230]**)**

The synchronous measurement is realized by using a GPS clock. The clock is obtained from a receiver that could be integrated with the PMU or externally installed inside the substation

building. The external receiver is capable of sending the signal to the PMU and to any other device that requires the time tag. Normally, the PMU will provide the positive-sequence of voltage and current for the three phases.

5.2.1 Concepts of PMUs

In practical situations, frequency and magnitude of the sinusoidal signals are not stationary. Therefore, a fixed phasor data will defeat the purpose of the measurement devices. Instead, the data are updated frequently with the time. The frequency of recording is very high complaining with the existing measurement devices. The window of data recorded by PMUs is one cycle of the fundamental frequency of voltage and current signals. The PMU has the ability of frequency tracking as it measures the frequency of the signal. The input signal may have both fundamental and other harmonics. The PMU is able to segregate the fundamental frequency from the overall signal and produce its phasor equivalent.

One of the techniques for identifying the phasor equivalent for the input sinusoidal signal is to apply the discrete Fourier transform on the sampled data of the waveform to calculate the phasor representation. It is important to filter the input signal before sampling and obtaining the phasor representation. This is to obtain the fundamental frequency from the input signal using the following formula [125]:

$$X = \frac{\sqrt{2}}{N} \sum_{K=1}^{N} X_k e^{-ik\frac{2\pi}{N}} \tag{5.1}$$

Where N represents the total number of samples per one period of the input signal, X is the measure signal in phasor representation, and X_k is the samples of the input waveform.

This method of calculation rejects the harmonics of the input waveform. Nevertheless, the noisy signals lead to an error in approximating the phasor. The error of calculation due to such effects has been presented in this chapter (Chapter 5).

This methodology of obtaining the phasor has the advantage of using samples N of the input signal. It produces an accurate phasor representation for under different electrical system conditions. The accuracy is improved as more samples and accurate synchronizations are aligned with the universal time (UTC).

X is the most proper equivalent of the fundamental harmonic frequency even if other harmonics exist. The PMU calculates the phasors at each phase, producing the three-phase phasors $X_{a,}\ X_b, and\ X_c$. The sequence components (positive, negative and zero) are calculate for each phase using the below transformation matrix:

$$\begin{bmatrix} X_1 \\ X_2 \\ X_0 \end{bmatrix} = \frac{1}{3}\begin{bmatrix} 1 & \alpha & \alpha^2 \\ 1 & \alpha^2 & \alpha \\ 1 & 1 & 1 \end{bmatrix}\begin{bmatrix} X_1 \\ X_1 \\ X_1 \end{bmatrix} \tag{5.2}$$

Where $\alpha = 1\ e^{i\frac{2}{3}\pi}$

5.2.2 PMU Architecture

Generally, PMUs are installed in electrical substations or in any desired location in the network. The selection of PMU placement depends the purpose of installation, expected outputs and cost-benefit analysis. The PMU optimal placement along with its applications are discussed in Chapter 4.

Usually, the phasor measure units are installed in remote locations from the place where are the data needed. Therefore, a hierarchy as shown in Figure 5-2 should be developed that

includes PMUs, communication connectivity, data concentrators and PCCs. This is to realize the full advantages of PMU recording system.

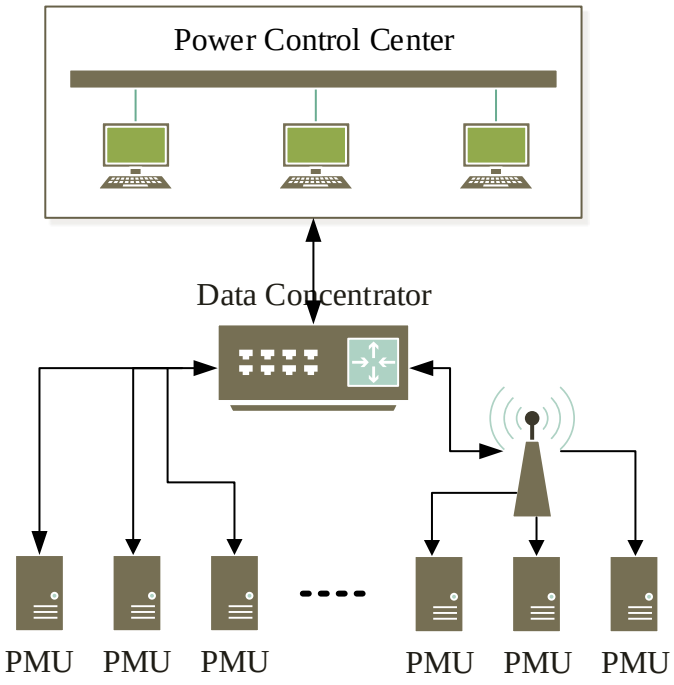

Figure 5-2: PMU System hierarchy diagram (the concepts are obtained from [231]**)**

In Figure 5-2, the PMUs are distributed in electrical system substations or in the filed subject to the availability of communication infrastructure. This is to measure the power system conditions with the time stamp. The measured data could be the positive-sequence of voltages and currents of all observable feeder and buses, in addition to the system actual frequency. The readings are stored locally in the PMU device itself or in an external data storage system. The PMU data, current and historical records, should be accessible remotely in order to perform the required applications. The storage should have sufficient capacity to store data in such a way that the event of interest will not be overwritten when the storage size is exhausted. The data are available locally for real-time purpose such as measurements are required on the

spot by the operator. However, the key driver of installing PMUs is for higher level tasks where numerous PMUs are integrated with each other.

The next building block level in the PMU system hierarchy is the data concentrator. The interface object between the PMU and the concentrator is a PMU internal or external remote terminal unit (RTU). The RTU could be connected to the data concentrator through a wire system (fiber optics) or wireless (router). Both fiber optics and the router connected PMUs are linked to a local control room where the data concentrator is located. The purpose of the data concentrator is to collect data from different PMUs, reject undesired input, ensure the alignment of the time tag, and create a simultaneous and coherent measurements. Local storage could be installed along with the data concentrator for different applications such the analysis performed by the central control room professionals.

The intermediate building blocks will definitely create data latency. However, the main advantage of the PMU is that the data will arrive with a short delay, but with a time stamp. Accordingly, the analysis will not be affected by the latency as all the data will be synchronized with the GPS time.

The highest level in the hierarchy is the PCC where the central applications, monitoring, control, and analysis are performed. Usually, the brain of the power system custodies (such as the planning engineers, consultants, and designers, etc.) are tapped into the PCC. The ultimate objectives of installing the PMUs will be realized at the PCC. The applications of PMUs are discussed in Section 4.1.2.

The connections links shown in Figure 5-2 are bidirectional. In most cases, the direction of data flow is from the PMU to the PCC. There are few cases where the data flow is downward.

These cases are for power system control and protection. This includes turning off a breaker for operation or maintenance purpose, tripping a breaker, load shedding, islanding and so on and so forth.

Although the science and new technologies support the automation in lieu of human performance, still some critical facilities permit monodirectional data flow only (open feedback) for monitoring and analytical purposes. The control is achieved locally through a local control room or manually through an operator. This is to reduce the potential errors associated with the control systems and increase the accountability of personnel.

5.2.3 Global Positioning System

The GPS is a space-based navigation owned, operated and maintained by the United States Air Force. The GPS is an international navigation system with the aim of providing time and geolocation data to a GPS receiver anywhere on the Earth [232].

The GPS system provides signals independently of any telephonic or internet lines and does not necessitate the receiver to send any information. The internet and telephonic reception could enhance the GPS positioning performance. It offers positioning and timing capabilities to global users for any purpose. The GPS service is available to anyone with a GPS receiver without any fee [233].

In 1978, the GPS was started with the time of launching the first Block I satellites by US. The complete 24 satellites constellation was put in place around 1995. By 2007, there were a total of 30 active satellites in orbit. The additional satellites provide an improved accuracy level. The satellites are arranged in six orbits apart from each other by 60 degrees and with inclination of 55° from the equator as shown in Figure 5-3. Their orbital radius is 26,554 km

and orient around the earth two times per day. Six satellites are available all the times at the majority of locations on our planet. Most of the times, a total of ten satellites could be visible for view [125].

The key use of the GPS is to provide coordinates and time to the GPS receiver which could be a pulse per second. The same pulse is received by all the GPS receivers on the Earth in a coincident manner within one microsecond. The accuracy of synchronization has been improving over years as the PMU technology evolves as recently an order of magnitude of a hundred nanoseconds has been recognized [234].

The GPS satellites clocks keep the accuracy of providing one pulse per second that will be received by GPS receivers in time better than a fraction of millisecond. The time procured by the GPS is called “GPS time” which disregard the earth movement and local time. Subsequently, a time adjustment is required by GPS receivers to consider this difference and show UTC clock time. Converting the GPS clock timing with the UTC clock time is required as the count of number of pulse per seconds started on January 6, 1980 [125].

Currently, numerous similar GPS systems have been developed by other countries. However, it is predicted that PMU technology is more prone to continue basing on the global GPS system.

5.2.4 GPS Integration with PMU

The configuration of GPS integration with PMUs is not unique. This is due to the diversity of PMU manufacturers and specifications. The PMU could be a very sophisticated system such as the ones installed at the islanded systems to perform all power monitoring, control, protection, load shedding and so forth. On the other hand, it could be as simple as the other

digital relays except for the time stamp and the sampling frequency. The diversity of PMU specifications creates difficulties of developing a unique PMU-GPS integration hardware scheme. Instead, a generic configuration could be developed that includes major components of PMUs [31, 37-38]. Figure 5-3 shows the block logic diagram of PMU integration with GPS. It is to be noted that the development of PMU technology had evolved from the concepts of "symmetrical component distance relay" [125].

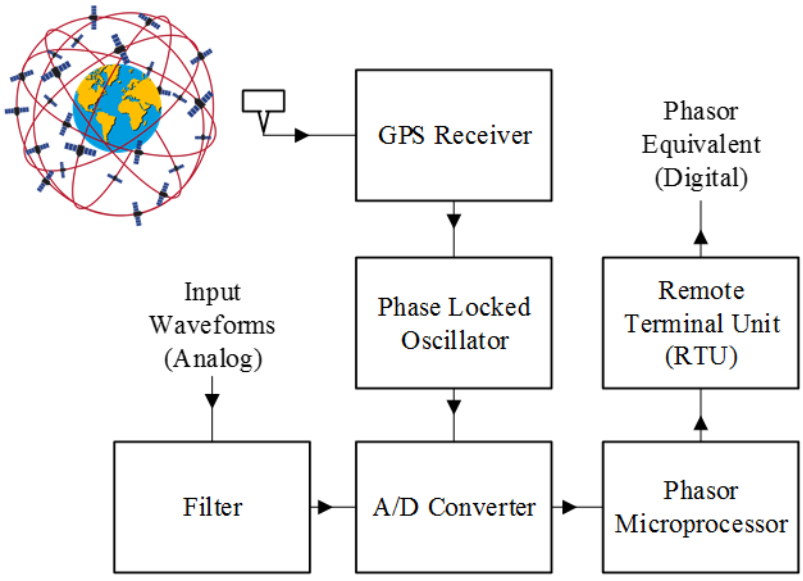

Figure 5-3: GPS integration with PMU block diagram (the concepts are obtained from [236]**)**

Analog input waveforms are received from the secondary winding of voltage and CTs. All three-phase conditions will be measured simultaneously to provide the positive-sequence components. The noise associated with the input waveform is rejected at the first building block which is the filter. The current and voltage waveforms at the secondary side of the instrumentation transformers are with low magnitude (typically within the range of 1-5 V in / 4-20 mA). These signals match the requirements of the analog to digital converter. The sampling rate must be at least double the filter cut-off frequency to satisfy the Nyquist criterion [125]. To get more accuracy of data, more samples are needed [237].

The GPS receiver produces a pulse per second to the oscillator in order to freeze the sampling clock phase. It, also, creates time tag for the microprocessor outputs with a negligible synchronization error.

The digital signal is delivered to the microprocessor by the A/D converter to identify the phasor equivalent. The phasor measurements are produced irrespective of any time delay resulted from the communication infrastructure as they will be compared using the time tag as the reference.

5.3 Techniques of Distribution Line Parameters Estimation

Three different techniques are discussed in this section with the objectives of identifying the DL parameters. The techniques leverage the PMU voltage and current signals obtained at the two terminals of the line. In order to perform DL parameters estimation, the line is represented in a π-model equivalent circuit as illustrated in Figure 5-4.

The study considers the positive-sequence of the voltage and current phasors in addition to the phase values. This aims to explore accuracy enhancement opportunities and compare the results. Additionally, the sequence quantities are required for developing any asymmetrical analysis. The positive-sequence equivalent π-model is shown in Figure 5-5.

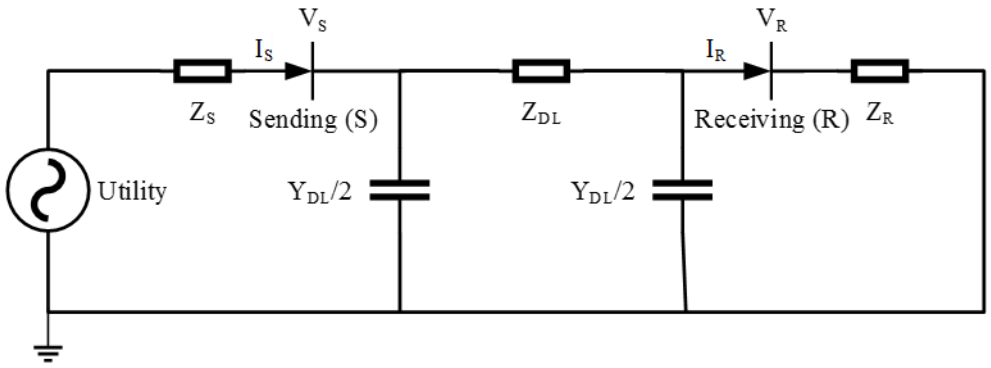

Figure 5-4: Distribution line equivalent model (π-Type)

The parameters of the above figure are described as follows:

Z_S	:	Equivalent impedance at the source side
Z_R	:	Equivalent impedance at the receiving end
Z_{DL}	:	Distribution line impedance
Y_{DL}	:	Distribution line admittance
V_S	:	Phase voltages at sending end
V_R	:	Phase voltages at receiving end
I_S	:	Phase current at sending end
I_R	:	Phase current at receiving end

The positive-sequence equivalent π-model is shown in Figure 5-5.

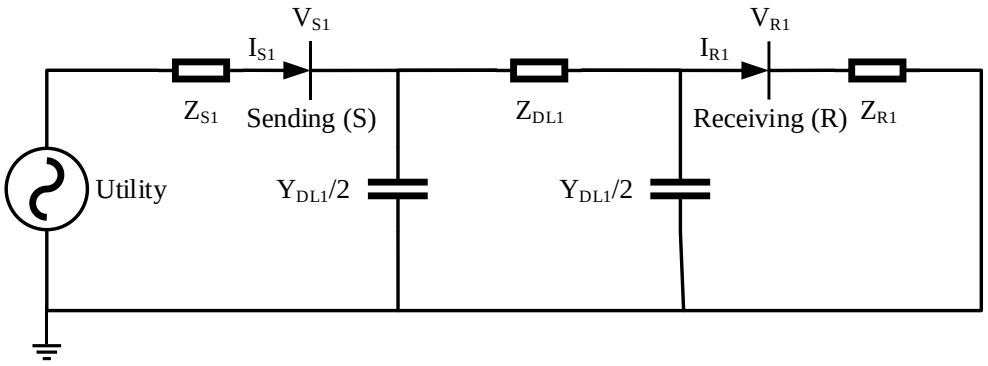

Figure 5-5: Positive-sequence distribution line equivalent model (π-Type)

The parameters of the above figure are defined as follows:

Z_{S1}	:	Positive-sequence equivalent impedance at the source side
Z_{R1}	:	Positive-sequence equivalent impedance at the receiving end
Z_{DL1}	:	Positive-sequence distribution Line impedance
Y_{DL1}	:	Positive-sequence distribution Line admittance
V_{S1}	:	Positive-sequence phase voltages at sending end
V_{R1}:	:	Positive-sequence phase voltages at receiving end
I_{S1}:	:	Positive-sequence phase current at sending end
I_{R1}	:	Positive-sequence phase current at receiving end

5.3.1 Ohm's Formula Technique

The proposed ohm's formula technique (OFT) depends on the ohm's law. Under this method, both phase and positive-sequence voltage and current phasors are used. This method requires

only single set of voltage and current samples of the phasor voltage and current signals produced by PMUs.

The developed OFT equations to calculate the DL parameters are described below:

$$Z_{DL1} = \frac{2(V_{S1} - V_{R1})}{I_{R1} + I_{S1}} \tag{5.3}$$

$$Y_{DL1} = \frac{I_{S1} - I_{R1}}{V_{S1}} \tag{5.4}$$

5.3.2 Single Measurement Technique

The proposed single measurement technique (SMT) aims to find DL resistance, reactive inductance and shunt admittance. It uses both the phase and positive-sequence of the voltage and current signals that are obtained from PMUs at the steady state. The SMT equations are formulated as follows:

$$Z_{DL1} = \frac{V_{S1}^2 - V_{R1}^2}{V_{R1}I_{S1} + V_{S1}I_{R1}} \tag{5.5}$$

$$Y_{DL1} = \frac{2(V_{S1} - V_{R1})}{I_{R1} + I_{S1}} \tag{5.6}$$

5.3.3 Two-Port Circuit Measurement Technique

The two-port circuit measurement technique (TPCMT) requires two sets of synchronized measurement samples at different loading conditions. The samples are taken from the DL terminals to calculate the two-port circuit parameter known as A, B, C, & D. The DL impedance and admittance are identified from the ABCD matrix.

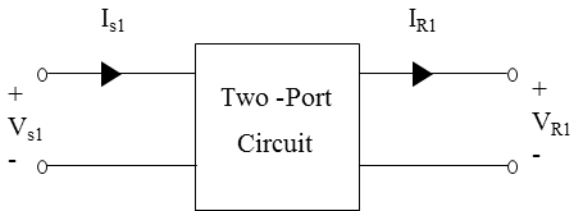

Figure 5-6: Representation of positive-sequence two-port circuit for distribution line

The TPCMT is conventionally used to represent transmission lines. Additionally, it provides adequate accuracy for DLs at some cases. Representation of positive-sequence TPCMT for DL is shown in Figure 5-6, where V_{S1}, V_{R1}, I_{R1} and I_{S1} are the positive-sequence of the sending and receiving ends voltage and current signals, respectively.

The following equations form the relation between the sending end and the receiving end quantities:

$$V_{S1} = A\,V_{R1} + B\,I_{R1} \tag{5.7}$$

$$I_{S1} = C\,V_{R1} + D\,I_{R1} \tag{5.8}$$

Where the parameters A, B, C and D are influenced by the DL resistance, inductance, capacitance and conductance. The ABCD parameters are complex numbers in which A and D are unit less, B is measured in ohms, and C has a unit of Siemens. The concepts of two port circuits are detailed in Reference [238].

The ABCD parameters of the DL equivalent π-model shown in Figure 5-5 are obtained by the following equations:

$$V_{S1} = V_{R1} + Z_{DL1}\left(I_{R1} + \frac{V_{R1}Y_{DL1}}{2}\right)$$

$$= (1 + \frac{Z_{DL1}Y_{DL1}}{2})V_{R1} + Z_{DL1}I_{R1} \quad (5.9)$$

By applying the Kirchhoff current law (KCL) at the sending end, the following equation is obtained:

$$I_{S1} = I_{R1} + \frac{Y_{DL1}(V_{R1} + V_{S1})}{2} \quad (5.10)$$

Combining the previous two equations yields:

$$I_{S1} = I_{R1} + \frac{Y_{DL1}V_{R1}}{2} + [(1 + \frac{Z_{DL1}Y_{DL1}}{2})V_{R1} + Z_{DL1}I_{R1}]\frac{Y_{DL1}}{2} \quad (5.11)$$

$$= Y_{DL1}(1 + \frac{Z_{DL1}Y_{DL1}}{4})V_{R1} + (1 + \frac{Z_{DL1}Y_{DL1}}{2})I_{R1} \quad (5.12)$$

Comparing the last above formula with the ABCD equations yields:

$$A = D \quad (5.13)$$

$$= (1 + \frac{Z_{DL1}Y_{DL1}}{2}) \quad \text{per unit} \quad (5.14)$$

$$C = Y_{DL1}\left(1 + \frac{Z_{DL1}Y_{DL1}}{4}\right) \quad \text{ohm} \quad (5.15)$$

From the simple DL (only series impedance representation) analysis and derivation B is obtained to be:

$$B = Z_{DL1} \quad \text{ohm} \quad (5.16)$$

The above A, B, C and D equations are solved to find Z_{DL1} and Y_{DL1}which will be as follows:

$$Z_{DL1} = B \quad \text{ohm}$$

$$Y_{DL1} = \frac{2(A-1)}{B} \quad \text{Siemens} \tag{5.17}$$

This method could be extended to accommodate two sets of PMU measurements. The two sets could be obtained from two different redundant PMUs, or from two readings recorded at different timing or loading conditions. The ABCD equations for the two sets are as follows:

$$V_{S1}{}' = A\, V_{R1}{}' + B\, I_{R1}{}' \tag{5.18}$$

$$I_{S1}{}' = C\, V_{R1}{}' + D\, I_{R1}{}' \tag{5.19}$$

$$V_{S1}{}'' = A\, V_{R1}{}'' + B\, I_{R1}{}'' \tag{5.20}$$

$$I_{S1}{}'' = C\, V_{R1}{}'' + D\, I_{R1}{}'' \tag{5.21}$$

The samples of the voltages and currents for the receiving and sending ends are as the following:

- $V_{S1}{}'$, $V_{R1}{}'$, $I_{S1}{}'$and $I_{R1}{}'$ are for the first set;
- $V_{S1}{}''$, $V_{R1}{}''$, $I_{S1}{}''$and $I_{R1}{}''$ are for the second set.

The ABCD parameters are calculated to account for the two sets to be as follows:

$$A = \frac{I_{R1}{}'\, V_{S1}{}'' - I_{R1}{}''\, V_{S1}{}'}{I_{R1}{}'\, V_{R1}{}'' - I_{R1}{}'' V_{R1}{}'} \tag{5.22}$$

$$B = \frac{V_{R1}{}''\, V_{S1}{}' - V_{R1}{}'\, V_{S1}{}''}{I_{R1}{}'\, V_{R1}{}'' - I_{R1}{}'' V_{R1}{}'} \tag{5.23}$$

$$C = \frac{I_{R1}{}' I_{S1}{}'' - I_{R1}{}'' I_{S1}{}'}{I_{R1}{}' V_{R1}{}'' - I_{R1}{}'' V_{R1}{}'} \quad (5.24)$$

$$D = \frac{I_{S1}{}' V_{R1}{}'' - I_{S1}{}'' V_{R1}{}', }{I_{R1}{}' V_{R1}{}'' - I_{R1}{}'' V_{R1}{}'} \quad (5.25)$$

5.4 Inaccuracy Prediction and Mitigation

It is observed form the simulated case studies shown in Appendix B that the error follows specific trend under different fault resistance and loading conditions. Knowing the error trend will ease predicting its magnitude and hence mitigating it. This section proposes to apply inaccuracy mitigation measures to improve the line parameters online estimation. The measures are developed based on line characteristics and possible faults' types and impedances. The proposed inaccuracy mitigation measure concept is illustrated in Figure 6-5 and given by the following formula:

$$\ddot{y} = \dot{y}(1 + \varepsilon(\dot{y})) \quad (5.26)$$

Where $\dot{y}$ is the originally calculated value and $\ddot{y}$ is the enhanced estimation. The symbol ε is taken from the pre-developed inaccuracy mitigation measures demonstrated in Figure 5-7. The inaccuracy mitigation curve could take different shapes based on line loadings and characteristics. The inaccuracy mitigation measure (IMM) can be developed for each line as appropriate by the design consultant firms during the design phase of the lines, part of the protection and coordination studies.

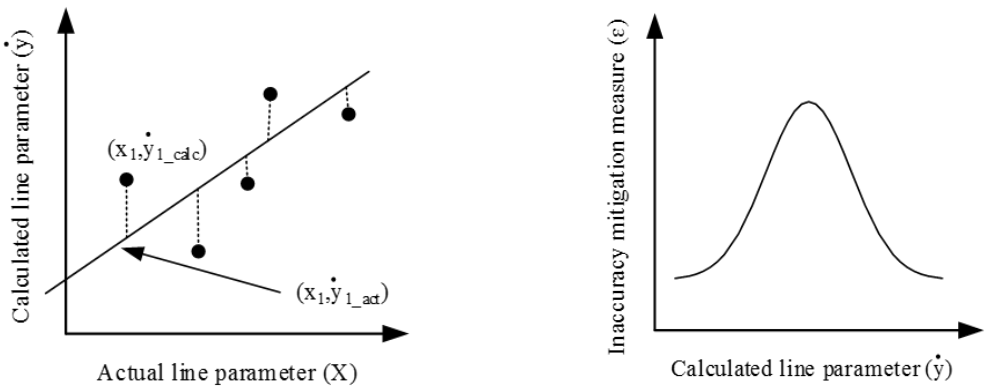

a) Actual vs. calculated line parameters **b) Proposed inaccuracy mitigation measure**

Figure 5-7: Indicative graphs of the proposed inaccuracy mitigation measure concept

5.5 Accuracy Evaluation Measures

The accuracy of the proposed methods is evaluated using different statistical measures. This is to ensure that the measures will converge for all case studies analyzed in this section. That is, in case one statistical measure fails to perform in one of the cases, the evaluation will be achieved by the other measures.

5.5.1 Percentage Error

The first step toward accepting or rejecting the proposed methods is assessing its accuracy using the percentage error given by the following equation:

$$Error\ (\%) \ = \frac{|Actual\ values - Calculated\ value|}{Actual\ value} \times 100 \qquad (5.27)$$

5.5.2 Coefficient of Determination

The coefficient of determination (CoD), denoted by R^2, is used to indicate the difference of the obtained values by a proposed formula compared to the actual ones. It measures the strength of the proposed formula and benchmark it with the ideal situation which will result

in a coefficient of determination of 100%. It is, also, called the squared error which is the error between the curve obtained by the proposed formula and the actual curve. The range of coefficient of determination varies between 0 to 1. The higher the number means the proposed formula is more descriptive and reflective to the actual values. Figure 5-8 is an explanatory sketch for calculating the CoD.

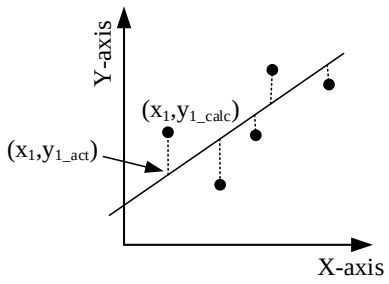

Figure 5-8: Coefficient of determination explanatory sketch

The coefficient of determination equation is formulated as follows [239]:

$$CoD = 1 - \frac{\sum_1^k (y_{calc} - y_{act})^2}{\sum_1^k (y_{calc} - \overline{y_{act}})^2}$$

$$= 1 - \frac{SE}{TV} \tag{5.28}$$

$$SE = \sum_1^k (y_{calc} - y_{act})^2 \tag{5.29}$$

$$TV = \sum_1^k (y_{calc} - \overline{y_{act}})^2 \tag{5.30}$$

The parameters are described as follows:

CoD	:	Coefficient of determination
SE	:	Total square error between the calculated points and the actual values
TV	:	Total variation between the calculated points and the actual values
$\overline{y_{act}}$	:	Mean of the actual values
y_{calc}	:	Calculated value
y_{act}	:	Actual value

5.5.3 Other Accuracy Statistical Measures

Other accuracy statistical measures are required to be integrated with the percentage error and CoD. This is due to the fact that the percentage error does not represent the correlation and the CoD has certain shortfalls, especially for small scientific numbers.

The following additional statistical measures are used to evaluate the proposals presented in this section:

1- Mean absolute deviation (MAD) which is the summation of the absolute deviation between the actual and calculated values over the number of records (or the length of the range). The MAD is given by the following formula:

$$\text{MAD} = \frac{\sum_{tc=1}^{nc} |A_{tc} - C_{tc}|}{nc} \tag{5.31}$$

Where nc is the number of simulations, A is the actual result and C is the calculated value.

2- Mean square error (MSE) which is considered as the most common error metric. It is mainly the summation of the squared errors over the number of records. The MSE is given by the following formula:

$$\text{MSE} = \frac{\sum_{tc=1}^{nc}(A_{tc} - C_{tc})^2}{nc} \tag{5.32}$$

3- Root mean square error (RMSE) is obtained by applying the square root to the RMSE. The RMSE is given by the following formula:

$$\text{RMSE} = \sqrt{\frac{\sum_{tc=1}^{nc}(A_{tc} - C_{tc})^2}{nc}} \tag{5.33}$$

4- Mean absolute percentage error (MAPE) is the average of absolute errors over the actual records. The MAPE is given by the following formula:

$$\text{MAPE} = \frac{\sum_{tc=1}^{nc}\left|\frac{A_{tc} - C_{tc}}{A_{tc}}\right|}{nc} \tag{5.34}$$

5.6 Case Studies

A 25 kV distribution system is modeled in MATLAB/Simulink to verify the effectiveness of the three line parameters identification techniques, see Figure 5-9. A total of 12,960 different case studies have been performed for the three techniques and three DL parameters. This is completed under six main loading scenarios and four categories with changing of the line parameters. The line parameters have been varied in 60 steps. Descriptions of the case studies,

loading scenarios and categories are tabulated in below tables. The total number of case studies is obtained from the fact that the areas of study (described in Figure 5-1) are repeated in each other. That is the 60 steps are considered for each category, each category is simulated for each loading scenario, each scenario is calculated for each parameter and so forth.

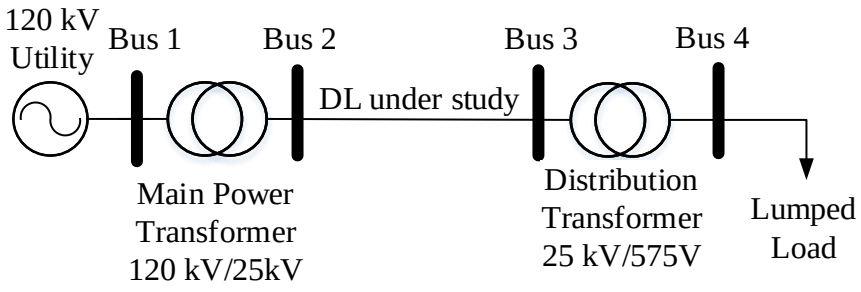

Figure 5-9: The 4-bus 25 kV distribution system under consideration

Table 5-1: Case studies descriptions for the Chapter 5

No.	**Area of Study**		**Additional Information/Reference**
	Area	**No.**	
1.	Techniques	3	OFT, SMT and TPCMT
2.	Parameters	3	R, L and C
3.	Loading scenarios	6	Table 5-2
4.	Study categories	4	Table 5-3
5.	Parameters values	60	The line parameters have been varied in 60 steps
	Total	**12,960**	The total is calculated by multiplying the number of areas of study

Table 5-2: Simulations loading scenarios

Scenario	Load	
	Active (MW)	Reactive (MVar)
1	1	0.25
2	2	0.5
3	3	0.75
4	4	1
5	5	1.25
6	6	1.5

Table 5-3: Categories of the study

Category	Description
1	Phase quantities
2	Positive-sequence quantities
3	Phase quantities with noise
4	The proposed inaccuracy mitigation applied to Category 3

The large number of case studies have been developed to test the robustness and accuracy of this section proposals. The 12,960 simulations differ in the loading conditions, line lengths, noise and inaccuracy mitigations.

The selected DL is modeled as three-phase DL with a π-type. The model consists of one set of resistance and inductance elements in series connected between sending and receiving

terminals. Two sets of shunt capacitances lumped are, also, included at both ends as illustrated in Figure 5-4. The initial DL parameters are stated in Table 5-4.

Table 5-4: Initial parameters of the distribution line test circuits

Parameter	**Actual Value**	**Dimension**
r	0.1153	(Ohms/km)
l	1.05e-3	(H/km)
c	11.33e-009	(F/km)

Where r, l, and c are the resistance, inductance and capacitance per unit length, respectively.

The total series resistance, reactive inductance and shunt admittance are given by the following formulas, respectively:

$$R = r\ell \tag{5.35}$$

$$X_{DL1} = \omega L\ell \tag{5.36}$$

$$Y_{DL} = \omega C\ell \tag{5.37}$$

Where R, L and C are the total DL resistance, inductance and capacitance, and ℓ is the total length of the line.

In MATLAB, two sets of simulated PMUs are placed at both terminals of the selected DL to measure the voltages and currents waveforms simultaneously. The recorded waveforms are in the shape of sinusoidal signals and then converted into phasor equivalents.

5.7 Results and Discussions

The simulation results of the 12,960 cases are summarized in this part and organized into four categories. Under each category, the resistance, reactive inductance and shunt admittance are calculated using the three methods for different loading conditions and parameter values. The calculation is based on the voltage and current signals obtained from PMUs that are installed at both ends of the line. Figure 5-10 shows the voltage and current signals obtained from PMU devices considering noise free system. Appendix B display the detailed simulation results for the discussion in the following sections.

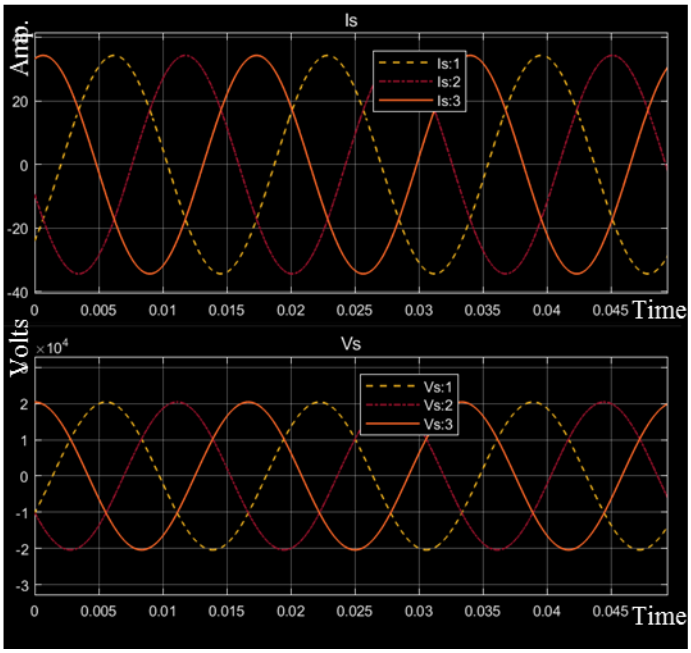

Figure 5-10: PMU current and voltage signals with noise free

5.7.1 Phase Quantities

In this category, the phase quantities of voltage and current are used to perform the analysis. This type of analysis is required for asymmetrical related studies such as unbalanced fault analysis.

The values of resistance, reactive inductance and shunt admittance are changing in 60 steps. The parameters identification errors of the six loading scenarios are averaged for the three methods. The voltage and current waveforms are assumed to be noise free. Results of the average errors for the resistance, reactive inductance and shunt admittance are shown in Figure 5-11. The maximum errors for each method are displayed in Table 5-6. The TPCMT shows weakness in calculating the shunt admittance for short lines. This is expected as the method was developed specifically for medium transmission lines. However, it performs very well when the DL length is ranging between 10 and 30 km which is a common sort of DLs.

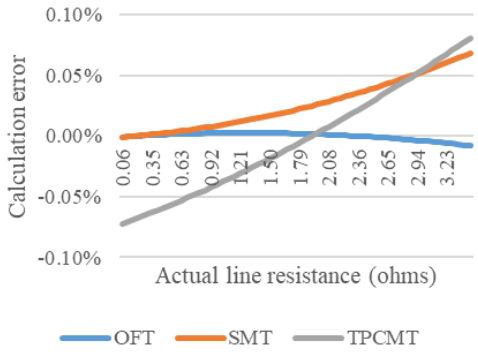

a) **Resistance**

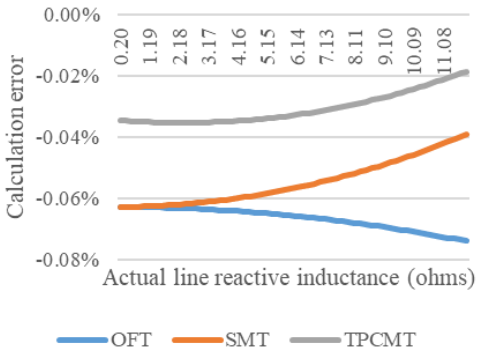

b) **Reactive inductance**

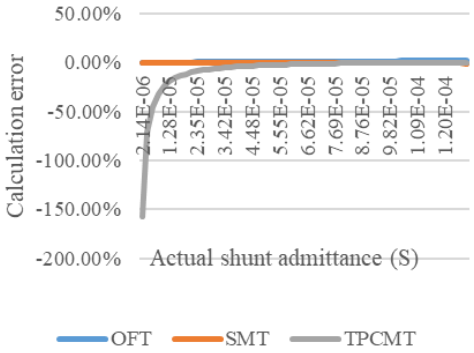

c) **Shunt admittance**

Figure 5-11: Calculation average errors of the six loading scenarios for the three methods under Category 1

5.7.2 Positive-sequence Quantities

Both OFT and SMT have excellent performance in identifying the DL parameters using positive-sequence quantities. The average and maximum errors recorded in the simulated studies are presented in Figure 5-12 and Table 5-6, separately. It is observed form the results that TPCMT fails to calculate the line parameters using positive-sequence voltage and current quantities. Therefore, the results were excluded from Figure 5-12. The results demonstrate that SMT is superior to OFT in calculating the line parameters using positive-sequence quantities.

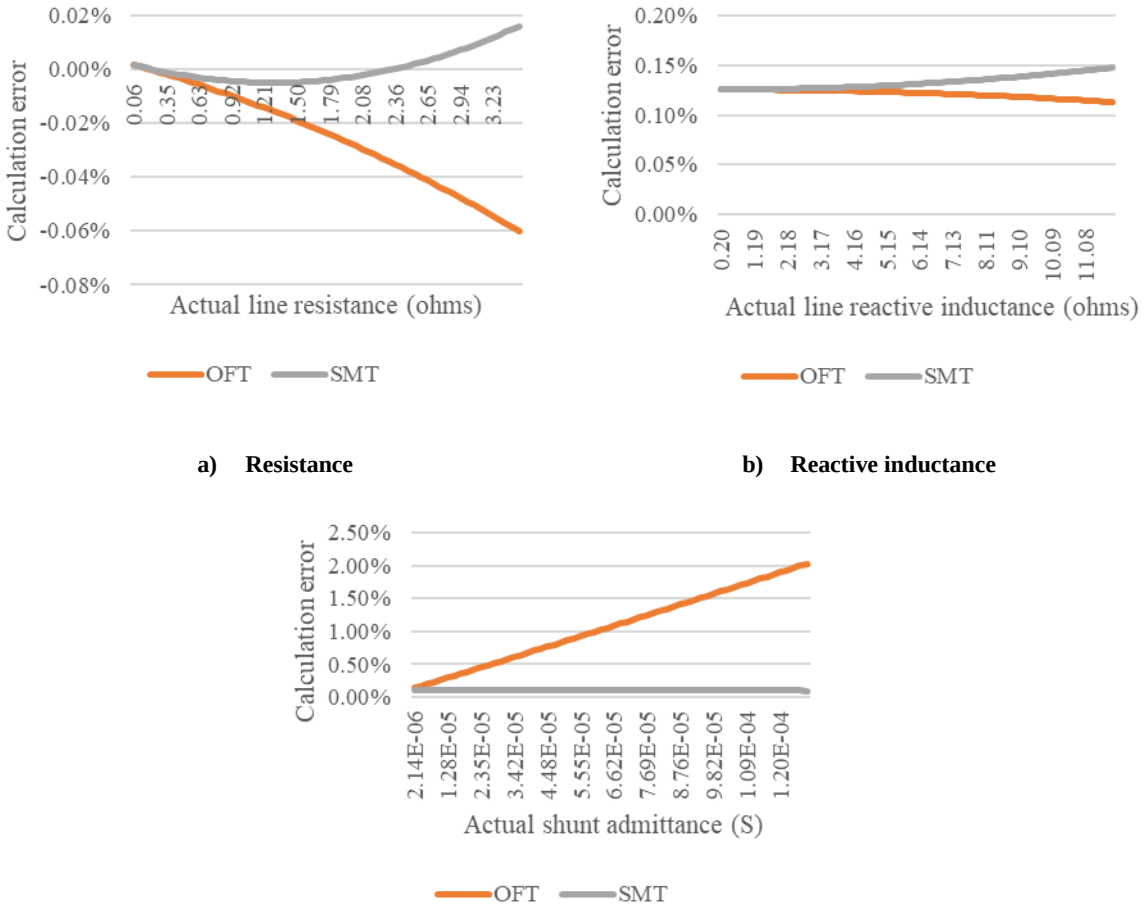

a) Resistance

b) Reactive inductance

c) Shunt admittance

Figure 5-12: Calculation average errors of the six loading scenarios for the OFT and SMT techniques under Category 2

5.7.3 Phase Quantities with Noise

Actual voltage and current signals of any distribution system are not pure sinusoidal. Noise is always impeded in the signals due to several factors, e.g. harmonics produced from electronic based devices. The electronic devices could be at residential areas such as televisions, computers, laptops, electronic games and so on. There are a number of applications that produce harmonics at the industrial sector, for example capacitor bank, variable frequency drives and other electronic based equipment.

Accordingly, all input signals to PMUs will be associated with additional harmonics beside the fundamental frequency (60 Hz) as in the Kingdome power system. Although PMU measurements showed an improved accuracy compared to other devices, this performance is not fully materialized in the actual field due to errors from other channels such as instrumentation, CT, and potential transformer and etc.

Figure 5-13 shows the voltage and current signals obtained from PMU devices considering noisy system.

The OFT and SMT have extraordinary performance when applying the phase values to noisy system, see Figure 5-14. TPCMT still shows weakness in estimating the line parameters, especially for short lines capacitance. As the line length increases as TPCMT converges for identifying the X_C.

The maximum error recorded in the simulated studies are shown in Table 5-6. From the calculated average and maximum errors of the six loading scenarios for the three methods considering phasor quantities, it is concluded that SMT is superior to the other techniques for noisy system.

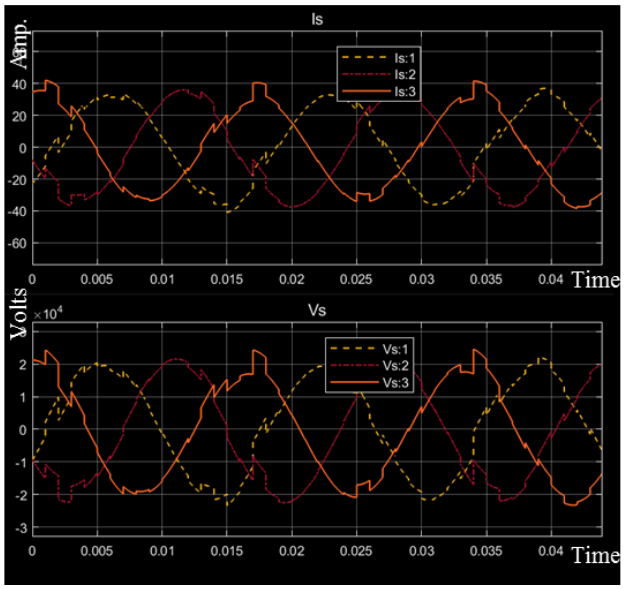

Figure 5-13: PMU current and voltage signals with noise

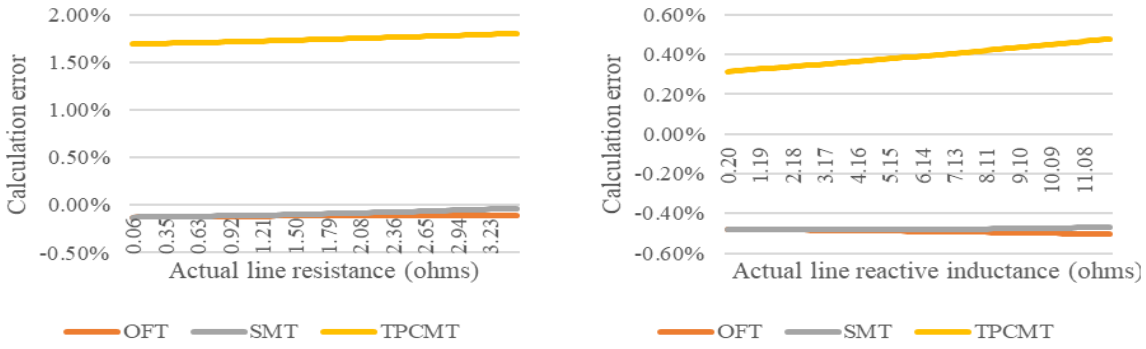

a) Resistance **b) Reactive inductance**

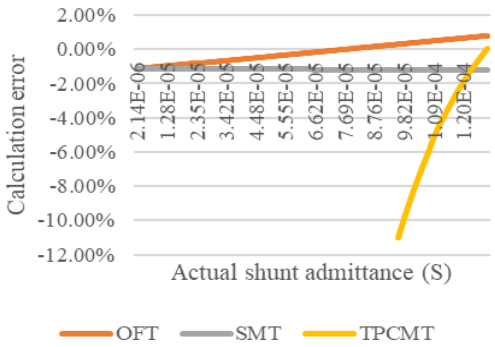

c) Shunt admittance

Figure 5-14: Calculation average errors of the six loading scenarios for the three methods under Category 3

5.7.4 Phase Quantities with the Proposed Inaccuracy Mitigation for Noisy Systems

It is observed form the simulated case studies shown in Appendix B that the error follows specific trend under different line parameters, irrespective of the loading conditions. Knowing the error trend will ease predicting the error magnitude and hence mitigating it. This category proposes to apply inaccuracy mitigation measures to improve the line parameter calculation errors. The measures are developed based on line characteristics and possible loadings. The proposed inaccuracy mitigation measure concept is illustrated in Figure 5-15 and given by the following formula:

$$\ddot{y} = \dot{y}(1 + \varepsilon(\dot{y})) \tag{5.38}$$

Where $\dot{y}$ is the originally calculated value and $\ddot{y}$ is the enhanced measurement. The symbol ε is taken from the pre-developed inaccuracy mitigation measures demonstrated in Figure 5-15. The inaccuracy mitigation curve could take different shapes based on line loading and characteristics.

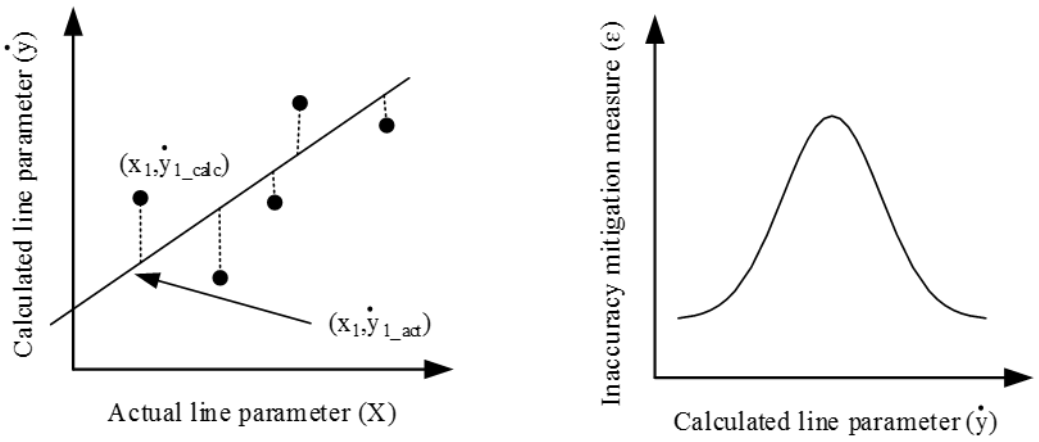

a) Actual vs. calculated line parameters **b) Proposed inaccuracy mitigation measure**

Figure 5-15: Indicative graphs of the proposed inaccuracy mitigation measure concept

The proposed concept has been applied to Category 3 and the simulation results are illustrated in Figure 5-16. The results reveal significant improvements of Category 4 compared to Category 3 in Figure 5-14.

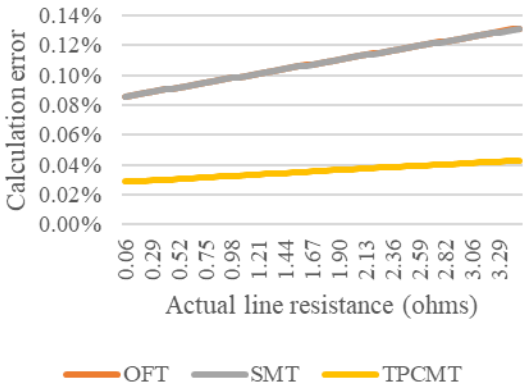

a) **Resistance**

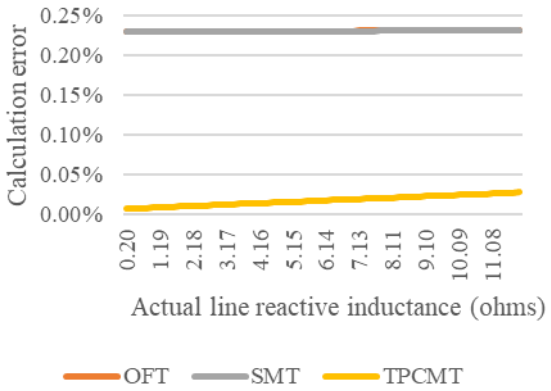

b) **Reactive inductance**

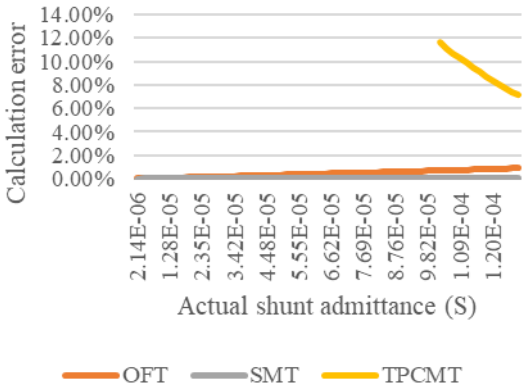

c) **Shunt admittance**

Figure 5-16: Calculation average errors of the six loading scenarios for the three methods under Category 4

5.7.5 Methods Evaluation

The MAD, MSE, RMSE, MAPE and CoD have been applied to the four categories and six loading scenarios. The results for the latter are averaged into one value for each category and

parameter. The results are tabulated in Table 5-5 to evaluate the robustness of this section proposals. It is noticed from the table that generally the values under the proposed inaccuracy mitigation measures category (Category 4) are improved compared to those in Category 3. This shows the strength of the proposed inaccuracy mitigation concept which could be applied for ideal and noisy systems. The use of positive-sequence quantities will perform very well when using OFT and SMT. However, the phase quantities will result in more accurate line parameters estimation. Unlike OFT and SMT, TPCMT does not function when using the positive-sequence values. Therefore, ABCD should not be used for any asymmetrical related studies in DLs.

MAPE is found to be the only method applicable for calculating the line shunt admittance since the values of the capacitances are very small scientific numbers. MAD, MSE, RMSE, MAPE and R^2 resulted in zero values as shown in Table 5-5. The zeros do not demonstrate the correlation as they do not work for small scientific numbers.

The inaccuracy mitigation measures will result in accuracy improvement up to 98% of the maximum error of Category 3. The maximum errors for the four categories and six loading scenarios considering the variation of the line parameters are tabulated in Table 5-6. The results confirm that the TPCMT does not perform for the sequence components and the capacitance identification as the errors as very high, refer to Table 5-6.

Table 5-5: Statistical measures results for all cases (in %)

Parameter	Statistical Measure	OFT				SMT				TPCMT			
		Category											
		1	2	3	4	1	2	3	4	1	2	3	4
Resistance	MAD	0.05	0.14	0.41	0.41	0.13	0.09	0.38	0.41	0.14	0.00	6.20	0.14
	MSE	0.00	0.00	0.00	0.00	0.00	0.00	0.00	0.00	0.00	0.00	0.26	0.00
	RMSE	0.04	0.14	0.34	0.34	0.14	0.08	0.33	0.34	0.15	0.00	5.07	0.12
	MAPE	0.02	0.06	0.24	0.22	0.05	0.04	0.22	0.22	0.08	0.00	3.49	0.07
	R^2	99.99	99.98	99.88	99.90	99.98	99.98	99.89	99.90	99.96	0.00	98.40	99.97
Inductance	MAD	0.83	1.44	5.97	2.78	0.61	1.65	5.76	2.78	0.34	0.00	5.08	0.25
	MSE	0.00	0.01	0.32	0.08	0.00	0.02	0.30	0.08	0.00	0.00	0.18	0.00
	RMSE	0.69	1.16	4.88	2.27	0.48	1.37	4.67	2.26	0.26	0.00	4.28	0.23
	MAPE	0.13	0.24	0.98	0.46	0.11	0.27	0.96	0.46	0.06	0.00	0.79	0.03
	R^2	99.99	99.99	99.96	99.98	100.0	99.99	99.96	99.98	100.0	0.00	99.97	100.0
Capacitance	MAD	-	-	-	-	-	-	-	-	-	-	-	-
	MSE	-	-	-	-	-	-	-	-	-	-	-	-
	RMSE	-	-	-	-	-	-	-	-	-	-	-	-
	MAPE	1.83	2.15	1.42	0.88	0.12	0.21	2.36	0.03	16.68	0.00	high	high
	R^2	-	-	-	-	-	-	-	-	-	-	-	-

Table 5-6: Maximum errors of the six loading scenarios considering the variation of the line parameters

Category	Method	R	X_L	X_C
1	OFT	0.04%	0.07%	3.35%
	SMT	0.09%	0.15%	0.07%
	TPCMT	0.12%	0.04%	high
2	OFT	0.11%	0.13%	3.45%
	SMT	0.08%	0.15%	0.11%
	TPCMT	high	high	high
3	OFT	0.45%	1.10%	2.22%
	SMT	0.38%	1.08%	1.22%
	TPCMT	1.87%	0.52%	high
4	OFT	0.34%	0.59%	1.49%
	SMT	0.34%	0.59%	0.03%
	TPCMT	0.10%	0.05%	high

5.8 Conclusion

To carry out any asymmetrical related analysis at DLs such as asymmetrical fault studies, the symmetrical components should be leveraged to identify the positive, negative and zero sequences. Therefore, robust and accurate line parameters calculation techniques are required. Based on that, three line parameters identification techniques have been applied to different case studies and evaluated using different statistical measures. The outcomes of this analysis along with the associated recommendations are as follows:

1. SMT is ranked to be the most robust technique for identifying all DL parameters under different conditions and OFT comes the second. Therefore, it is recommended to use SMT for any distribution related case studies.
2. TPCMT fails to produce results using positive-sequence voltage and current signals. Therefore, it should not be applied for any asymmetrical studies at the distribution level.
3. The proposed inaccuracy mitigation concept will result in accuracy improvement up to 98% of the maximum error. Therefore, it is recommended to use this concept for any online impedance and admittance calculations using PMUs.
4. The inaccuracy of the line parameters estimation follows a specific trend over different scenarios. This will allow proper inaccuracy prediction and hence mitigation.
5. The proposed inaccuracy prediction and mitigation have resulted in a negligible deviation between calculated and actual DL parameters. This proves the robustness of the proposals of this section.
6. Both OFT and SMT have extraordinary performance in calculating the DL parameters using positive-sequence quantities. Therefore, it is recommended to use them for any asymmetrical-based analysis such as unbalanced fault studies.
7. SMT is superior to OFT in calculating the line parameters using positive-sequence quantities.
8. TPCMT does not perform when the line resistance is small (short line) and using phase quantities. This is expected as the method was developed for medium transmission lines. As the line impedance or length increase, TPCMT will boost up its resistance calculation accuracy.

9. It is expected the TPCMT will not perform very well for capacitance identification of short DLs. Therefore, it is unrecommended to use this method for short DLs.
10. Some statistical measures do not function under certain conditions, such as in case of small scientific figures. Therefore, there is a need for a wide range of statistical measures to ensure covering all study cases.

CHAPTER 6

IMPEDANCE-BASED FAULT LOCATION

This chapter proposes a new impedance-based fault location model for distribution grids. The concept of accuracy improvement, namely inaccuracy mitigation measures (IMMs) have been, also, considered. This is to reduce the error associated with the fault location estimation and hence expedite power restoration. The model includes asymmetrical and symmetrical fault classification and location algorithms. The algorithms along with the mitigation measures have been evaluated using different statistical measures. A total of 7,254 different case studies have been simulated and analyzed for different scenarios, cases, fault types and fault distances. The results demonstrate the effectiveness of this research proposals and their superiority to other publications in similar subjects. The inputs of the model are calculated online using voltage and current signals obtained from PMUs placed at the line two terminals. Finally, the study outcomes and the associated recommendations have been summarized for future works considerations.

6.1 Introduction

Fault location accuracy in distribution systems is the main intent of fault location studies. This is due to the fact that it will result in advancement of line repair and system restoration, and subsequently shorten the outage and interruption durations.

The majority of PMU-based fault location techniques have been developed for transmission. The available works associated with the fault location application of PMUs at distribution

grid is very limited. Fault location in distribution networks has the same criticality level, if not more, comparing to transmission due to the following reasons:

1. In numerous cases, DLs are installed underground, especially in residential and industrial areas for different justification. The justifications include that the aerial lines could be safety risky to people and affecting scene of the city. However, underground installation usually crosses roads and passes under third parties' territories which make the coordination more complicated. The issue is exacerbated further by the fact that underground circuits require feet patrolling and inspection in case of maintenance and abnormal situations. Patrolling to inspect aerial transmission lines is performed by vehicles.
2. Live downed-conductors are common problems in distribution networks which create a safety risk. Hence, quick and accurate protective and fault location schemes are necessary.
3. Transmission lines are designed with acceptable redundancy to tolerate any planned and forced outages. Therefore, the faults could cause line outages but not necessarily power interruption to the customers. Unlike transmission, most of distribution circuits are designed to be radial type. Accordingly, any fault in the radial configuration DL will cause interruptions. This could result in tremendous amount of opportunity loss and actual money loss.
4. Distribution system faults account for more than 80% of customer interruptions [3]. This large percentage confirms the high priority of fault location in distribution grids.

The above four considerations justify the innovation and creation for swift and accurate fault location in distribution networks.

The literature publications of fault location methods in distribution networks using PMUs could be organized into four (4) main categories as follows:

1. Impedance-based methods considering the fundamental voltage and current signals and the network parameters to find the fault locations [95]–[99], [240]–[245].
2. Travelling wave techniques utilizing the travelling waves of the voltage and current between the network terminals during the fault [102], [162], [246]–[248].
3. Wavelet which is a mathematical model used for digital signal processing with similar principles to Fourier analysis [100], [101].
4. Other techniques based on different approaches that are uncommonly used for fault location such as state estimation [103], [104].

In general, there is little efforts devoted for the impedance-based fault location application of PMUs at distribution grid. Paper [95] presented a method that works for different networks including active and passive, radial and looped with ranging precision in order of magnitude of 1%. A new PMU-based method was introduced in [96] to locate faults in distribution networks and the method was proven via simulations using MATLAB/Simulink for different types of faults. In Reference [97], an algorithm for optimal PMU placement was validated for a 7-bus test circuit in addition to IEEE 14 and 30-bus networks. The optimal PMU placement was performed to identify the fault location in both ring and radial types distribution systems, which was tested using 11-bus radial and 14-bus ring networks. Patynowski et al. in [98] discussed a new approach that collects the data from different sources for high impedance grounded or ungrounded lines. A new algorithm for HIF was introduced in [99] by Kargar and Zanjani. This type of faults is difficult to detect by over current protection relays because of low fault current. The algorithm is sensitive to any change in current phasor. The best

accuracy of fault location studies in distribution networks was achieved is 99.8% in Reference [100]. The method was based on a wavelet technique. The accuracies of References [95] and [96] were 99% which is the highest for impedance-based fault location techniques in distribution networks.

However, there are a number of factors influencing fault location accuracy using impedance-based techniques have not been addressed in these publications. In general, the main factors are itemized below:

1. Inaccuracy of identifying fault types for fault-locating algorithms. This affects the accuracy as some algorithms are effective in some fault types, e.g. LG.
2. Unaccepted deviation between the line parameters and the actual ones. This could be resulted from the total length of the line which could be identified with error, although the geometry of conductors and parameters are accurate.
3. Insufficient accuracy due to change in the line parameters resulted from surrounding circumstances (such as weather conditions: Snow, dusts, winter, and summer, etc.), loading conditions and aging of the network.
4. Uncertainty of the zero-sequence impedance as it impacted by soil resistivity which varies under different conditions including the weather (e.g. rainy, sunny and dry, etc.).
5. Lack of accurate line models that take into account transposition, inhomogeneity, shunt admittance, mutual effects and so on.

Accordingly, considering fixed line parameters will play a major role in increasing the calculation error. The accurate data of DL parameters improves the precision of locating faults.

This chapter proposes inaccuracy prediction and mitigation of impedance-based fault location in DLs using PMUs. Swift and accurate fault location will advance the faulty lines restoration in the industry in which currently it is heavily depends on manual foot patrols with electronic locators and fault finders [249]. Superposition is introduced in Section 6.2. which will be used in developing the asymmetrical fault location method. Section 6.3 explains the four-sample method that is used to produce the phasor quantities from the sampled signals. In Section 6.4, the line parameters are identified online through the voltage and current waves obtained from the installed PMUs. This is to overcome the deficiencies associated with the fixed predefined line parameters. Fault classification is presented in Section 6.5. Sections 6.6 and 6.7 describe the proposed fault location model along with inaccuracy prediction and mitigation, respectively. Section 6.8 presents the percentage error formula which is used along with others to evaluate the effectiveness of proposed model in detecting the fault with high accuracy level under different scenarios. The developed case studies along with their results and discussion are presented in Sections 6.9 and 6.10, respectively. Finally, the study recommendations and outcomes are stipulated in Section 6.11.

6.2 Superposition for Fault Location

Linear systems obey the superposition principle which separates the faulty system (post-fault) into two circuits; steady state (pre-fault) and during fault circuits [250]. This will result in a

new circuit called superposed network. The superposed distribution system is converted into sequence electrical distribution system that is illustrated in Figure 6-1.

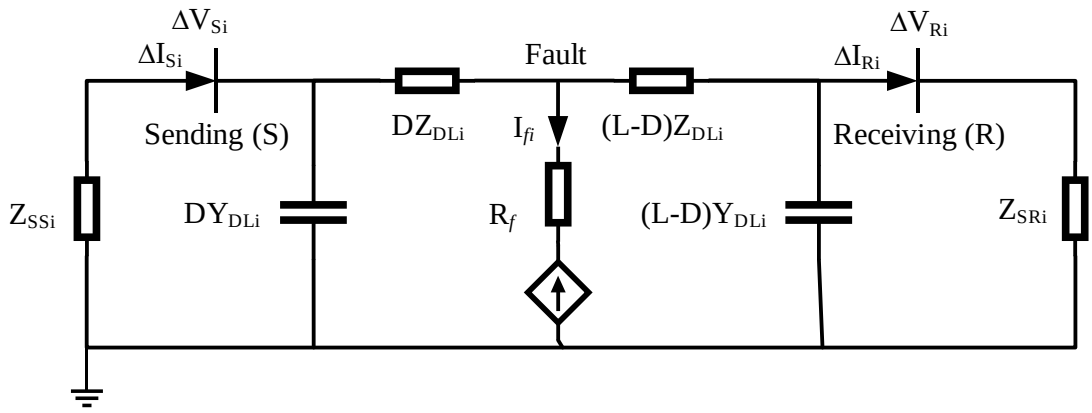

Figure 6-1: Superposed network of distribution system

The parameters of the above figure are described as follows:

i	:	Zero, positive and negative sequences (i=0,1,2)
Z_{SSi}	:	Equivalent i^{th} sequence source impedance at the sending end
Z_{SRi}	:	Equivalent i^{th} sequence source impedance at the receiving end
Z_{DL}	:	i^{th} sequence of distribution line impedance
Y_{DL}	:	i^{th} sequence of distribution line admittance
R_f	:	Fault resistance
I_{fi}	:	i^{th} sequence of the fault current

ΔV_{Si}	:	i^{th} sequence of superposed voltage at sending end
ΔV_{Ri}	:	i^{th} sequence of superposed voltage at receiving end
ΔI_{Si}	:	i^{th} sequence of superposed current at sending end
ΔI_{Ri}	:	i^{th} sequence of superposed current at receiving end
L	:	|Total distribution line length
D	:	Distance of the fault from the sending end

Consider dV_{Sk}, dV_{Rk}, dI_{Sk}, and $dI_{Rk}$to be the superposed phase voltage and current at the two terminals of a DL, where k reflects the phase a, b or c. Applying the concepts of symmetrical components transformation method, the following yields:

$$\Delta V_{Si} = M^{-1} \times dV_{Sk} \tag{6.1}$$

$$\Delta V_{Ri} = M^{-1} \times dV_{Rk} \tag{6.2}$$

$$\Delta I_{Si} = M^{-1} \times dI_{Sk} \tag{6.3}$$

$$\Delta I_{Ri} = M^{-1} \times dI_{Rk} \tag{6.4}$$

Where, $M^{-1}$is the reciprocal of M that is known as the symmetrical component transformation matrix (SCTM) which converts the phasor quantities into their symmetrical components and it is given by the following:

$$M^{-1} = \frac{1}{3}\begin{bmatrix} 1 & 1 & 1 \\ 1 & a & a^2 \\ 1 & a^2 & a \end{bmatrix} \tag{6.5}$$

$$a = 1e^{i120^{\circ}} \tag{6.6}$$

The Z_{SSi} and Z_{SRi} are the equivalent source impedances at the source and load sides, respectively. Their values are directly related to the change of generation mode and load of the distribution system. In the current practice, these equivalent impedances are obtained from the Power bureau and they are changing every now and then. However, it is beneficial to calculate these values online for using them in the fault location model to reflect more practical and synchronized values. This work proposes to calculate the source impedances online at the two terminals of a DL using the superposed sequence voltage and current phasors. From Figure 6-1, the source impedances are estimated by applying Kirchhoff Laws as follows:

$$Z_{SSi} = \frac{\Delta V_{Si}}{\Delta I_{Si}} \tag{6.7}$$

$$Z_{SRi} = \frac{\Delta V_{Ri}}{\Delta I_{Ri}} \tag{6.8}$$

The equivalent source impedances will reflect the generation and load modes of the distribution grids during faults.

The utilization of superposition system configuration in fault location will reduce the effects of the distribution system pre-fault conditions on the location accuracy.

6.3 Four-Sample Method

The four-sample method is used in this section to convert the samples into phasors. The method is much similar to Fourier analysis in term of obtaining the fundamental (60 Hz)

component from noisy signals. The advantage of using the four-sample method is the simplicity and no trigonometric functions are involved.

This method also identifies the phase of the input waveform which is with respect to a zero reference. The reference is the midway between the first and second sampling instants. Figure 6-2 illustrates identification of a sinusoidal waveform in the presence of noise which is called also "Walsh function method". The figure indicates the simplicity of four-sample method.

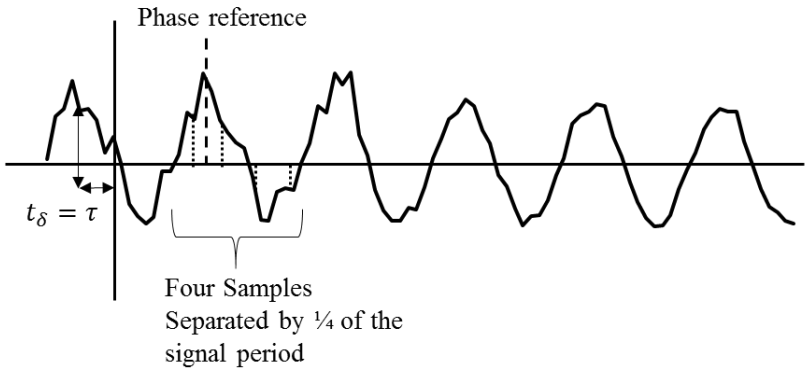

Figure 6-2: Four-sample method explanatory diagram (the concepts are obtained from [251]**)**

$$S = i_1 + i_2 - i_3 - i_4 \tag{6.9}$$

$$C = i_1 - i_2 - i_3 + i_4 \tag{6.10}$$

$$i_p = \frac{\sqrt{2}}{4}\sqrt{S^2 + C^2} \tag{6.11}$$

$$\delta = \tan^{-1}(\frac{C}{S}) \tag{6.12}$$

Where S and C are arbitrary parameters, i_p is the peak value of the measured signal and δ is the waveform phase angle. The δ value must be adjusted to account for the proper quadrant.

6.4 Online DL Parameters Identification Algorithms

To overcome line parameters related influencing factors on fault location accuracy, the line parameters are identified online. The identification is based on voltage and current signals obtained from PMUs placed at the line two terminals. The effects of ±20% inaccuracy of line parameters could result in substantial errors of fault location. The resulted error can reach up to 6.6% as per Reference [79].

The SMT is used to identify DL resistance, reactive inductance and shunt admittance. DL capacitance has been considered despite the fact that it does not play the same major role in the electrical power studies as in transmission. This is to ensure the high accuracy of the model is maintained. The SMT uses symmetrical components of the voltage and current signals that are obtained from PMUs at the steady state. The SMT equations are formulated as follows:

$$Z_{DLi} = \frac{V_{Si}^2 - V_{Ri}^2}{V_{Ri}I_{Si} + V_{Si}I_{Ri}} \tag{6.13}$$

$$Y_{DLi} = \frac{2(V_{Si} - V_{Ri})}{I_{Ri} + I_{Si}} \tag{6.14}$$

The effectiveness of this method in finding the symmetrical components of DL parameters have been investigated in Chapter 5.

The pre-fault symmetrical components of voltage and current at the sending and receiving ends are used. In case of symmetrical faults, either phase or positive-sequence voltage and current quantities are used to find the phase line parameters as recommended by Chapter 5.

6.5 Fault Classification

Fault classification method is an important pillar toward fault location. It is required for fault location algorithms selection and settings. That is, some methods are applicable for specific type of faults (e.g. symmetrical vs. asymmetrical). Additionally, identification of the exact faulty conductor is required for the maintenance crew to splice the effected section and perform the required repair.

A fault classification method has been proposed to classify the fault type in distribution networks. The method has been verified for all the case studies simulated for fault location. The simulation results confirm that the proposed algorithm is effective and applicable for detecting fault types in distribution network.

The fault type classification method is based on pre-fault, post-fault and superposed values of current signals obtained from PMUs. The method determines, first, the superposed phase current that has the minimum change. Then, the superposed phase currents are divided by that minimum change to produce value $k1_i$, where i represents the phases A, B or C. To ensure that it a fault and not overshooting, a new factor is developed which called fault check. This factor measures the superposed current values over the mean of pre-fault current to generate value $k2_i$. In case there is a real fault, $k2_i$ will be higher than one and multiplying it with $k1_i$ will magnify the sudden change. Therefore, a new factor $k3_i$ is introduced and given by the below equations. This factor value reflects the faulty phase.

$$k3_i = k1_i \, k2_i \tag{6.15}$$

$$k3_i = \begin{cases} 1, k3_i \geq average\ [k4 * k3_i, k1_i] \\ 0, k3_i < 0 \end{cases} \quad (6.16)$$

The constant $k4$ could take different values less than 1 (e.g. 0.8). Similar concepts apply to identify if a ground fault exists. The zero-sequence current is divided by the aforementioned minimum change. It is set to one if the resulted value is above pre-identified value ($k5$) and otherwise it will be zero. The factors $k4$ and $k5$ could be obtained by interfacing with the prospective fault analysis program to get the most likely ratios based on system characteristics and parameters. It is noticed during the simulations that the unfaulty phase for ground-involved faults is always a little bit higher compared if no ground-involved. This observation could help in developing the algorithm for the ground-involved faults.

The analysis of the fault location model presented in this work will use the knowledge of the fault type if it is balanced or unbalanced only. It will not require further details about the fault type to provide the fault location.

6.6 Impedance-based Fault Location Model

The proposed impedance-based fault location model for distribution grids using PMUs is demonstrated in Figure 6-3. The model consists mainly of two fault location techniques for asymmetrical and symmetrical fault types. The other components such as superposition, conversion to phasors, line parameters identification and fault type classification are explained in Sections 6.2, 6.3, 6.4 and 6.5, separately. The asymmetrical and symmetrical techniques are presented in Sections 6.6.1 and 6.6.2, respectively. Additionally, the model involves the inaccuracy mitigation measures which are introduced in Section 6.7.

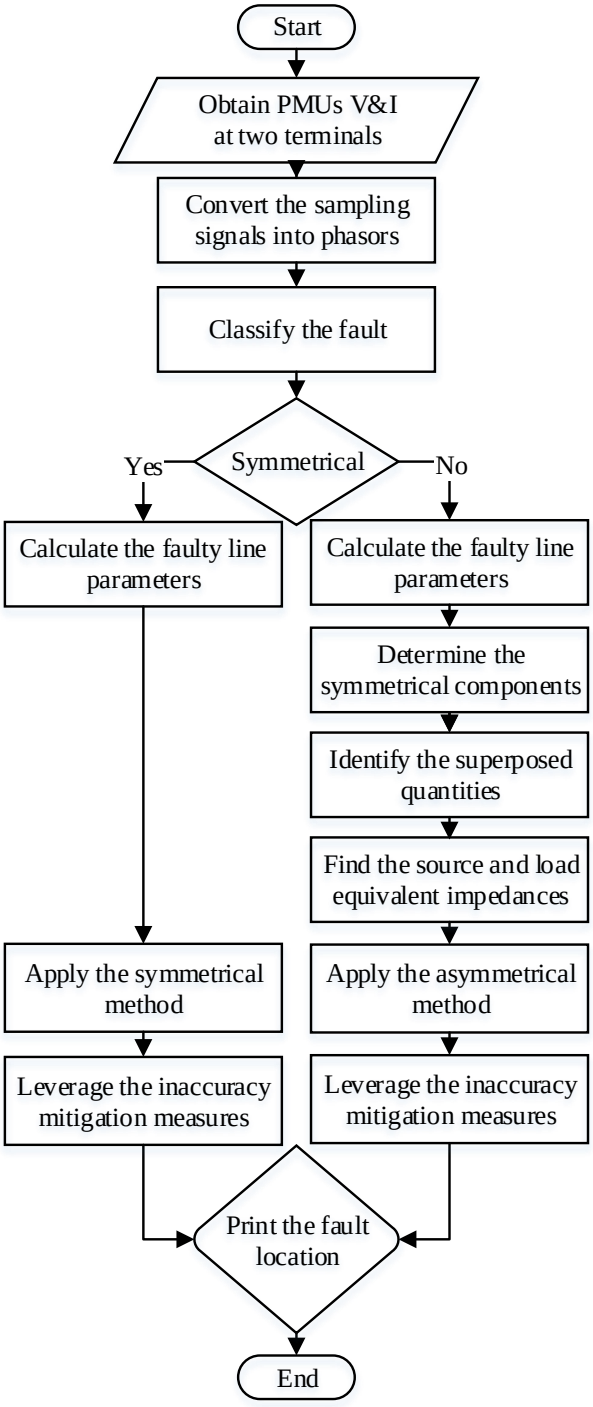

Figure 6-3: Flowchart of the proposed impedance-based fault location model

6.6.1 Asymmetrical Fault Location Algorithm

The proposed asymmetrical impedance-based technique leverages the sudden change of the system conditions resulted from the fault. This is to solve for the symmetrical components of voltages at the sending and receiving ends. The sudden change of voltage and current signals of the faulty DL shown in Figure 6-1 are defined by in the following fault location equations:

$$V_{SFi} = (\Delta I_{Si} - D\Delta V_{Si} Y_{DL}) \left(\frac{Z_{SSi}}{1 + DZ_{SSi} Y_{DL}} + DZ_{DL} \right) \tag{6.17}$$

$$V_{RFi} = (\Delta I_{Ri} - (L - D)\Delta V_{Ri} Y_{DL}) \left(\frac{Z_{RSi}}{1 + (L - D)Z_{SSi} Y_{DL}} + (L - D)Z_{DL} \right) \tag{6.18}$$

The $V_{SFi}$and V_{RFi}must be equal at the fault location when calculated from the sending and receiving terminals, respectively. This is achieved by considering the data of the two terminals are absolutely synchronous. This will not take place unless synchronous measurement units are employed which shows the advantage of applying PMUs for fault location. Therefore, the fault location model will be as follows:

$$\begin{aligned} &\left| (\Delta I_{Si} - D\Delta V_{Si} Y_{DL}) \left(\frac{Z_{SSi}}{1 + DZ_{SSi} Y_{DL}} + DZ_{DL} \right) \right| = \\ &\left| (\Delta I_{Ri} - (L - D)\Delta V_{Ri} Y_{DL}) \left(\frac{Z_{RSi}}{1 + (L - D)Z_{SSi} Y_{DL}} + (L - D)Z_{DL} \right) \right| \end{aligned} \tag{6.19}$$

The above model is to be solved for D which is the distance between the fault point and the sending bus. The solution can, also, be obtained graphically by plotting $V_{SFi}$and $V_{RFi}$for the full line length. The intersection point is the solution for the above fault location model that will provide the estimated D. Alternatively, the solution can be found through the following objective function:

$$D = \min(|V_{SFi}| - |V_{RFi}|) \tag{6.20}$$

The flowchart of the proposed asymmetrical impedance-based fault location algorithm is shown in Figure 6-3.

6.6.2 Symmetrical Fault Location Algorithm

In general, symmetrical fault analysis is less involved compared to the asymmetrical approach. The proposed symmetrical impedance-based fault location approach builds on the principle of voltage drop. First, the approach identifies the voltage rise as it is calculated from the receiving end using the receiving end voltage and current and moving toward the sending terminal. Similarly, it calculates the voltage reduction as it moves from the sending end toward the receiving end using the sending terminal quantities.

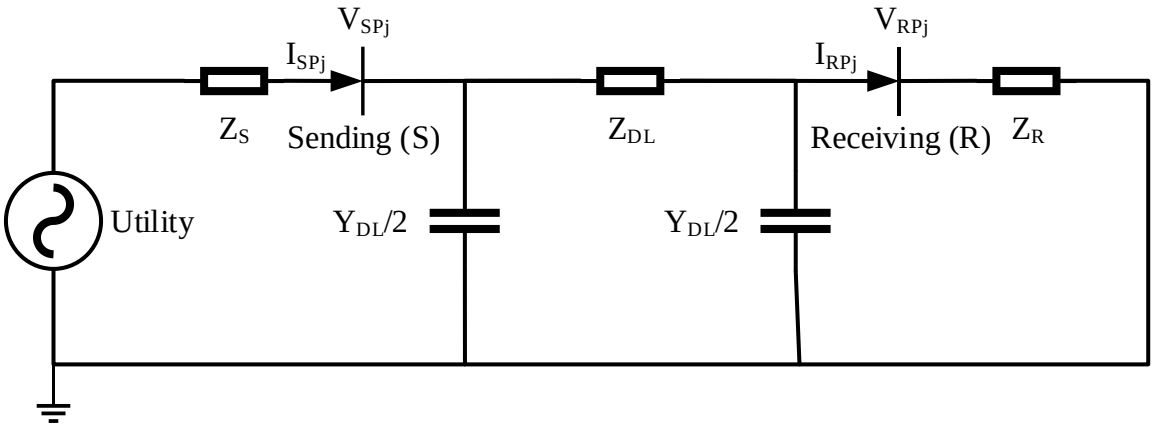

Figure 6-4: Distribution network for Symmetrical algorithm

The parameters of the above figure are described as follows:

j : Represents the phase (j= a, b and c).

Z_S : Equivalent impedance at the sending end

Z_R : Equivalent impedance at the receiving end

Z_{DL} : i^{th} sequence of distribution line impedance

Y_{DL} : i^{th} sequence of distribution line admittance

V_{SPj} : Post-fault phase voltage at sending end

V_{RPj} : Post-fault phase voltage at receiving end

I_{SPj} : Post-fault line current at sending end

I_{RPj} : Post-fault line current at receiving end

L : |Total distribution line length

The approach performs the fault location steps using post-fault phase quantities, applying them to the pre-fault circuit arrangement, i.e. assuming there is no fault in the DL. The novel equations developed for symmetrical fault location are as follows:

$$V_{SFj} = V_{Spj} - \left(I_{Spj} - D\, V_{Spj} Y_{DL}\right) D Z_{DL} \tag{6.21}$$

$$V_{RFj} = V_{Rpj} + \left(I_{Rpj} - (L - D)\, V_{Rpj} Y_{DL}\right)(L - D)\, Z_{DL} \tag{6.22}$$

The fault calculated distance D can be found by one of the following equations:

$$\left|V_{SFj}\right| = \left|V_{RFj}\right|, \text{ Solving for D} \tag{6.23}$$

$$D = first \min\left(\left|V_{SFj}\right| - \left|V_{RFj}\right|\right) \tag{6.24}$$

6.7 Inaccuracy Prediction and Mitigation

It is observed form the simulated case studies shown in Appendix C that the error follows specific trend under different fault resistance and loading conditions. Knowing the error trend will ease predicting its magnitude and hence mitigating it. This section proposes to apply inaccuracy mitigation measures to improve the fault location accuracy. The measures are developed based on line characteristics and possible faults' types and impedances. The proposed inaccuracy mitigation measure concept is illustrated in Figure 6-5 and given by the following formula:

$$\ddot{y} = \dot{y}(1 + \varepsilon(\dot{y})) \tag{6.25}$$

Where $\dot{y}$ is the originally calculated value and $\ddot{y}$ is the enhanced estimation. The symbol ε is taken from the pre-developed inaccuracy mitigation measures demonstrated in Figure 6-5. The inaccuracy mitigation curve could take different shapes based on line loadings and characteristics.

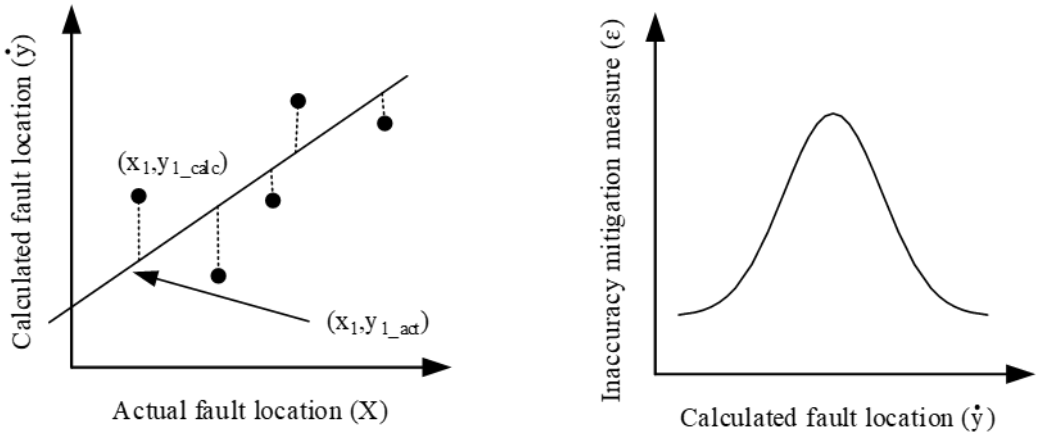

a) Actual vs. calculated fault location **b) Proposed inaccuracy mitigation measure**

Figure 6-5: Indicative graphs of the proposed inaccuracy mitigation measure concept

The inaccuracy mitigation measures (IMMs) can be organized into two categories as follows:

- Global-based inaccuracy mitigation measure (GIMM) which considers the average of all fault type errors for a specific case and under a specific algorithm;
- Local-based inaccuracy mitigation measure (LIMM) which develops a specific measure for each fault type.

The above two IMMs can be developed for each line as appropriate by the design consultant firms during the design phase of the lines, part of the protection and coordination studies.

6.8 Percentage Error

The first step toward accepting or rejecting the proposed methods is assessing its accuracy using the percentage error given by the following equation:

$$Error\ (\%) = \frac{|Actual\ values - Calculated\ value|}{Line\ length} \times 100 \tag{6.26}$$

6.9 Case Studies

The effectiveness of the proposed impedance-based fault location model has been validated using the 25 kV distribution systems shown Figure 6-6. A total of 7,254 different case studies have been performed under three different scenarios summarized in Table 6-2. Different fault types including LG, double line (LL), double line-to-ground (LLG), and three-phase faults.

Different fault locations have been selected starting from 0.50 km to approximately the total line length with a step size of 0.5 km.

The large number of case studies have been developed to test the robustness and accuracy of the proposed fault location model. The 7,254 simulations differ in the line lengths, fault locations, loading conditions, line parameters and applying IMMs.

The selected DL is modeled as three-phase DL with a π-type. The model consists of one set of resistance and inductance elements in series connected between sending and receiving terminals. Two sets of shunt capacitances lumped are, also, included at both ends as illustrated in Figure 6-1 and Figure 6-4.

In MATLAB, two sets of simulated PMUs are placed at both terminals of the selected DL to measure the voltages and currents waveforms simultaneously. The recorded waveforms are in the shape of sinusoidal signals and then converted into phasor equivalents.

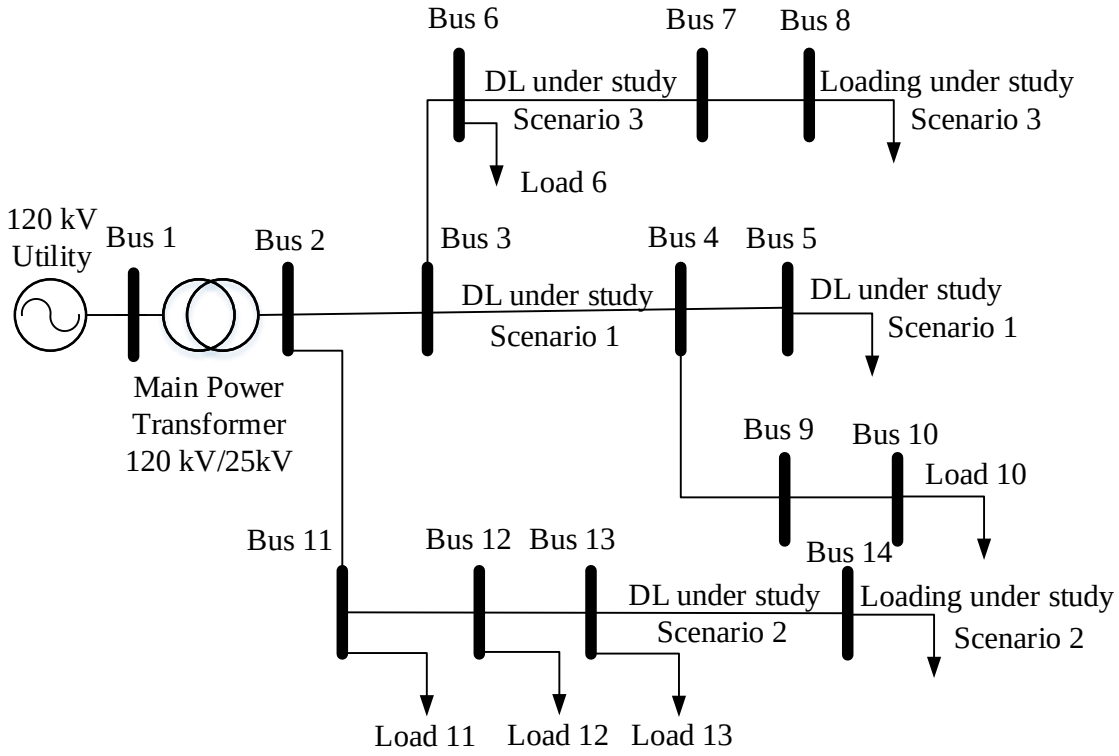

Figure 6-6: The 25 kV 14-bus test distribution network under consideration

Table 6-1: Case studies descriptions for Chapter 6

No.	Area of Case Study		Additional Information/Reference
	Area	No.	
6.	Unbalanced fault	3	LG, LL and LLG
7.	Balanced fault	1	LLLG
8.	Fault resistance (for asymmetrical)	6	0.001 Ω, 0.01 Ω, 0.1 Ω, 1 Ω, 10 Ω and 100 Ω
9.	Fault resistance (symmetrical)	4	0.001 Ω, 0.01 Ω, 0.1 Ω and 1 Ω
10.	Case (for asymmetrical)	3	1) Without IMM, 2) GIMM, and 3) LIMM

No.	Area of Case Study		Additional Information/Reference
	Area	**No.**	
11.	Case (for symmetrical)	2	1) Without and 2) with IMM
12.	Fault placement	117	The fault placements starting from 0.50 km to approximately the total line length with a step size of 0.5 km. That is 59, 39 and 19 different fault locations for the three scenarios presented in Table 6-2, respectively.
Total		**7,254**	(3 unbalanced fault) (6 fault resistances) (3 cases) (117 fault placements) + (1 balanced fault) (4 fault resistances) (2 cases) (117 fault placements)

Table 6-2: Parameters of the different simulation scenarios

Specification		Details		
		Scenario 1	**Scenario 2**	**Scenario 3**
Distribution line length (km)		30	20	10
Frequency (Hz)		60		
Loading Condition	MW	2	4	6
	MVar	0.5	2	3
R (Ω/km)	Positive & negative seq.	0.1153	0.0769	0.1153
	Zero-sequence	0.413	0.2753	0.413
L (H/km)	Positive & negative seq.	1.05e-3	0.0007	1.05e-3
	Zero-sequence	3.32e-3	0.0022	3.32e-3
C (F/km)	Positive & negative seq.	11.33e-9	0.1700e-7	11.33e-9
	Zero-sequence	5.01e-9	0.0751e-7	5.01e-9

6.10 Results and Discussions

This section summarizes the simulation results of the 7,254 cases and organizes them into two categories; asymmetrical and symmetrical. Under each category, the three simulation scenarios, in Table 6-2, are considered. The following cases are simulated for each scenario:

- Case 1: Base case which includes the results obtained directly from the proposed fault location methods shown in Figure 6-3 without applying the concept of IMM.
- Case 2: Global-based inaccuracy mitigation measure (GIMM).
- Case 3: Local-based inaccuracy mitigation measure (LIMM).

One inaccuracy mitigation measure is applied for the symmetrical approach as the three phases and three phases to ground faults use the same balanced faults analysis.

The calculation is performed based on the voltage and current signals obtained from PMUs that are installed at both ends of the line. Figure 6-7 and Figure 6-8 show the voltage and current signals obtained from PMU devices at the sending and receiving ends, respectively. The line considered is 30 km and the fault location is 25 k m away from the sending bus at the 0.05 second. In these specific two figures, Phase A to ground fault is applied. It is noticed that after 0.05 second both sending and receiving ends Phased A of the voltage is reduced and the current is increased. This is a normal phenomenon during LG faults. Therefore, certain models can be developed to detect and place these faults which is the intent of this study.

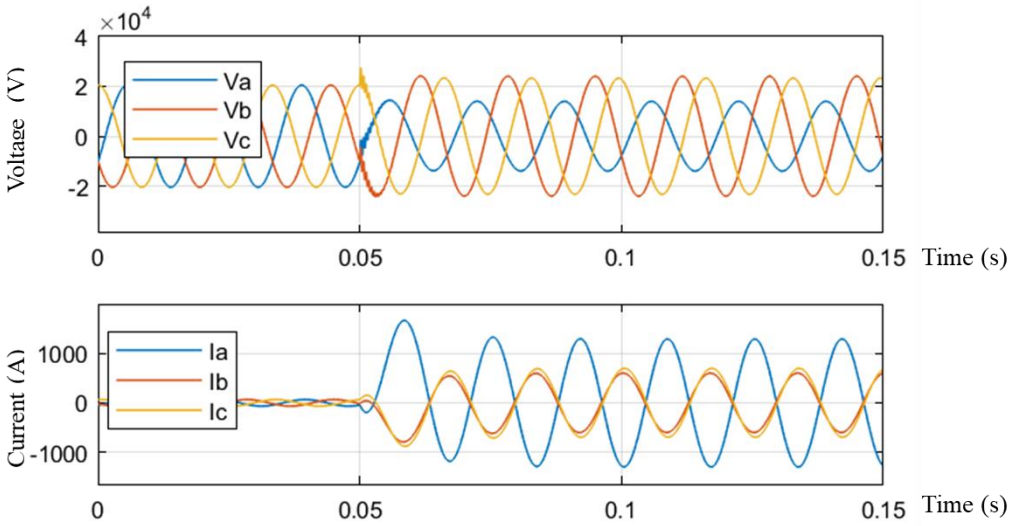

Figure 6-7: PMU voltage and current signals at the sending end with line-to-ground (AG) fault at the 0.05 second

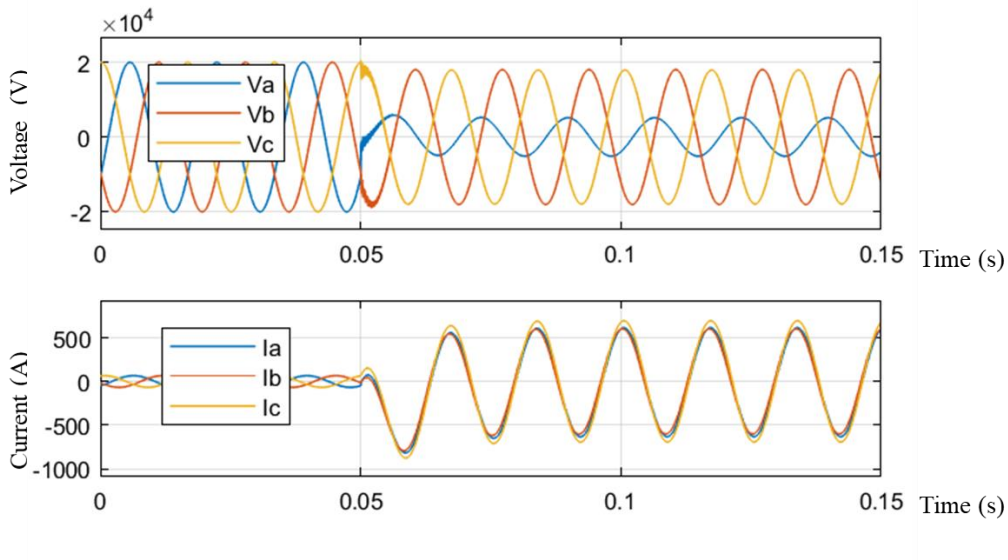

Figure 6-8: **PMU voltage and current signals at the receiving end with line-to-ground (AG) fault at the 0.05 second**

6.10.1 Asymmetrical Faults

The asymmetrical algorithms described in Section 6.6.1 have been applied to different types of unbalanced faults (LG, LL and LLG) for the three scenarios tabulated in Table 6-2. The faults have been placed at different distances in the studied systems starting from 0.50 km to approximately the total line length with a step size of 0.5 km. In each fault distance, the fault resistance has been varied to be 0.001 Ω, 0.01 Ω, 0.1 Ω, 1 Ω, 10 Ω and 100 Ω. The fault location at each distance has been averaged for the aforementioned fault resistance values.

The results are detailed in this part for the three cases; base case, GIMM and LIMM.

A. Base Case

The scenarios of Table 6-2 have been simulated by the proposed asymmetrical method for different fault distances and resistances. The average errors of fault resistances for fault distances and unbalanced fault types are demonstrated in Figure 6-9. The detailed actual fault errors are shown in Appendix C.

The results reveal that the error curves follow a particular concaved-down parabolic graph. The parabolic shape is almost similar for all asymmetrical method related simulations with minor differences. Subsequently, the error can be predicted and hence mitigated.

The maximum and average errors for the three scenarios considering the variation of both the distance and resistance of fault are displayed in Table 6-5. It is observed that as the line length decreases as the maximum and average errors drops. The best numbers are obtained for the LG and LL and then for LLG. The base case overall average error for all scenarios is 0.62% which reflects the accuracy of proposed asymmetrical fault location method using PMUs.

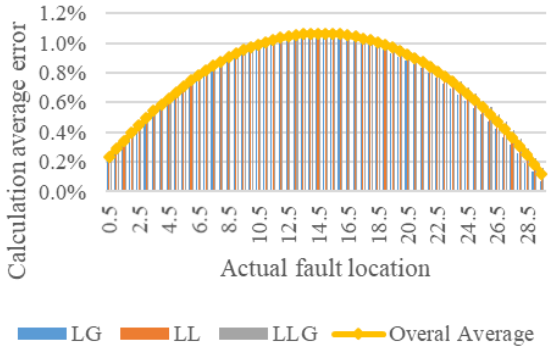

a) **Scenario 1**

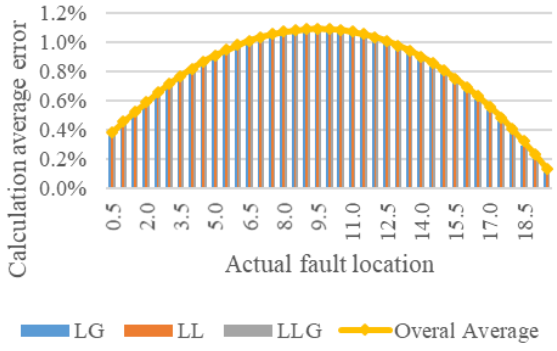

b) **Scenario 2**

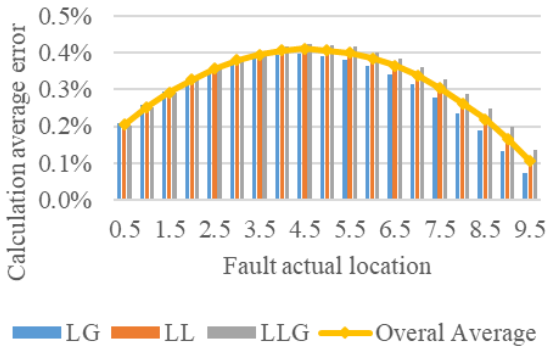

c) **Scenario 3**

Figure 6-9: Calculation average errors of fault resistances for the three scenarios under the proposed asymmetrical fault method (Case 1)

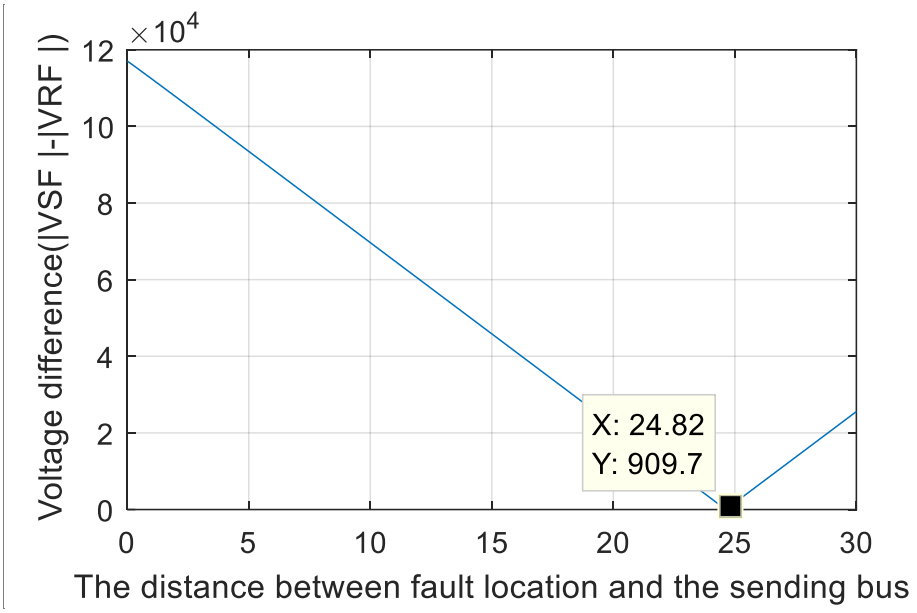

Figure 6-10: Fault location solution for line-to-ground (AG) fault at 25 km and 0.05 second using the asymmetrical

Figure 6-10 represents an example of fault location solitons using the proposed asymmetrical fault location algorithm. The line considered is 30 km and the fault location is 25 km away from the sending bus at the 0.05 second. The minimum point of $(|V_{SFi}| - |V_{RFi}|)$ reflects the calculated fault distance from the sending bus. More examples are shown in Appendix C.

B. Global-based Inaccuracy Mitigation Measure

The GIMM considers the average of all unbalanced fault types errors for a specific scenario. This is under different loading conditions and the change of both distance and resistance of the fault. The results are averaged for fault resistances at specific distance and shown in Figure 6-11. The detailed actual fault errors are shown in Appendix C.

The concept of global inaccuracy prediction and mitigation has revealed on a tremendous enhancement of the fault location accuracy. The inaccuracy reduction could reach up to 96% of the base case. This is observed in the maximum error of LL fault under Scenario 2 as shown

in Table 6-5 as the maximum error has been reduced from 1.12% to 0.05% (above 22 times of reduction). In simple terminologies, the error for the base case is equivalent to 224 meters. By the introduction of this novel concept, the uncertainty will drop to only 10 meters. The table includes the maximum and average errors for the three scenarios considering the variation of both distance and resistance of the faults.

The overall average error obtained by the GIMM for all scenarios is 0.030% which is more than 20 times less than the base case. This prove the robustness and effectiveness of the proposed GIMM.

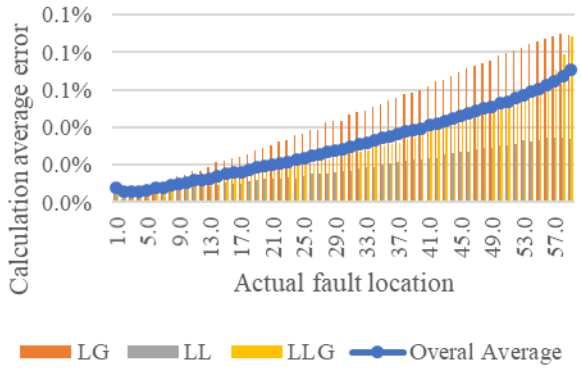

a) **Scenario 1**

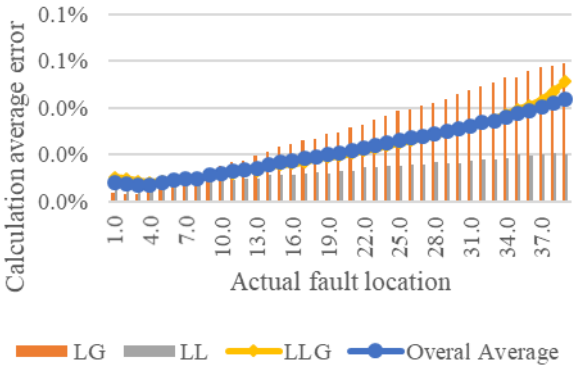

b) **Scenario 2**

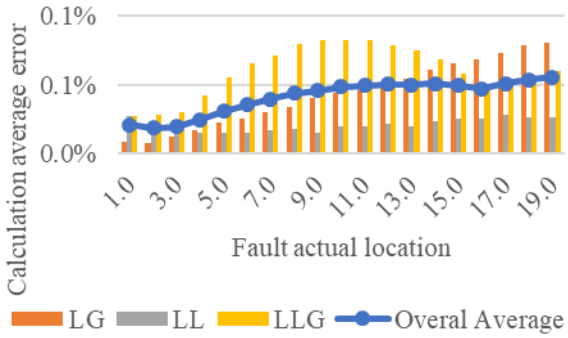

c) **Scenario 3**

Figure 6-11: Calculation average errors of fault resistances for the three scenarios under the GIMM (Case 2)

C. Local-based Inaccuracy Mitigation Measure

The LIMM measure is almost similar to the global except that it uses a specific measure for each type of faults. The measures are developed based on the change of both distance and resistance of the fault. The results are averaged for fault resistances at specific distance and presented in Figure 6-12. The detailed actual fault errors are included in Appendix B.

The concept of local inaccuracy prediction and mitigation has resulted in a similar tremendous enhancement of the fault location accuracy as in the global approach. It has achieved the same reduction level as the global of above 22 times comparing to the base case. The overall average error obtained by the LIMM measure for all scenarios is 0.027%. This number is less than both the base and global cases by 22.38 and 0.13 times, respectively. This proves the robustness and effectiveness of the proposed LIMM measure.

Table 6-5 presents the maximum and average errors for the three scenarios considering the variation of both distance and resistance of the faults.

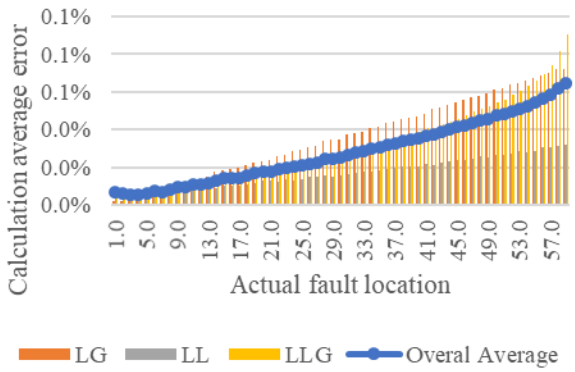

a) Scenario 1

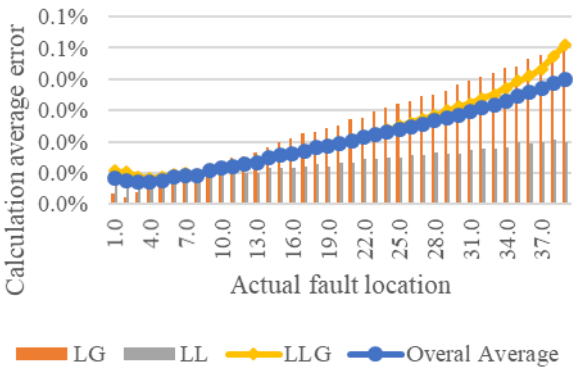

b) Scenario 2

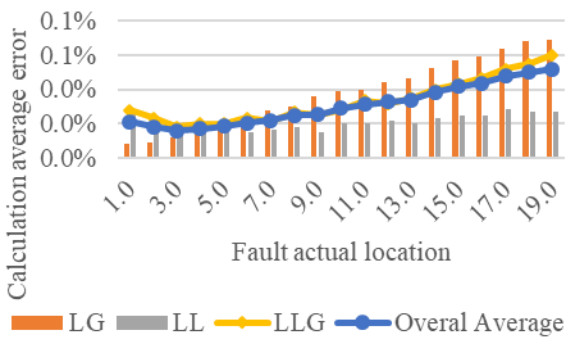

c) Scenario 3

Figure 6-12: Calculation average errors of fault resistances for the three scenarios under the LIMM measure (Case 3) under asymmetrical

6.10.2 Symmetrical Faults

The symmetrical algorithms described in Section 6.6.2 have been applied to different balanced faults for the three scenarios tabulated in Table 6-6. The faults have been placed at different distances in the studied line starting from 0.50 km to approximately the total line length with a step size of 0.5 km. In each fault distance, the fault resistance has been varied to be 0.001 Ω, 0.01 Ω, 0.1 Ω and 1 Ω.

The results are detailed in this part for two cases; base case and inaccuracy-based measures. The global will be the same as the local as the three phases and three phases to ground faults use the same balanced faults analysis.

A. Base Case

The scenarios of Table 6-2 have been simulated by the proposed symmetrical method for different fault distances and resistances. The average errors of fault resistances for fault distances and unbalanced fault types are demonstrated in Figure 6-13.

The results reveal that the error curves follow particular predictable trends. The curvature trends are almost similar for the three scenarios. Therefore, the error can be predicted and hence mitigated.

The maximum and average errors for the three scenarios considering the variation of both the distance and resistance of fault are displayed in Table 6-6. It is observed that as the line length decreases as the maximum and average errors drops. The base case overall average error for all scenarios is 0.067%. This very low number reflects the high accuracy of proposed symmetrical fault location method using PMUs.

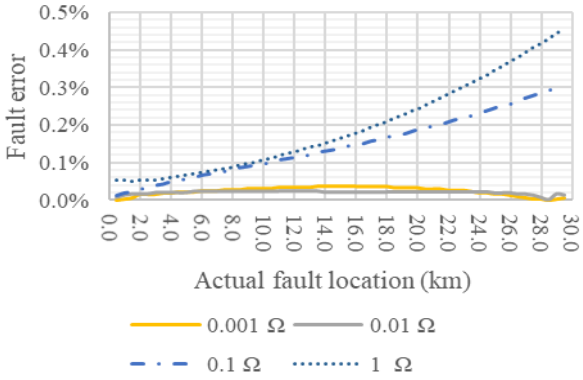

a) **Scenario 1**

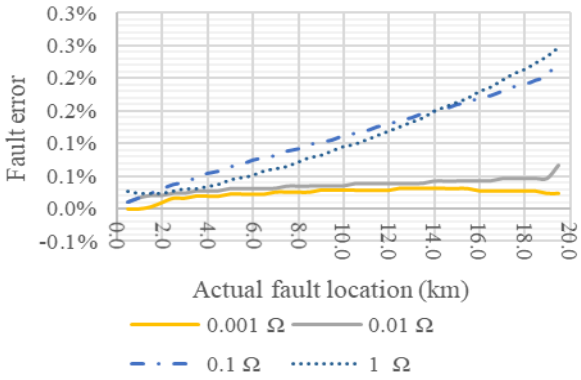

b) **Scenario 2**

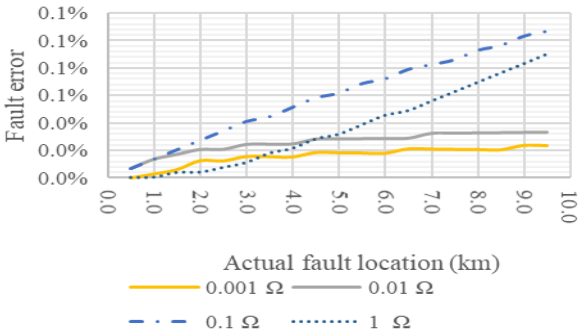

c) **Scenario 3**

Figure 6-13: Calculation errors of fault resistances for the three scenarios under the proposed symmetrical fault method (Base Case)

B. Inaccuracy Mitigation Measure

The resulted calculation errors of varying fault resistances for the three scenarios using the proposed inaccuracy mitigation measure are displayed in Figure 6-14.

The concept of inaccuracy prediction and mitigation has revealed on an enhancement of the fault location accuracy. The inaccuracy reduction could reach up to 43% of the base case maximum errors and 29% of their average. This confirms the robustness and effectiveness of the proposed inaccuracy mitigation measure.

Table 6-6 demonstrates the maximum and average errors for the three scenarios considering the variation of both distance and resistance of the faults.

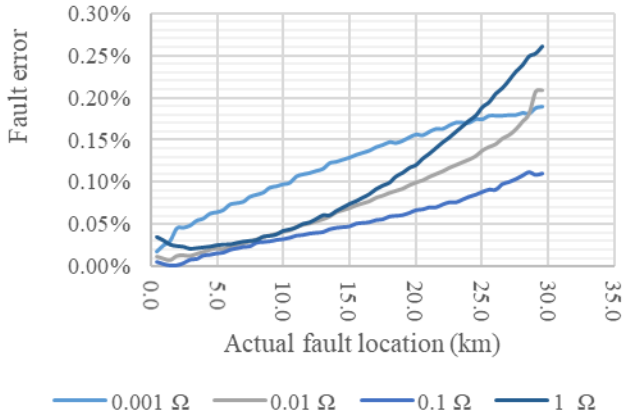

a) Scenario 1

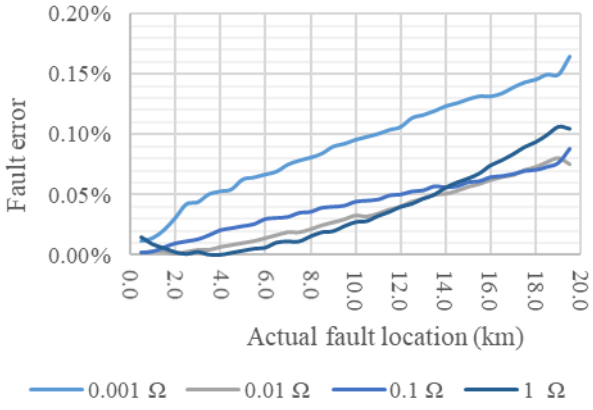

b) Scenario 2

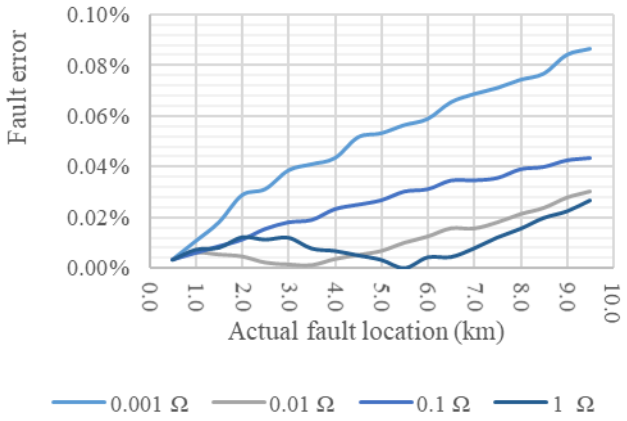

c) Scenario 3

Figure 6-14: Calculation errors of fault resistances for the three scenarios under the proposed symmetrical fault method

6.10.3 Model Evaluation

The MAD, MSE, RMSE, MAPE and CoD have been applied to the three scenarios, three cases and different resistance values. The results for the latter are averaged into one value for each scenario and case. The results are tabulated in Table 6-3 and Table 6-6 to evaluate the robustness of this section proposals. It is noticed from the tables that generally the values under the proposed IMMs categories are improved compared to those in the base case (Case1). This shows the strength of the proposed inaccuracy mitigation concept. Case 3 is superior to all cases and will provide super accurate results.

With the consideration of maximum and average errors presented in Table 6-5, the proposed IMMs concept is between 99.81% and 99.97%. The accuracy could reach more than four 9s if the minimum errors are considered.

Considering maximum and average errors shown in Table 6-6, the proposed IMMs concept is between 99.74% and 99.95%. The accuracy could reach more than four 9s if the minimum errors are considered.

Table 6-3: Statistical measures results for all asymmetrical-based simulations (in %)

Scenario	Statistical Measure	LG			LL			LLG		
		Case								
		1	2	3	1	2	3	1	2	3
1	MAD	21.95	1.36	1.08	22.98	0.55	0.51	23.42	0.89	0.93
	MSE	5.53	0.03	0.02	5.97	0.00	0.00	6.17	0.02	0.02
	RMSE	23.49	1.58	1.25	24.43	0.62	0.57	24.83	1.09	1.13
	MAPE	2.55	0.09	0.07	2.60	0.05	0.05	2.62	0.07	0.07
	R^2	99.97	100.00	100.00	99.96	100.00	100.00	99.96	100.00	100.00
2	MAD	23.50	0.92	0.77	24.01	0.40	0.40	24.27	0.67	0.67
	MSE	6.19	0.01	0.01	6.41	0.00	0.00	6.53	0.01	0.01
	RMSE	24.86	1.05	0.88	25.32	0.43	0.43	25.55	0.77	0.77
	MAPE	4.26	0.09	0.08	4.30	0.07	0.07	4.32	0.09	0.09
	R^2	99.88	100.00	100.00	99.88	100.00	100.00	99.88	100.00	100.00
3	MAD	2.99	0.43	0.38	3.16	0.21	0.21	3.28	0.60	0.33
	MSE	0.10	0.00	0.00	0.11	0.00	0.00	0.12	0.00	0.00
	RMSE	3.14	0.49	0.43	3.29	0.22	0.22	3.40	0.65	0.36
	MAPE	1.06	0.09	0.08	1.08	0.08	0.08	1.10	0.17	0.10
	R^2	99.86	99.99	99.99	99.86	99.99	99.99	99.85	99.98	99.99

Table 6-4: Statistical measures results for all symmetrical-based simulations (in %)

Statistical Measure	Scenario 1		Scenario 2		Scenario 3	
	Case					
	1	2	1	2	1	2
MAD	2.92	2.61	2.07	1.54	1.04	0.73
MSE	0.19	0.10	0.08	0.04	0.02	0.01
RMSE	3.36	3.06	2.35	1.81	1.19	0.83
MAPE	0.24	0.20	0.24	0.16	0.21	0.16
R^2	100.00	100.00	99.99	99.99	99.97	99.98

Table 6-5: Maximum and average errors for the three cases and scenarios considering the variation of both distance and resistance of fault under asymmetrical

Case	**Scenario**	**Error**							
		Maximum				**Average**			
		LG	LL	LLG	Overall	LG	LL	LLG	Overall
1	1	1.11%	1.11%	1.14%	1.14%	0.73%	0.77%	0.78%	0.76%
	2	1.12%	1.12%	1.13%	1.13%	0.78%	0.80%	0.81%	0.80%
	3	0.45%	0.44%	0.47%	0.47%	0.30%	0.32%	0.33%	0.31%
2	1	0.11%	0.06%	0.19%	0.19%	0.05%	0.02%	0.03%	0.03%
	2	0.07%	0.05%	0.14%	0.14%	0.03%	0.01%	0.02%	0.02%
	3	0.10%	0.06%	0.14%	0.14%	0.04%	0.02%	0.06%	0.04%
3	1	0.14%	0.07%	0.19%	0.19%	0.04%	0.02%	0.03%	0.03%
	2	0.08%	0.05%	0.11%	0.11%	0.03%	0.01%	0.02%	0.02%
	3	0.11%	0.06%	0.12%	0.12%	0.04%	0.02%	0.03%	0.03%

Table 6-6: Maximum and average errors for the three cases and scenarios considering the variation of both distance and resistance of fault under symmetrical

Case	Scenario	Maximum	Average
1	1	0.46%	0.10%
	2	0.25%	0.07%
	3	0.11%	0.03%
2	1	0.26%	0.09%
	2	0.17%	0.05%
	3	0.09%	0.02%

6.11 Conclusion

To advance the DL repair and system restoration, a prompt and accurate fault location approach is required. Based on that, an impedance-based fault location model has been developed and evaluated for different simulations by statistical measures. The model consists of two fault location techniques for asymmetrical and symmetrical faults. Additionally, global and local IMMs have been proposed to improve the fault location. The outcomes of this analysis along with the associated recommendations are as follows:

1. The proposed IMMs have significantly improved the fault location estimate up to 23 times compared to the base case. Their accuracies based on the maximum errors are 99.81% and 99.74% for the asymmetrical and symmetrical respectively. By applying the measures, fault location can be identified within few meters of the exact location if not at the actual location. These accuracies demonstrate the effectiveness of this research proposal and its superiority to other publications in similar subjects. This is

compared with the accuracies of References [95] and [96] which were 99% and represented the highest for impedance-based fault location techniques in distribution networks using PMUs.

2. Both asymmetrical and symmetrical techniques resulted in high-level of accuracy with overall average error of 0.62% and 0.067%, respectively.
3. It is observed that as the line length decreases as the maximum and average errors drops for both symmetrical and asymmetrical techniques.
4. The above two IMMs can be developed for each line by the design consultant firms during the design phase of the lines, part of the protection studies.
5. The proposed model does not suffer from the line impedance inaccuracy issues under the idea situation (homogeneous, radial, and uncompensated, etc.). This is due to this research's recommendation to calculate the line parameters online.

CHAPTER 7

IMPEDANCE-BASED FAULT LOCATION FOR INHOMOGENEOUS DISTRIBUTION GRIDS WITH PMUS

This chapter proposes a novel impedance-based fault location model for inhomogeneous distribution lines. The accuracy improvement method, namely Inaccuracy mitigation measures (IMMs) have, also, been considered. This is to improve the accuracy of fault location and hence advance power restoration. The proposed model includes asymmetrical and symmetrical fault classification and location algorithms. The fault location algorithms along with the mitigation measures have been evaluated using different statistical measures. A total of 9,477 different case studies have been simulated and analyzed for different scenarios, cases, fault types and fault distances. The results demonstrate the effectiveness of this research proposals. The inputs of the model are calculated online using voltage and current signals obtained from PMUs placed at the line two terminals. Finally, the study outcomes and the associated recommendations have been summarized for future works considerations.

7.1 Introduction

In general, numerous existing DLs are inhomogeneous. The inhomogeneity could be a result of the following:

1- Initial installation of DLs with different sections due to site conditions. Examples are an onshore power supply that feeds an offshore facility and power supply consists of both overhead conductors and underground cables.
2- Initial installation of homogeneous DLs with the same design parameters all over the line. However, the effective parameters are not homogeneous due to the installation at different environments. For example, the line will be underground and then over cable tray full of other cables. The clearances with the other cables and ambient temperature play major roles in changing the effective line parameters.
3- Splicing cables due to different reasons such as failure in the initially installed DL and rerouting the cable which will require additional length.

The combined or inhomogeneous DLs present a challenge for fault location, considering the traditional homogeneous-based techniques. This is due to the inequality of the parameters and their positive, negative and zero sequences for the different line sections. This mandates development of specific types of fault location methods for inhomogeneous lines. This is to support the utilities to locate faults in their distribution networks swiftly and accurately.

The available fault location techniques for inhomogeneous lines can be classified into two main techniques; impedance-based and travelling waves methods.

Regarding the first category, Reference [252] proposes to use currents and voltages obtained from a distance relaying to improve the impedance error. It addresses actual complicated situations of inhomogeneous transmission lines. In [253], a combination of overhead and underground power lines are considered. The method uses synchronized voltage and current signals. The authors emphasized on the importance of high accuracy fault location methods for combined transmission lines. Paper [34] recommended the use of a fault location algorithm in lieu of the line differential relays. Lin in [254] presented a fault location method for three-terminal multi-section inhomogeneous transmission lines. The method extended two-terminal fault location technique to three and included the use of PMUs. Reference [36] is a PMU-based fault location for inhomogeneous two terminals transmission lines.

Regarding travelling waves-based methods, Reference [93] demonstrated high-speed synchrophasor data that is not impacted by fault resistance, inhomogeneous voltage angles and mutual coupling. The authors of [255] propose a smart reclose scheme for combined transmission lines that consist of both underground cable and overhead line. This scheme leverages both the derived voltage module and travelling wave fault location methods to improve robustness and accuracy. Finally, [256] presents a method based on Hilbert-Huang transform for fault location in combined transmission lines was proposed. The method uses the concept of travelling waves without the use of synchronizer.

However, critical issues related to fault location for inhomogeneous (combined) lines have not been addressed yet. Such as the use of PMUs to locate faults in inhomogeneous distribution grids. Subsequently, this chapter proposes a novel impedance-based fault location model for inhomogeneous DLs. IMMs have, also, been considered. This is to improve the accuracy of fault location and hence advance power restoration. This chapter builds on the

concept of impedance-based fault location model in distribution grids that is presented in Chapter 6. The model presented in this part uses the concept of superposition, online parameters identification and fault classification presented in Sections 6.2, 6.4 and 6.5, respectively. Additionally, the fault location model along with inaccuracy prediction and mitigation presented in Sections 6.6 and 6.7 are used as initial building blocks. Building on these concepts, Section 7.2 describes the proposed fault location model for the inhomogeneous DLs. The developed case studies along with the results and discussions are presented in Sections 7.3 and 7.4, separately. Finally, the study recommendations and outcomes are stipulated in Section 7.5.

7.2 Impedance-based Fault Location Model for Inhomogeneous DLs

The proposed impedance-based fault location model for inhomogeneous distribution grids using PMUs is demonstrated in Figure 7-1. The model consists mainly of inhomogeneous DL fault location algorithms integrated with both asymmetrical and symmetrical fault location techniques. These two techniques are presented in Sections 6.6.1 and 6.6.2, separately. Additionally, the model involves the IMMs which are introduced in Section 6.7. The other components such as superposition, line parameters identification and fault type classification are explained in Sections 6.2, 6.4 and 6.5, separately.

The superposed sequence distribution system for the proposed method is illustrated in Figure 7-2. The figure is mainly for the asymmetrical fault type. However, the principle of the DL impedances representation and the developed algorithms apply to both asymmetrical and symmetrical methods.

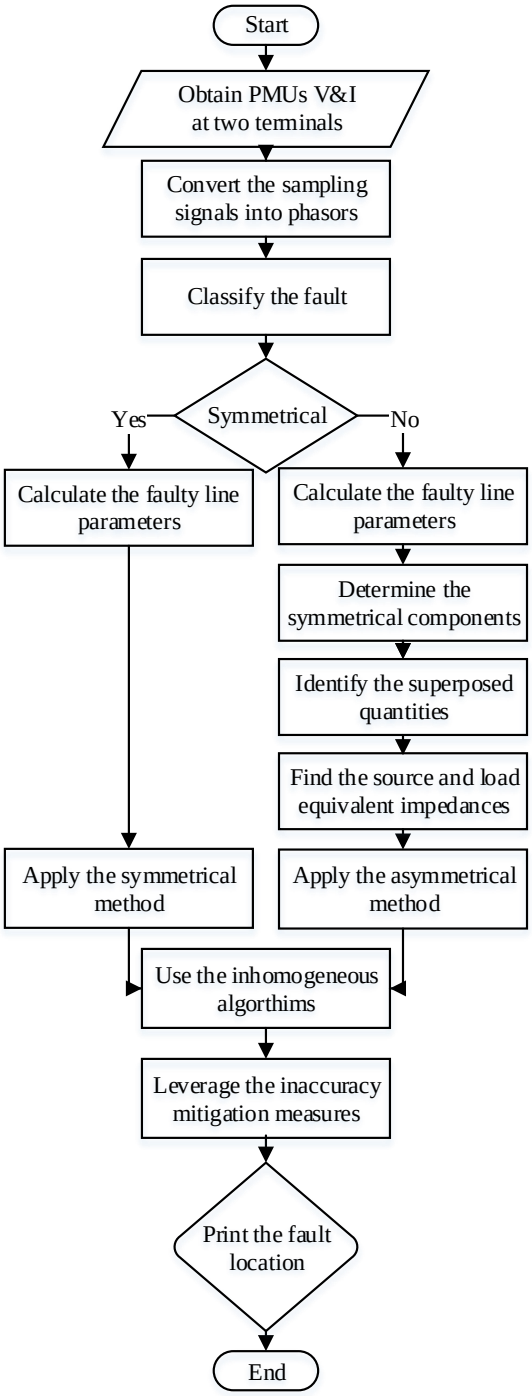

Figure 7-1: Flowchart of the proposed impedance-based fault location model for inhomogeneous DLs

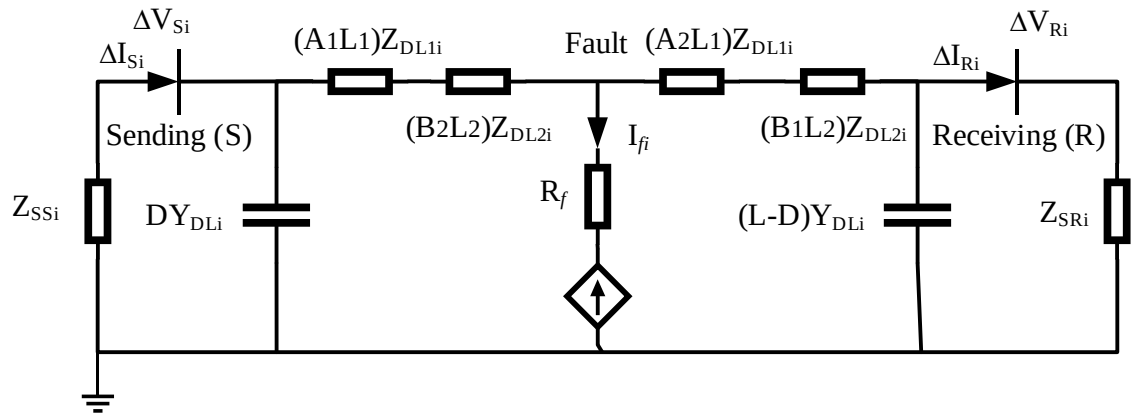

Figure 7-2: Superposed circuit of inhomogeneous distribution system

The parameters of the above figure are described as follows:

i	:	Zero, positive and negative sequence (i=0,1,2)
Z_{SSi}	:	Equivalent i^{th} sequence source impedance at the sending end
Z_{SRi}	:	Equivalent i^{th} sequence source impedance at the receiving end
Z_{DL1i}	:	i^{th} sequence of distribution line impedance (Conductor 1)
Z_{DL2i}	:	i^{th} sequence of distribution line impedance (Conductor 2)
Y_{DLi}	:	i^{th} sequence of distribution line admittance (combined for both conductors)
R_f	:	Fault resistance
I_{fi}	:	i^{th} sequence of the fault current

ΔV_{Si}	:	i^{th} sequence of superposed voltage at sending end
ΔV_{Ri}	:	i^{th} sequence of superposed voltage at receiving end
ΔI_{Si}	:	i^{th} sequence of superposed current at sending end
ΔI_{Ri}	:	i^{th} sequence of superposed current at receiving end
L	:	Total distribution line length
L_1	:	Total length of Conductor 1
L_2	:	Total length of Conductor 2
D	:	Actual distance of the fault from the sending end
A_1	:	Length of Conductor 1 from the sending end side and just before the fault point
A_2	:	Length of Conductor 1 after the fault point from the sending end side and up to the remaining length
B_1	:	Length of Conductor 2 after the fault point from the sending end side
B_2	:	Length of Conductor 2 before the fault point from the sending end side

The parameters A_1, A_2, B_1 and B_2can be calculated using the below relations:

Table 7-1: The equations of the parameters A_1, A_2, B_1 and B_2

Parameter	Equality	Equivalent under the conditions	
		$\boldsymbol{D \leq L_1}$	$\boldsymbol{D > L_1}$
A_1	$=$	D	L_1
A_2	$=$	$L_1 - D$	0
B_1	$=$	L_2	$L_2 - (D - L_1)$
B_2	$=$	0	$D - L_1$

The online DL parameters identification approach using PMUs will not detect the inhomogeneity of the line. Instead, it will calculate equivalent impedance of the line sections. In case two lines are spliced with each other with different parameters, the equivalent impedance will be calculated by the following:

$$Z_{eq} = \frac{L_1 Z_{DL1} + L_2 Z_{DL2i}}{L} \tag{7.1}$$

This is with the assumption that both shunt admittances line sections are combined and placed at the two ends of the DL. The two conductors are contributing to the above $Z_{eq}$by the following factors for the first and second conductors, respectively:

$$C_1 = \frac{L_1 Z_{DL1}}{L_1 Z_{DL1} + L_2 Z_{DL2i}} \tag{7.2}$$

$$C_2 = \frac{L_2 Z_{DL2}}{L_1 Z_{DL1} + L_2 Z_{DL2i}} \tag{7.3}$$

The below proposed simplified formula is basically projecting the fault estimation produced by the proposed model in Chapter 6 from a homogeneous-base line to the corresponding actual DL.

$$D_2 = \begin{cases} \left(\frac{D_1}{L} \div C_1\right) L_1, & \frac{D_1}{L} \leq C_1; \\ \frac{\left(\frac{D_1}{L} - C_1\right)}{C_2} L_2 + L_1, & Otherwise. \end{cases} \quad (7.4)$$

The above relation is called homogeneity-to-inhomogeneity relation (H2IR), in which D_1represents the calculated fault distance using the homogeneous-based techniques. The calculated fault distance using the proposed inhomogeneous is denoted by D_2.

7.3 Case Studies

The same case studies developed in Chapter 6 for fault location in homogeneous DLs are simulated in this chapter for inhomogeneous lines. A total of 9,477 different case studies have been performed under three different scenarios described in Table 7-2, Table 6-2 and Table 7-3. Different fault types including line to ground (LG), double line (LL), double line-to-ground (LLG), and three-phase faults. Different line lengths have been selected and the simulation starts from 0.50 km to approximately the total line length with a step size of 0.5 km.

The inhomogeneity is represented by two different line parameters connected to each other. The details of Conductor 1 of the line are presented in Table 7-3 with little change in loading conditions.

Table 7-2: Case studies descriptions for Chapter 7

No.	Area of Case Study		Additional Information/Reference
	Area	**No.**	
13.	Unbalanced fault	3	LG, LL and LLG
14.	Balanced fault	1	LLLG
15.	Fault resistance (for asymmetrical)	6	0.001 Ω, 0.01 Ω, 0.1 Ω, 1 Ω, 10 Ω and 100 Ω
16.	Fault resistance (for symmetrical)	3	0.001 Ω, 0.01 Ω and 0.1 Ω
17.	Case (for asymmetrical)	4	1) Without IMM and H2IR., 2) H2IR. 3) H2IR.and GIMM, and 4) H2IR. And LIMM
18.	Case (for symmetrical)	3	1) Without IMM and H2IR., 2) with IMM, 3) with H2IR and IMM
19.	Fault placement	117	The fault placements starting from 0.50 km to approximately the total line length with a step size of 0.5 km. That is 59, 39 and 19 different fault locations for the three scenarios presented in Table 6-2 and Table 7-3, respectively.
Total		**9,477**	(3 unbalanced) (6 fault resistances) (4 cases) (117 fault placements) + (1 balanced) (3 fault resistances) (3 cases) (117 fault placements)

Table 7-3: Details of Conductor 1 of the three different simulation scenarios

Specification		Details		
		Scenario 1	**Scenario 2**	**Scenario 3**
Total Distribution line length (km)		30	20	10
Conductor 1 total length		10	5	4
Loading Condition	MW	4	6	5
	MVar	2	1.5	1.25
R (Ω/km)	Positive & negative seq.	0.3459	0.3076	0.17295
	Zero-sequence	1.239	1.1012	0.6195
L (H/km)	Positive & negative seq.	0.00315	0.0028	0.001575
	Zero-sequence	0.00996	0.0088	0.00498
C (F/km)	Positive & negative seq.	3.78E-09	4.25E-09	7.55E-09
	Zero-sequence	1.67E-09	1.88E-09	3.34E-09

The large number of case studies have been developed to test the robustness and accuracy of the proposed fault location model. The 9,477 simulations differ in the line lengths, fault locations, loading conditions, line parameters and applying IMM.

The selected DL is modeled as three-phase DL with two series π-type. The model consists of two sets of resistance and inductances elements in series connected between sending and receiving terminals. Two sets of shunt capacitances lumped are, also, included at both ends as illustrated in Figure 7-2.

In MATLAB, two sets of simulated PMUs are placed at both terminals of the selected DL to measure the voltages and currents waveforms simultaneously. The recorded waveforms are in the shape of sinusoidal signals and then converted into phasor equivalents.

7.4 Results and Discussions

This section summarizes the simulation results of the 9,477 cases and organizes them into two categories; asymmetrical and symmetrical. Under each category, the three simulation scenarios, in Table 6-2 and Table 7-3, are considered. The following cases are simulated for each scenario:

- Case 1: Considering the proposed homogeneous fault location methods shown in Figure 6-3 without applying the concepts of H2IR or IMM.
- Case 2: H2IR.
- Case 3: GIMM.
- Case 4: LIMM.

One inaccuracy mitigation measure is applied for the symmetrical approach as the three phases and three phases to ground faults use the same balanced faults analysis.

7.4.1 Asymmetrical Faults

The inhomogeneous asymmetrical algorithms have been applied to different types of unbalanced faults (LG, LL and LLG) for the three scenarios tabulated in Table 6-2 and Table 7-3. The faults have been placed at different distances in the studied systems starting from 0.50 km to approximately the total line length with a step size of 0.5 km. In each fault distance, the fault resistance has been varied to be 0.001 Ω, 0.01 Ω, 0.1 Ω, 1 Ω, 10 Ω and 100 Ω. The

fault location at each distance has been averaged for the aforementioned fault resistance values.

The results are detailed in this part for the four cases; homogeneous model, H2IR, GIMM and LIMM.

A. Homogeneous Approach

The scenarios of Table 6-2 and Table 7-3 have been simulated by the proposed asymmetrical method in Chapter 6 for different fault distances and resistances. The average errors of fault resistances for fault distances and unbalanced fault types are demonstrated in Figure 7-3.

The maximum and average errors for the three scenarios considering the variation of both the distance and resistance of fault are displayed in Table 7-6. It is observed that as the line length decreases as the maximum and average errors drops. The homogeneous case overall average error for all scenarios is -7.41% which shows that it is not reliable technique to be used for inhomogeneous cases.

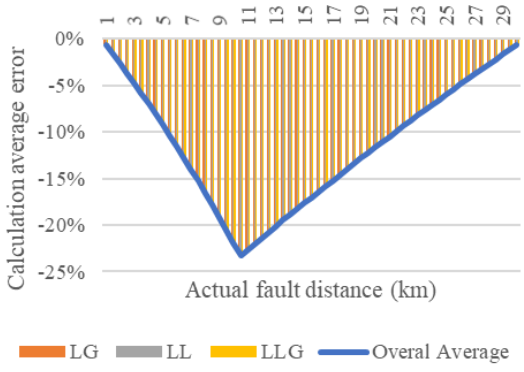

a) **Scenario 1**

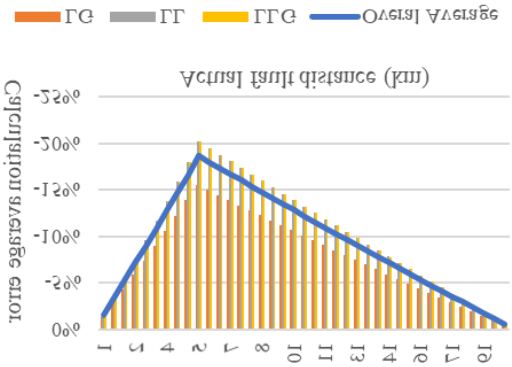

b) **Scenario 2**

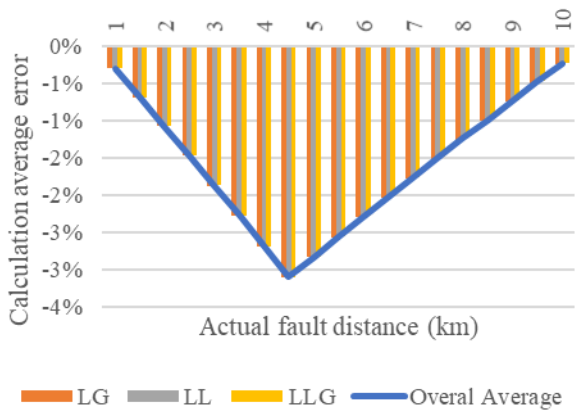

c) Scenario 3

Figure 7-3: Calculation average errors of fault resistances for the three scenarios under the proposed inhomogeneous asymmetrical fault method (Case 1)

B. H2IR Approach

The scenarios of Table 6-2 and Table 7-3 have been simulated by the proposed inhomogeneous asymmetrical method for different fault distances and resistances. The average errors of fault resistances for fault distances and unbalanced fault types are demonstrated in Figure 7-4.

The results reveal that the error curves follow a particular graph. The shape is almost similar for all asymmetrical method related simulations with minor differences. Subsequently, the error can be predicted and hence mitigated.

The maximum and average errors for the three scenarios considering the variation of both the distance and resistance of fault are displayed in Table 7-6. It is observed that as the line length decreases as the average errors drops. The H2IR case overall average error for all scenarios is 1.65% which reflects the accuracy of proposed inhomogeneous asymmetrical fault location method using PMUs.

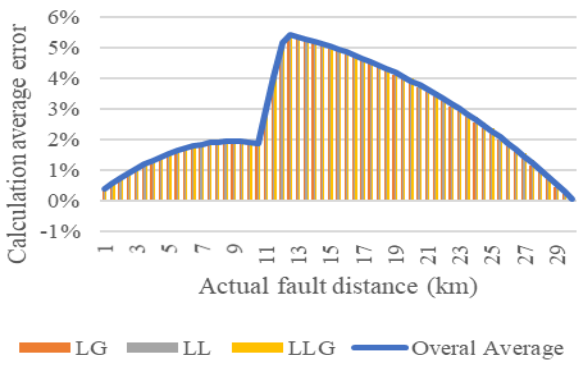

a) **Scenario 1**

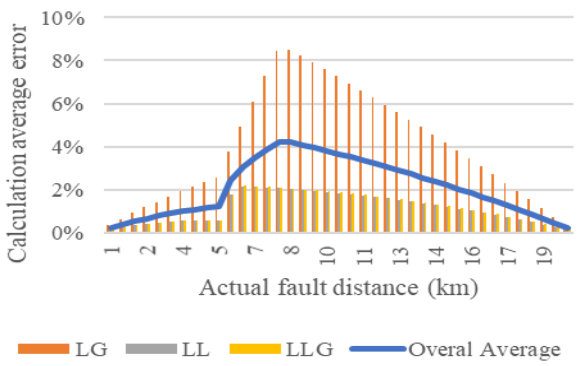

b) **Scenario 2**

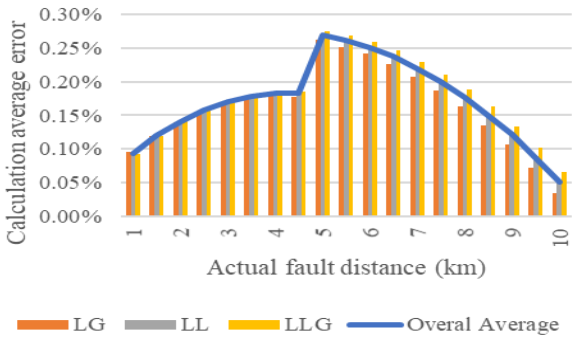

c) **Scenario 3**

Figure 7-4: **Calculation average errors of fault resistances for the three scenarios under the proposed inhomogeneous asymmetrical fault method (Case 2)**

C. Global-based Inaccuracy Mitigation Measure

The GIMM considers the average of all unbalanced fault types errors for a specific scenario. This is under different loading conditions and the change of both distance and resistance of the fault. The results are averaged for fault resistances at specific distance and shown in Figure 7-5.

The concept of global inaccuracy prediction and mitigation has revealed on a tremendous enhancement of the fault location accuracy. The inaccuracy reduction could reach up to 96% of the inhomogeneous case. This is observed in the maximum error of LG fault under Scenario

1 as shown in Table 7-6 as the maximum error has been reduced from 5.51% to 0.20% (approximately 28 times of reduction). In simple terminologies, the error for the homogeneous case is equivalent to 1653 meters. By the introduction of this novel concept, the uncertainty will drop to only 60 meters. The table includes the maximum and average errors for the three scenarios considering the variation of both distance and resistance of the faults.

The overall average error obtained by the GIMM for all scenarios is 0.45% which is approximately four times less than the inhomogeneous case. This prove the robustness and effectiveness of the proposed GIMM.

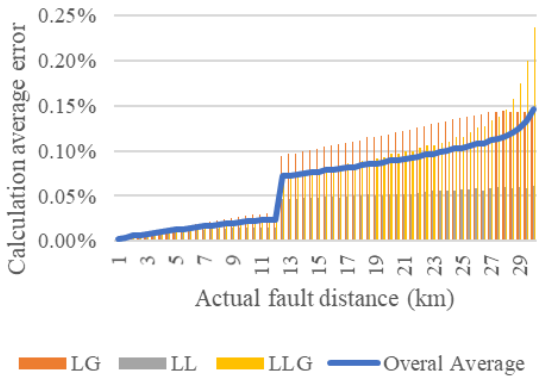

a) **Scenario 1**

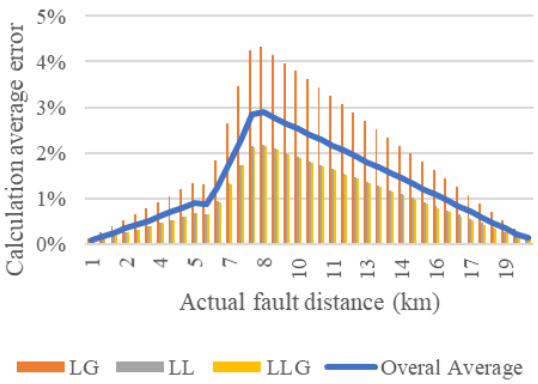

b) **Scenario 2**

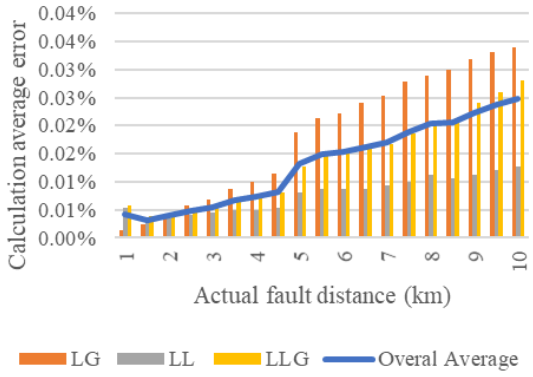

c) **Scenario 3**

Figure 7-5: Calculation average errors of fault resistances for the three scenarios under the GIMM (Case 3)

D. Local-based Inaccuracy Mitigation Measure

The LIMM measure is almost similar to the global except that it uses a specific measure for each type of faults. The measures are developed based on the change of both distance and resistance of the fault. The results are averaged for fault resistances at specific distance and presented in Figure 7-6.

The concept of local inaccuracy prediction and mitigation has resulted in a similar tremendous enhancement of the fault location accuracy as in the global approach. It has achieved major reduction of above 50 times comparing to the inhomogeneous case. This is observed in the maximum error of LG fault under Scenario 2 as shown in Table 7-6 as the maximum error has been reduced from 8.63% to 0.17%.

The overall average error obtained by the LIMM measure for all scenarios is 0.04%. This number is less than both the inhomogeneous and global cases by 41.25 and 11.25 times, respectively. This proves the robustness and effectiveness of the proposed LIMM measure.

Table 7-6 presents the maximum and average errors for the three scenarios considering the variation of both distance and resistance of the faults.

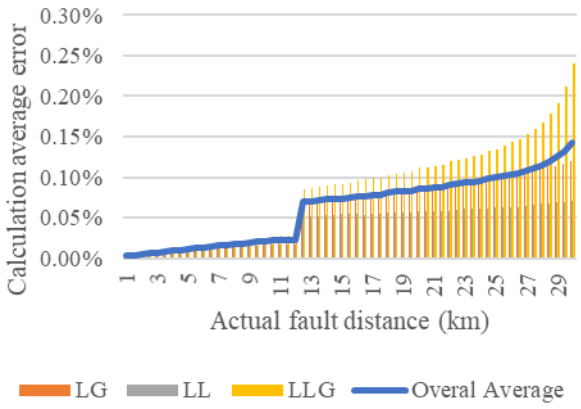

a) **Scenario 1**

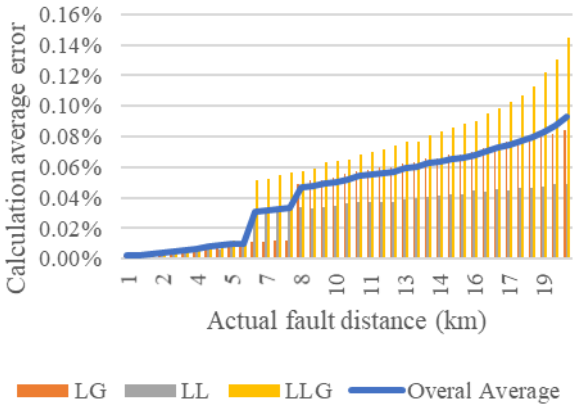

b) **Scenario 2**

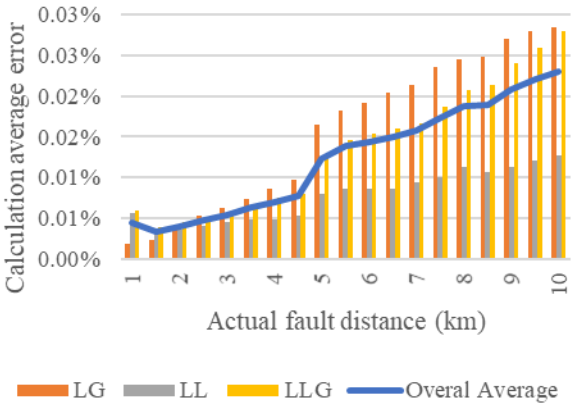

c) **Scenario 3**

Figure 7-6: Calculation average errors of fault resistances for the three scenarios under the LIMM measure (Case 4) considering asymmetrical and inhomogeneous

7.4.2 Symmetrical Faults

The inhomogeneous symmetrical algorithms have been applied to different balanced faults for the three scenarios tabulated in Table 6-6 and Table 7-3. The faults have been placed at different distances in the studied line starting from 0.50 km to approximately the total line length with a step size of 0.5 km. In each fault distance, the fault resistance has been varied to be 0.001 Ω, 0.01 Ω and 0.1 Ω.

The results are detailed in this part for three cases; homogeneous approach, H2IR approach and inaccuracy-based measures. The global will be the same as the local as the three phases and three phases to ground faults use the same balanced faults analysis.

A. Homogeneous Approach

The scenarios of Table 6-2 and Table 7-3 have been simulated by the proposed symmetrical algorithms for different fault distances and resistances. The average errors of fault resistances for fault distances and balanced fault types are demonstrated in Figure 7-7.

The results reveal that the error curves follow particular trends. The curvature trends are almost similar for the three scenarios. Therefore, the error can be predicted and hence mitigated.

The maximum and average errors for the three scenarios considering the variation of both the distance and resistance of fault are displayed in Table 7-7. It is observed that as the line length decreases as the maximum and average errors drops. The homogeneous approach overall average error for all scenarios is 8.86%. This shows the unreliability of this method for inhomogeneous lines.

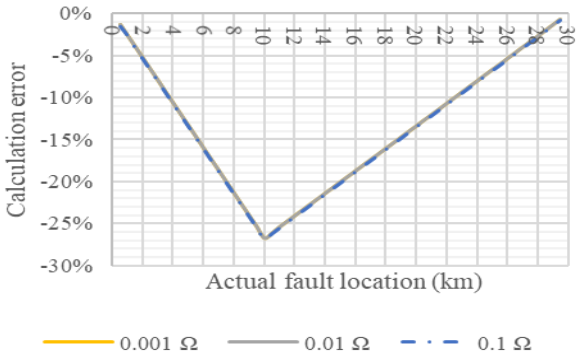

e) Scenario 1

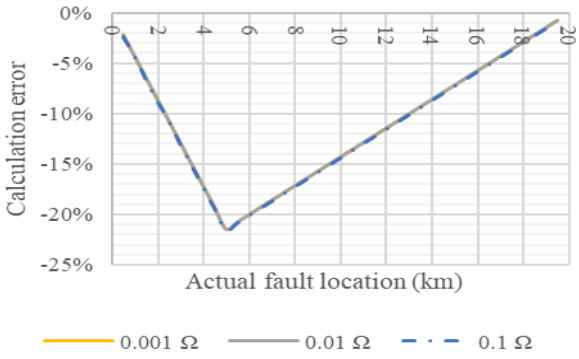

f) Scenario 2

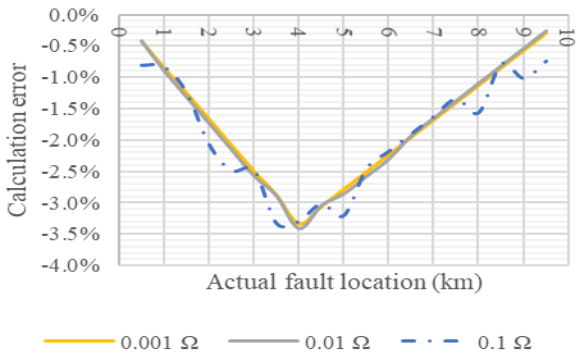

g) Scenario 3

Figure 7-7: Calculation errors of fault resistances for the three scenarios under the proposed symmetrical fault method (homogeneous Case)

B. Inhomogeneous Approach

The scenarios of Table 6-2 and Table 7-3 have been simulated by the proposed inhomogeneous asymmetrical method for different fault distances and resistances. The average errors of fault resistances for fault distances and unbalanced fault types are demonstrated in Figure 7-8.

The results reveal that the error curves follow a particular graph. The parabolic shape is almost similar for all inhomogeneous asymmetrical method related simulations with minor differences. Subsequently, the error can be predicted and hence mitigated.

The maximum and average errors for the three scenarios considering the variation of both the distance and resistance of fault are displayed in Table 7-7. The overall average error for all scenarios is 0.13% which reflects the accuracy of proposed inhomogeneous asymmetrical fault location method using PMUs.

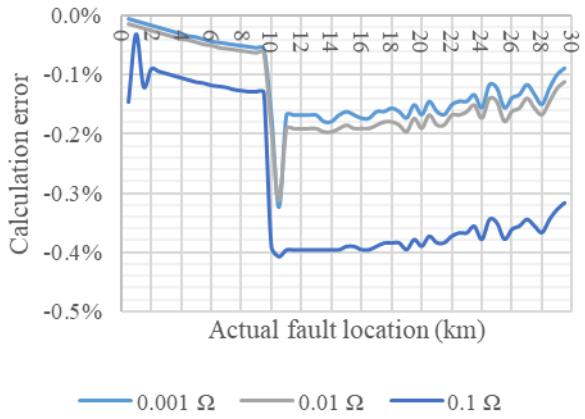

a) Scenario 1

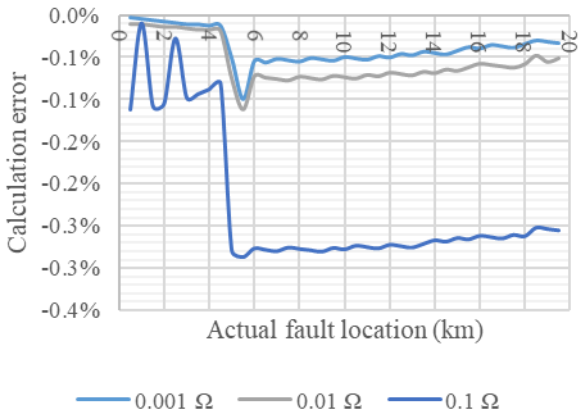

b) Scenario 2

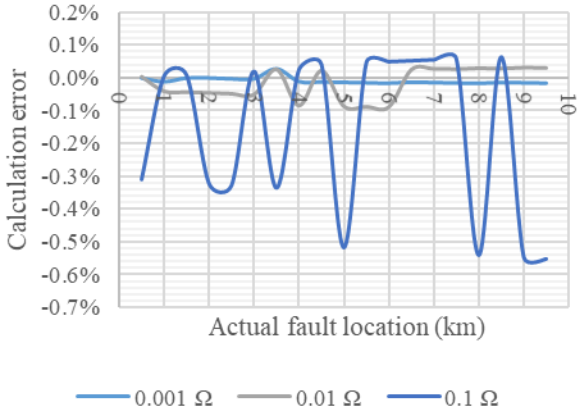

c) Scenario 3

Figure 7-8: Calculation average errors of fault resistances for the three scenarios under the proposed inhomogeneous symmetrical fault method (Case 2)

C. Inaccuracy Mitigation Measure

The resulted calculation errors of varying fault resistances for the three scenarios using the proposed inaccuracy mitigation measure are displayed in Figure 7-9.

The concept of inaccuracy prediction and mitigation has revealed on acceptable accuracy level of the fault location accuracy. The inaccuracy reduction could reach up to 35% of

inhomogeneous case maximum errors and 18% of their average. This confirms the robustness and effectiveness of the proposed inaccuracy mitigation measure.

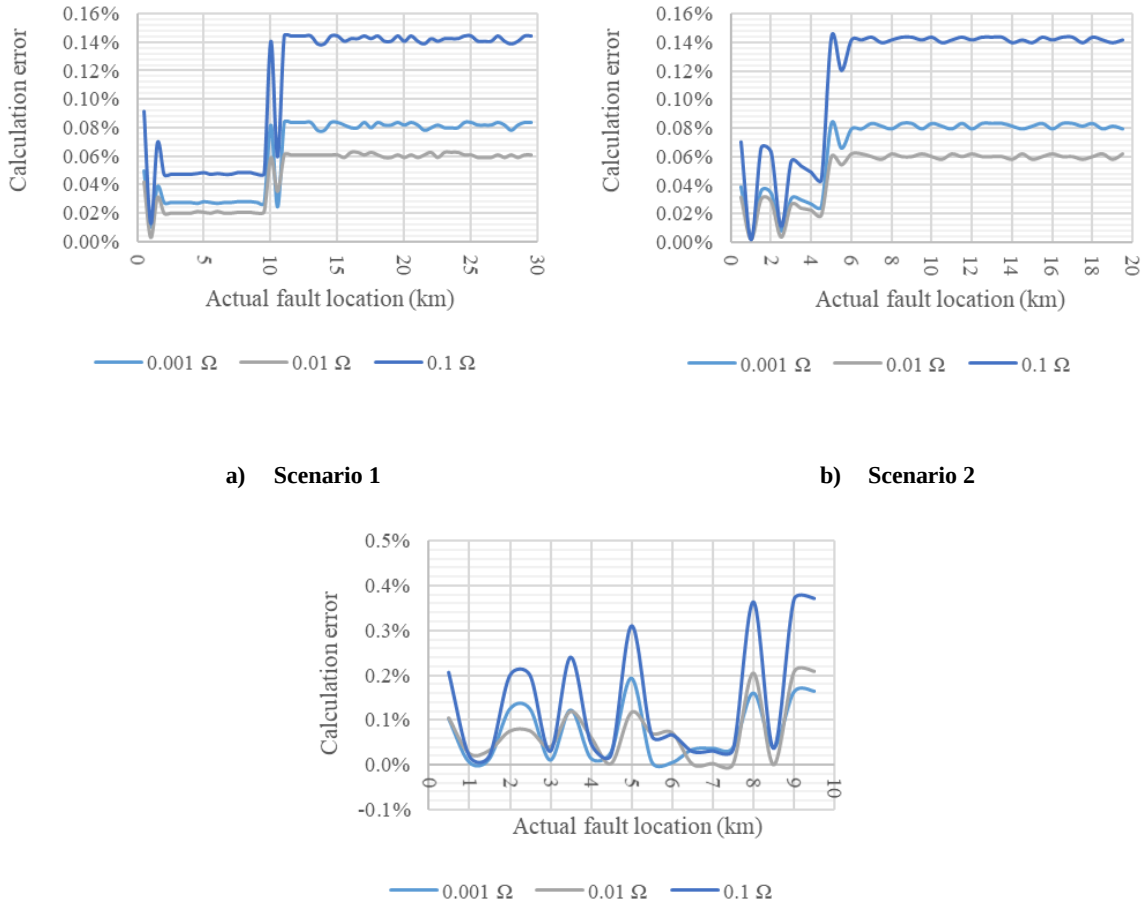

a) Scenario 1 **b) Scenario 2**

c) Scenario 3

Figure 7-9: Calculation errors of fault resistances for the three scenarios under the proposed inhomogeneous symmetrical fault method (case 3)

7.4.3 Model Evaluation

The MAD, MSE, RMSE, MAPE and CoD have been applied to different scenarios, cases and resistance values. The results for the latter are averaged into one value for each scenario and case. The results are tabulated in Table 7-4 and Table 7-5 to evaluate the robustness of this chapter proposals. It is noticed from the tables that generally the values under the proposed

IMMs categories are improved compared to those in the inhomogeneous case. This proves the strength of the proposed inaccuracy mitigation concept.

Table 7-4 (a): Statistical measures results for all asymmetrical-based simulations under inhomogeneous approach in percentage (%) (1/2)

Scenario	Statistical Measure	LG				LL			
		Case							
		1	2	3	4	1	2	3	4
1	MAD	340.04	79.40	2.45	1.84	338.70	81.24	1.11	1.24
	MSE	1554.19	85.04	0.10	0.06	1545.24	88.40	0.03	0.02
	RMSE	394.23	92.19	2.92	2.20	393.09	94.01	1.29	1.45
	MAPE	35.17	7.48	0.15	0.11	35.07	7.59	0.08	0.09
	R^2	99.58	99.91	100.00	100.00	99.58	99.91	100.00	100.00
2	MAD	233.51	120.48	57.33	1.31	304.14	34.21	28.95	0.90
	MSE	719.27	204.57	47.96	0.03	1218.11	15.75	12.19	0.01
	RMSE	268.19	143.02	69.24	1.58	349.01	39.68	34.90	1.02
	MAPE	41.51	15.61	7.24	0.12	54.01	4.73	3.64	0.09
	R^2	98.77	99.58	99.79	100.00	98.49	99.87	99.89	100.00
3	MAD	47.75	4.90	0.55	0.47	47.51	5.17	0.23	0.23
	MSE	29.57	0.28	0.00	0.00	29.34	0.30	0.00	0.00
	RMSE	54.38	5.22	0.64	0.55	54.17	5.47	0.26	0.26
	MAPE	13.64	1.60	0.10	0.09	13.61	1.64	0.06	0.07
	R^2	98.37	99.81	99.99	100.00	98.38	99.81	99.99	100.00

Table 7-4 (b): Statistical measures results for all asymmetrical-based simulations under inhomogeneous approach in percentage (%) (2/2)

Scenario	Statistical Measure	LG			
		Case			
		1	2	3	4
1	MAD	338.22	82.07	2.19	2.49
	MSE	1542.06	89.93	0.13	0.11
	RMSE	392.69	94.80	2.79	3.08
	MAPE	35.04	7.63	0.13	0.15
	R^2	99.58	99.91	100.00	100.00
2	MAD	303.80	34.76	28.48	1.83
	MSE	1216.05	16.25	11.85	0.06
	RMSE	348.72	40.27	34.38	2.19
	MAPE	53.97	4.78	3.60	0.16
	R^2	98.49	99.87	99.89	100.00
3	MAD	47.37	5.34	0.41	0.41
	MSE	29.22	0.32	0.00	0.00
	RMSE	54.06	5.63	0.48	0.48
	MAPE	13.58	1.67	0.09	0.09
	R^2	98.38	99.80	99.99	100.00

Table 7-5: Statistical measures results for all symmetrical-based simulations under inhomogeneous approach (in %)

Statistical Measure	Scenario 1			Scenario 2			Scenario 3		
	Case								
	1	2	3	1	2	3	1	2	3
MAD	450.01	62.08	59.61	356.56	36.35	34.74	60.57	8.89	9.35
MSE	2916.26	482.39	475.61	1769.68	233.95	231.68	52.08	7.28	7.14
RMSE	526.34	106.55	103.82	414.93	77.04	75.90	69.45	13.86	14.15
MAPE	53.16	9.24	9.07	67.30	7.87	7.73	18.47	3.43	3.74
R^2	99.41	99.89	99.88	98.23	99.77	99.83	97.70	99.56	99.96

With the consideration of maximum and average errors presented in Table 7-6, the proposed IMMs concept is between 95.57% and 99.76%. The accuracy could reach more than four 9s if the minimum errors are considered.

Considering maximum and average errors shown in Table 7-7, the proposed IMMs concept is between 96.60% and 99.31%. The accuracy could reach more than four 9s if the minimum errors are considered.

Table 7-6: Maximum and average errors for the three cases and scenarios considering the variation of both distance and resistance of fault under inhomogeneous asymmetrical

Scenario	Case	Error							
		Maximum				Average			
		LG	LL	LLG	Overall	LG	LL	LLG	Overall
1	1	23.36%	23.32%	23.32%	23.36%	-11.33%	-11.29%	-11.28%	-11.30%
	2	5.51%	5.50%	5.57%	5.57%	2.64%	2.71%	2.73%	2.69%
	3	0.20%	0.20%	0.40%	0.40%	0.08%	0.04%	0.07%	0.06%
	4	0.26%	0.20%	0.39%	0.39%	0.06%	0.04%	0.08%	0.06%
2	1	15.57%	20.19%	20.19%	20.19%	-7.78%	-10.14%	-10.13%	-9.35%
	2	8.63%	2.21%	2.26%	8.63%	4.02%	1.14%	1.16%	2.10%
	3	4.43%	2.20%	2.20%	4.43%	1.91%	0.96%	0.95%	1.28%
	4	0.17%	0.08%	0.24%	0.24%	0.04%	0.03%	0.06%	0.04%
3	1	3.12%	3.11%	3.11%	3.12%	-1.59%	-1.58%	-1.58%	-1.58%
	2	0.29%	0.28%	0.30%	0.30%	0.16%	0.17%	0.18%	0.17%
	3	0.04%	0.03%	0.07%	0.07%	0.02%	0.01%	0.01%	0.01%
	4	0.05%	0.03%	0.06%	0.06%	0.02%	0.01%	0.01%	0.01%

Table 7-7: Maximum and average errors for the three cases and scenarios considering the variation of both distance and resistance of fault under inhomogeneous symmetrical

Case	Scenario	Maximum	Average
1	1	26.90%	13.69%
	2	21.59%	11.06%
	3	3.40%	1.82%
2	1	0.41%	0.18%
	2	0.29%	0.11%
	3	0.55%	0.09%
3	1	0.76%	0.36%
	2	0.45%	0.21%
	3	0.75%	0.15%

7.5 Conclusion

This chapter addresses an important issue associated with impedance-based fault location for inhomogeneous DLs. To advance inhomogeneous DL repair and system restoration, a prompt and accurate fault location approach is required. Based on that, an impedance-based fault location model for inhomogeneous DL has been developed and evaluated for different simulations by statistical measures. The model consists of two fault location techniques for asymmetrical and symmetrical faults. Additionally, it includes a novel relation denoted by H2IR to ensure projecting the fault estimation produced by the proposed model in Chapter 6 from a homogeneous-base line to the corresponding actual DL. Global and local IMMs have

been included to improve the fault location. The outcomes of this analysis along with the associated recommendations are as follows:

1. This study's proposal to integrate H2IR method with the homogeneous impedance-based methods resulted in a novel approach that is able to locate the faults accurately with an average error of approximately1.3% for both asymmetrical and symmetrical.
2. The proposed IMMs have significantly improved the fault location estimate up to 41 times compared to the inhomogeneous case. Their accuracies based on the maximum errors are 4.43% and 0.76% for the inhomogeneous asymmetrical and symmetrical, respectively. By applying the measures, fault location can be identified within few meters of the exact distance if not at the actual location.
3. Both asymmetrical and symmetrical techniques resulted in high-level of accuracy with overall average error of 0.24 for each.
4. The above two IMMs can be developed for each line by the design consultant firms during the design phase of the lines, part of the protection studies.
5. The proposed model does not suffer from the line impedance inaccuracy issues under the idea situation (homogeneous, radial, and uncompensated, etc.). This is due to this research's recommendation to calculate the line parameters online.

CHAPTER 8

CONCLUSION AND FUTURE WORK

This chapter summarizes the outcomes, recommendations, conclusions and contributions of this thesis work. The challenges and important aspects have been, also, highlighted for further investigation in future.

8.1 Summary and Conclusion

A comprehensive survey has been completed on the works reported in literature since 2000 till 2017, addressing the problem of fault location using PMUs. The survey is exhaustive to all available researches in the subject of PMU use for fault location. These publications have been tabulated to summarize the problems, pros and cons, accuracy, methods implemented, and locations with respect to energy chain. This is to support power system engineers and academic researchers as a reference for their prospective relevant problems.

Additionally, two novel load flow analysis for distribution networks are developed and compared against BFS. The approaches are EBFS and Zig Zag-based load flow analysis. Both approaches can be applied for extended radial system where multiterminal lines exist. A total of nine different cases are simulated to show the effectiveness of the proposed methods. The numerical results demonstrate that these two methods are very robust and have excellent convergence characteristics. They will result in reduction of the number of iterations while maintaining the required load flow accuracy. It is concluded that Zig Zag is the best technique

for the studied systems which results in considerably better solutions. There is a chance to achieve less convergence time from the two proposed techniques by further optimization to their respective MATLAB codes.

Furthermore, the optimal placement of PMUs problem is considered using single objective function (ABC). It is one of the robust and reliable techniques to find the optimal solution. Additionally, multi-objective optimization technique (SPEA) is discussed. It represents a considerable contribution to the subject of PMUs in distribution. Using multi-objective approach will give diversified optimal options to the decision makers to select the most appropriate one that meet their needs.

Online DL parameters identification is, also, discussed. The symmetrical component based analysis has been investigated which is required for asymmetrical related studies such as unbalanced fault analysis. The analysis considers noisy distribution networks. It compares the performance of three line parameters identification techniques by using different statistical measures. A total of 12,960 different case studies are simulated and analyzed. The line parameters are calculated online using voltage and current signals obtained from phasor measurement units (PMUs) placed at the line two terminals.

A new impedance-based fault location model for distribution grids is proposed. The model includes asymmetrical and symmetrical fault classification and location algorithms. The algorithms along with the mitigation measures have been evaluated using different statistical measures. The results demonstrate the effectiveness of this research proposals and their superiority to other publications in similar subjects.

Inhomogeneous DLs fault location model has, also, been proposed. This is achieved by the introduction of a novel relation denoted by H2IR to ensure projecting the fault estimation from a homogeneous-base line to the corresponding actual DL.

Novel IMMs have been proposed. This is to improve the accuracy of fault location and hence advance power restoration. The measures can be organized into two categories as follows:

- GIMM which considers the average of all fault type errors for a specific case and under a specific algorithm.
- LIMM measure which develops a specific measure for each fault type.

The above two IMMs can be developed for each line as appropriate by the design consultant firms during the design phase of the lines, part of the protection and coordination studies.

8.2 Future Work

The recommendations of this thesis work along with the challenges and important aspects are itemized below for further investigation in future:

1. Leverage the concepts of IMM proposed in this work to improve the accuracy of fault location and advance the DL repair and system restoration.
2. Consider the H2IR for other techniques other than the proposed model.
3. Investigate the impedance-based fault location techniques for further actual systems simulations, experiments and field piloting. This is to increase the utilities confidence of deploying PMUs in wide scales.

4. Study the aged and inhomogeneous lines fault locations in distribution grids by travelling wavers and wavelets as they are critical and common problems for a number of utilities.
5. Continue using the two- and multiterminal-based fault location techniques are they are proven reliable and robust under different conditions.
6. Consider both impedance and wavelet-based techniques for distribution as the work is very limited and the they should provide the same accuracy level as in transmission.
7. Explored more wavelet-base techniques for transmission due to its improved accuracy which is superior to the recorded average impedance-based. The investigation in this area is more promising which may achieve super accuracy results comparing to the others as the accuracy matters the most.
8. Research for PMU-based fault location at the generation side. Although the distance is not that long from the generation unit to the substation, the expeditious and accurate fault location is required. This is to put back into surface the affected unit and avoid unnecessary additional excavation which might damage other cables in the process.
9. Consider PMU-based fault location at the load side. Prompt and accurate fault location for loads is important, especially when the cables are in critical process area where hand digging is the only permitted option. This is associated with very high cost and execution time. The lines supplying offshore hydrocarbon facilities are also very critical and require more cost and time for power restoration.
10. Study renewable integration with the conventional grid which has not been paid adequate attention and this type of systems are increasing.

11. Explore further the communication infrastructure and associated cyber security issues as they represent major challenges for the rolling-out of PMUs. This is due to their costs and vulnerability to attacks and leakage of private information.
12. Consider optimal placement of PMUs in distribution grids using intelligent techniques for large-scale networks.

REFERENCES

[1] S. Gazette, “Saudi electricity demand posts 8% annual growth,” *Saudi Gazette*, Riydh, 01-Apr-2014.

[2] A. News, “KSA power demand posts 8% average annual growth rate,” *Arab News*, Apr-2014.

[3] D. Chowdhury, Ali ; Koval, *Power distribution system reliability: practical methods and applications*, Second. Wiley-Blackwell, 2009.

[4] I. P. & E. Society, *C37.118.1-2011 - IEEE Standard for Synchrophasor Measurements for Power Systems*, vol. 2011, no. December. 2011.

[5] M. Korkali, H. Lev-Ari, and A. Abur, “Traveling-Wave-Based Fault-Location Technique for Transmission Grids Via Wide-Area Synchronized Voltage Measurements,” *IEEE Trans. Power Syst.*, vol. 27, no. 2, pp. 1003–1011, May 2012.

[6] A. H. Al-Mohammed and M. A. Abido, “A Fully Adaptive PMU-Based Fault Location Algorithm for Series-Compensated Lines,” *IEEE Trans. Power Syst.*, vol. 29, no. 5, pp. 2129–2137, Sep. 2014.

[7] J. Sadeh and A. Adinehzadeh, “Accurate fault location algorithm for transmission line in the presence of series connected FACTS devices,” *Int. J. Electr. Power Energy Syst.*, vol. 32, no. 4, pp. 323–328, 2010.

[8] M. Kezunovic and B. Perunicic, “Automated transmission line fault analysis using synchronized sampling at two ends,” in *Proceedings of Power Industry Computer Applications Conference*, 1995, pp. 407–413.

[9] A. H. Al-Mohammed and M. A. Abido, “Fault Location Based on Synchronized Measurements: A Comprehensive Survey,” *Sci. World J.*, vol. 2014, no. i, pp. 1–10, 2014.

[10] F. Aminifar, M. Fotuhi-Firuzabad, A. Safdarian, A. Davoudi, and M. Shahidehpour, “Synchrophasor Measurement Technology in Power Systems: Panorama and State-of-the-Art,” *IEEE Access*, vol. 2, pp. 1607–1628, 2014.

[11] M. Shafiullah and M. A. Abido, “A Review on Distribution Grid Fault Location Techniques,” *Electr. Power Components Syst.*, vol. 45, no. 8, pp. 807–824, May 2017.

[12] R. Mahanty and P. Gupta, “Application of RBF neural network to fault classification and location in transmission lines,” *IEE Proceedings-Generation, Transm. …*, vol. 151, no. 3, pp. 201–212, 2004.

[13] T. Takagi, Y. Yamakoshi, M. Yamaura, R. Kondow, and T. Matsushima, “Development of a New Type Fault Locator Using the One-Terminal Voltage and Current Data,” *IEEE Trans. Power Appar. Syst.*, vol. PAS-101, no. 8, pp. 2892–2898,

Aug. 1982.

[14] L. Eriksson, M. M. Saha, and G. D. Rockefeller, “An Accurate Fault Locator with Compensation for Apparent Reactance in the Fault Resistance Resulting from Remote-End Infeed,” *IEEE Power Eng. Rev.*, vol. PER-5, no. 2, pp. 44–44, Feb. 1985.

[15] A. Gopalakrishnan, M. Kezunovic, S. M. McKenna, and D. M. Hamai, “Fault location using the distributed parameter transmission line model,” *Power Deliv. IEEE Trans.*, vol. 15, no. 4, pp. 1169–1174, 2000.

[16] D. Novosel, D. G. Hart, E. Udren, and J. Garitty, “Unsynchronized two-terminal fault location estimation,” *IEEE Trans. Power Deliv.*, vol. 11, no. 1, pp. 130–136, 1996.

[17] E. G. Silveira and C. Pereira, “Transmission line fault location using two-terminal data without time synchronization,” *IEEE Trans. Power Syst.*, vol. 22, no. 1, pp. 498–499, 2007.

[18] C. S. Yu, C. W. Liu, S. L. Yu, and J. A. Jiang, “A New PMU-Based Fault Location Algorithm for Series Compensated Lines,” *IEEE Power Eng. Rev.*, vol. 21, no. 11, pp. 58–58, Nov. 2001.

[19] Chi-Shan Yu, Chih-Wen Liu, Sun-Li Yu, and Joe-Air Jiang, “A new PMU-based fault location algorithm for series compensated lines,” *IEEE Trans. Power Deliv.*, vol. 17, no. 1, pp. 33–46, 2002.

[20] Ying-Hong Lin, Chih-Wen Liu, and Chi-Shan Yu, “A new fault locator for three-terminal transmission lines using two-terminal synchronized voltage and current phasors,” *IEEE Trans. Power Deliv.*, vol. 17, no. 2, pp. 452–459, Apr. 2002.

[21] A. M. Ranjbar and A. Salehi-Dobakhshari, “Robust fault location of transmission lines by synchronised and unsynchronised wide-area current measurements,” *IET Gener. Transm. Distrib.*, vol. 8, no. 9, pp. 1561–1571, Sep. 2014.

[22] Z. Jiang, S. Miao, H. Xu, P. Liu, and B. Zhang, “An effective fault location technique for transmission grids using phasor measurement units,” *Int. J. Electr. Power Energy Syst.*, vol. 42, no. 1, pp. 653–660, Nov. 2012.

[23] S. Azizi, M. Sanaye-Pasand, and M. Paolone, “Locating Faults on Untransposed, Meshed Transmission Networks Using a Limited Number of Synchrophasor Measurements,” *IEEE Trans. Power Syst.*, vol. 31, no. 6, pp. 4462–4472, Nov. 2016.

[24] C.-S. Chen, C. Liu, and J. Jiang, “A New Adaptive PMU Based Protection Scheme for Transposed / Untransposed Parallel Transmission Lines,” *IEEE Trans. Power Deliv.*, vol. 17, no. 2, pp. 395–404, 2002.

[25] C. Wang, Q.-Q. Jia, X.-B. Li, and C.-X. Dou, “Fault location using synchronized sequence measurements,” *Int. J. Electr. Power Energy Syst.*, vol. 30, no. 2, pp. 134–139, Feb. 2008.

[26] T. Becejac, P. Dehghanian, and M. Kezunovic, “Impact of the errors in the PMU

response on synchrophasor-based fault location algorithms," in *NAPS 2016 - 48th North American Power Symposium, Proceedings*, 2016, pp. 1–6.

[27] V. Terzija, Z. M. Radojevic, and G. Preston, "Flexible Synchronized Measurement Technology-Based Fault Locator," *IEEE Trans. Smart Grid*, vol. 6, no. 2, pp. 866–873, Mar. 2015.

[28] C. Fan, X. Du, S. Li, and W. Yu, "An adaptive fault location technique based on PMU for transmission line," in *2007 IEEE Power Engineering Society General Meeting, PES*, 2007, pp. 1–6.

[29] C. J. Lee, J. B. Park, J. R. Shin, and Z. M. Radojevie, "A New Two-Terminal Numerical Algorithm for Fault Location, Distance Protection, and Arcing Fault Recognition," *IEEE Trans. Power Syst.*, vol. 21, no. 3, pp. 1460–1462, Aug. 2006.

[30] V. Terzija, G. Preston, V. Stanojevic, N. I. Elkalashy, and M. Popov, "Synchronized Measurements-Based Algorithm for Short Transmission Line Fault Analysis," *IEEE Trans. Smart Grid*, vol. 6, no. 6, pp. 2639–2648, Nov. 2015.

[31] Z. Y. He, R. K. Mai, W. He, and Q. Q. Qian, "Phasor-measurement-unit-based transmission line fault location estimator under dynamic conditions," *IET Gener. Transm. Distrib.*, vol. 5, no. 11, p. 1183, 2011.

[32] S. El Safty, M. M. Abo El Nasr, S. F. Mekhemer, and M. M. Mansour, "New technique for fault location in interconnected networks using phasor measurement unit," in *2008 12th International Middle-East Power System Conference*, 2008, pp. 6–10.

[33] H. W. H. Wen, H. Z. H. Zhengyou, M. R. M. Ruikun, W. He, Z. He, and R. Mai, "A PMU-based Dynamic Fault Location Estimation for Transmission Lines," in *2010 Asia-Pacific Power and Energy Engineering Conference*, 2010, no. 2, pp. 1–4.

[34] P. Eguia, I. Martin, I. Zamora, and R. Cimadevilla, "Fault location in combined transmission lines using PMUs for recloser control," in *2011 IEEE Trondheim PowerTech*, 2011, pp. 1–8.

[35] T.-C. Lin, P.-Y. Lin, and C.-W. Liu, "An Algorithm for Locating Faults in Three-Terminal Multisection Nonhomogeneous Transmission Lines Using Synchrophasor Measurements," *IEEE Trans. Smart Grid*, vol. 5, no. 1, pp. 38–50, Jan. 2014.

[36] C.-W. Liu, T.-C. Lin, C.-S. Yu, and J.-Z. Yang, "A Fault Location Technique for Two-Terminal Multisection Compound Transmission Lines Using Synchronized Phasor Measurements," *IEEE Trans. Smart Grid*, vol. 3, no. 1, pp. 113–121, Mar. 2012.

[37] P. Y. Lin, T. C. Lin, and C. W. Liu, "An intranet-based transmission grid fault location platform using synchronized IED data for the Taiwan power system," in *2013 IEEE PES Innovative Smart Grid Technologies Conference, ISGT 2013*, 2013, pp. 1–6.

[38] R. K. Mai *et al.*, "Dynamic fault locator for three-terminal transmission lines for phasor measurement units," *IET Gener. Transm. Distrib.*, vol. 7, no. 2, pp. 183–191, Feb. 2013.

[39] Y.-H. Lin, C.-W. Liu, J.-A. Jiang, and J.-Z. Yang, "An adaptive fault locator for transmission lines tapped with a source of generation - using synchronized voltage and current phasors," in *Proceedings of the IEEE Power Engineering Society Transmission and Distribution Conference*, 2000, vol. 3, pp. 1379–1383.

[40] Chi-Shan Yu, Chih-Wen Liu, and Ying-Hong Lin, "A fault location algorithm for transmission lines with tapped leg-PMU based approach," in *2001 Power Engineering Society Summer Meeting. Conference Proceedings (Cat. No.01CH37262)*, 2001, vol. 2, no. C, pp. 915–920 vol.2.

[41] A. H. Al-Mohammed, M. M. Mansour, and M. A. Abido, "Application of Phasor Measurement Units (PMUs) for fault location in SEC-EOA interconnected network," in *2010 IEEE International Energy Conference and Exhibition, EnergyCon 2010*, 2010, pp. 435–439.

[42] A. H. Al-Mohammed, M. M. Mansour, and M. A. Abido, "Fault location in SEC interconnected network based on synchronized phasor measurements," in *44th International Conference on Large High Voltage Electric Systems 2012*, 2012.

[43] A. H. Al-Mohammed and M. A. Abido, "An adaptive fault location algorithm for power system networks based on synchrophasor measurements," *Electr. Power Syst. Res.*, vol. 108, no. January, pp. 153–163, Mar. 2014.

[44] A. Esmaeilian, M. Mohseninezhad, M. Doostizadeh, and M. Khanabadi, "A precise PMU based fault location method for multi terminal transmission line using voltage and current measurement," in *2011 10th International Conference on Environment and Electrical Engineering*, 2011, pp. 1–4.

[45] A. H. Al-Mohammed and M. A. Abido, "Adaptive fault location for three-terminal lines using synchrophasors," in *2014 IEEE International Workshop on Applied Measurements for Power Systems, AMPS 2014 - Proceedings*, 2014, pp. 69–74.

[46] Y. H. Lin, C. W. Liu, and C. S. Yu, "A New Fault Locator for Three-Terminal Transmission Lines Using Two Terminal Synchronized Voltage and Current Phasors," *IEEE Power Eng. Rev.*, vol. 21, no. 11, pp. 58–58, Nov. 2001.

[47] Q. Jiang, B. Wang, and X. Li, "An Efficient PMU-Based Fault-Location Technique for Multiterminal Transmission Lines," *IEEE Trans. Power Deliv.*, vol. 29, no. 4, pp. 1675–1682, Aug. 2014.

[48] K.-M. Lee, S.-C. Choi, S.-H. Yoon, and C.-W. Park, "A Study on Smart Fault Locator Based on Time-Synchronized Phasor," *IFAC-PapersOnLine*, vol. 49, no. 27, pp. 224–229, Jul. 2016.

[49] S. M. Brahma, "New Fault-Location Method for a Single Multiterminal Transmission Line Using Synchronized Phasor Measurements," *IEEE Trans. Power Deliv.*, vol. 21, no. 3, pp. 1148–1153, Jul. 2006.

[50] S. M. Brahma, "Fault Location Scheme for a Multi-Terminal Transmission Line Using

Synchronized Voltage Measurements," *IEEE Trans. Power Deliv.*, vol. 20, no. 2, pp. 1325–1331, Apr. 2005.

[51] C. A. Apostolopoulos and G. N. Korres, "A novel algorithm for locating faults on transposed/untransposed transmission lines without utilizing line parameters," *IEEE Trans. Power Deliv.*, vol. 25, no. 4, pp. 2328–2338, 2010.

[52] M. B. Djurić, Z. M. Radojević, and V. V. Terzija, "Distance protection and fault location utilizing only phase current phasors," *IEEE Trans. Power Deliv.*, vol. 13, no. 4, pp. 1020–1024, 1998.

[53] S. M. Brahma, "Fault Location Scheme for a Multi-Terminal Transmission Line Using Synchronized Voltage Measurements," *IEEE Trans. Power Deliv.*, vol. 20, no. 2, pp. 1325–1331, Apr. 2005.

[54] M. S. Sachdev and R. Agarwal, "A technique for estimating transmission line fault locations from digital impedance relay measurements," *IEEE Trans. Power Deliv.*, vol. 3, no. 1, pp. 121–129, 1988.

[55] J. Gracia, A. J. Maz??n, and I. Zamora, "Best ANN structures for fault location in single- and double-circuit transmission lines," *IEEE Trans. Power Deliv.*, vol. 20, no. 4, pp. 2389–2395, 2005.

[56] T. Funabashi, H. Otoguro, Y. Mizuma, L. Dube, and A. Ametani, "Digital fault location for parallel double-circuit multi-terminal transmission lines," *IEEE Trans. Power Deliv.*, vol. 15, no. 2, pp. 531–537, Apr. 2000.

[57] D. J. Lawrence, L. Z. Cabeza, and L. T. Hochberg, "Development of an Advanced Transmission Line Fault Location System. II. Algorithm Development and Simulation," *IEEE Trans. Power Deliv.*, vol. 7, no. 4, pp. 1972–1983, 1992.

[58] Y. Liao and S. Elangovan, "Digital Distance Relaying Algorithm for First-Zone Protection for Parallel Transmission Lines," *IEEE Power Eng. Soc. Winter Meet.*, vol. 145, no. 5, pp. 531–536, 1998.

[59] Q. Zhang, Y. Zhang, W. Song, and Y. Yu, "Transmission line fault location for phase-to-earth fault using one-terminal data," *IEE Proc. - Gener. Transm. Distrib.*, vol. 146, no. 2, p. 121, 1999.

[60] G. Song, J. Suonan, Q. Xu, P. Chen, and Y. Ge, "Parallel Transmission Lines Fault Location Algorithm Based on Differential Component Net," *IEEE Trans. Power Deliv.*, vol. 20, no. 4, pp. 2396–2406, 2005.

[61] S.-H. K. S.-H. Kang, Y.-J. A. Y.-J. Ahn, Y.-C. K. Y.-C. Kang, and S.-R. N. S.-R. Nam, "A fault location algorithm based on circuit analysis for untransposed parallel transmission lines," *2008 IEEE Power Energy Soc. Gen. Meet. - Convers. Deliv. Electr. Energy 21st Century*, vol. 24, no. 4, pp. 1850–1856, 2008.

[62] C. S. Chen, C. W. Liu, and J. a. Jiang, "A New Adaptive PMU-Based Protection Scheme for Transposed/Untransposed Parallel Transmission Lines," *IEEE Power Eng.*

Rev., vol. 22, no. 3, pp. 61–62, 2002.

[63] T. Kawady and J. Stenzel, "A practical fault location approach for double circuit transmission lines using single end data," *IEEE Trans. Power Deliv.*, vol. 18, no. 4, pp. 1166–1173, 2003.

[64] Li Shengfang, "A new phase measurement unit (PMU) based fault location algorithm for double circuit lines," in *Eighth IEE International Conference on Developments in Power System Protection*, 2004, vol. 2004, no. I, pp. 188–191.

[65] N. Kang and Y. Liao, "Double-Circuit Transmission-Line Fault Location Utilizing Synchronized Current Phasors," *IEEE Trans. Power Deliv.*, vol. 28, no. 2, pp. 1040–1047, Apr. 2013.

[66] S. V. Unde and S. S. Dambhare, "PMU based fault location for double circuit transmission lines in modal domain," in *IEEE Power and Energy Society General Meeting*, 2016, vol. 2016–Novem, pp. 1–4.

[67] Chi-Shan Yu, Chih-Wen Liu, and Joe-Air Jiang, "A new fault location algorithm for series compensated lines using synchronized phasor measurements," in *2000 Power Engineering Society Summer Meeting (Cat. No.00CH37134)*, 2000, vol. 3, no. c, pp. 1350–1354.

[68] C. A. Apostolopoulos and G. N. Korres, "Accurate fault location algorithm for double-circuit series compensated lines using a limited number of two-end synchronized measurements," *Int. J. Electr. Power Energy Syst.*, vol. 42, no. 1, pp. 495–507, Nov. 2012.

[69] A. N. Zeinhom, "Phasor measurement unit-based distance protection & fault location algorithm for series-compensated transmission lines," in *2014 Saudi Arabia Smart Grid Conference (SASG)*, 2014, pp. 1–7.

[70] A. M. Ranjbar and A. Salehi-Dobakhshari, "Application of synchronised phasor measurements to wide-area fault diagnosis and location," *IET Gener. Transm. Distrib.*, vol. 8, no. 4, pp. 716–729, Apr. 2014.

[71] M. Rezaei Jegarluei, A. Salehi Dobakhshari, A. M. Ranjbar, and A. Tayebi, "A new algorithm for fault location on transmission lines by optimal PMU placement," *Int. Trans. Electr. Energy Syst.*, vol. 25, no. 10, pp. 2071–2086, Oct. 2015.

[72] K.-P. Lien, C.-W. Liu, C.-S. Yu, and J.-A. Jiang, "Transmission Network Fault Location Observability With Minimal PMU Placement," *IEEE Trans. Power Deliv.*, vol. 21, no. 3, pp. 1128–1136, Jul. 2006.

[73] S. M. Brahma, "Fault Location Scheme for a Multi-Terminal Transmission Line Using Synchronized Voltage Measurements," *IEEE Trans. Power Deliv.*, vol. 20, no. 2, pp. 1325–1331, Apr. 2005.

[74] A. S. Dobakhshari, "Wide-area Fault Location of Transmission Lines by Hybrid Synchronized/Unsynchronized Voltage Measurements," *IEEE Trans. Smart Grid*, vol.

3053, no. c, pp. 1–1, 2016.

[75] S. H. Mortazavi and J. Sadeh, “An analytical fault location method based on minimum number of installed PMUs,” *Int. Trans. Electr. Energy Syst.*, vol. 26, no. 2, pp. 253–273, Feb. 2016.

[76] M. Venugopal and C. Tiwari, “A novel algorithm to determine fault location in a transmission line using PMU measurements,” in *2013 IEEE International Conference on Smart Instrumentation, Measurement and Applications, ICSIMA 2013*, 2013, pp. 1–4.

[77] Quanyuan Jiang, Xingpeng Li, Bo Wang, and Haijiao Wang, “PMU-Based Fault Location Using Voltage Measurements in Large Transmission Networks,” *IEEE Trans. Power Deliv.*, vol. 27, no. 3, pp. 1644–1652, Jul. 2012.

[78] N. Parveen, A. S. Rana, and M. S. Thomas, “A practical approach for locating faults for overhead transmission lines using synchronized measurements from PMUs,” in *1st IEEE International Conference on Power Electronics, Intelligent Control and Energy Systems, ICPEICES 2016*, 2017, pp. 1–5.

[79] Joe-Air Jiang, Jun-Zhe Yang, Ying-Hong Lin, Chih-Wen Liu, and Jih-Chen Ma, “An adaptive PMU based fault detection/location technique for transmission lines. I. Theory and algorithms,” *IEEE Trans. Power Deliv.*, vol. 15, no. 2, pp. 486–493, Apr. 2000.

[80] Joe-Air Jiang, Ying-Hong Lin, Jun-Zhe Yang, Tong-Ming Too, and Chih-Wen Liu, “An adaptive PMU based fault detection/location technique for transmission lines. II. PMU implementation and performance evaluation,” *IEEE Trans. Power Deliv.*, vol. 15, no. 4, pp. 1136–1146, Apr. 2000.

[81] Y.-H. Lin, C.-W. Liu, and C.-S. Chen, “A New PMU-Based Fault Detection/Location Technique for Transmission Lines With Consideration of Arcing Fault Discrimination—Part I: Theory and Algorithms,” *IEEE Trans. Power Deliv.*, vol. 19, no. 4, pp. 1587–1593, Oct. 2004.

[82] Y.-H. Lin, C.-W. Liu, and C.-S. Chen, “A New PMU-Based Fault Detection/Location Technique for Transmission Lines With Consideration of Arcing Fault Discrimination—Part II: Performance Evaluation,” *IEEE Trans. Power Deliv.*, vol. 19, no. 4, pp. 1594–1601, Oct. 2004.

[83] D. K. Mohanta, P. Gopakumar, and M. J. B. Reddy, “Transmission line fault detection and localisation methodology using PMU measurements,” *IET Gener. Transm. Distrib.*, vol. 9, no. 11, pp. 1033–1042, Aug. 2015.

[84] C.-J. Lee, Z. Radojević, H.-H. Kim, J.-B. Park, and J.-R. Shin, “A new numerical algorithm for fault location estimation using two-terminal synchronized voltage and current phasors,” in *Power Plants and Power Systems Control 2006*, vol. 5, no. PART 1, Elsevier, 2007, pp. 131–136.

[85] M. Korkali and A. Abur, “Fault location in meshed power networks using synchronized

measurements," in *North American Power Symposium 2010*, 2010, pp. 1–6.

[86] H. Yin and L. Fan, "PMU data-based fault location techniques," in *North American Power Symposium 2010*, 2010, pp. 1–7.

[87] N. Ghaffarzadeh, M. Parpaei, and M. Z. Tayar, "A fast fault location method based on detecting the minimum number of phasor measurement units using a novel adaptive binary differential evolution optimization algorithm," *Int. Trans. Electr. Energy Syst.*, vol. 25, no. 11, pp. 2933–2947, Nov. 2015.

[88] E. Nashawati, R. Garcia, and T. Rosenberger, "Using synchrophasor for fault location identification," in *2012 65th Annual Conference for Protective Relay Engineers*, 2012, pp. 14–21.

[89] A. Esmaeilian and M. Kezunovic, "Fault Location Using Sparse Synchrophasor Measurement of Electromechanical-Wave Oscillations," *IEEE Trans. Power Deliv.*, vol. 31, no. 4, pp. 1787–1796, Aug. 2016.

[90] C.-S. Chen and C.-W. Liu, "Fast and accurate fault detection/location algorithms for double-circuit/three-terminal lines using phasor measurement units," *J. Chinese Inst. Eng.*, vol. 26, no. 3, pp. 289–299, 2003.

[91] S. S. Mousavi-Seyedi, F. Aminifar, M. R. Rezaei, and R. Hasani, "Optimal fault location algorithm for series-compensated transmission lines based on PMU data," in *Smart Grid Conference, SGC 2015*, 2017, pp. 105–109.

[92] C. L. Chuang, J. A. Jiang, Y. C. Wang, C. P. Chen, and Y. T. Hsiao, "An adaptive PMU-based fault location estimation system with a fault-tolerance and load-balancing communication network," in *2007 IEEE Lausanne POWERTECH, Proceedings*, 2007, pp. 1197–1202.

[93] S. D. Picard, M. G. Adamiak, and V. Madani, "Fault location using PMU measurements and wide-area infrastructure," in *2015 68th Annual Conference for Protective Relay Engineers*, 2015, pp. 272–277.

[94] M. Kezunovic, C. Zheng, and C. Pang, "Merging PMU, operational, and non-operational data for interpreting alarms, locating faults and preventing cascades," in *Proceedings of the Annual Hawaii International Conference on System Sciences*, 2010, pp. 1–9.

[95] J. Ren, S. S. Venkata, and E. Sortomme, "An Accurate Synchrophasor Based Fault Location Method for Emerging Distribution Systems," *IEEE Trans. Power Deliv.*, vol. 29, no. 1, pp. 297–298, Feb. 2014.

[96] Z. Mengsheng, W. Yi, Z. Zhou, and Z. Li, "Research on fault location based on PMU for multi-source distribution network," in *Asia-Pacific Power and Energy Engineering Conference, APPEEC*, 2016, vol. 2016–Decem, pp. 1877–1882.

[97] A. Rajeev, T. S. Angel, and F. Z. Khan, "Fault location in distribution feeders with optimally placed PMU's," in *Proceedings of IEEE International Conference on*

Technological Advancements in Power and Energy, TAP Energy 2015, 2015, pp. 438–442.

[98] D. Patynowski *et al.*, "Fault Locator approach for high-impedance grounded or ungrounded distribution systems using synchrophasors," in *2015 68th Annual Conference for Protective Relay Engineers, CPRE 2015*, 2015, pp. 302–310.

[99] M. M. Ghalei, H. K. Kargar, and M. G. M. M. G. M. Zanjani, "High impedance fault detection of distribution network by phasor measurement units," in *Electrical Power Distribution Networks (EPDC), 2012 Proceedings of 17th Conference on*, 2012, no. Proceedings of 17th Conference on, pp. 1–5.

[100] E. S. Tag El Din, M. Gilany, M. M. Abdel Aziz, and D. K. Ibrahim, "An PMU double ended fault location scheme for aged power cables," in *IEEE Power Engineering Society General Meeting, 2005*, 2005, pp. 423–429.

[101] A. A. P. Bescaro, R. A. F. Pereira, and J. R. S. Mantovani, "Optimal Phasor Measurement Units Placement for fault location on overhead electric power distribution feeders," in *2010 IEEE/PES Transmission and Distribution Conference and Exposition: Latin America (T&D-LA)*, 2010, pp. 37–43.

[102] J. Lee, "Automatic Fault Location on Distribution Networks Using Synchronized Voltage Phasor Measurement Units," in *Volume 2: Simple and Combined Cycles; Advanced Energy Systems and Renewables (Wind, Solar and Geothermal); Energy Water Nexus; Thermal Hydraulics and CFD; Nuclear Plant Design, Licensing and Construction; Performance Testing and Performance Test Codes; St*, 2014, vol. 2, p. V002T14A008.

[103] M. Pignati, L. Zanni, P. Romano, R. Cherkaoui, and M. Paolone, "Fault Detection and Faulted Line Identification in Active Distribution Networks Using Synchrophasors-Based Real-Time State Estimation," *IEEE Trans. Power Deliv.*, vol. 32, no. 1, pp. 381–392, Feb. 2017.

[104] R. A. F. Pereira, L. G. W. da Silva, and J. R. S. Mantovani, "PMUs optimized allocation using a tabu search algorithm for fault location in electric power distribution system," in *2004 IEEE/PES Transmision and Distribution Conference and Exposition: Latin America (IEEE Cat. No. 04EX956)*, 2004, pp. 143–148.

[105] J. A. M. Rupa and S. Ganesh, "Power Flow Analysis for Radial Distribution System Using Backward / Forward Sweep Method," vol. 8, no. 10, pp. 1537–1541, 2014.

[106] D. Shirmohammadi, H. W. Hong, A. Semlyen, and G. X. Luo, "A compensation-based power flow method for weakly meshed distribution and transmission networks," *IEEE Trans. Power Syst.*, vol. 3, no. 2, pp. 753–762, May 1988.

[107] M. E. Baran and F. F. Wu, "Network reconfiguration in distribution systems for loss reduction and load balancing," *IEEE Trans. Power Deliv.*, vol. 4, no. 2, pp. 1401–1407, Apr. 1989.

[108] Xiaofeng Zhang, F. Soudi, D. Shirmohammadi, and C. S. Cheng, “A distribution short circuit analysis approach using hybrid compensation method,” *IEEE Trans. Power Syst.*, vol. 10, no. 4, pp. 2053–2059, Nov. 1995.

[109] Y. Ju, W. Wu, B. Zhang, and H. Sun, “An Extension of FBS Three-Phase Power Flow for Handling PV Nodes in Active Distribution Networks,” *IEEE Trans. Smart Grid*, vol. 5, no. 4, pp. 1547–1555, Jul. 2014.

[110] G. Chang, S. Chu, and H. Wang, “A Simplified Forward and Backward Sweep Approach for Distribution System Load Flow Analysis,” in *2006 International Conference on Power System Technology*, 2006, no. 4, pp. 1–5.

[111] J. Wang, L. Lu, J.-Y. Liu, and S. Zhong, “Reconfiguration of Distribution Network with Dispersed Generators Based on Improved Forward-Backward Sweep Method,” in *2010 Asia-Pacific Power and Energy Engineering Conference*, 2010, vol. 2015–Septe, no. 1, pp. 1–5.

[112] K. Kaur and S. Singh, “Optimization and comparison of distributed generator in distribution system using backward and forward sweep method,” in *2016 7th India International Conference on Power Electronics (IICPE)*, 2016, pp. 1–5.

[113] P. Samal and S. Ganguly, “A modified forward backward sweep load flow algorithm for unbalanced radial distribution systems,” in *2015 IEEE Power & Energy Society General Meeting*, 2015, vol. 2015–Septe, pp. 1–5.

[114] G. A. Setia, G. H. M. Sianipar, and R. T. Paribo, “The performance comparison between fast decoupled and backward-forward sweep in solving distribution systems,” in *2016 3rd Conference on Power Engineering and Renewable Energy (ICPERE)*, 2016, pp. 247–251.

[115] G. Benmouyal, “Synchronized phasor measurement in protective relays for protection, control, and analysis of electric power systems,” in *Eighth IEE International Conference on Developments in Power System Protection*, 2004, vol. 2004, pp. 814–820.

[116] A. Roy, J. Bera, and G. Sarkar, “A state-of-the-art PMU based monitoring system with Intelligent Electronic Device using microcontroller,” in *2012 1st International Conference on Power and Energy in NERIST (ICPEN)*, 2012, vol. 2004, pp. 1–4.

[117] M. Chenine and L. Nordstrom, “Modeling and Simulation of Wide-Area Communication for Centralized PMU-Based Applications,” *IEEE Trans. Power Deliv.*, vol. 26, no. 3, pp. 1372–1380, Jul. 2011.

[118] M. Farrokhabadi and L. Vanfretti, “State-of-the-art of topology processors for EMS and PMU applications and their limitations,” in *IECON 2012 - 38th Annual Conference on IEEE Industrial Electronics Society*, 2012, pp. 1422–1427.

[119] A. G. Phadke, “Synchronized phasor measurements-a historical overview,” *IEEE/PES Transm. Distrib. Conf. Exhib.*, vol. 1, no. Virginia Polytech. Inst. & State Univ.,

Blacksburg, VA, USA, pp. 476–479, 2002.

[120] M. Wache, “Application of phasor measurement units in distribution networks,” in *22nd International Conference and Exhibition on Electricity Distribution (CIRED 2013)*, 2013, no. 498, pp. 0498–0498.

[121] A. G. Phadke and J. S. Thorp, “History and applications of phasor measurements,” *2006 IEEE PES Power Syst. Conf. Expo. PSCE 2006 - Proc.*, pp. 331–335, 2006.

[122] Y. Min, “Phasor measurement applications in China,” *IEEE/PES Transm. Distrib. Conf. Exhib.*, vol. 1, pp. 485–489, 2002.

[123] F. Ding and C. D. Booth, “Applications of PMUs in Power Distribution Networks with Distributed Generation,” *Proc. 46th Int. Univ. Power Eng. Conf.*, no. September, pp. 1–5, 2011.

[124] D. Kumar, D. Ghosh, and D. K. Mohanta, “Simulation of phasor measurement unit (PMU) in MATLAB,” in *2015 International Conference on Signal Processing and Communication Engineering Systems*, 2015, no. 4, pp. 15–18.

[125] A. G. Phadke and J. S. Thorp, *Synchronized Phasor Measurements and Their Applications*. Boston, MA: Springer US, 2008.

[126] MISO, *PMU Installation and Configuration Requirements*, no. 1. 2012.

[127] D. of Energy, “Factors Affecting PMU Installation Costs,” no. October, 2014.

[128] K. E. Martin, J. F. Hauer, and T. J. Faris, “PMU Testing and Installation Considerations at the Bonneville Power Administration,” in *2007 IEEE Power Engineering Society General Meeting*, 2007, pp. 1–6.

[129] P. Romano, M. Pignati, and M. Paolone, “Integration of an IEEE Std. C37.118 compliant PMU into a real-time simulator,” in *2015 IEEE Eindhoven PowerTech*, 2015, pp. 1–6.

[130] V. Madani *et al.*, “A Guide for PMU Installation, Commissioning and Maintenance,” 2007.

[131] S. Rabiee, H. Ayoubzadeh, D. Farrokhzad, and F. Aminifar, “Practical aspects of phasor measurement unit (PMU) installation in power grids,” in *2013 Smart Grid Conference (SGC)*, 2013, pp. 20–25.

[132] S. T. Mak and E. So, “Integration of PMU, SCADA, AMI to accomplish expanded functional capabilities of Smart Grid,” in *29th Conference on Precision Electromagnetic Measurements (CPEM 2014)*, 2014, pp. 68–69.

[133] M. S. Almas, L. Vanfretti, S. Lovlund, and J. O. Gjerde, “Open source SCADA implementation and PMU integration for power system monitoring and control applications,” in *2014 IEEE PES General Meeting | Conference & Exposition*, 2014, pp. 1–5.

[134] V. Ramesh, U. Khanz, and M. D. Ili??, “Data aggregation strategies for aligning PMU and AMI measurements in electric power distribution networks,” *NAPS 2011 - 43rd North Am. Power Symp.*, 2011.

[135] C. Tsai and W. Lee, “PMU Based Generator Parameter Identification to,” *2012 IEEE Power Energy Soc. Gen. Meet.*, pp. 1–8, 2012.

[136] E. Jamil, M. Rihan, and M. A. Anees, “Towards optimal placement of phasor measurement units for smart distribution systems,” in *2014 6th IEEE Power India International Conference (PIICON)*, 2014, pp. 1–6.

[137] S. M. Mazhari, H. Monsef, H. Lesani, and A. Fereidunian, “Comments on ‘Minimizing the number of PMUs and their optimal placement in power systems’ in 83 (2012) 66–72,” *Electr. Power Syst. Res.*, vol. 114, pp. 146–148, Sep. 2014.

[138] S. P. Singh and S. P. Singh, “Optimal PMU Placement in Power System Considering the Measurement Redundancy,” *Adv. Electron. Electr. Eng.*, vol. 4, no. 6, pp. 593–598, 2014.

[139] H. A. Abdelsalam, A. Y. Abdelaziz, and V. Mukherjee, “Optimal PMU placement in a distribution network considering network reconfiguration,” in *2014 International Conference on Circuits, Power and Computing Technologies [ICCPCT-2014]*, 2014, pp. 191–196.

[140] A. K. zadeh, H. R. Mashhadi, and M. E. H. Abadi, “Optimal placement of a defined number of Phasor Measurement Units in power systems,” *Smart Grids (ICSG), 2012 2nd Iran. Conf.*, pp. 1–9, 2012.

[141] R. Sodhi, S. C. Srivastava, and S. N. Singh, “Optimal PMU placement method for complete topological and numerical observability of power system,” *Electr. Power Syst. Res.*, vol. 80, no. 9, pp. 1154–1159, Sep. 2010.

[142] A. Y. Abdelaziz, A. M. Ibrahim, and R. H. Salem, “Power system observability with minimum phasor measurement units placement,” *Int. J. Eng. Sci. Technol.*, vol. 5, no. 3, pp. 1–18, 2013.

[143] M. Hurtgen and J.-C. Maun, “Optimal PMU placement using Iterated Local Search,” *Int. J. Electr. Power Energy Syst.*, vol. 32, no. 8, pp. 857–860, Oct. 2010.

[144] D. Ghosh, C. Kumar, T. Ghose, and D. K. Mohanta, “Performance simulation of phasor measurement unit for wide area measurement system,” in *Proceedings of The 2014 International Conference on Control, Instrumentation, Energy and Communication (CIEC)*, 2014, pp. 242–245.

[145] C. Sharma and B. Tyagi, “Sequential PMU placement to monitor power flow in integrated power systems,” in *2014 IEEE PES T&D Conference and Exposition*, 2014, pp. 1–5.

[146] Fei Zeng, Hao Xu, Daonong Zhang, Xiaoyi Zhang, and Yubo Yuan, “A new strategy for optimal PMU placement based on limited exhaustive approach,” in *2014*

International Conference on Power System Technology, 2014, no. Powercon, pp. 67–74.

[147] H. A. Abdelsalam, A. Y. Abdelaziz, R. A. Osama, and R. H. Salem, "Impact of distribution system reconfiguration on optimal placement of phasor measurement units," in *2014 Clemson University Power Systems Conference*, 2014, pp. 1–6.

[148] H. D. Lashkari and J. B. Sarvaiya, "Matlab based Simulink Model of Phasor Measurement Unit and Optimal Placement Strategy for PMU Placement," *Int. J. Sci. Res. Dev.*, vol. 2, no. 3, pp. 135–138, 2014.

[149] B. Ramachandran and G. Thomas Bellarmine, "Improving observability using optimal placement of phasor measurement units," *Int. J. Electr. Power Energy Syst.*, vol. 56, pp. 55–63, Mar. 2014.

[150] S. Mousavian and M. J. Feizollahi, "An investment decision model for the optimal placement of phasor measurement units," *Expert Syst. Appl.*, vol. 42, no. 21, pp. 7276–7284, Nov. 2015.

[151] Q. Li, R. Negi, and M. D. Ilic, "Phasor measurement units placement for power system state estimation: A greedy approach," in *2011 IEEE Power and Energy Society General Meeting*, 2011, pp. 1–8.

[152] V. V., S. Chakrabarti, and S. C. Srivastava, "Power system load modelling under large and small disturbances using phasor measurement units data," *IET Gener. Transm. Distrib.*, vol. 9, no. 12, pp. 1316–1323, 2015.

[153] V. V., S. Chakrabarti, and S. C. Srivastava, "Power system load modelling under large and small disturbances using phasor measurement units data," *IET Gener. Transm. Distrib.*, vol. 9, no. 12, pp. 1316–1323, Sep. 2015.

[154] A. E. Kahunzire and K. O. Awodele, "Improving distribution network state estimation by means of Phasor Measurement Units," in *2014 49th International Universities Power Engineering Conference (UPEC)*, 2014, no. 2, pp. 1–6.

[155] M. Akbari and H. Kazemi, "PMU-Based Distribution Network Load Modelling Using Harmony Search Algorithm," in *Electrical Power Distribution Networks (EPDC), 2012 Proceedings of 17th Conference*, 2012, no. Im, pp. 1–6.

[156] F. Chen, X. Han, Z. Pan, and L. Han, "State estimation model and algorithm including PMU," *Electr. Util. Deregul. Restruct. Power Technol. 2008. DRPT 2008. Third Int. Conf.*, no. April, pp. 1097–1102, 2008.

[157] S. D. Picard, M. G. Adamiak, and V. Madani, "Fault location using PMU measurements and wide-area infrastructure," in *2015 68th Annual Conference for Protective Relay Engineers, CPRE 2015*, 2015, pp. 272–277.

[158] A. Rajeev, T. S. Angel, and F. Z. Khan, "Fault location in distribution feeders with optimally placed PMU's," in *Proceedings of IEEE International Conference on Technological Advancements in Power and Energy, TAP Energy 2015*, 2015, pp. 438–

442.

[159] J. Huang and N. E. Wu, “Fault-tolerant placement of phasor measurement units based on control reconfigurability,” *Control Eng. Pract.*, vol. 21, no. 1, pp. 1–11, Jan. 2013.

[160] J. Ren, S. S. Venkata, and E. Sortomme, “An accurate synchrophasor based fault location method for emerging distribution systems,” *IEEE Trans. Power Deliv.*, vol. 29, no. 1, pp. 297–298, Feb. 2014.

[161] S. Lotfifard, M. Kezunovic, and M. J. Mousavi, “Voltage sag data utilization for distribution fault location,” *IEEE Trans. Power Deliv.*, vol. 26, no. 2, pp. 1239–1246, Apr. 2011.

[162] A. T. Jahromi, P. Wolfs, and S. Islam, “Travelling wave fault location in rural radial distribution networks to reduce wild fire risk,” in *2015 Australasian Universities Power Engineering Conference: Challenges for Future Grids, AUPEC 2015*, 2015, pp. 1–6.

[163] Y. Dong, C. Zheng, and M. Kezunovic, “Enhancing accuracy while reducing computation complexity for Voltage-Sag-based distribution fault location,” *IEEE Trans. Power Deliv.*, vol. 28, no. 2, pp. 1202–1212, Apr. 2013.

[164] V. Terzija, G. Preston, V. Stanojevic, N. I. Elkalashy, and M. Popov, “Synchronized Measurements-Based Algorithm for Short Transmission Line Fault Analysis,” *IEEE Trans. Smart Grid*, vol. 6, no. 6, pp. 2639–2648, Nov. 2015.

[165] Y. Zhang, Y. Xu, and Z. Y. Dong, “Robust Ensemble Data-Analytics for Incomplete PMU Measurements-based Power System Stability Assessment,” *IEEE Trans. Power Syst.*, vol. 639798, pp. 1–1, 2017.

[166] A. Perez, J. Østergaard, and K. Martin, “Improved method for considering PMU ’ s uncertainty and its effect on real-time stability assessment methods based on Th ´ evenin equivalent,” *PowerTech*, 2015.

[167] J. H. Liu and C. C. Chu, “PMU measurement-based voltage stability indicators by modified multi-port equivalent models,” *IEEE Power Energy Soc. Gen. Meet.*, pp. 1–5, 2013.

[168] C. Wang and Y. Hou, “A PMU-based three-step controlled separation with transient stability considerations,” *2014 IEEE PES Gen. Meet. | Conf. Expo.*, no. 51277155, pp. 1–5, 2014.

[169] P. Chusovitin and A. Pazderin, “Small-signal stability monitoring using PMU,” *ENERGYCON 2014 - IEEE Int. Energy Conf.*, pp. 267–272, 2014.

[170] O. Gomez, C. Portilla, and M. A. Rios, “Reliability analysis of substation monitoring systems based on branch PMUs,” *IEEE Trans. Power Syst.*, vol. 30, no. 2, pp. 962–969, 2015.

[171] C. D. Vournas, C. Lambrou, and P. Mandoulidis, “Voltage Stability Monitoring from

a Transmission Bus PMU," *IEEE Trans. Power Syst.*, vol. 8950, no. 1, pp. 1–1, 2016.

[172] M. Rashidi and E. Farjah, "Lyapunov exponent-based optimal PMU placement approach with application to transient stability assessment," *IET Sci. Meas. Technol.*, vol. 10, no. 5, pp. 492–497, 2016.

[173] L. M. Putranto, R. Hara, H. Kita, and E. Tanaka, "Voltage stability-based PMU placement considering N- 1 line contingency and power system reliability," *Proc. - ICPERE 2014 2nd IEEE Conf. Power Eng. Renew. Energy 2014*, pp. 120–125, 2014.

[174] G. Ravikumar, S. Member, S. A. Khaparde, and S. Member, "Taxonomy of PMU Data Based Catastrophic Indicators for Power System Stability Assessment," pp. 1–13, 2016.

[175] D. T. Duong and K. Uhlen, "Online voltage stability monitoring based on PMU measurements and system topology," *2013 3rd Int. Conf. Electr. Power Energy Convers. Syst. EPECS 2013*, pp. 4–9, 2013.

[176] A. Abdlrahem, G. K. Venayagamoorthy, and K. A. Corzine, "Frequency stability and control of a power system with large PV plants using PMU information," *45th North Am. Power Symp. NAPS 2013*, 2013.

[177] P. Pourbeik and G. Stefopoulos, "Validation of generic models for stability analysis of two large static var systems in new york using PMU data," *Proc. IEEE Power Eng. Soc. Transm. Distrib. Conf.*, pp. 1–4, 2014.

[178] H. Y. Su and C. W. Liu, "Estimating the Voltage Stability Margin Using PMU Measurements," *IEEE Trans. Power Syst.*, vol. 31, no. 4, pp. 3221–3229, 2016.

[179] C. Chen, J. Wang, S. Member, Z. Li, H. Sun, and S. Member, "PMU Uncertainty Quantification in Voltage Stability Analysis," vol. 30, no. 4, pp. 2196–2197, 2015.

[180] C. Sharma and B. Tyagi, "Fuzzy type-2 controller design for small-signal stability considering time latencies and uncertainties in PMU measurements," *IEEE Syst. J.*, vol. PP, no. 99, pp. 1–12, 2014.

[181] A. Reddy, K. Ekmen, V. Ajjarapu, and U. Vaidya, "PMU based real-time short term voltage stability monitoring — Analysis and implementation on a real-time test bed," *2014 North Am. Power Symp.*, pp. 1–6, 2014.

[182] G. Wang and C. Liu, "PMU-Based Monitoring of Power System Stability Incorporating Load and Voltage Dynamics," vol. 0, no. 1, pp. 1–5.

[183] J. Lavenius, L. Vanfretti, and G. N. Taranto, "Performance assessment of PMU-based estimation Methods of Thevenin Equivalents for real-time voltage stability monitoring," *2015 IEEE 15th Int. Conf. Environ. Electr. Eng. EEEIC 2015 - Conf. Proc.*, pp. 1977–1982, 2015.

[184] A. Perez, J. Møller, and J. Østergaard, "Uncertainty in real-time voltage stability assessment methods based on Th ´ evenin equivalent due to PMU ' s accuracy," pp. 1–

6, 2014.

[185] C. V. V. S. Bhaskara Reddy, S. Chakrabarti, and S. C. Srivastava, “Reduced network based voltage stability monitoring by using PMU measurements,” *IEEE Reg. 10 Annu. Int. Conf. Proceedings/TENCON*, pp. 762–765, 2017.

[186] T. F. Mazibuko, L. J. Ngoma, J. L. Munda, A. O. Akumu, and S. P. Chowdhury, “Transient Stability of a Multi-machine System based on Synchronised PMU ’ s.”

[187] H. Shah and K. Verma, “Stability Monitoring,” 2016.

[188] M. Adamiak and R. Hunt, “Application of Phasor Measurement Units for Disturbance Recording,” pp. 18–26.

[189] M. K. Neyestanaki and A. M. Ranjbar, “An Adaptive PMU-Based Wide Area Backup Protection Scheme for Power Transmission Lines,” *IEEE Trans. Smart Grid*, vol. 6, no. 3, pp. 1550–1559, May 2015.

[190] S. N. Muneshwar, R. Hasabe, D. Shelar, and P. Kose, “A new adaptive PMU based protection scheme for interconnected transmission network system,” in *2014 International Conference on Circuits, Power and Computing Technologies [ICCPCT-2014]*, 2014, pp. 197–202.

[191] R. A. Guardado and J. L. Guardado, “A PMU Model for Wide-Area Protection in ATP/EMTP,” *IEEE Trans. Power Deliv.*, vol. 31, no. 4, pp. 1953–1960, Aug. 2016.

[192] A. Shaik and P. Tripathy, “Development of Phasor Estimation Algorithm for P-class PMU suitable in Protection Applications,” *IEEE Trans. Smart Grid*, vol. 3053, no. c, pp. 1–1, 2016.

[193] G. Noida and U. Pradesh, “Phasor Measurement Unit (PMU) Based Wide,” pp. 97–99, 2015.

[194] P. Mohammadi and H. El-Kishky, “A robust initialization algorithm for k-means clustering in power distribution networks with PMU-based adaptive protection system,” in *2014 IEEE International Power Modulator and High Voltage Conference (IPMHVC)*, 2014, pp. 252–255.

[195] M. Rahmatian, W. G. Dunford, and A. Moshref, “PMU Based System Protection Scheme,” in *2014 IEEE Electrical Power and Energy Conference*, 2014, pp. 35–40.

[196] A. Saran, “Comparison between overcurrent relay and developed PMU based protection,” in *2013 North American Power Symposium (NAPS)*, 2013, pp. 1–6.

[197] A. Ghorbani, S. Soleymani, and B. Mozafari, “A PMU-Based LOE Protection of Synchronous Generator in the Presence of GIPFC,” *IEEE Trans. Power Deliv.*, vol. 31, no. 2, pp. 551–558, Apr. 2016.

[198] S. Mirsaeidi, D. M. Said, M. W. Mustafa, M. H. Habibuddin, and K. Ghaffari, “A Protection Strategy for Micro-Grids Based on Positive-Sequence Impedance,” *Distrib.*

Gener. Altern. Energy J., vol. 31, no. 3, pp. 7–32, Jun. 2016.

[199] J. O'Brien *et al.*, "Use of synchrophasor measurements in protective relaying applications," in *2014 67th Annual Conference for Protective Relay Engineers*, 2014, pp. 23–29.

[200] X. Gao, L. Bai, and J. J. Cui, "The DTW synchronized MPCA on-line monitoring and fault detection predicted with GCC," in *Chinese Control and Decision Conference, 2008, CCDC 2008*, 2008, no. June, pp. 551–555.

[201] D. Wang and D. Wilson, "PMU-based angle constraint active management on 33kV distribution network," *Electr. Distrib. (…*, no. June, pp. 10–13, 2013.

[202] B. Singh, N. K. Sharma, A. N. Tiwari, K. S. Verma, and S. N. Singh, "Applications of phasor measurement units (PMUs) in electric power system networks incorporated with FACTS controllers," *Int. J. Eng. Sci. Technol.*, vol. 3, no. 3, pp. 64–82, 2011.

[203] Y. Hou, S. Liu, and Z. Qin, "Construction of system restoration strategy with PMU measurements," *Energy Procedia*, vol. 12, pp. 377–386, 2011.

[204] A. Riepnieks and S. Member, "An Introduction to Goodness of Fit for PMU Parameter Estimation," pp. 1–8, 2016.

[205] M. Asprou and E. Kyriakides, "Identification and Estimation of Erroneous Transmission Line Parameters Using PMU Measurements," *IEEE Trans. Power Deliv.*, vol. 8977, no. c, pp. 1–1, 2017.

[206] M. Zhou, V. A. Centeno, A. G. Phadke, Y. Hu, D. Novosel, and H. A. R. Volskis, "A preprocessing method for effective PMU placement studies," *3rd Int. Conf. Deregul. Restruct. Power Technol. DRPT 2008*, no. April, pp. 2862–2867, 2008.

[207] B. Mogharbel, L. Fan, and Z. Miao, "Least squares estimation-based synchronous generator parameter estimation using PMU data," *IEEE Power Energy Soc. Gen. Meet.*, vol. 2015–Septe, pp. 1–5, 2015.

[208] N. Nayak, H. Chen, W. Schmus, and R. Quint, "Generator parameter validation and calibration process based on PMU data," *Proc. IEEE Power Eng. Soc. Transm. Distrib. Conf.*, vol. 2016–July, pp. 4–8, 2016.

[209] Z. Wu, L. T. Zora, and A. G. Phadke, "Simultaneous transmission line parameter and PMU measurement calibration," *IEEE Power Energy Soc. Gen. Meet.*, vol. 2015–Septe, pp. 1–5, 2015.

[210] S. V. Unde and S. S. Dambhare, "Double circuit transmission line parameter estimation using PMU," *2016 IEEE 6th Int. Conf. Power Syst. ICPS 2016*, 2016.

[211] S. Pal, B. Sikdar, and J. Chow, "Classification and Detection of PMU Data Manipulation Attacks Using Transmission Line Parameters," *IEEE Trans. Smart Grid*, vol. 3053, no. c, pp. 1–1, 2017.

[212] D. Shi, D. Tylavsky, K. Koellner, D. Wheeler, and N. Logic, “Transmission Line Parameter Identification using PMU Measurements,” *Iran. J. Sci. Technol. - Trans. Electr. Eng.*, vol. 36, no. E1, pp. 51–66, 2010.

[213] I. Oleinikova, A. Mutule, E. Grebesh, and A. Lvovs, “Line parameter estimation based on PMU application in the power grid,” *2015 IEEE 5th Int. Conf. Power Eng. Energy Electr. Drives*, vol. 5, pp. 453–457, 2015.

[214] K. V. Khandeparkar, S. A. Soman, and G. Gajjar, “Detection and Correction of Systematic Errors in Instrument Transformers along with Line Parameter Estimation using PMU Data,” *IEEE Trans. Power Syst.*, vol. 8950, no. c, pp. 1–1, 2016.

[215] S. D. Chowdhury, “PMU Data Based Online Parameter Estimation of Synchronous Generator,” 2016.

[216] D. Shi, D. J. Tylavsky, N. Logic, and K. M. Koellner, “Identification of short transmission-line parameters from synchrophasor measurements,” *40th North Am. Power Symp. NAPS2008*, pp. 1–8, 2008.

[217] E. C. M. Costa and S. Kurokawa, “Estimation of transmission line parameters using multiple methods,” *IET Gener. Transm. Distrib.*, vol. 9, no. 16, pp. 2617–2624, 2015.

[218] C. Borda, A. Olarte, and H. Diaz, “Estimation,” 2009.

[219] B. Akay and D. Karaboga, “Artificial bee colony algorithm for large-scale problems and engineering design optimization,” *J. Intell. Manuf.*, vol. 23, no. 4, pp. 1001–1014, Aug. 2012.

[220] E. Zitzler and L. Thiele, “An Evolutionary Algorithm for Multiobjective Optimization : The Strength Pareto Approach,” no. 43, p. 43, 1998.

[221] R. E. Wilson, Gary A. Zevenbergen, Dan, “Calculation of Transmission Line Parameters From Synchronized Measurements,” *Electr. Mach. Power Syst.*, vol. 27, no. 12, pp. 1269–1278, Nov. 1999.

[222] D. Shi, D. J. Tylavsky, N. Logic, and K. M. Koellner, “Identification of short transmission-line parameters from synchrophasor measurements,” in *2008 40th North American Power Symposium*, 2008, pp. 1–8.

[223] Yuan Liao and M. Kezunovic, “Online Optimal Transmission Line Parameter Estimation for Relaying Applications,” *IEEE Trans. Power Deliv.*, vol. 24, no. 1, pp. 96–102, Jan. 2009.

[224] A. M. Dan and D. Raisz, “Estimation of transmission line parameters using wide-area measurement method,” in *2011 IEEE Trondheim PowerTech*, 2011, pp. 1–6.

[225] I. W. Slutsker, S. Mokhtari, and K. A. Clements, “Real time recursive parameter estimation in energy management systems,” *IEEE Trans. Power Syst.*, vol. 11, no. 3, pp. 1393–1399, 1996.

[226] Y. Liao, “Algorithms For Fault Location And Line Parameter Estimation Utilizing Voltage and Current Data During the Fault,” in *2008 40th Southeastern Symposium on System Theory (SSST)*, 2008, pp. 183–187.

[227] Dongli Jia, Wanxing Sheng, Xiaohui Song, and Xiaoli Meng, “A system identification method for smart distribution grid,” in *2014 International Conference on Power System Technology*, 2014, no. Powercon, pp. 14–19.

[228] G. D’Antona and M. Davoudi, “Effect of Phasor Measurement Unit on power State Estimation considering parameters uncertainty,” in *2012 IEEE International Workshop on Applied Measurements for Power Systems (AMPS) Proceedings*, 2012, pp. 1–5.

[229] A. M. Prostejovsky, O. Gehrke, A. M. Kosek, T. Strasser, and H. W. Bindner, “Distribution Line Parameter Estimation Under Consideration of Measurement Tolerances,” *IEEE Trans. Ind. Informatics*, vol. 12, no. 2, pp. 726–735, Apr. 2016.

[230] A. E. Pachpinde, “Real Time Monitoring of Distribution Networks Using Internet based PMU,” University at Buffalo, State University of New York, 2014.

[231] A. G. Phadke and J. S. Thorp, “Synchronized Phasor Measurements and their Applications,” *Springer*, p. 246, 2008.

[232] U. S. A. Force, “Global Positioning System.” [Online]. Available: http://www.gps.gov/. [Accessed: 19-May-2017].

[233] Wikipedia, “Global Positioning System.” [Online]. Available: https://en.wikipedia.org/wiki/Global_Positioning_System. [Accessed: 01-Jan-2017].

[234] F. Ding and C. D. Booth, “Applications of PMUs in Power Distribution Networks with Distributed Generation,” in *2011 46th International Universities’ Power Engineering Conference (UPEC)*, 2011, no. September, pp. 1–5.

[235] Feng Ding and C. D. Booth, “Protection and stability assessment in future distribution networks using PMUs,” in *11th IET International Conference on Developments in Power Systems Protection (DPSP 2012)*, 2012, pp. P34–P34.

[236] C. Sutar, “Application of Phasor Measurement Unit in,” vol. 1, no. 2, pp. 26–31, 2013.

[237] A. G. Phadke, “Computer relaying: its impact on improved control and operation of power systems,” *IEEE Comput. Appl. Power*, vol. 1, no. 4, pp. 5–10, Oct. 1988.

[238] J. D. G. M. S. S. T. J. Overbye, *Power System Analysis And Design*, Fifth. Cengage Learning - Global Engineering, 2012.

[239] S. Khan, “R-squared or coefficient of determination,” *khan Academy*, 2011. [Online]. Available: https://www.khanacademy.org/math/ap-statistics/bivariate-data-ap/assessing-fit-least-squares-regression/v/r-squared-or-coefficient-of-determination. [Accessed: 12-Aug-2017].

[240] J. Mora-Flòrez, J. Meléndez, and G. Carrillo-Caicedo, “Comparison of impedance

based fault location methods for power distribution systems," *Electr. Power Syst. Res.*, vol. 78, no. 4, pp. 657–666, Apr. 2008.

[241] K. Ramar and E. E. Ngu, "Generalized Impedance-Based Fault Location for Distribution Systems," *IEEE Trans. Power Deliv.*, vol. 27, no. 1, pp. 449–451, 2012.

[242] R. Dashti and J. Sadeh, "Accuracy improvement of impedance-based fault location method for power distribution network using distributed-parameter line model," *Int. Trans. Electr. Energy Syst.*, vol. 24, no. 3, 2014.

[243] R. Dashti and J. Sadeh, "Applying Dynamic Load Estimation and Distributed-parameter Line Model to Enhance the Accuracy of Impedance-based Fault-location Methods for Power Distribution Networks," *Electr. Power Components Syst.*, vol. 41, no. 14, pp. 1334–1362, 2013.

[244] S. F. Alwash and V. K. Ramachandaramurthy, "New impedance-based fault location method for unbalanced power distribution systems," *Int. Trans. Electr. Energy Syst.*, vol. 25, no. 6, pp. 1008–1021, 2015.

[245] R. H. Salim, K. C. O. Salim, and A. S. Bretas, "Further improvements on impedance-based fault location for power distribution systems," *IET Gener. Transm. Distrib.*, vol. 5, no. 4, pp. 467–478, 2011.

[246] A. T. Jahromi, "A Travelling Wave Detector Based Fault Location Device and Data Recorder for Medium Voltage Distribution Systems," in *2016 Australasian Universities Power Engineering Conference (AUPEC)*, 2016, pp. 3–7.

[247] H. Ye, K. Rui, Z. Zhu, X. Zeng, D. Yang, and Y. Cao, "A novel single-phase grounding fault location method with traveling wave for distribution networks," in *2015 5th International Conference on Electric Utility Deregulation and Restructuring and Power Technologies (DRPT)*, 2015, pp. 1175–1179.

[248] J. Zhao, T. He, C.-M. Liu, and K. Li, "Travelling Wave Fault Location for Distribution Line Based on Improved Morphological Gradient Algorithm," in *2016 International Symposium on Computer, Consumer and Control (IS3C)*, 2016, pp. 156–159.

[249] T. W. Stringfield, D. J. Marihart, and R. F. Stevens, "Fault Location Methods for Overhead Lines," *Trans. Am. Inst. Electr. Eng. Part III Power Appar. Syst.*, vol. 76, no. 3, pp. 518–529, Apr. 1957.

[250] J. J. Grainer and W. Stevenson, *Power System Analysis*. McGraw-Hill, 1994.

[251] D. M. Abido, "EE541 Power System Protection II (Course Handouts)." Dhahran, p. 150, 2010.

[252] J. B. Lee, C. W. Ha, and C. H. Jung, "Development of digital distance relaying algorithm in combined transmission lines with underground power cables," in *2001 Power Engineering Society Summer Meeting. Conference Proceedings (Cat. No.01CH37262)*, 2001, vol. 0, no. C, pp. 611–616 vol.1.

[253] M. Gilany, E. S. Tag El Din, M. M. Abdel Aziz, and D. Khalil Ibrahim, “An accurate scheme for fault location in combined overhead line with underground power cable,” in *IEEE Power Engineering Society General Meeting, 2005*, pp. 1105–1111.

[254] T.-C. Lin, P.-Y. Lin, and C.-W. Liu, “An Algorithm for Locating Faults in Three-Terminal Multisection Nonhomogeneous Transmission Lines Using Synchrophasor Measurements,” *IEEE Trans. Smart Grid*, vol. 5, no. 1, pp. 38–50, Jan. 2014.

[255] Zhentao Xin, Lei Wang, Hongyan Jiang, Baodong Chai, and Jun Yang, “Smart re-close scheme of combined overhead line with underground power cable,” in *2010 International Conference on Power System Technology*, 2010, no. 2, pp. 1–6.

[256] Wang Yang, Zeng Xiangjun, Qin Xiaoan, Zhao Zhenfeng, and Pan Hui, “HHT based single terminal traveling wave fault location for lines combined with overhead-lines and cables,” in *2010 International Conference on Power System Technology*, 2010, pp. 1–6.

APPENDIX A
DETAILS OF DISTRIBUTION SYSTEMS USED IN LOAD FLOW

Table A-1: 5-Bus radial distribution system - bus data

Bus no.	Power (in p.u.)	
	Real	Reactive
1	0	0
2	1.2200	0.9160
3	0.0320	0.2400
4	0.7780	0.5840
5	0.0260	0.0220

Table A-2: 5-Bus radial distribution system - line data

In-bus	Out-bus	Resistance (in p.u.)	Reactance (in p.u.)
1	2	0.0078	0.0187
2	3	0.0078	0.0187
3	4	0.0234	0.0563
3	5	0.3922	0.4594

Table A-3: 7-Bus radial distribution system - bus data

Bus no.	Power (in p.u.)	
	Real	Reactive
1	0	0
2	1.2200	0.9160
3	0.0320	0.0240
4	0.7780	0.5840
5	0.6730	0.5950
6	1.2200	0.9160
7	0.0488	0.0366

Table A-4: 7-Bus radial distribution system - line data

In-bus	Out-bus	Resistance (in p.u.)	Reactance (in p.u.)
1	2	0.0500	0.0664
2	3	0.0233	0.0331
1	4	0.0466	0.0620
1	5	0.0208	0.0277
5	6	0.0250	0.0332
1	7	0.0267	0.0354

Table A-5: 11-Bus radial distribution system - bus data

Bus no.	Power (in p.u.)	
	Real	**Reactive**
1	0	0
2	1.2200	0.9160
3	0.0320	0.0240
4	0.7780	0.5840
5	0.6730	0.5950
6	1.2200	0.9160
7	0.0488	0.0366
8	0.9560	0.7170
9	0.6980	0.5230
10	1.2650	0.9490
11	0.2650	0.0949

Table A-6: 11-Bus radial distribution system - line data

In-bus	Out-bus	Resistance (in p.u.)	Reactance (in p.u.)
1	2	0.0500	0.0664
2	3	0.0233	0.0331
1	4	0.0466	0.0620
1	5	0.0208	0.0277
5	6	0.0250	0.0332
1	7	0.0267	0.0354
7	8	0.0275	0.0365
1	9	0.0333	0.0443
1	10	0.0208	0.0277
2	11	0.0208	0.0277

Table A-7: 25-Bus radial distribution system - bus data

Bus no.	Power (in p.u.)	
	Real	Reactive
1	0	0
2	0.0180	0.0066
3	0.0031	0.0011
4	0	0
5	0.0095	0.0034
6	0.0302	0.0032
7	0.0116	0.0034
8	0	0
9	0.0235	0.0063
10	0.0105	0.0045
11	0	0
12	0.0280	0.0091
13	0.0086	0.0012
14	0.0152	0.0016
15	0.0081	0.0017
16	0.0126	0.0037
17	0.0041	0.0005
18	0.0117	0.0045
19	0.0306	0.0098
20	0	0

Bus no.	Power (in p.u.)	
	Real	Reactive
21	0.0498	0.0101
22	0.0136	0.0043
23	0.0185	0.0032
24	0.0111	0.0027
25	0.0324	0.0076

Table A-8: 25-Bus radial distribution system - line data

In-bus	Out-bus	Resistance (in p.u.)	Reactance (in p.u.)
1	2	0.0225	0.0182
2	3	0.0375	0.0304
3	4	0.0337	0.0274
4	5	0.0487	0.0396
5	6	0.0187	0.0152
6	7	0.0187	0.0152
7	8	0.0375	0.0304
8	9	0.0075	0.0060
9	10	0.0187	0.0152
10	11	0.0750	0.0608
11	12	0.0112	0.0091
12	13	0.0750	0.0608
13	14	0.0562	0.0457
11	15	0.0375	0.0304
15	16	0.0375	0.0304
16	17	0.0375	0.0304
8	18	0.0562	0.0457
18	19	0.0281	0.0228
19	20	0.0056	0.0045
20	21	0.0262	0.0212
4	22	0.0037	0.0030

22	23	0.0225	0.0182
20	24	0.0938	0.0762
24	25	0.0131	0.0106

Table A-9: 28-Bus radial distribution system - bus data

Bus no.	Power (in p.u.)	
	Real	Reactive (1.0e-03 *)
1	0.0014	0.9000
2	0.0008	0.5000
3	0.0008	0.6000
4	0.0010	0.6000
5	0.0008	0.5000
6	0.0009	0.4000
7	0.0009	0.4000
8	0.0008	0.5000
9	0.0009	0.5000
10	0.0008	0.5000
11	0.0008	0.4000
12	0.0009	0.5000
13	0.0007	0.4000
14	0.0007	0.4000
15	0.0007	0.4000
16	0.0006	0.3000
17	0.0006	0.3000
18	0.0007	0.4000
19	0.0005	0.3000
20	0.0005	0.3000

Bus no.	Power (in p.u.)	
	Real	Reactive (1.0e-03 *)
21	0.0004	0.2000
22	0.0005	0.3000
23	0.0005	0.2000
24	0.0006	0.3000
25	0.0004	0.2000
26	0.0004	0.2000
27	0.0004	0.2000
28	0	0

Table A-10: 28-Bus radial distribution system - line data

In-bus	Out-bus	Resistance (in p.u.)	Reactance (in p.u.)
1	2	1.5055	0.6264
2	3	1.8405	0.7831
3	4	1.1291	0.4698
4	5	0.7587	0.3132
5	6	3.0109	1.2529
6	7	2.2582	0.9397
7	8	1.2044	0.5012
8	9	2.2582	0.9397
9	10	3.0109	1.2529
10	11	2.2744	0.6430
11	12	1.1372	0.3215
12	13	3.4116	0.9645
13	14	3.4116	0.7073
14	15	2.5018	0.6430
15	16	2.2744	0.9645
16	17	3.4116	0.6430
17	18	2.2744	0.6430
2	19	2.8430	0.8037
19	20	1.1372	0.3215
20	21	2.2744	0.6430
21	22	4.0939	1.1574

3	23	2.9567	0.8359
23	24	2.5018	0.7073
24	25	4.5488	1.2860
6	26	2.2744	0.6430
26	27	1.1372	0.3215
27	28	1.1372	0.3215

Table A-11: 30-Bus radial distribution system - bus data

Bus no.	Power (in p.u.)	
	Real	Reactive
1	0	0
2	0.0042	0.0026
3	0	0
4	0.0042	0.0026
5	0.0042	0.0026
6	0	0
7	0	0
8	0.0042	0.0026
9	0.0042	0.0026
10	0.0041	0.0025
11	0.0042	0.0026
12	0.0025	0.0015
13	0.0011	0.0007
14	0.0011	0.0007
15	0.0011	0.0007
16	0.0002	0.0001
17	0.0044	0.0027
18	0.0044	0.0027
19	0.0044	0.0027
20	0.0044	0.0027

Bus no.	Power (in p.u.)	
	Real	Reactive
21	0.0044	0.0027
22	0.0044	0.0027
23	0.0044	0.0027
24	0.0044	0.0027
25	0.0044	0.0027
26	0.0044	0.0027
27	0.0026	0.0016
28	0.0017	0.0011
29	0.0017	0.0011
30	0.0017	0.0011

Table A-12: 30-Bus radial distribution system - line data

In-bus	Out-bus	Resistance (in p.u.)	Reactance (in p.u.)
1	2	0.0967	0.0397
2	3	0.0886	0.0364
3	4	0.1359	0.0377
4	5	0.1236	0.0343
5	6	0.1236	0.0343
6	7	0.2598	0.0446
7	8	0.1732	0.0298
8	9	0.2598	0.0446
9	10	0.1732	0.0298
10	11	0.1083	0.0186
11	12	0.0866	0.0149
3	13	0.1299	0.0223
13	14	0.1732	0.0298
14	15	0.0866	0.0149
15	16	0.0433	0.0074
6	17	0.1483	0.0412
17	18	0.1359	0.0377
18	19	0.1718	0.0391
19	20	0.1562	0.0355
20	21	0.1562	0.0355
21	22	0.2165	0.0372

22	23	0.2165	0.0372
23	24	0.2598	0.0446
24	25	0.1732	0.0298
25	26	0.1083	0.0186
26	27	0.0866	0.0149
7	28	0.1299	0.0223
28	29	0.1299	0.0223
29	30	0.1299	0.0223

Table A-13: 33-Bus radial distribution system - bus data

Bus no.	Power (in p.u.)	
	Real	Reactive
1	0	0
2	0.0010	0.0006
3	0.0009	0.0004
4	0.0012	0.0008
5	0.0006	0.0003
6	0.0006	0.0002
7	0.0020	0.0010
8	0.0020	0.0010
9	0.0006	0.0002
10	0.0006	0.0002
11	0.0004	0.0003
12	0.0006	0.0004
13	0.0006	0.0004
14	0.0012	0.0008
15	0.0006	0.0001
16	0.0006	0.0002
17	0.0006	0.0002
18	0.0009	0.0004
19	0.0009	0.0004
20	0.0009	0.0004

Bus no.	Power (in p.u.)	
	Real	Reactive
21	0.0009	0.0004
22	0.0009	0.0004
23	0.0009	0.0005
24	0.0042	0.0020
25	0.0042	0.0020
26	0.0006	0.0003
27	0.0006	0.0003
28	0.0006	0.0002
29	0.0012	0.0007
30	0.0020	0.0060
31	0.0015	0.0007
32	0.0021	0.0010
33	0.0006	0.0004

Table A-14: 33-Bus radial distribution system - line data

In-bus	Out-bus	Resistance (in p.u.)	Reactance (in p.u.)
1	2	0.0085	0.0043
2	3	0.0453	0.0231
3	4	0.0336	0.0171
4	5	0.0350	0.0178
5	6	0.0752	0.0649
6	7	0.0172	0.0568
7	8	0.0653	0.0216
8	9	0.0946	0.0680
9	10	0.0959	0.0680
10	11	0.0181	0.0060
11	12	0.0344	0.0114
12	13	0.1348	0.1061
13	14	0.0497	0.0655
14	15	0.0543	0.0483
15	16	0.0685	0.0500
16	17	0.1184	0.1580
17	18	0.0672	0.0527
2	19	0.0151	0.0144
19	20	0.1381	0.1245
20	21	0.0376	0.0439
21	22	0.0651	0.0861

3	23	0.0414	0.0283
23	24	0.0825	0.0651
24	25	0.0823	0.0644
6	26	0.0186	0.0095
26	27	0.0261	0.0133
27	28	0.0972	0.0857
28	29	0.0738	0.0643
29	30	0.0466	0.0237
30	31	0.0895	0.0884
31	32	0.0285	0.0332
32	33	0.0313	0.0487

Table A-15: 34-Bus radial distribution system - bus data

Bus no.	Power (in p.u.)	
	Real	Reactive
1	0	0
2	0.0042	0.0026
3	0	0
4	0.0042	0.0026
5	0.0042	0.0026
6	0	0
7	0	0
8	0.0042	0.0026
9	0.0042	0.0026
10	0.0041	0.0025
11	0.0042	0.0026
12	0.0025	0.0015
13	0.0011	0.0007
14	0.0011	0.0007
15	0.0011	0.0007
16	0.0002	0.0001
17	0.0044	0.0027
18	0.0044	0.0027
19	0.0044	0.0027
20	0.0044	0.0027

Bus no.	Power (in p.u.)	
	Real	Reactive
21	0.0044	0.0027
22	0.0044	0.0027
23	0.0044	0.0027
24	0.0044	0.0027
25	0.0044	0.0027
26	0.0044	0.0027
27	0.0026	0.0016
28	0.0017	0.0011
29	0.0017	0.0011
30	0.0017	0.0011
31	0.0017	0.0011
32	0.0017	0.0011
33	0.0017	0.0011
34	0.0017	0.0011

Table A-16: 34-Bus radial distribution system - line data

In-bus	Out-bus	Resistance (in p.u.)	Reactance (in p.u.)
1	2	0.0967	0.0397
2	3	0.0886	0.0364
3	4	0.1359	0.0377
4	5	0.1236	0.0343
5	6	0.1236	0.0343
6	7	0.2598	0.0446
7	8	0.1732	0.0298
8	9	0.2598	0.0446
9	10	0.1732	0.0298
10	11	0.1083	0.0186
11	12	0.0866	0.0149
3	13	0.1299	0.0223
13	14	0.1732	0.0298
14	15	0.0866	0.0149
15	16	0.0433	0.0074
6	17	0.1483	0.0412
17	18	0.1359	0.0377
18	19	0.1718	0.0391
19	20	0.1562	0.0355
20	21	0.1562	0.0355
21	22	0.2165	0.0372

22	23	0.2165	0.0372
23	24	0.2598	0.0446
24	25	0.1732	0.0298
25	26	0.1083	0.0186
26	27	0.0866	0.0149
7	28	0.1299	0.0223
28	29	0.1299	0.0223
29	30	0.1299	0.0223
30	31	0.1299	0.0223
31	32	0.1299	0.0223
32	33	0.1299	0.0223
33	34	0.1299	0.0223

Table A-17: 69-Bus radial distribution system - bus data

Bus no.	Power (in p.u.)	
	Real	Reactive
1	0	0
2	0	0
3	0	0
4	0	0
5	0.0000	0.0000
6	0.0004	0.0003
7	0.0008	0.0005
8	0.0003	0.0002
9	0.0003	0.0002
10	0.0014	0.0010
11	0.0014	0.0010
12	0.0001	0.0001
13	0.0001	0.0001
14	0	0
15	0.0005	0.0003
16	0.0006	0.0003
17	0.0006	0.0003
18	0	0
19	0.0000	0.0000
20	0.0011	0.0008

Bus no.	Power (in p.u.)	
	Real	Reactive
21	0.0001	0.0000
22	0	0
23	0.0003	0.0002
24	0	0
25	0.0001	0.0001
26	0.0001	0.0001
27	0.0003	0.0002
28	0.0003	0.0002
29	0	0
30	0	0
31	0	0
32	0.0001	0.0001
33	0.0001	0.0001
34	0.0001	0.0000
35	0.0003	0.0002
36	0.0003	0.0002
37	0	0
38	0.0002	0.0002
39	0.0002	0.0002
40	0.0000	0.0000
41	0	0

Bus no.	Power (in p.u.)	
	Real	Reactive
42	0.0001	0.0000
43	0	0
44	0.0004	0.0003
45	0.0004	0.0003
46	0	0
47	0.0008	0.0006
48	0.0038	0.0027
49	0.0038	0.0027
50	0.0004	0.0003
51	0.0000	0.0000
52	0.0000	0.0000
53	0.0003	0.0002
54	0.0002	0.0002
55	0	0
56	0	0
57	0	0
58	0.0010	0.0007
59	0	0
60	0.0124	0.0089
61	0.0003	0.0002
62	0	0

Bus no.	Power (in p.u.)	
	Real	Reactive
63	0.0023	0.0016
64	0.0006	0.0004
65	0.0002	0.0001
66	0.0002	0.0001
67	0.0003	0.0002
68	0.0003	0.0002
69	0.0003	0.0002

Table A-18: 69-Bus radial distribution system - line data

In-bus	Out-bus	Resistance (in p.u.)	Reactance (in p.u.)
1	2	0.0003	0.0008
2	3	0.0003	0.0008
3	4	0.0010	0.0025
4	5	0.0174	0.0204
5	6	0.2542	0.1294
6	7	0.2647	0.1348
7	8	0.0640	0.0326
8	9	0.0342	0.0174
9	10	0.5687	0.1880
10	11	0.1300	0.0430
11	12	0.4940	0.1633
12	13	0.7153	0.2361
13	14	0.7250	0.2396
14	15	0.7347	0.2428
15	16	0.1365	0.0451
16	17	0.2600	0.0860
17	18	0.0033	0.0011
18	19	0.2275	0.0752
19	20	0.1462	0.0479
20	21	0.2372	0.0784
21	22	0.0097	0.0032
22	23	0.1105	0.0365
23	24	0.2405	0.0795

24	25	0.5200	0.1719
25	26	0.2145	0.0709
26	27	0.1203	0.0397
3	28	0.0031	0.0075
28	29	0.0444	0.1087
29	30	0.2762	0.0913
30	31	0.0488	0.0161
31	32	0.2437	0.0806
32	33	0.5826	0.1956
33	34	1.1861	0.3921
34	35	1.0236	0.3384
3	36	0.0031	0.0075
36	37	0.0444	0.1087
37	38	0.0731	0.0854
38	39	0.0211	0.0247
39	40	0.0013	0.0015
40	41	0.5058	0.5909
41	42	0.2153	0.2516
42	43	0.0285	0.0332
43	44	0.0064	0.0081
44	45	0.0756	0.0953
45	46	0.0006	0.0008
4	47	0.0024	0.0058

47	48	0.0591	0.1447
48	49	0.2013	0.4924
49	50	0.0571	0.1397
8	51	0.0644	0.0328
51	52	0.2305	0.0774
52	53	0.1208	0.0615
53	54	0.1410	0.0718
54	55	0.1974	0.1005
55	56	0.1953	0.0995
56	57	1.1042	0.3706
57	58	0.5442	0.1826
58	59	0.2112	0.0699
59	60	0.2681	0.0814
60	61	0.3524	0.1795
61	62	0.0676	0.0344
62	63	0.1007	0.0512
63	64	0.4934	0.2513
64	65	0.7229	0.3682
11	66	0.1397	0.0424
66	67	0.0033	0.0010
12	68	0.5135	0.1697
68	69	0.0033	0.0011

APPENDIX B
DETAILED SIMULATION RESULTS FOR LINE PARAMETERS IDENTIFICATION

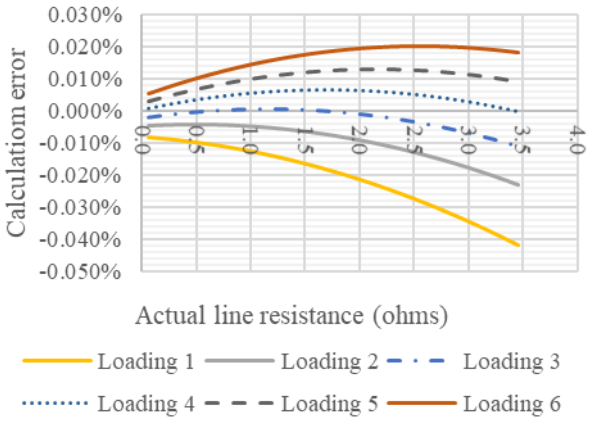

Figure B-1: Line resistance calculation (Method 1- Case 1)

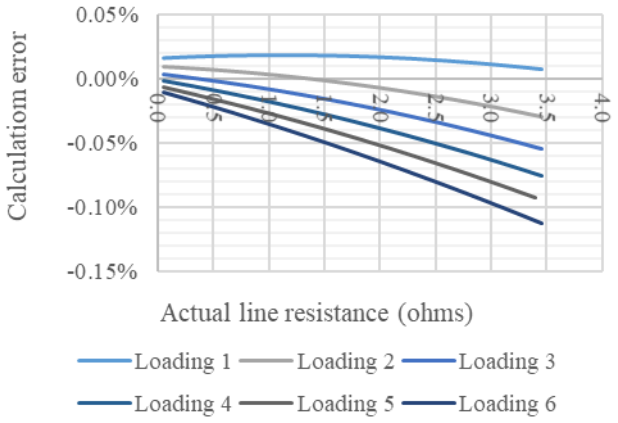

Figure B-2: Line resistance calculation (Method 1- Case 2)

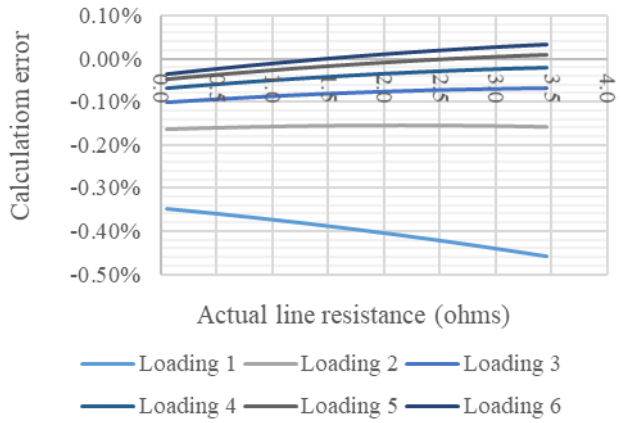

Figure B-3: Line resistance calculation (Method 1- Case 3)

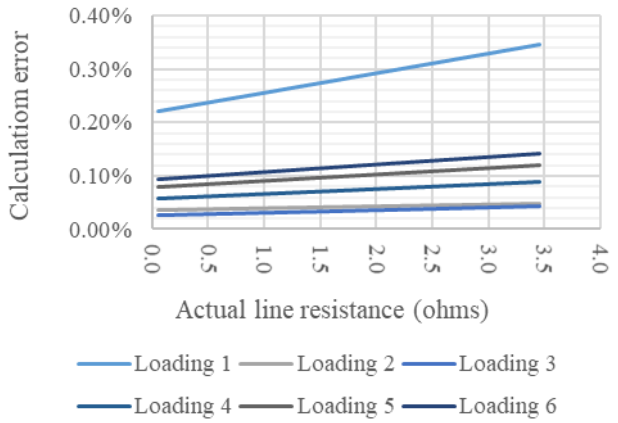

Figure B-4: Line resistance calculation (Method 1- Case 4)

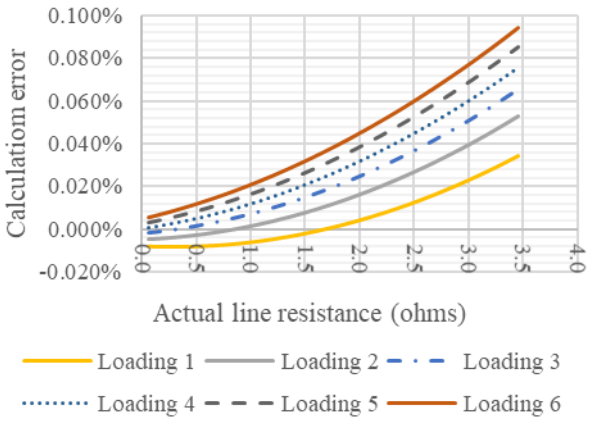

Figure B-5: Line resistance calculation (Method 2- Case 1)

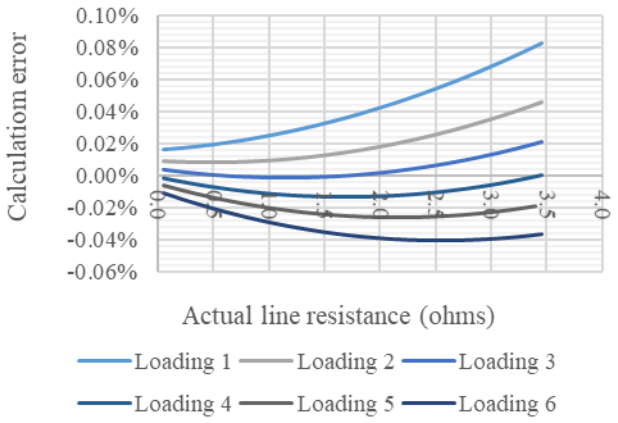

Figure B-6: Line resistance calculation (Method 2- Case 2)

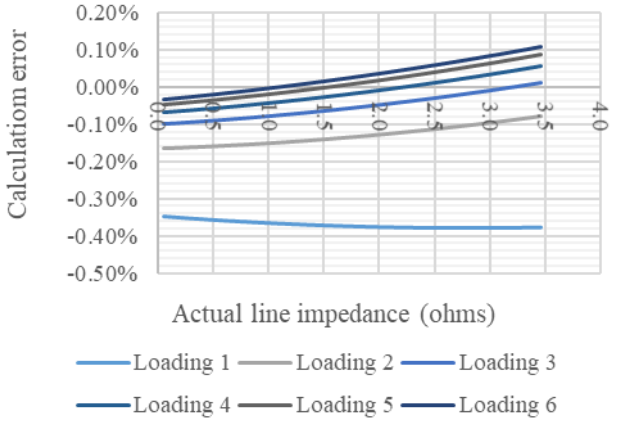

Figure B-7: Line resistance calculation (Method 2- Case 3)

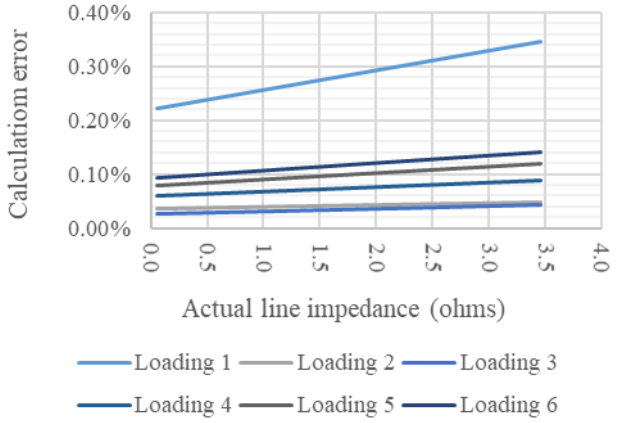

Figure B-8: Line resistance calculation (Method 2- Case 4)

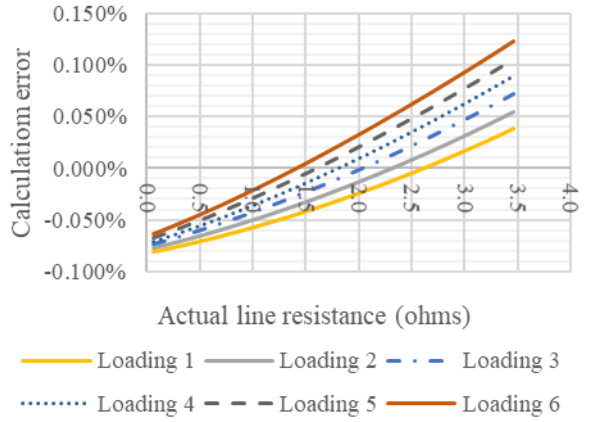

Figure B-9: Line resistance calculation (Method 3- Case 1)

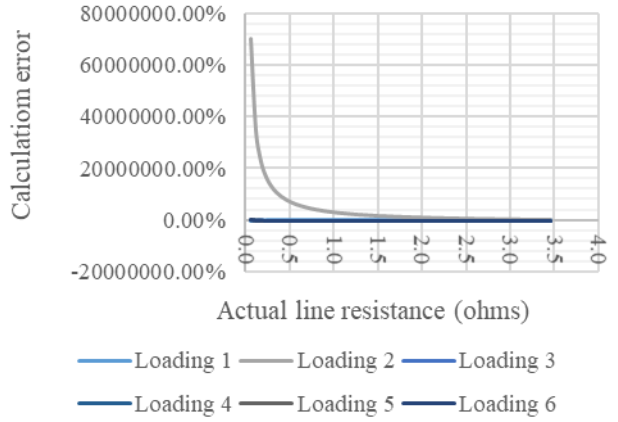

Figure B-10: Line resistance calculation (Method 3- Case 2)

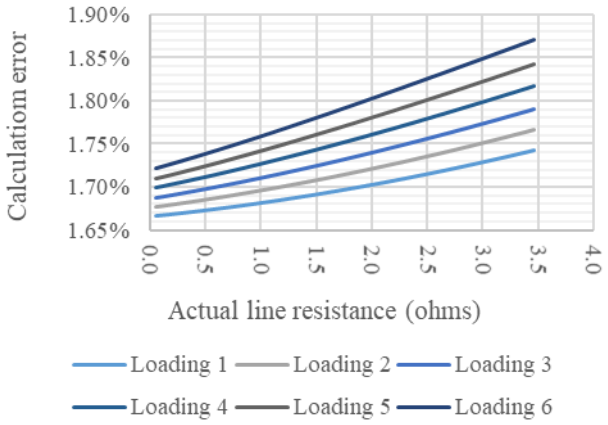

Figure B-11: Line resistance calculation (Method 3- Case 3)

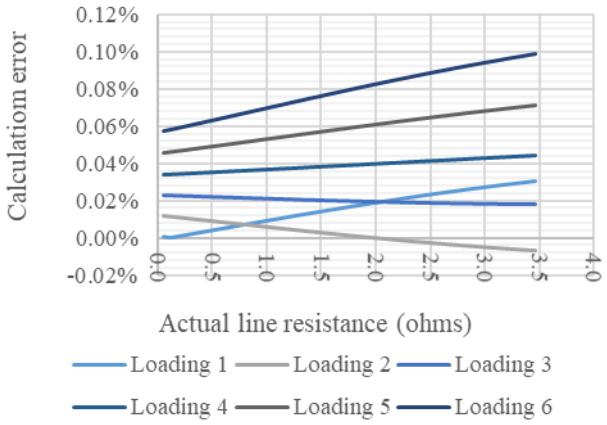

Figure B-12: Line resistance calculation (Method 3- Case 4)

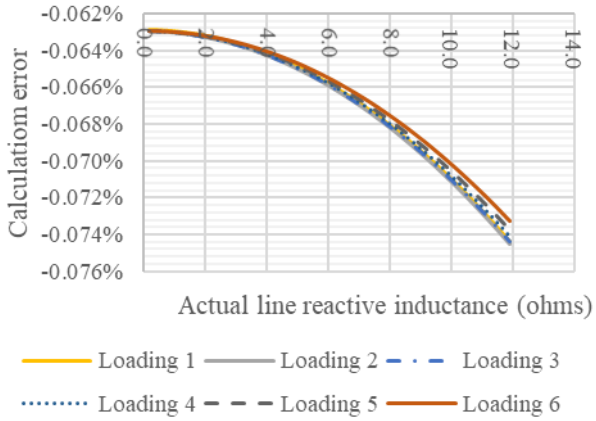

Figure B-13: Line reactive inductance calculation (Method 1- Case 1)

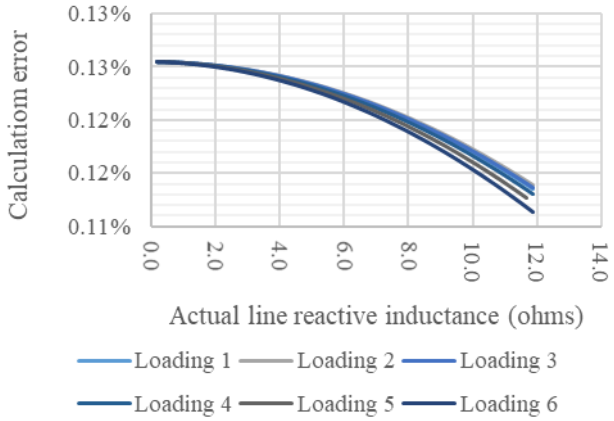

Figure B-14: Line reactive inductance calculation (Method 1- Case 2)

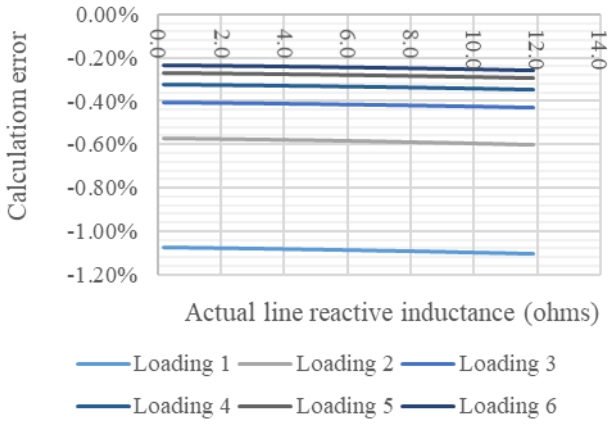

Figure B-15: Line reactive inductance calculation (Method 1- Case 3)

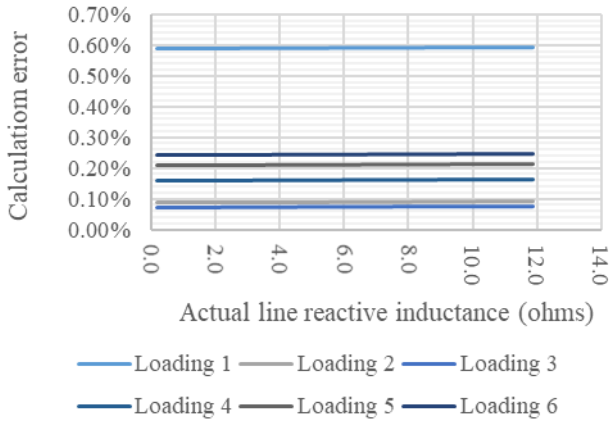

Figure B-16: Line reactive inductance calculation (Method 1- Case 4)

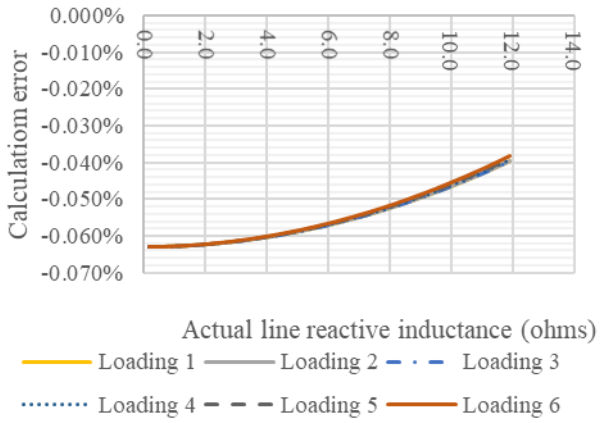

Figure B-17: Line reactive inductance calculation (Method 2-Case 1)

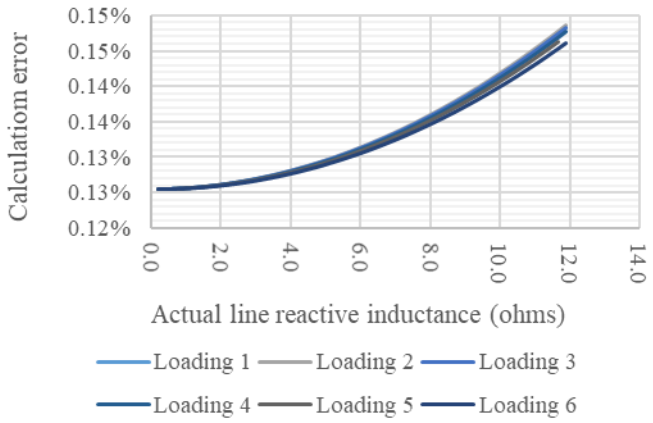

Figure B-18: Line reactive inductance calculation (Method 2-Case 2)

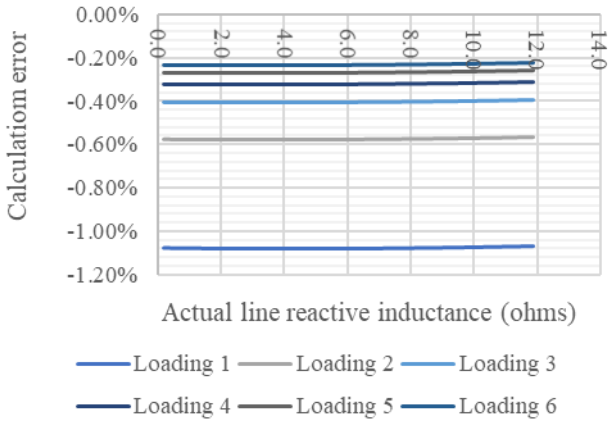

Figure B-19: Line reactive inductance calculation (Method 2-Case 3)

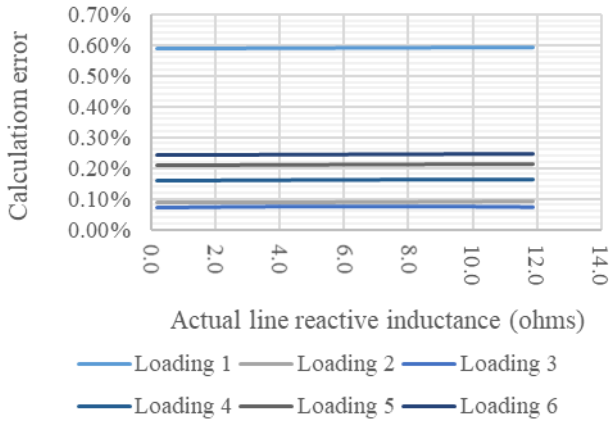

Figure B-20: Line reactive inductance calculation (Method 2-Case 4)

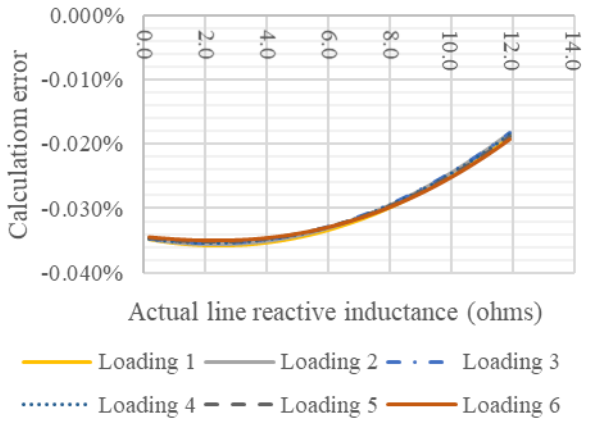

Figure B-21: Line reactive inductance calculation (Method 3-Case 1)

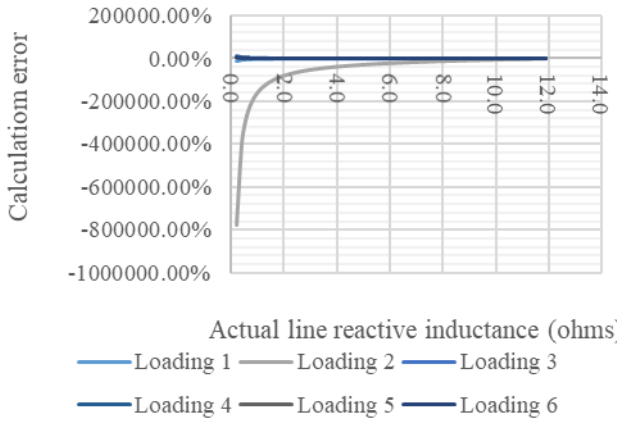

Figure B-22: Line reactive inductance calculation (Method 3-Case 2)

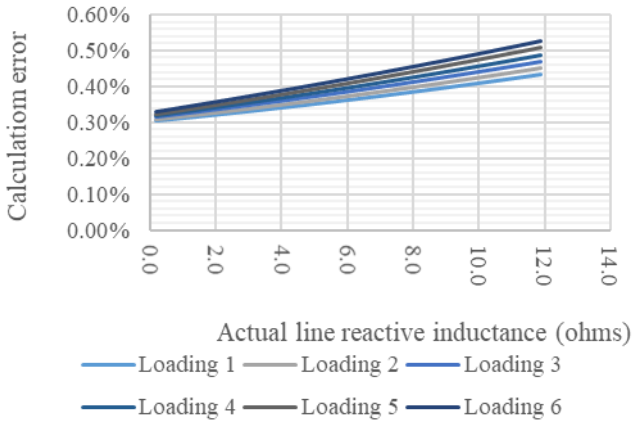

Figure B-23: Line reactive inductance calculation (Method 3- Case 3)

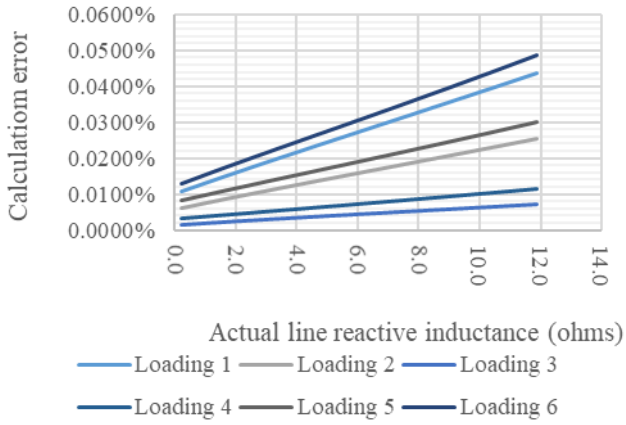

Figure B-24: Line reactive inductance calculation (Method 3- Case 4)

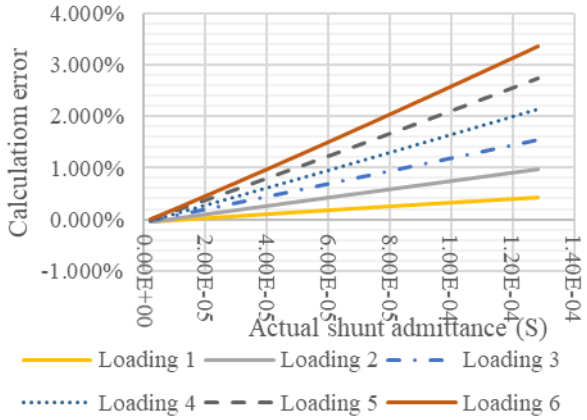

Figure B-25: Line shunt admittance calculation (Method 1- Case 1)

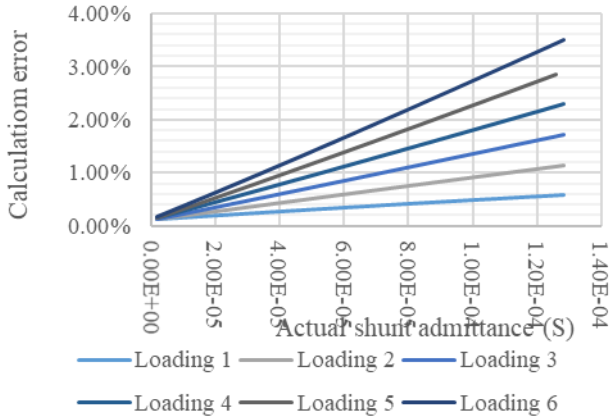

Figure B-26: Line shunt admittance calculation (Method 1- Case 2)

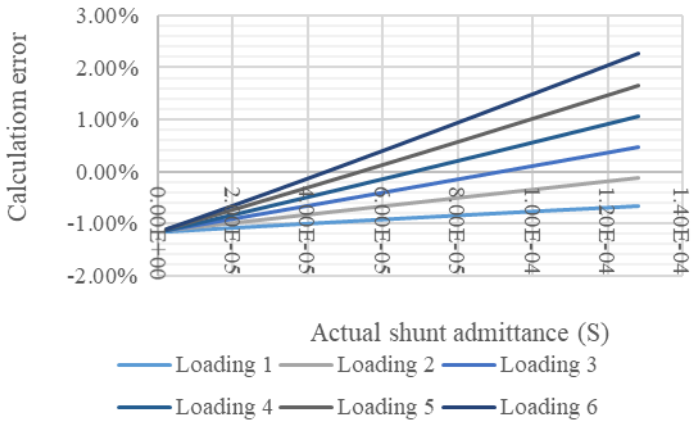

Figure B-27: Line shunt admittance calculation (Method 1- Case 3)

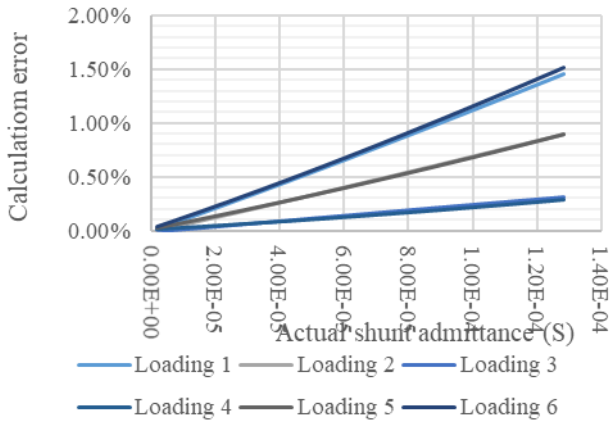

Figure B-28: Line shunt admittance calculation (Method 1- Case 4)

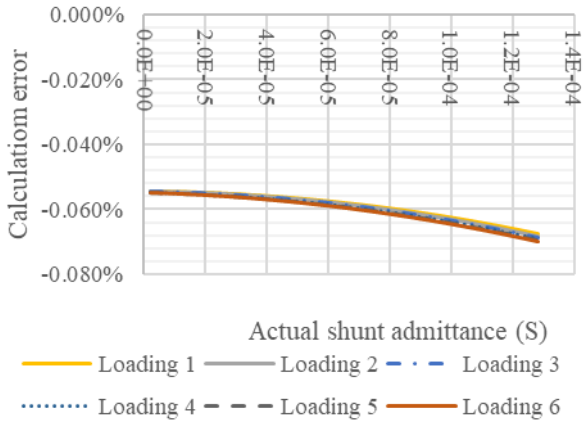

Figure B-29: Line shunt admittance calculation (Method 2- Case 1)

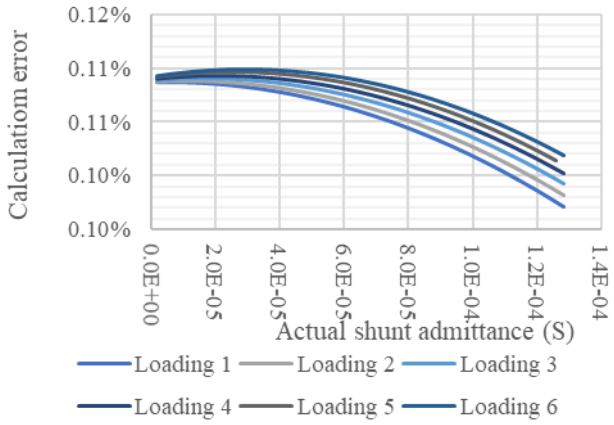

Figure B-30: Line shunt admittance calculation (Method 2- Case 2)

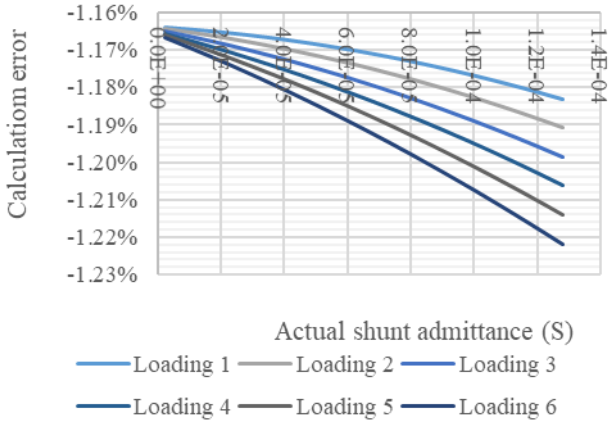

Figure B-31: Line shunt admittance calculation (Method 2- Case 3)

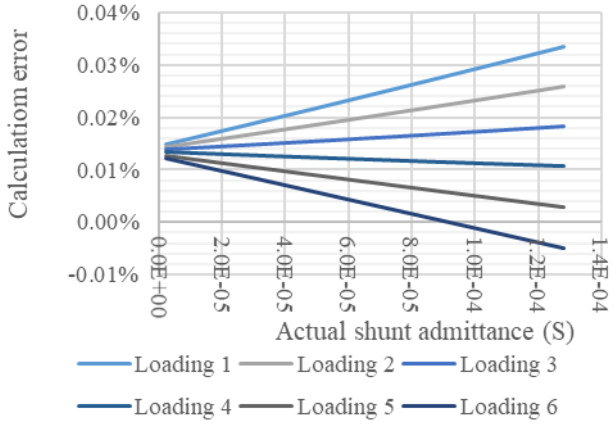

Figure B-32: Line shunt admittance calculation (Method 2- Case 4)

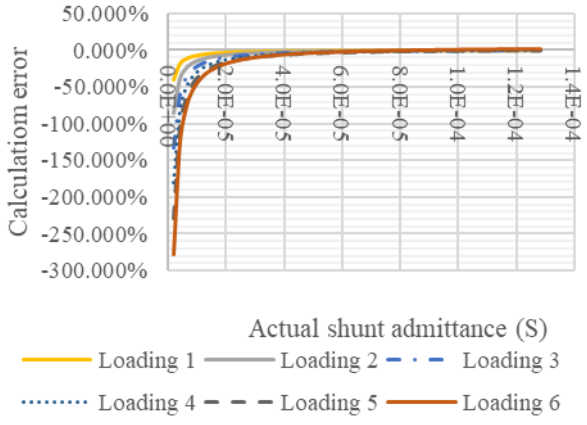

Figure B-33: Line shunt admittance calculation (Method 3- Case 1)

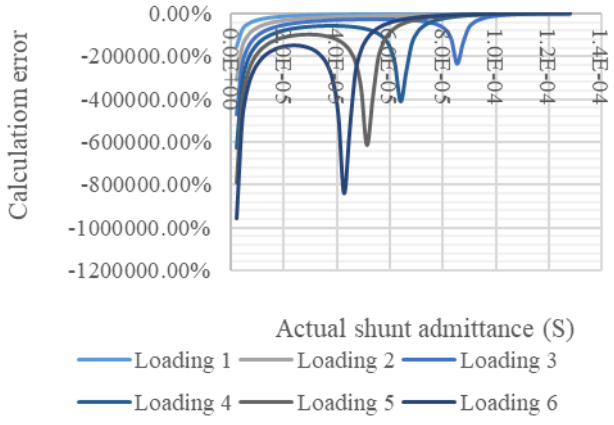

Figure B-34: Line shunt admittance calculation (Method 3- Case 2)

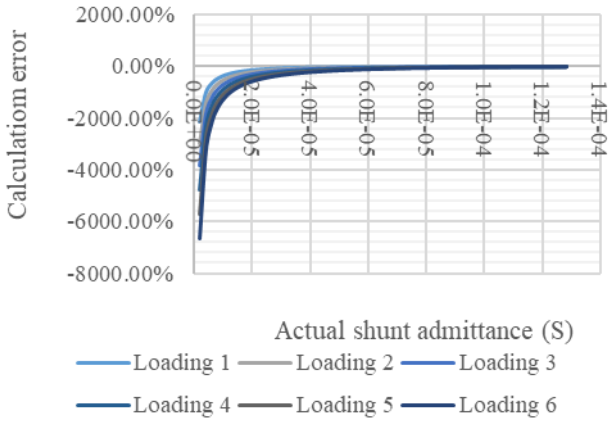

Figure B-35: Line shunt admittance calculation (Method 3- Case 3)

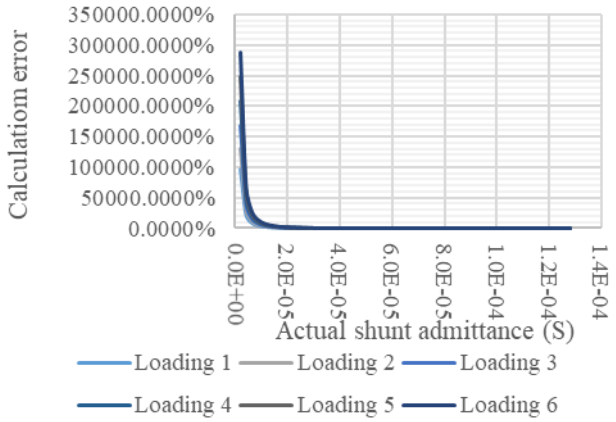

Figure B-36: Line shunt admittance calculation (Method 3- Case 4)

APPENDIX C
DETAILED SIMULATION RESULTS FOR IMPEDANCE-BASED FAULT LOCATION

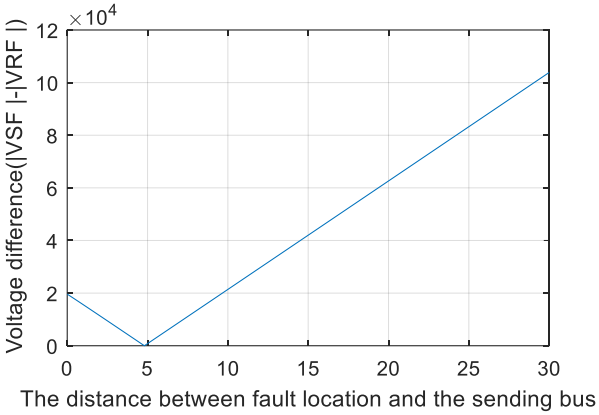

Figure C-1: Fault location solution for line-to-ground (AG) fault at 5 km from the sending bus under Scenario 1

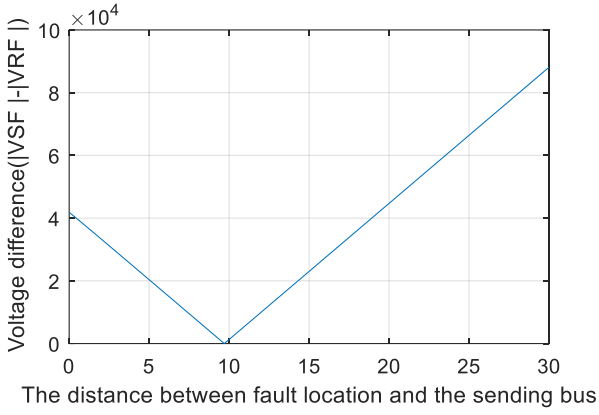

Figure C-2: Fault location solution for line-to-ground (BG) fault at 10 km from the sending bus under Scenario 1

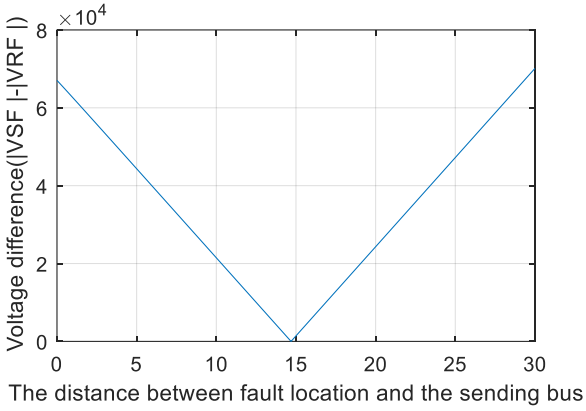

Figure C-3: Fault location solution for line-to-ground (CG) fault at 15 km from the sending bus under Scenario 1

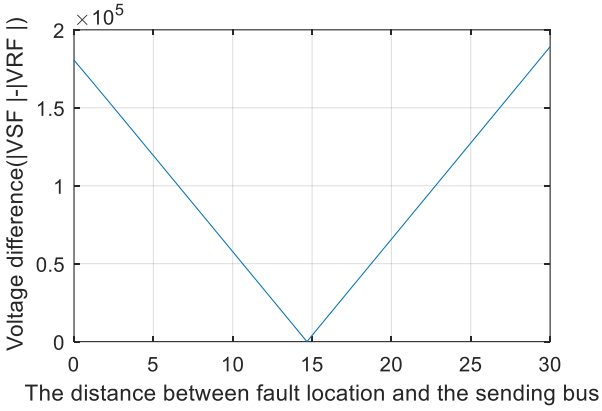

Figure C-4: Fault location solution for line-to-line (AB) fault at 15 km from the sending bus under Scenario 1

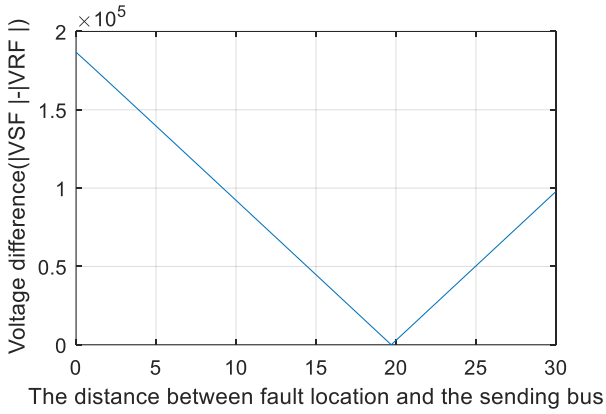

Figure C-5: Fault location solution for line-to-line (BC) fault at 20 km from the sending bus under Scenario 1

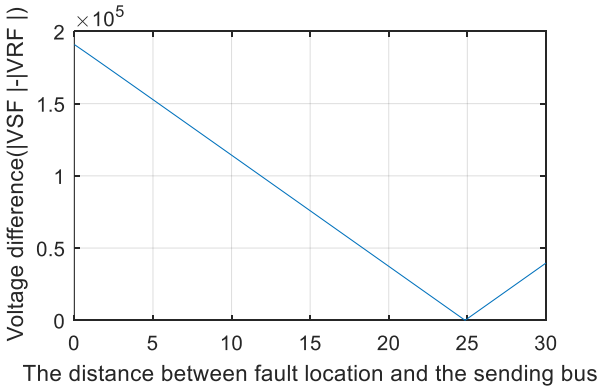

Figure C-6: Fault location solution for line-to-line (AC) fault at 25 km from the sending bus under Scenario 1

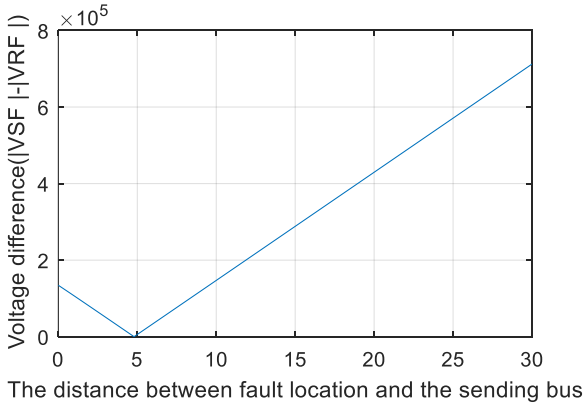

Figure C-7: Fault location solution for double line-to-ground (ABG) fault at 5 km from the sending bus under Scenario 1

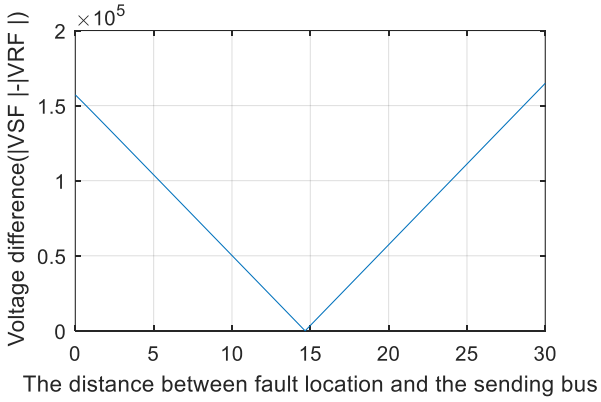

Figure C-8: Fault location solution for double line-to-ground (BCG) fault at 15 km from the sending bus under Scenario 1

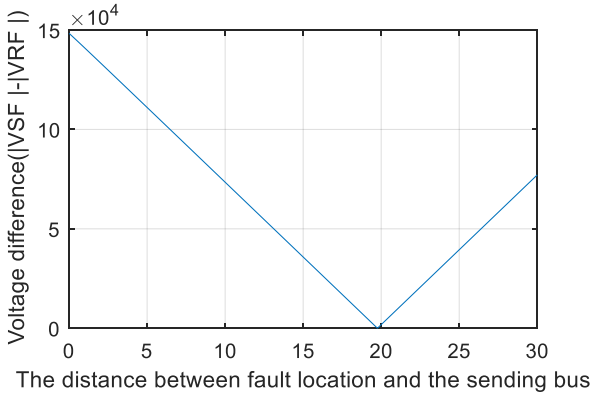

Figure C-9: Fault location solution for double line-to-ground (ACG) fault at 20 km from the sending bus under Scenario 1

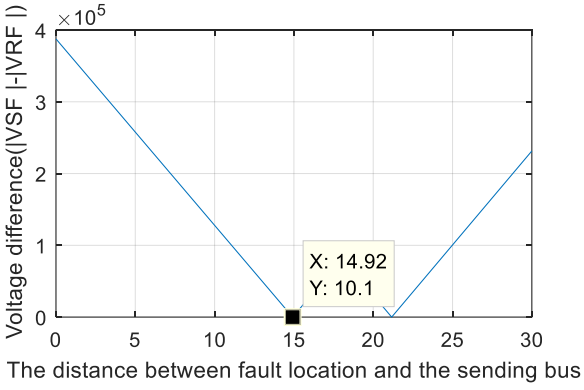

Figure C-10: Three-phase fault location solution at 15 km from the sending bus under Scenario 1

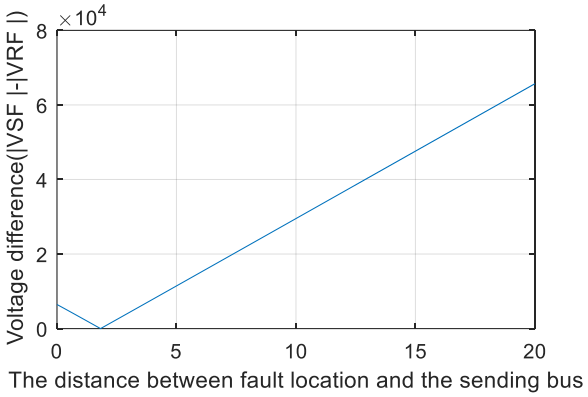

Figure C-11: Fault location solution for line-to-ground (AG) fault at 2 km from the sending bus under Scenario 2

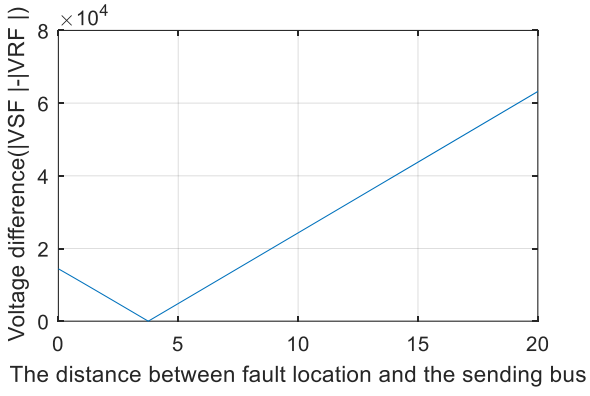

Figure C-12: Fault location solution for line-to-ground (BG) fault at 4km from the sending bus under Scenario 2

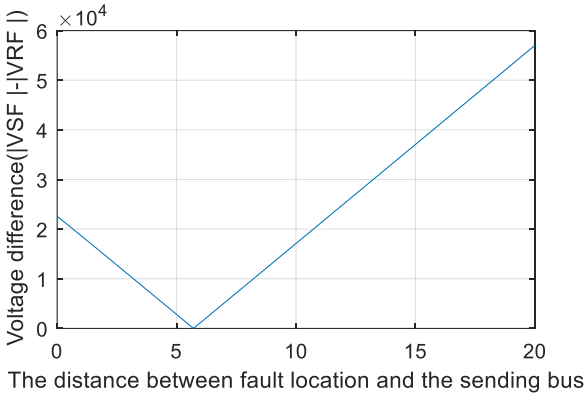

Figure C-13: Fault location solution for line-to-ground (CG) fault at 6 km from the sending bus under Scenario 2

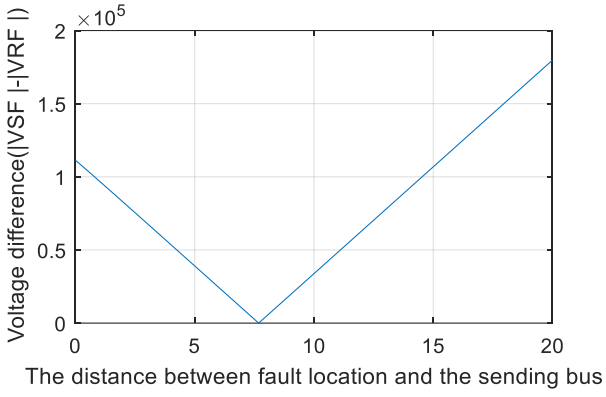

Figure C-14: Fault location solution for line-to-line (AB) fault at 8 km from the sending bus under Scenario 2

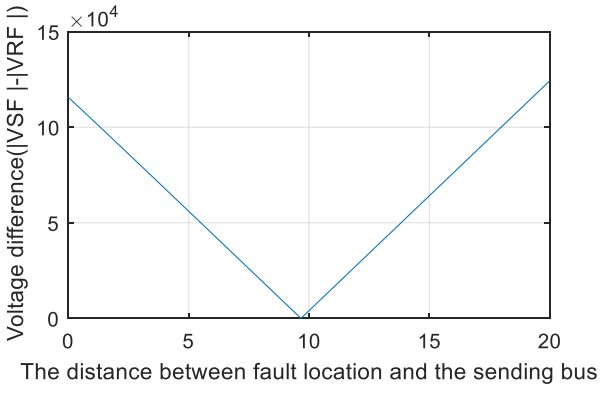

Figure C-15: Fault location solution for line-to-line (BC) fault at 10 km from the sending bus under Scenario 2

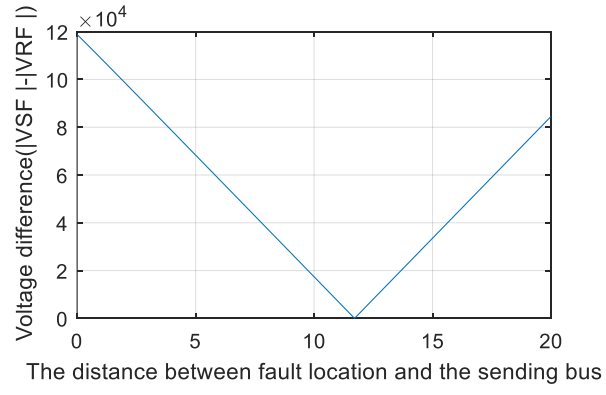

Figure C-16: Fault location solution for line-to-line (AC) fault at 12 km from the sending bus under Scenario 2

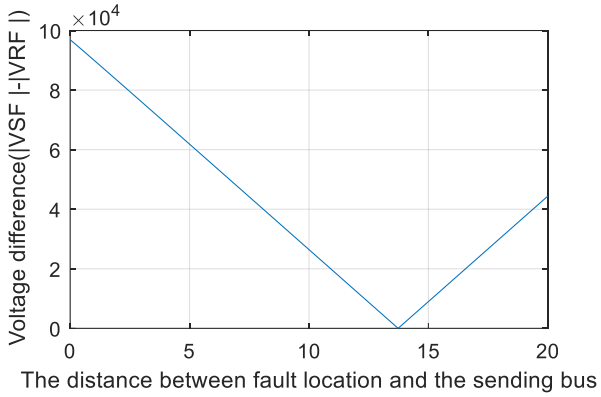

Figure C-17: Fault location solution for double line-to-ground (ABG) fault at 14 km from the sending bus under Scenario 2

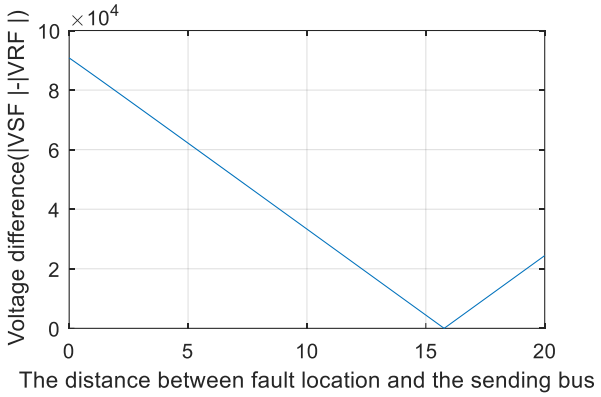

Figure C-18: Fault location solution for double line-to-ground (BCG) fault at 16 km from the sending bus under Scenario 2

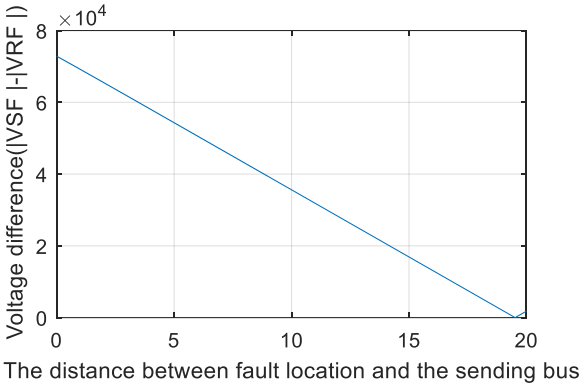

Figure C-19: Fault location solution for double line-to-ground (ACG) fault at 19.5 km from the sending bus under Scenario 2

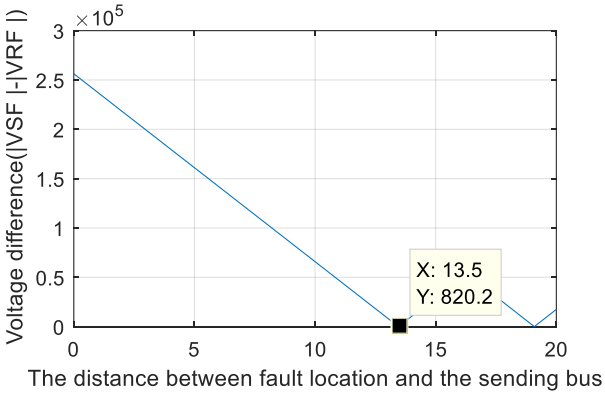

Figure C-20: Three-phase fault location solution at 13.5 km from the sending bus under Scenario 2

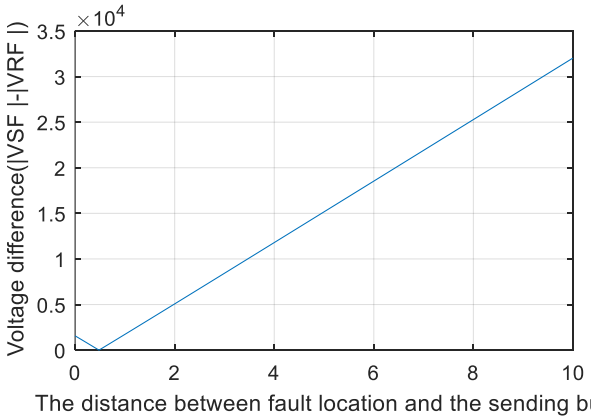

Figure C-21: Fault location solution for line-to-ground (AG) fault at 0.5 km from the sending bus under Scenario 3

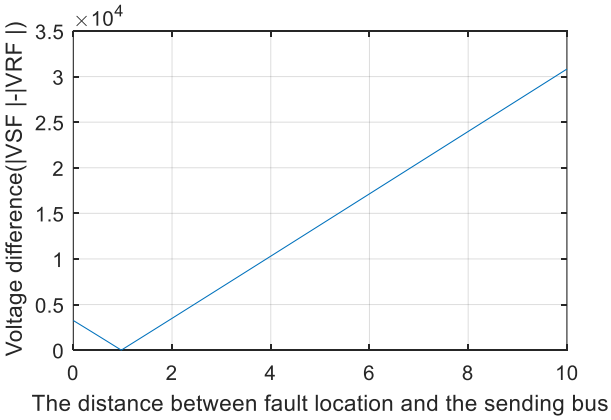

Figure C-22: Fault location solution for line-to-ground (BG) fault at 1 km from the sending bus under Scenario 3

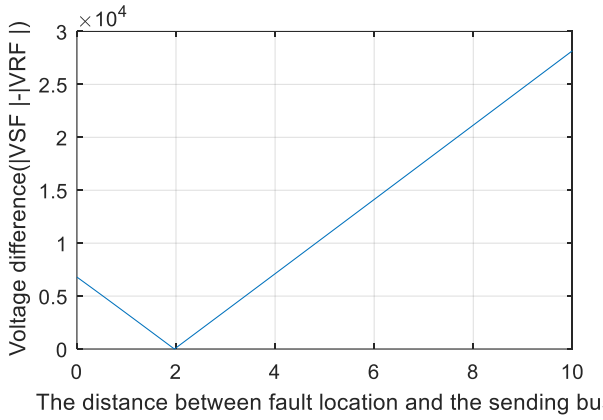

Figure C-23: Fault location solution for line-to-ground (CG) fault at 2 km from the sending bus under Scenario 3

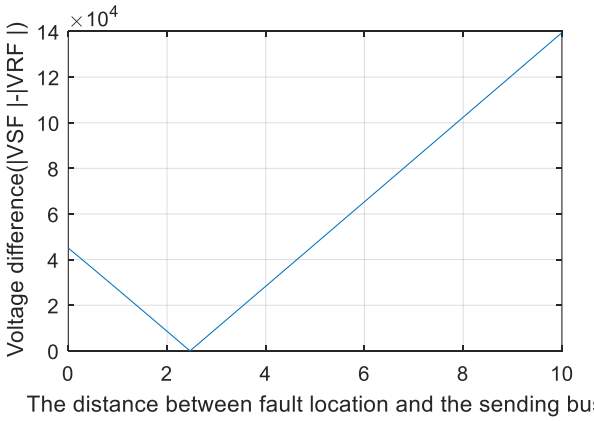

Figure C-24: Fault location solution for line-to-line (AB) fault at 2.5 km from the sending bus under Scenario 3

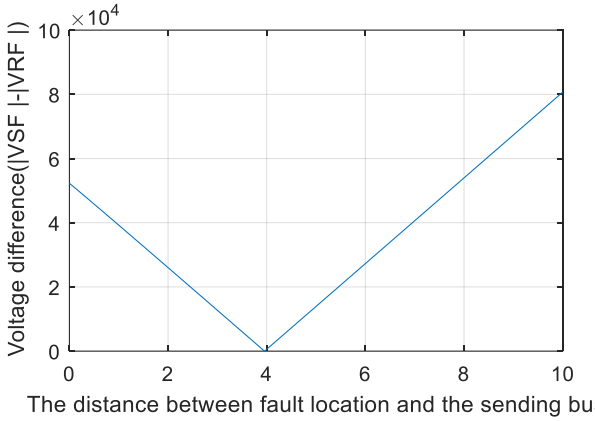

Figure C-25: Fault location solution for line-to-line (BC) fault at 4 km from the sending bus under Scenario 3

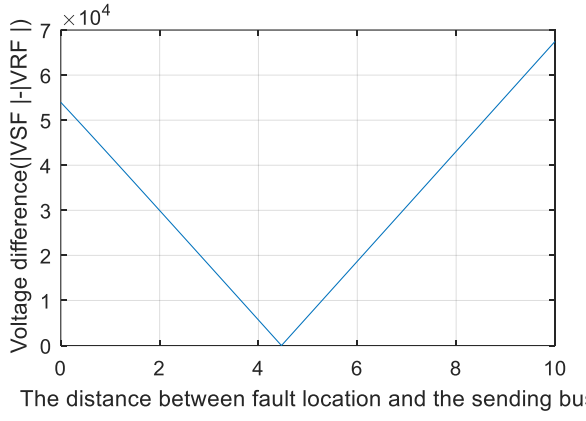

Figure C-26: Fault location solution for line-to-line (AC) fault at 4.5 km from the sending bus under Scenario 3

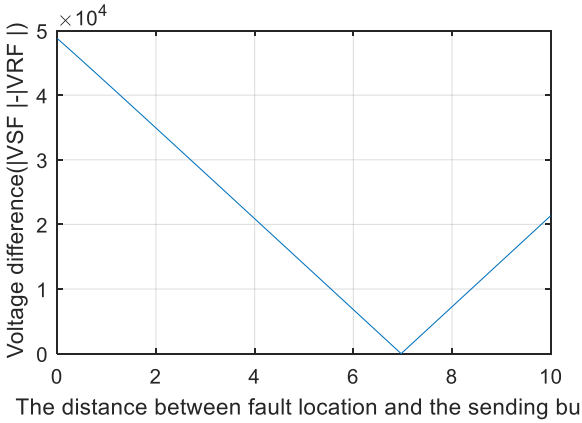

Figure C-27: Fault location solution for double line-to-ground (ABG) fault at 7 km from the sending bus under Scenario 3

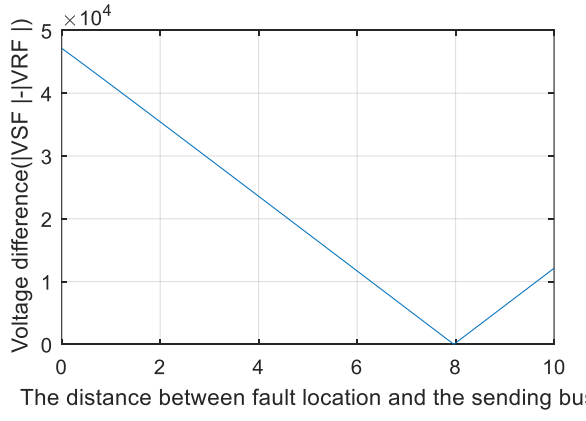

Figure C-28: Fault location solution for double line-to-ground (BCG) fault at 8 km from the sending bus under Scenario 3

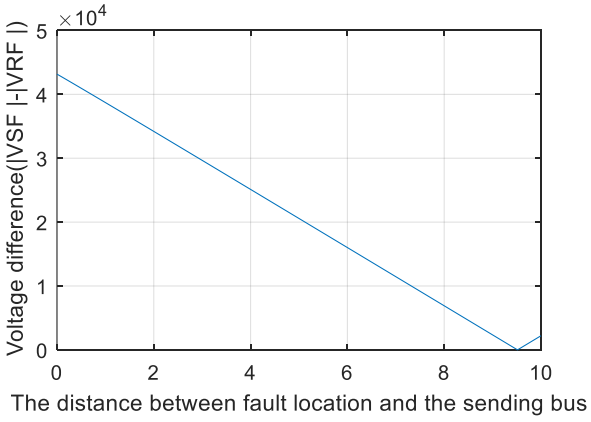

Figure C-29: Fault location solution for double line-to-ground (ACG) fault at 9.5 km from the sending bus under Scenario 3

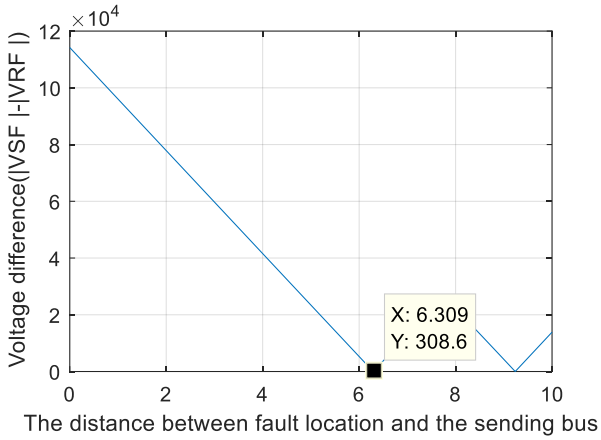

Figure C-30: Three-phase fault location solution at 6.3 km from the sending bus under Scenario 3

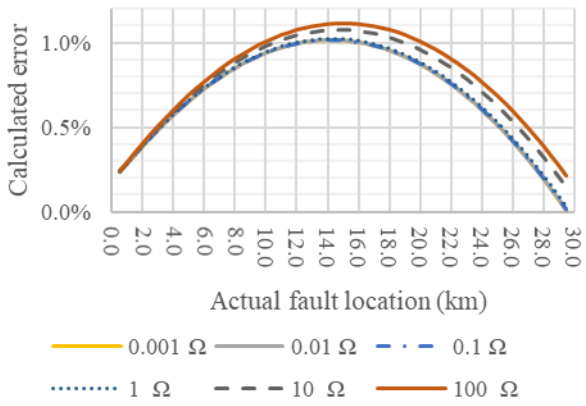

Figure C-31: Calculation errors of fault resistances for LG (Scenario 1–Case 1)

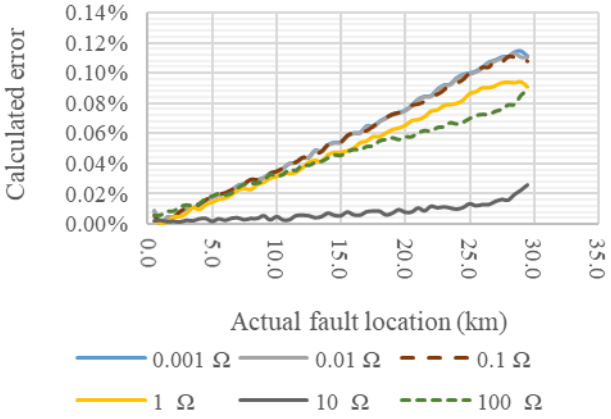

Figure C-32: Calculation errors of fault resistances for LG (Scenario 1–Case 2)

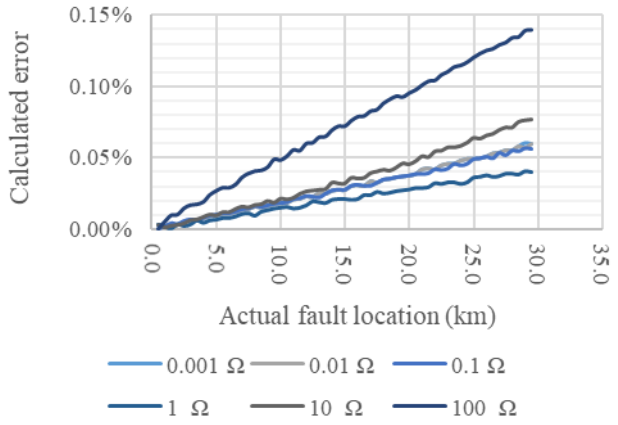

Figure C-33: Calculation errors of fault resistances for LG (Scenario 1–Case 3)

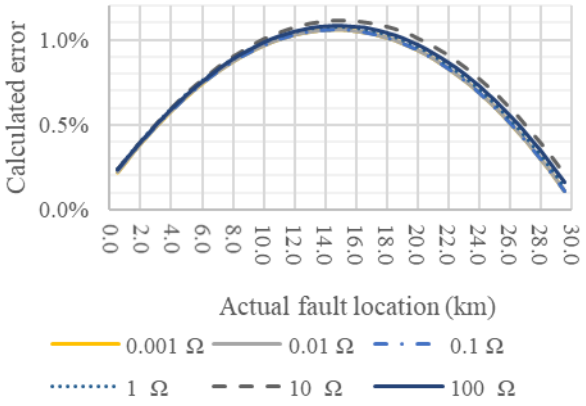

Figure C-34: Calculation errors of fault resistances for LL (Scenario 1–Case 1)

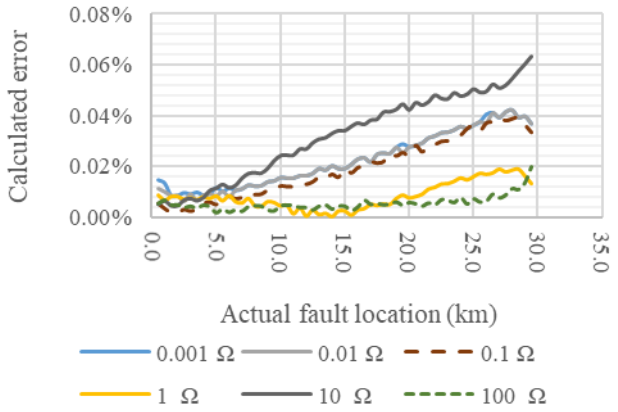

Figure C-35: Calculation errors of fault resistances for LL (Scenario 1–Case 2)

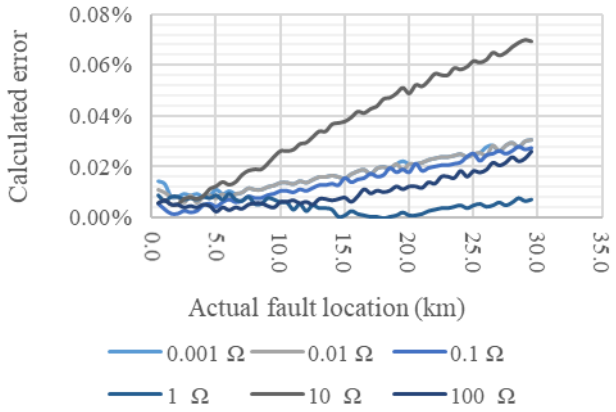

Figure C-36: Calculation errors of fault resistances for LL (Scenario 1–Case 3)

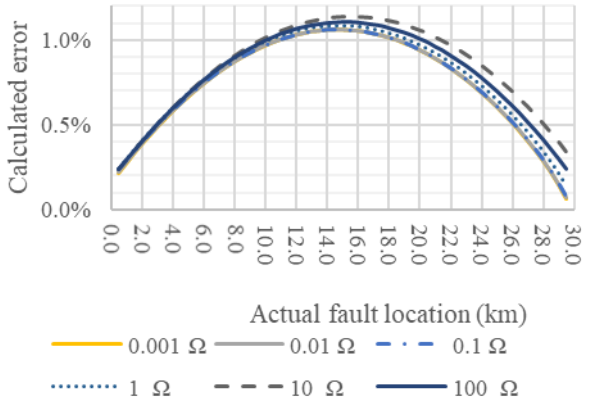

Figure C-37: Calculation errors of fault resistances for LLG (Scenario 1–Case 1)

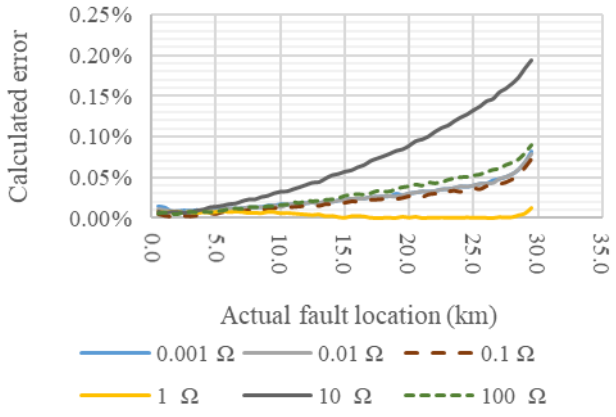

Figure C-38: Calculation errors of fault resistances for LLG (Scenario 1–Case2)

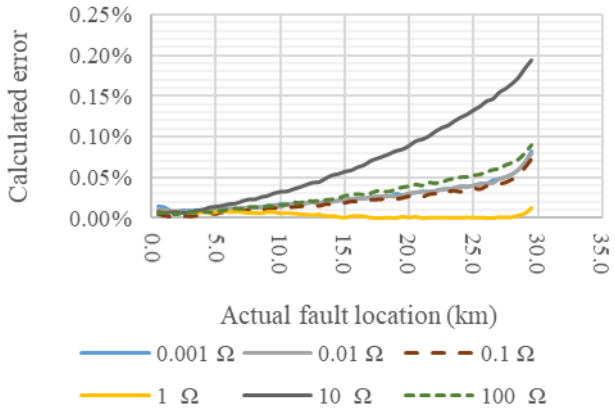

Figure C-39: Calculation errors of fault resistances for LLG (Scenario 1–Case 3)

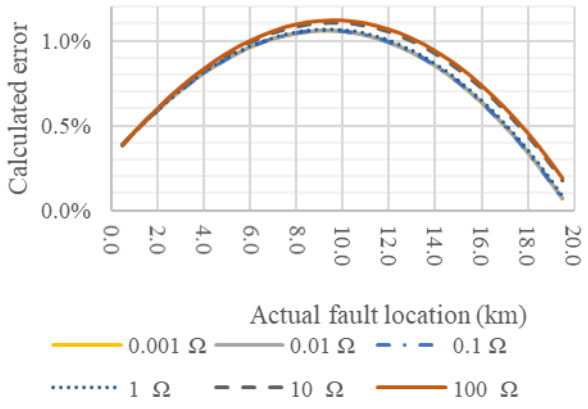

Figure C-40: Calculation errors of fault resistances for LG (Scenario 2–Case 1)

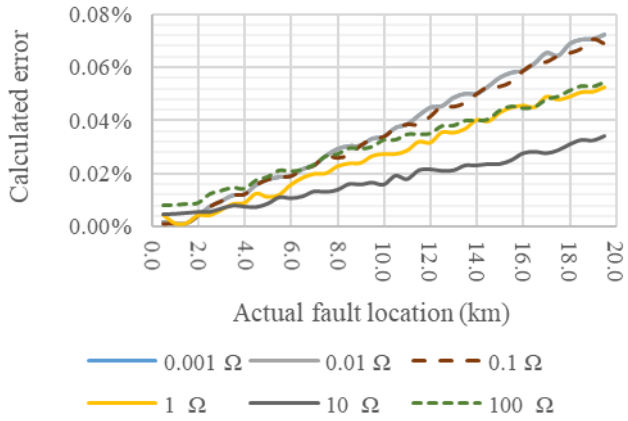

Figure C-41: Calculation errors of fault resistances for LG (Scenario 2–Case 2)

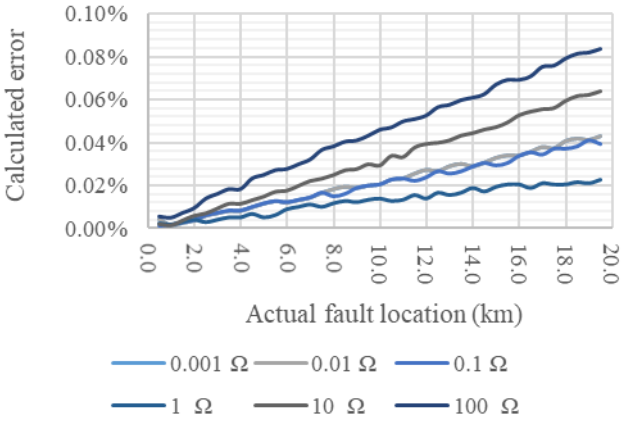

Figure C-42: Calculation errors of fault resistances for LG (Scenario 2–Case 3)

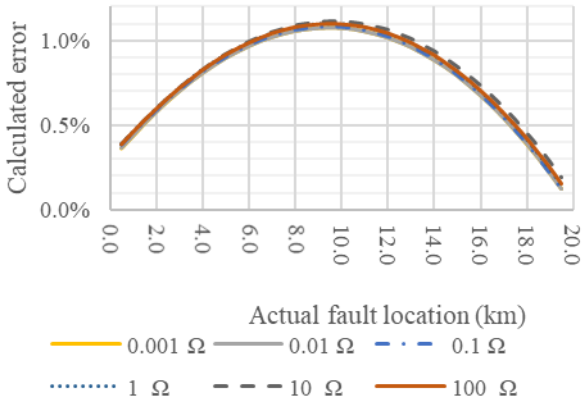

Figure C-43: Calculation errors of fault resistances for LL (Scenario 2–Case 1)

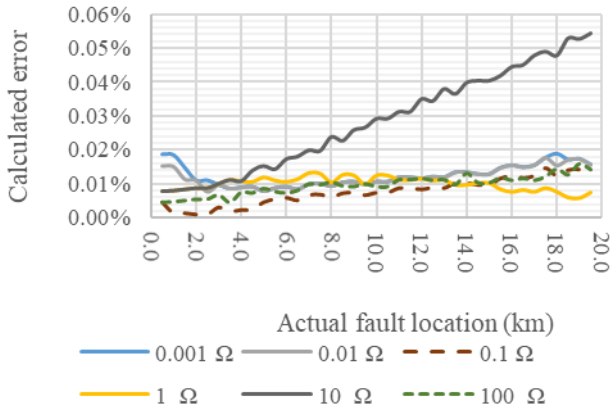

Figure C-44: **Calculation errors of fault resistances for LL (Scenario 2–Case 2)**

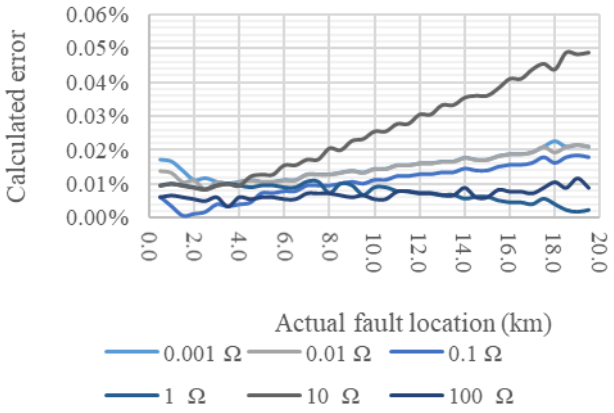

Figure C-45: **Calculation errors of fault resistances for LL (Scenario 2–Case 3)**

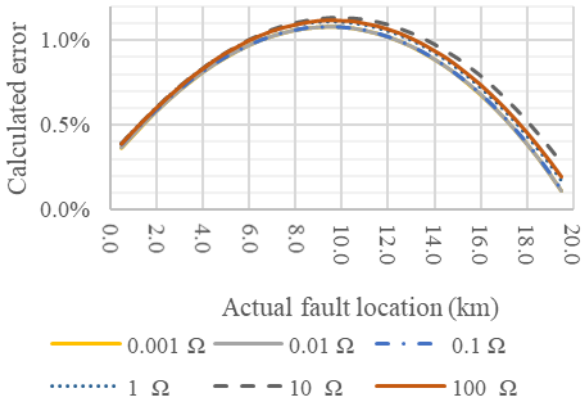

Figure C-46: **Calculation errors of fault resistances for LLG (Scenario 2–Case 1)**

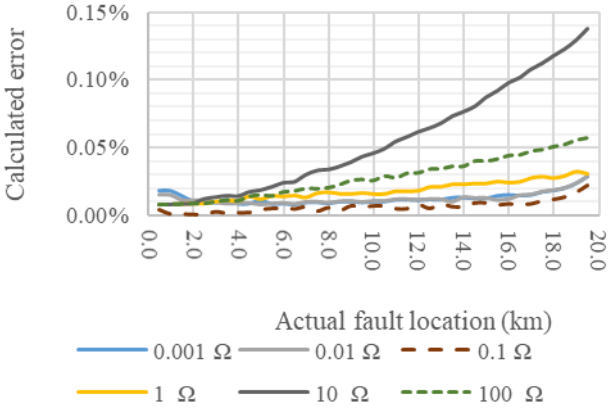

Figure C-47: **Calculation errors of fault resistances for LLG (Scenario 2–Case2)**

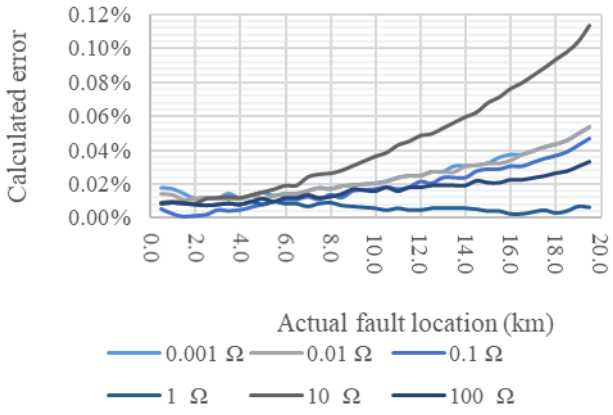

Figure C-48: **Calculation errors of fault resistances for LLG (Scenario 2–Case 3)**

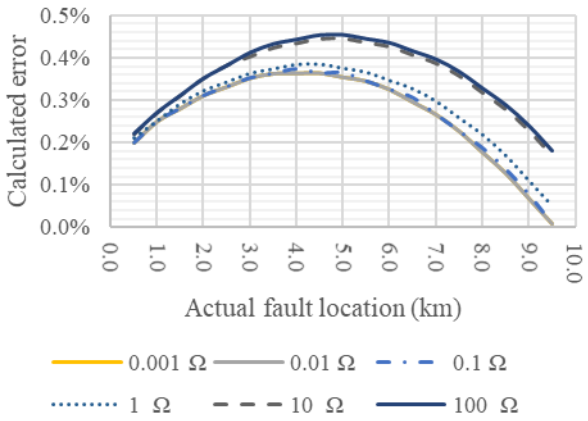

Figure C-49: Calculation errors of fault resistances for LG (Scenario 3–Case 1)

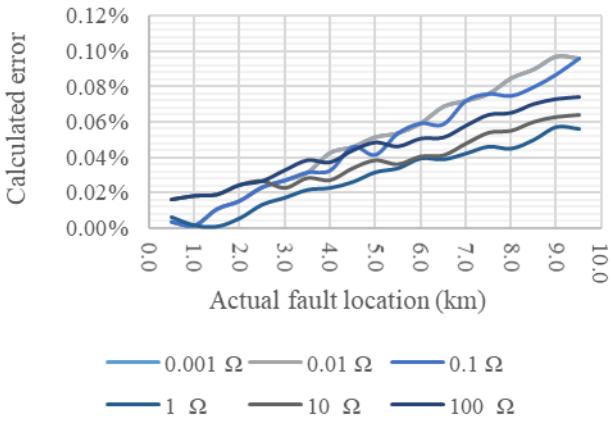

Figure C-50: Calculation errors of fault resistances for LG (Scenario 3–Case 2)

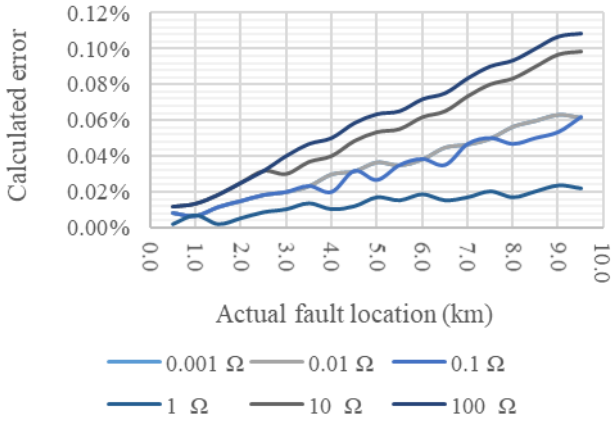

Figure C-51: Calculation errors of fault resistances for LG (Scenario 3–Case 3)

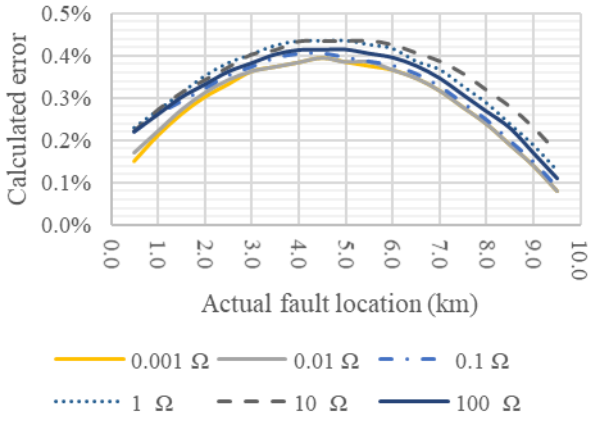

Figure C-52: Calculation errors of fault resistances for LL (Scenario 3–Case 1)

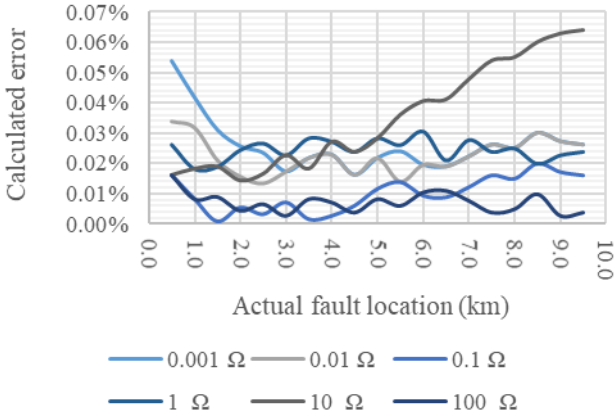

Figure C-53: Calculation errors of fault resistances for LL (Scenario 3–Case 2)

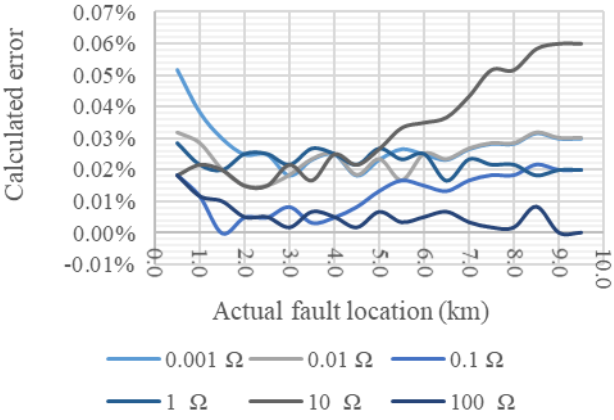

Figure C-54: Calculation errors of fault resistances for LL (Scenario 3–Case 3)

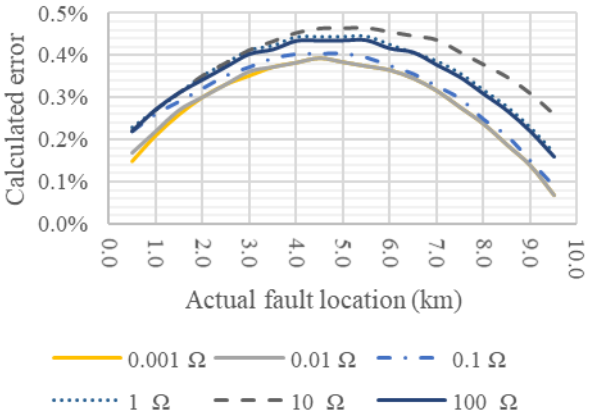

Figure C-55: Calculation errors of fault resistances for LLG (Scenario 3–Case 1)

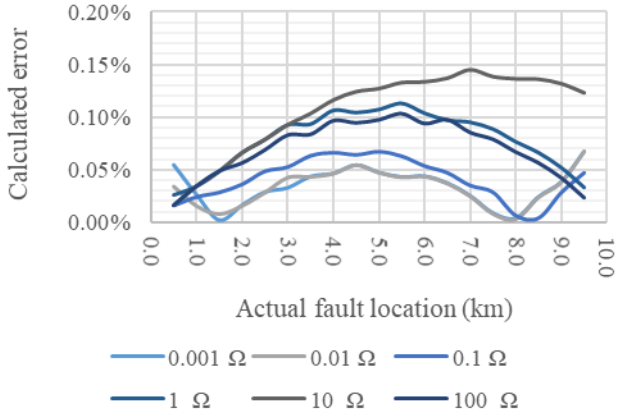

Figure C-56: Calculation errors of fault resistances for LLG (Scenario 3–Case2)

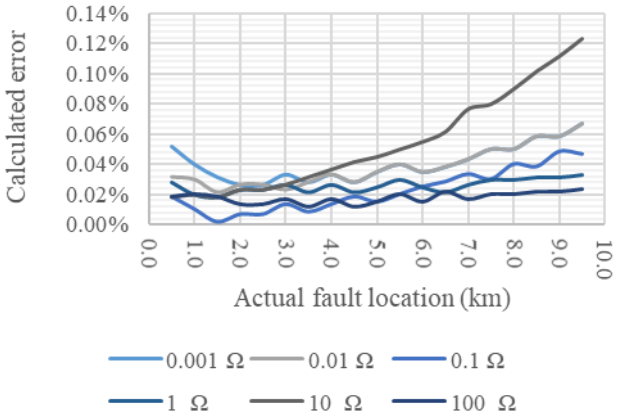

Figure C-57: Calculation errors of fault resistances for LLG (Scenario 3–Case 3)

VITAE

Name	:Mustafa Mohammed Jamal Al-Khabbaz
Nationality	:Saudi
Date of Birth	:11/4/1988
Email	:am.1@hotmail.com
Address	:Dhahran 31311, Saudi Arabia–P.O. Box 18377 (Saudi Aramco)
Academic Background	:Bachelor of Science in Electrical Engineering with honors from King Fahd University of Petroleum and Minerals, Dhahran, Saudi Arabia in 2011.
Research Experience	:Published several manuscripts in the field of power system at prestige forums of IEEE and IASTED during different events at Canada, Qatar, and Malaysia..
Area of Interest	:Power system planning and analysis, engineering economics, smart grid, renewables and PMU applications in power systems.
Work Experience	:Facilities Planning, Power System Engineering and Abqaiq Plants Operations Departments of Saudi Aramco since 2011.